NEW METHODS FOR TRACE ANALYSIS OF IODINE AND

PERCHLORATE IN BIOLOGICAL FLUIDS

by

CHARLES PHILLIP SHELOR

Presented to the Faculty of the Graduate School of

The University of Texas at Arlington in Partial Fulfillment

of the Requirements

for the Degree of

DOCTOR OF PHILOSOPHY

THE UNIVERSITY OF TEXAS AT ARLINGTON

MAY 2014

Acknowledgements

There are many people that have played an important role during my studies. Words cannot accurately express my gratitude to Dr. Purnendu K. Dasgupta who was not only my mentor but a friend. He provided me daily inspiration with his wealth of knowledge and endless words of motivation. Dr. Dasgupta, Thank you for your continued guidance. Without your support I would not have been able to accomplish what I have.

Many thanks to my committee members, Dr. Krishnan Rajeshwar, Dr. Richard Timmons, and Dr. Rasika Dias, for your support and valuable input during my time at UTA.

I'd like to thank all my coworkers. Many have come and gone and all have left something behind. You will all be remembered.   Mahitti Puanngam and Jason Dyke, your teaching during these years was invaluable. Martina Kroll, Brian Stamos, Catrina Campbell, and Veronica Waybright, our coffee breaks were often the highlight of my day when nothing else was working. To all the others, though you have not been named, you are no less important.

I'd especially like to thank my wife Kathryn. You have always been supportive of me, even when I've been more attentive to my studies than you. Now that I've written my last dissertation chapter, I look forward to starting the next chapter in our lives with you.

April 17, 2014

Abstract

NEW METHODS FOR TRACE ANALYSIS OF IODINE AND

PERCHLORATE IN BIOLOGICAL FLUIDS

Charles Phillip Shelor, PhD

The University of Texas at Arlington, 2014

Supervising Professor: Purnendu K. Dasgupta

Iodine is an essential element necessary for the production of the thyroid hormones T3 and T4. These hormones are necessary for metabolism and are especially important for brain development in infants and young children. Iodine is transported into the thyroid by the sodium iodide symporter. Perchlorate is known to inhibit iodine uptake into the thyroid by binding to the sodium iodide symporter, thus acting as a potential neurotoxicant for developing children.

The research in this dissertation consists of two goals. The primary is the development of novel methods for measuring iodine and perchlorate and the second is performing analyses to determine infant risk associated with perchlorate consumption via milk. Further research performed not relevant to the title theme is included in the appendices.

The iodine status of infants is not well known. Urinary iodine is used as the primary epidemiological marker for gauging the iodine status of an adult population. Infant risk assessment however, due to difficulties acquiring infant urine samples, is more frequently monitored via the feed, e.g. milk. Measurement of iodine and perchlorate in milk is no simple task.   Complete sample digestion is preferred for iodinalysis, but the harsh conditions often rule out such methods to be used for perchlorate analysis. Iodide

present in the milk may also be oxidized to molecular iodine which is volatile and may be lost prior to analysis. We have developed a new digestion procedure for the removal of organics based on the Fenton reaction: the Fe^{2+} catalyzed oxidation of organics by H_2O_2. The method is green, safe, inexpensive and effective. Iodine loss is kept to a minimum by controlling the temperature and pH of the reaction. Additionally, the reaction is mild enough such that perchlorate remains intact throughout the digestion.

The digestion procedure was used for the analysis of breast milk samples and corresponding infant urinary secretions. Using iodine as a conservative tracer in the infants, it is found that perchlorate is actually reduced in breastfed infants as opposed to their formula fed counterparts. One of the primary physiological differences between breastfed and formula fed infants is intestinal bacteria. Milk spiked with perchlorate was inoculated with *bifidobacteria,* the dominant intestinal bacteria in breastfed infants. Perchlorate reduction occurred in those samples with *bifidobacteria* compared to those with a bacteria blend that didn't contain it.

Currently there is no means of measuring an individual's iodine nutrition status. An inexpensive device was developed capable of measuring iodine to levels necessary for identifying severe deficiency. The system was based on a gas-phase preconcentration microplasma dielectric barrier discharge atomic emission spectrometer. Iodine is absorbed on a suitably coated tungsten filament of low thermal mass. The filament is heated rapidly and the iodine is vaporized and measured in the plasma. The biggest obstacle to final development of a working unit is the chemistry of iodine itself. Oxidation of I^- to I_2 and removal from solution is a seemingly easy task given that I^- is readily oxidized and I_2 is volatile with low solubility in water. However, disproportionation reactions are prevalent at low iodine concentrations and necessitate the need for alternative approaches such as generation of CH_3I.

Table of Contents

List of Illustrations

List of Tables

Chapter 1

Review of Analytical Methods for the Quantification of Iodine in Complex Matrices

1.1 Introduction

It is estimated that more than two billion people have insufficient iodine intake and are at risk of developing Iodine Deficiency Disorders (IDD).[1] Symptoms of Iodine Deficiency include goiter, hypothyroidism, and cretinism. In 1917, Marine and Kimball[2] first showed that iodine supplementation could reduce goiter, and prophylactic iodization of salt started in Switzerland in 1922;[3] in 1924, the U.S. followed suit.[4,5] In this review we refer to the US population most frequently as we are most familiar with the relevant literature. However, the status of most countries regarding iodine nutrition is not better than that of the US.

The U.S. Institute of Medicine (IOM) recommended daily allowance (RDA) or adequate intake (AI) of iodine for different population groups are as follows (in $\mu g\ d^{-1}$), 0-6 mo.: 110 (AI); 7-12 mo: 130 (AI), 1-8 yr: 90 (RDA), 9-13 yr: 120 (RDA); > 14 yr: 150 (RDA); pregnant women: 220 (RDA); Lactating women: 290 (RDA).[6] There are calls for further increasing the suggested iodine intake, especially for pregnant and lactating women.[7] Currently 91% of the global population, totaling some 130 countries, is regularly surveyed for their iodine nutrition status and iodization of salt and other measures of iodine supplementation are taken. In 1993, iodine deficiency was a recognized public health problem in 123 countries; by 2006 this number has decreased to 47. Some 63 countries still do not have regular screening procedures. The WHO recommends iodization of not just household salt but also livestock feed. Urinary iodine (UI) is the epidemiological indicator used for iodine nutrition status in a population.[8] Median UI levels are used to categorize a population as severely deficient (<20 $\mu g\ L^{-1}$), moderately

deficient (20-49 μg L^{-1}), mildly deficient (50-99 μg L^{-1}), adequate nutrition (100-199 μg L^{-1}), above requirements (200-299 μg L^{-1}), and excessive intake (>300 μg L^{-1}). The risks of excessive Iodine intake include hyperthyroidism and thyroid autoimmune diseases; however whether this occurs at a UI level of 300 μg L^{-1} is debatable. A mean urinary iodine volume of 1.5 L d^{-1} can be used to relate intake values to UI values. Backer and Hollowell[9] surveyed the extensive extant literature and concluded that the strongest data suggests that iodine intakes of 1000–5000 μg d^{-1} are safe for most people for *years*.

1.2 Iodine Deficiency and a Particular Perspective for the United States.

Iodine deficiency is the most common cause of cognitive impairment.[8] The brain is extremely sensitive to the effects of low iodine intake with the degree of impairment dependent on the timing and severity of the deficit.[10] Even a mild iodine deficiency may seriously affect the intelligence and function of children.[11,12] In the US, iodine nutrition status is monitored through the National Health and Nutrition Examination Surveys (NHANES). Evaluations of iodine nutrition made through NHANES I and III have indicated that iodine intake has decreased over the last decades, potentially leaving more infants at risk of iodine deficiency.[13] The decrease in intake may be due to changing practices among dairies and cereal manufacturers[14] removal of iodate-based conditioners from store-bought bread[15] and increased reliance on pre-prepared, prepackaged and fast foods, which may contain a lot of salt but not iodized salt.[16] There is also decreasing use of salt at home because of potential adverse health concerns of excessive sodium consumption;[17] ironically, the bulk of the salt consumed outside the home is *not* iodized. Salt, the primary source of iodine for many within the US, is now widely perceived as unhealthy, because it increases hypertension risks. The American Medical Association has taken the extraordinary step to ask the US Food and Drug Administration to take salt

off the "Generally Recognized As Safe" (GRAS) list. As households seek to reduce their sodium consumption, the likely end result is that iodine intake will further decrease. Salt content will be reduced at home, the only place most individuals encounter iodized salt, as the population typically does not go to restaurants and ask that less salt be used in cooking or ask fast food /prepackaged food vendors to reduce salt in their products. Recently, however, some US vendors of prepackaged food now have voluntarily pledged gradual reduction of salt content. Pregnant and lactating women, many of whom attempt to "eat healthy" while pregnant or in early motherhood, may thus become the most susceptible when salt consumption at home is cut back.

Actual infant iodine nutritional status in the US is not directly known: infants are not a part of the NHANES cohort. Breastfed infants, who rely on their mothers' milk for iodine, will be particularly vulnerable if their mothers fall short on iodine nutrition. The recent decrease in iodine intake has been associated with increasing rates of congenital hypothyroidism,[18] a serious condition known to have permanent effects on neurological function.[19] The most recently available NHANES data indicate that the median UI value for lactating white women is 106 μg L^{-1} (and even then 6%, 22% and 11% of the population are respectively in the severely, moderately and mildly iodine deficient categories). The median UI value for lactating Hispanic women in the US is a dismal 50 μg L^{-1}.[20]

Even mild iodine deficiency is associated with behavioral and cognitive dysfunction. Children with UI <100 μg L^{-1} have lower IQ and higher prevalence of behavioral disorders than their higher UI peers.[21] Mild iodine deficiencies in women correlate with attention deficit hyperactivity disorders (ADHD) in their children.[22] The present scenario on iodine nutrition is complicated by the fact that the relationship between iodine assimilation and intake may be affected by the ubiquitous environmental

presence of iodide transport inhibitors. Perchlorate is the most potent of iodide transport inhibitors. For a discussion of this issue see a special issue of this journal[23] and other recent commentaries.[24] Whether or not perchlorate plays a role, presently there is real concern about the iodine nutritional status of US mothers.[25]

1.3 Analytical Methods for Iodine in Biological Samples.

To properly assess iodine nutrition, methods are required to affordably and accurately quantify iodine in soil, plants, various foods and in physiological samples, notably milk, serum, and urine. Presently, iodine measurement in biological samples is carried out almost exclusively by one of two methods: One is an age-old kinetic spectrophotometric method called the Sandell-Kolthoff reaction.[26] The reduction of yellow Ce(IV) by As(III) to colorless Ce(III) is normally very slow. This reaction is catalyzed by trace amounts of iodide. The reaction follows the following scheme:

$$2Ce^{4+} + 2I^{-} \longrightarrow 2Ce^{3+} + I_2$$

$$As^{3+} + I_2 \longrightarrow As^{5+} + 2I^{-}$$
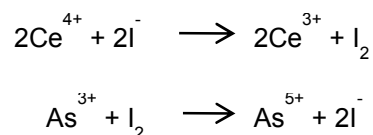
It is also catalyzed to a much smaller extent by iodate, which in any case, is readily converted to iodide in the presence of arsenite in an acidic medium. Organoiodine compounds do not react without decomposition. The rate of disappearance of the yellow color in a Ce(IV)-As(III) mixture is measured as a measure of iodine content. Ce(III) is fluorescent (λ_{ex} 254 nm, λ_{em} 350 nm)[27] and in principle the reaction can be fluorometrically followed as well. In practice because of the variable amounts of UV-absorbing species that may be present, the reaction is rarely used in this fashion. As may be intuitive, many organic substances can potentially interfere[26,28] by chelating Ce(IV) or Ce(III) or otherwise directly affecting the reaction rate. Complete mineralization

4

of the sample to digest the organics is thus a necessity. This digestion step typically

involves perchloric acid. This requires special hoods and precautions because of

explosion hazards. The other method used is at the opposite end of sophistication;

Inductively Coupled Mass Spectrometry (ICP-MS) permits superb sensitivity, and as

such, in some cases (e.g., urine) will permit direct sample analysis after dilution.

Nevertheless, it is still necessary to have an internal standard to account for matrix

effects.[29]

In this review, we critically evaluate all methods, including variants of the above,

actually used for the measurement of trace iodine in biological samples. We have

deliberately avoided extensive discussion of methods that have been used only with

simple matrices, e.g., salt, as such applications do not provide the analytical challenges

posed by biological matrices. The references cited here are representative rather than

comprehensive. Far too many applications of iodine measurements in biological samples

are in the extant literature but few contain analytical innovations. The heart of this review

is a summary table of the methods presented with key analytical figures of merit provided

in Appendix A,Table A - 1.

1.4 The Sandell-Kolthoff Reaction.

The Sandell-Kolthoff Reaction[26] is likely the most widely used technique for

quantifying iodine. The reduction of absorbance due to Ce(III) is typically measured at

405 - 420 nm; although the maximum sensitivity can be achieved at 310-317 nm;[30,31] this

is not often used because of the same reasons that the previously stated sensitive

method of Ce(III) fluorescence measurement is not used. Aside from uncharacterized

organics, the reaction is interfered with by higher concentrations of thiocyanate (both milk

and urine typically contain much larger amounts of thiocyanate than iodide[32, 33]);

5

thiocyanate levels are especially high for smokers.[34] Traces of metal ions such as silver or mercury that bind iodide also interfere. Substances that readily undergo oxidation, notably nitrite, ascorbic acid, and ferrous iron[26,28] also interfere.

Determination of iodide using the S-K method can be carried out two different ways: (a) record the complete absorbance profile with time (b) measure the sample absorbance after some preset time interval following mixing of all components. Most often b is used for higher throughput. The iodine concentration can be determined directly from the difference in absorbance between a blank and the sample at any time following mixing.[30]

1.4.1 Digestion Procedures Used Prior to Sandell-Kolthoff Measurement.

Barker et al.[35] reported an alkaline digestion procedure to measure protein bound iodine (PBI, synonymously used for thyroglobulin (TG), etc.); cited some 322 times, this approach has been much used. The method involves precipitation of the protein as the Zinc conjugate ($ZnSO_4$ solution is typically added[36]), addition of excess alkali, slow evaporation to dryness overnight @ 85-95 °C, ashing for 2.5 h @ 600 °C followed by extraction of the ash with dilute HCl. However, latter work has indicated that much loss can occur in the procedure at pre-ashing temperatures; this can be minimized by choosing a vessel that minimizes circulation of gases and using KOH instead of NaOH.[37] Glass vessels used for ashing cannot be reused; the etched surface tends to strongly adsorb iodine.[37] Acid digestion procedures do not have this problem. However acid digestion conditions can lead to losses as elemental I_2; iodide in acid solution is readily oxidized by air. Traditional perchloric acid digestion (sulfuric, nitric, perchloric acids[38] or nitric and perchloric acids[39]) does work and radiotracer studies show that iodine loss is consistent and is typically below 20%.[39] Traditional perchloric acid digestion as outlined

in[38] (see[40] for an update that involves overnight digestion with HNO_3 followed by digestion with conc. H_2SO_4 and 70% $HClO_4$) is still the method of choice for sample preparation for iodine determination by the US Food and Drug Administration.[41] Perchloric acid digestion does require special hoods and special precautions.

Zak et al.[42] had earlier developed a procedure that uses chloric acid ($HClO_3$) as the active oxidant to oxidize iodide more rapidly and effectively to nonvolatile iodate. Chloric acid is not commercially available as such; this was prepared by adding a stoichiometric amount of 70% $HClO_4$ to a concentrated solution of $KClO_3$. The resulting $KClO_4$ was allowed to precipitate while the mixture was refrigerated overnight. It is not known how much free $HClO_4$ remains but based on the residual potassium in solution, the amount is likely small. The chloric acid digestion procedure was adopted by Benotti et al.[43] for urine, feces, tissues and food; this work has been much cited. Some other chloric acid procedures actually use significant amount of other oxidizing acids including perchloric and chromic acids; again, appropriate precautions must be taken.[44] A mixture of sodium chlorate and perchloric acid has also been used for digestion.[45] It is not clear to the present authors why chloric acid must be prepared with $HClO_4$ with removal of the counterion as $KClO_4$ and cannot be used e.g., as a stoichiometric mixture of $KClO_3$ and H_2SO_4. It is possible but unlikely that the presence of excess potassium sulfate results in interferences.

Pino et al.[46] has advocated ammonium persulfate (AP) digestion of urine samples that is completed in 30 min. This avoids the needs for a specialized fume hood. In our experience, this method is indeed effective for digesting urine samples but is not necessarily applicable to other sample types, e.g., human milk. For UI, the AP digestion method was validated against automated acid digestion in a Technicon autoanalyzer[47,48] and reversed phase ion-pair HPLC.[47] Results obtained by the S-K method after AP

digestion has also been compared with parallel ICP-MS analysis.[49] For UI, in-line digestion at 38 °C with acidic permanganate and dichromate in a flow-injection format has also been shown to be viable.[50]

Rollman et al. combusted the sample in a closed flask in an oxygen atmosphere and converted the iodine formed to iodate by hypochlorite. Any chlorine formed was purged by N_2 prior to analysis.[51] Oxygen flask combustion followed by oxidation of iodine to iodate by a chloric acid absorber was used by Zaroda to measure PBI.[52]

Pyrohydrolysis, a process where the sample is heated to 1200-1300 °C while water vapor/steam and O_2/air is passed over it, has been used with geological samples.[53,54] The apparatus is complex.

The S-K method is an effective way to measure iodine in complex samples but it will be apparent that the sample preparation methods listed above are onerous, do not lend themselves well to automation and will constitute the major bottleneck when a large number of samples are to be analyzed. In some of the digestion methods, if digestion is conducted with multiple samples in a closed system, some iodine escapes into the gas phase from high concentration samples and is reabsorbed by other samples.[55] In specific cases, iodine can be liberated from organoiodine compounds. If the sample is already chromatographically purified, thyroxine (T_4) can be thus determined by adding bromine (generated in-situ by bromide, bromate and acid) prior to measurement by the S-K method.[56] Autoanalyzer adaptations of this have been reported.[57] The bromine addition procedure is broadly applicable to 3-iodotyrosine (monoiodotyrosine, MIT), 3,5-diiodotyrosine (DIT), 3,3',5-triiodotironine (T_3), T_4 and TG.[58] Chlorine can be used in the same manner as bromine.[59] Even without prior decomposition MIT, DIT, T_3 and T_4 respond to the S-K reaction but at rates lower than an equivalent amount of mineralized iodide and response of each compound must therefore be individually calibrated for.[60]

8

Other efforts at bypassing digestion have later been shown to lead to errors. On-line dialysis instead of digestion was adapted to measure UI[61] but thiocyanate is also transported and produces erroneously high values for UI.[28]

1.4.2 Chemical Modifications of the Sandell-Kolthoff (S-K) Method.

Modifications to the S-K method that result in different measurands have been proposed. The reaction can be quenched with brucine sulfate[50] and the absorbance of the resulting brucine-cerium complex measured at 428 nm.[62] Addition of excess Fe(II) can also stop the reaction by reacting with Ce(IV) to produce Fe(III); the latter can then be determined by adding excess thiocyanate to form the well known red ferrithiocyanate complex that can be measured at 460 nm.[63] These methods only allow a single point measurement, obtaining reaction rate profile is not possible and they have not been much used.

1.4.3 Measurement Platforms Used With the Sandell-Kolthoff Method.

The early years of strictly manual assays was rapidly replaced by adaptation on the Technicon Autoanalyzer[36,38,40,46,52,56,64] which also provided for in-line digestion. Equivalent segmented flow analyzers are still in use in many laboratories and still constitute the typical comparison benchmark for new methods [65-67]. A very effective current adaptation of the S-K method is on microtiter plates with corresponding multichannel plate readers. These can provide high sample throughput and reduce the amount of waste per sample[65-67]. Both acid and AP digestion have been performed on the plates. Ohashi et al.[68] pioneered the adaptation of the microplates. Using a specially designed sealing cassette to prevent loss of vapor and cross-contamination among wells, AP digestion was performed in a microplate in an oven at 110 °C for 60 min. Afterwards,

the digestion mixture was transferred to a transparent microplate and the S-K reaction was performed at 25 °C for 30 min and absorbance measured at 405 nm. An advantage of the microplate method is the ability to load multiple blanks and standards and monitor for cross contamination. The flow-injection format[50] also allows for rapid assays. However, it does this in a sequential manner and cannot provide a kinetic profile. A rate profile can in principle be obtained by adopting an intermittent stopped flow arrangement but at the expense of throughput.

1.4.4 Representative Applications of the Sandell-Kolthoff Method.

The S-K reaction has successfully been applied to the analysis of protein bound and total inorganic serum iodine,[30,55,56,58-60,62,65,66,69,70] UI,[43,47,48,50,61,67,68], plant material,[36] food,[38,40,43] tissue,[43,45] feces,[43] amniotic fluid[64,69] and coal.[53,54] Serum PBI per se is no longer measured as T_3 and T_4 can be measured by immunoassay techniques.[65] Serum T_3 and T_4 have also been measured by anion exchange separation and iodine liberation by bromine treatment prior to the S-K reaction.[56-59]

The sensitivity of the S-K assay is excellent. In an interesting twist, iodine, instead of radionuclides, was used to tag antibodies so that the iodine labeled antibodies could be detected by the S-K method.[71] The response in a human IgG was linear below 40 ng/well compared to that of horseradish peroxidase that was linear up to 25 ng/well.

1.5 Inductively Coupled Plasma Mass Spectrometry (ICP-MS)

In a typical Inductively Coupled Plasma-Mass Spectrometer, microwave or radio frequency power is applied through an induction coil to generate high temperature argon plasmas, 4500-8000 K, with an electron temperature of 8000-10,000 K. The plasma atomizes the sample and strips the atoms of one or more valence electrons. The

resulting positive ions then typically enter a single quadrupole mass analyzer for sorting out ions of different m/z and are then detected.[72] Iodine has a relatively high first ionization potential (IP, to form I^+) of 10 eV;[73] thus the iodine present is only partially ionized (~25%). Despite partial ionization, the sensitivity is exceptional and a very large linear dynamic range can be attained. Urine cannot be introduced into the instrument directly; some dilution is needed to minimize the very high salt/dissolved solids content. In addition, the extent of ionization in the plasma is susceptible to other ionizable material being present; salt content will notably vary from sample to sample. It is essential to correct for such matrix effects. Matrix effects are best compensated for by using isotope dilution mass spectrometry, using [129]I as an isotopic tracer.[29,73] [129]I has negligible natural abundance. It is a fission byproduct of uranium and plutonium and is also produced in very small quantities in the upper atmosphere by cosmic radiation acting on xenon. In the absence of fallouts from nuclear explosions or reactor accidents, the amount of *naturally occurring* [129]I is negligible in urine or other biological samples. Although it is radioactive, with a half life of 16 million years, the amounts used as an analytical tracer do not pose a radiological hazard. If all the [129]I typically used to spike 20,000 samples was ingested, not totaling much over 2 mg, the radiation dosage would be of the same order as that experienced by the average person yearly (~2 mSv y^{-1}).[73] At the level that [129]I is spiked into biological samples in our laboratory (prior to processing for ICP-MS analysis), 20,000 samples would consume 0.6 mg [129]I. One report has explored the use of [115]In (IP 5.78 eV) and [103]Rh (IP 7.46 eV) as internal standards for UI measurements and report acceptable results with both.[74] A detailed discussion of the superiority of [129]I for iodine analysis by ICP-MS appears in;[29] these authors conclude that [129]I provides reproducible results regardless of sample type, while other internal standards may work with one matrix but may not work with another. In the rare case that the amount of [129]I

needed for isotope dilution exceeds permitted local radiological standards, double isotope dilution[75] can be used. This involves adding a dilute amount of standard at the beginning of the experiment during treatment and dilution processes and a second aliquot of standard is added just before ICP-MS analysis.

The ^{127}I content of the ^{129}I tracer can be measured *a priori*; the ^{127}I added in the tracer addition process can thus be corrected for. Xenon occurs as an impurity in the argon plasma gas, the natural abundance of ^{129}Xe is 26.4%. The ^{129}Xe content of the plasma gas can interfere with the measurement of ^{129}I. A correction can be made by measuring ^{131}Xe (natural abundance 21.2%) at m/z 131 and thus correcting for ^{129}Xe based on the respective natural abundances. The correction can also be made in a simpler manner by subtracting the m/z 129 count in a reagent blank without any ^{129}I added. It is not generally necessary to use ultra-high purity grade Ar as plasma gas to reduce the ^{129}Xe background.[73]

The limit of detection (LOD) for UI ranges from 2.5 μg L^{-1} [73] (or better for present generation instruments) for a quadrupole mass analyzer to 10 ng L^{-1} for a magnetic sector instrument.[76] Either LOD is sufficient for measuring UI even in populations with severe iodine deficiency (<20 μg L^{-1}). Care must be taken when using ICP-MS to ensure that adequate rinse out occurs between samples. Iodide is easily oxidized to iodine in acidic solutions and can also react with iodate to form iodine. In acidic media, long rinse outs are required.[73] Thus, any sample preparation procedure that involves oxidation of iodide to iodate must be carefully monitored to prevent carryover contamination. Alkaline solutions, preferably ammonia or some other suitable amine that will not deposit additional solids on the cones, often provide the best results.

Of the National Health and Nutritional Examination Surveys (NHANES), the 2000 survey was the first to use ICP-MS to measure UI;[77] to assure continuity, the technique

was fully validated against the S-K method used until then.[49] Urine samples were diluted with a dilute aqueous solution of NMe_4OH and ^{130}Te (IP 9.01 eV) was used as an internal standard in this work.

An ICP-MS can be used as an element specific detector; although it cannot itself distinguish between different species of a particular element, it is invaluable as a detector when used in conjunction with liquid or ion chromatography[76, 78-81] or capillary electrophoresis[82] for speciation studies. Other types of mass spectrometry, e.g., electrospray ionization-MS may be preferred if different iodine species cannot be completely resolved by chromatography but ICP-MS generally provides better detection limits. Tandem MS should also be of particular value in speciation and provide much better sensitivity than single quadrupole MS but has not been used for iodine speciation to our knowledge. The most prevalent method used is anion exchange Ion Chromatography(IC).[76,78,79] In normal urine, essentially all the iodine is in the form of iodide[79] and chromatographic separation does not provide added value. However, speciation is of interest for subjects given iodine containing drugs/contrast agents. IC-ICP-MS has been used to study metabolites from subjects given 2,4,6-triiodophenol, an anti-inflammatory drug;[78] both 2- and 4-iodophenol metabolites as well as the unaltered drug were detectable in urine. Stark et al.[79] looked at various iodide species formed under different sample pretreatment/digestion conditions with a view to identify potential loss as elemental iodine. For milk powder, microwave digestion with an oxidizing acid was satisfactory. In contrast, for seaweed neither acidic nor basic digestion conditions provided good recovery. When samples of untreated urine were immediately analyzed, only iodide was observed in the chromatogram. When the same sample was stored overnight at room temperature and re-measured, the iodide signal decreased and an iodate signal appeared, presumably due to air oxidation. If the urine was acidified with

HNO_3, the oxidation rate to iodate clearly accelerated. By addition of H_2O_2, the iodide signal disappeared almost completely: the iodate signal increased and a number of additional peaks appeared, likely from the iodination of organic compounds present.

Leiterer et al.[80] report that when speciation analysis was done for cow's milk using IC-ICP-MS, most of the iodine was in the form of iodide with some iodate and traces of organoiodine compounds. Iodide to total iodine ratio exceeded 85% for 38 of 52 samples analyzed. Compared to direct analysis by ICP, the total iodine species eluted from the column amounted to 89%; suggesting that ~10% is protein bound and never elutes from the column. It is also possible that there were quantitation errors with individual peaks due to ionization suppression.

Sanchez et al. used size exclusion chromatography-ICP-MS for milk speciation.[81] A variety of milk samples (cow, goat, human) from several European countries, as well as milk powder and infant formulae, were studied. Whey obtained after centrifugation of the fresh milk or reconstituted milk powder contained 95% of the iodine present in the samples. With infant formulae, however, 50-85% of the iodine was *not* in the whey. Addition of sodium dodecyl Sulfate (SDS) improved the release of this iodine into the whey. The majority of the iodine in formulae was shown to be present in a large molecular weight (>1000 kDa) fraction.

Capillary electrophoresis coupled to ICP-MS has been used for the separation and quantification of T_3, T_4, iodide, and iodate.[82] The separation method used a buffer sandwich of phosphate (pH 2.3), SDS, and borate for stacking. The intended separation was complete in 15 min and then the separated bands were pressure driven into the ICP-MS. The serum from a healthy individual showed iodide (13 μg I L^{-1}), T_4-TG (61 μg I L^{-1}) and T_3-TG (7.5 μg I L^{-1}) peaks while that from a patient with the thyroid removed showed no T_3-TG peak. Addition of free T_4 or T_3 was shown to bind to TG immediately. This

technique is obviously capable of providing complete information on the iodine nutrition status of an individual.

Although reversed phase high performance liquid chromatography (RP-HPLC) is the most commonly used HPLC mode; it is not as commonly used with ICP-MS. Organic solvents used in RP-HPLC tend to modify the characteristics of the plasma, cooling it down[78,83] causing instability and can even extinguish it. Gradient elution typically involves a continuous change in the hydroorganic composition and results in a continuous change in the background. Diluting the column eluent with water before introduction to the ICP is possible[78] but deteriorates detection limits and cannot solve the gradient elution problem. A commercially available PTFE-membrane based desolvating nebulizer was explored for the determination of iodine and other halogen containing drugs.[83] Some analytes were partially lost in the desolvating unit, but the authors conclude that gradient elution (0-100% methanol) is possible. A different solvent removal device where anionic species are transmitted without loss has been described;[84] this should be readily applicable for iodinated species.

A direct injection high efficiency nebulizer was investigated for use with micro high performance liquid chromatography (μHPLC)-ICP-MS using 300 μm bore columns with an eluent flow rate of 4 μL min^{-1}.[85] The authors minimized the volume within the nebulizer by inserting a 20 μm bore capillary to carry the column effluent to the nebulizer tip to make it compatible with μ-HPLC. Although the modified nebulizer was slightly less sensitive, it not only provided superior chromatographic performance, but spray stability was better and it exhibited less sensitivity to solvent composition. In this case, maximum iodine response was observed not with pure water but with 60% acetonitrile in the eluent. The authors successfully separated and measured T_3 and T_4, reaching a 10 fmol

detection limit for T_4. The T_4 to T_3 ratio observed in their sample was further confirmed by nano HPLC-ESI-MS.

For solid samples, digestion is obligatory before the samples can be analyzed by ICP-MS. Commonly microwave assisted digestion,[79] combustion in an oxygen flask,[52,86] or wet ashing (nitric/perchloric acids) in a closed vessel[87] are used. Detection limits in such analyses tend to be blank limited[86,87] and result in LODs in the 30-50 ng I g^{-1} range. In a novel twist, Mesko et al.[88] ignited sample masses of up to 500 mg using NH_4NO_3 as a flux/oxidizer in a closed vessel containing 15 bar O_2, using microwave energy to initiate the combustion. Water, H_2O_2, $(NH_4)_2CO_3$ and NMe_4OH were explored as absorbers; the latter two provided better results. Applicability to diverse samples, including bovine liver, corn starch, milk powder, and wheat flour, was shown.

1.6 Inductively Coupled Plasma Optical Emission Spectrometry (ICP-OES).

ICP-OES [89] predates ICP-MS. It is also commonly referred to as ICP-atomic emission spectrometry (ICP-AES). Both ICP-OES and ICP-MS make use of the plasmas for atomization and excitation/ionization. In ICP-OES the light emission from the excited atom is measured at a specific wavelength characteristic of that element.

Relative to ICP-MS, fewer studies have been done on iodine measurement because the sensitivities are not as good. Further, the most useful emission lines for iodine are located in the vacuum UV range.[90] Iodine has 3 prominent emission lines in vacuum UV at 142.549, 178.276, and 183.038 nm. (The exact locations of the lines differ from one publication to another; a reference compendium[91] for example lists the most intense emission line being at 178.218 nm and the ~183 nm line being located at 182.980 nm.) The major problem with using the most intense emission line for the measurement for iodine is a neighboring emission line of phosphorus, which is located only 0.007[92] or

0.011[93] nm apart, depending on the source. With a good monochromator, some resolution is possible but if the phosphorus to iodine ratio is high, as will be true in most biological samples, large errors will be unavoidable unless the iodine content is high. Braselton et al.[93] separately measured the P emission at 214.914 nm to correct for its contribution to the 178 nm emission line. They measured Iohexol, an iodinated contrast agent in serum; the linear range was 15-600 mg/L, the precision decreased below an I concentration of 15 mg L^{-1}. Although less sensitive, the 183 nm line is free from P interference. In green algae Chlorella enriched with iodine, after sample solubilization with NMe_4OH, an LOD of 3 $\mu g\ g^{-1}$ was possible by measurement at 183 nm.[94]

Another alternative is to isolate the iodine from the matrix. Naozuka et al.[95] digested milk or egg powder samples in closed or open vessels in a microwave oven and then isolated the iodine by precipitation as AgI. Followed by dissolution in 20% NH_4OH, the iodine could be directly measured with the respective LODs being 280 and 40 $\mu g\ g^{-1}$ for closed and open vessel digestions.

Iodine can be also isolated as the elemental vapor. Nakahara and Wasa[96] pioneered this technique, using $HClO_4$ or H_2O_2 for oxidation. They did not use the 178 nm emission line but were still able to reach a 2 $\mu g\ L^{-1}$ LOD. Cave and Green[97] used a silicone rubber membrane for gas liquid separation and also obtained low $\mu g\ L^{-1}$ LODs for groundwater samples. Niedobová et al.[98] used ethanolic KOH and $Ca(NO_3)_2$ as an ashing aid for the digestion of milk or milk powder. Sample ash was then treated with HCl and Na_2SO_3 to acidify without iodine loss and eliminate CO_2. I_2 vapor was then generated by adding 1 M acidic H_2O_2. LODs were down to 20 $\mu g\ L^{-1}$. Vtorushina et al.[90] optimized the vapor generation technique with different oxidants, found *in-situ* generated HONO as the most suitable oxidant and were able to reach an LOD of 0.4 $\mu g\ L^{-1}$ for aqueous samples using the 178 nm line (whereas the 183 nm line gave an order of

magnitude poorer LOD); in comparison, with nebulization the LOD was 38 μg L^{-1} with the same 178 nm line. Dolan et al[99] preconcentrated 10 mL of sample on an anion exchange membrane disk, then eluted it with HNO_3 and added H_2O_2 prior to entry into a He-plasma, attaining an LOD of 0.75 μg L^{-1}.

Specific details of sample preparation (digestion) can often be the most critical step in any trace analysis task. Souza et al.[100] describe combustion in an O_2-pressurized (25 bar) commercial bomb for milk samples. Recovery of spiked iodide showed a great dependence on whether the bomb was allowed to cool for an extended period prior to pressure release. Even under the favored conditions of incorporating a cool down period, recovery of added iodide ranged from 75-105%, depending on the amount added.

<div align="center">1.7 Neutron Activation Analysis.</div>

Despite the fact that it is readily accessible to few, instrumental neutron activation analysis (INAA) is often considered the gold or benchmark standard. In his review[91] on iodine determination in foodstuff, Kucera, an expert on INAA, states that neutron activation analysis is the second most widely reported technique for the analysis of iodine in foods and biological materials. Even though he does not provide evidence for this conclusion, his review is excellent in summarizing the neutron activation techniques used for iodine analysis.

In INAA, the sample is irradiated with neutrons and the characteristic emission from a radioactive isotope formed is monitored. One great advantage is that sample preparation is not needed as long as self-shielding can be avoided. Iodine is a monoisotopic element (all isotopes other than ^{127}I are radioactive). Upon neutron absorption, ^{128}I is formed from ^{127}I. ^{128}I decays to ^{128}Xe by β-emission with energies of 2.1 and 1.7 MeV[101] and to ^{128}Te by electron capture with a half-life of 25 min.[102] Gamma

radiation is emitted by electron capture with values of 442.9 and 526.6 keV. The 442.9

keV γ-emission is most often used because the absolute intensity is ten times greater

than that at 526.6 keV. Thermal neutron (energy 0.025 eV) activation is most commonly

used in INAA but in the case of measuring iodine, interferences from sodium, potassium,

bromine, and chlorine can cause problems.[102] The background from these ubiquitous

elements can be vastly reduced by the use of epithermal neutrons (energy 1 eV to 10

keV) rather than thermal neutrons.[103-105] Reactors with high epithermal to thermal

neutron ratios are especially suited for Epithermal INAA (EINAA)[103,104] but any reactor

can be used and the thermal neutron flux filtered with a cadmium or boron filter.[106] The

thermal neutron count can be further reduced with the use of boron containing filters or

capsules. Normal EINAA detection is limited by the effect of Compton scattering. Using

an anti-coincidence counting system, Compton scattering errors can be compensated

for[103]. A NaI(Tl) detector can be set up to itself act as a shield to background radiation

but the arrangement is not simple. An LOD as low as 20 ng g^{-1} can be reached for the

determination of iodine in foodstuffs. A ~100 ng g^{-1} LOD was achieved[104] in sea lettuce

using flexible boron filters without anticoincidence counting. Hou et al.[106] reported LODs

of 10-95 ng g^{-1} for environmental and biological standard reference materials (SRMs)

using EINAA without Compton suppression One caveat in comparing LODs for different

NAA techniques is that the LOD is most often calculated based on the sample counts vs

background and counts from potentially interfering radiation.[107] Samples of similar

composition are thus likely to exhibit similar LOD's.

Hou et al.[108] described a procedure for measuring iodate and iodide in milk,

seawater or urine. The sample (10 mL) was passed through an anion exchange resin

column (housed in a disposable pipette) to capture both iodate and iodide. Using a low

strength eluent, iodate only was eluted, reduced to iodide by bisulfite and captured on

another column again. After thorough washing, a suitably cut portion of the column bearing the resin material was transferred to a polyethylene vials and subjected to thermal INAA. The LOD was 10 ng I.

Under conditions that iodine can be captured without simultaneous presence of the interfering elements, excellent LODs are possible without much ado. Parry[109] reports an LOD of 0.1 ng ^{127}I absorbed on 1 g activated charcoal. It is interesting that based on his experiments involving radiochemical separations, Bowen predicted the same LOD for ^{127}I by Radiochemical NAA (RNAA) in 1959.[110] In general, neutron activation followed by a fast separation of the ^{128}I formed from the potential interfering nuclides provides very good LODs and reliability; this has been practiced for a long time.[110,111] Precipitation as silver iodide is common in RNAA.

INAA has long had the moniker "gold standard." However, Heckman[112] performed a round robin study in 1979 to determine the iodine content in food. The general correlation amongst the different results were poor, including the results of the two INAA labs. INAA provided the great convenience of making the measurement without sample preparation. However, its premier status relies more on the judicious development of proper treatment of the sample following irradiation. This includes, for example, exercising care in RNAA[110,111] or appropriate compensation of interferences as done in EINAA, and cross validation of the proposed technique with an SRM.

1.8 Atomic Absorption Spectrometry (AAS)

Bermejo-Barrera et al.[113] reviewed in detail the use of atomic absorption spectrometry for iodine measurement until 1998. Direct determination of Iodine is difficult because no commercial lamp is available and the best iodine absorption bands lie in the vacuum UV region where inert gas purging of the optical path is needed However, good

limits of detection are achievable by indirect analysis, e.g., AgI can be precipitated, redissolved and measured as silver[114]. Iodide in solutions obtained from alkaline ashing of samples was precipitated with silver ion in a precipitation–dissolution flow manifold that allowed the retention of the AgI precipitate formed on a filter. The precipitate is washed with dilute (not concentrated) ammonia that washes off other silver salts and then dissolved in dilute thiosulfate followed by on-line determination of silver. The determination range was 11-350 μg I L^{-1} with a throughput rate of 17 samples an hour and a relative precision of 1.3-6.8%.

A similar indirect determination procedure relies on mercury determination by standard cold vapor AAS; a fixed amount of mercuric ion is added in a flow manifold to the sample where Hg(II) is in excess relative to iodide. Iodide causes precipitation of HgI$_2$; the residual Hg(II) is measured after SnCl$_2$ reduction.[115] The LOD was 2 μg I L^{-1}.

1.9 Electrochemical and Potentiometric Probes:

Ion selective electrodes (ISE) are commercially available for iodide and have been applied to the determination of iodide in milk from early on.[116,117] One study[116] compared direct measurement of iodine in milk and similar beverages by ISE and INAA (which compared well) with the S-K method (after ashing). The S-K method produced lower results which the authors attributed to losses during digestion. The response of the ISE was found to be nonlinear below 20 μM but was linear up to 1 mM. It takes 5-10 minutes to stabilize and a residue builds up after 10-15 hours of use.

A recent study[118] compared established iodide-selective electrode results for milk (obtained directly in the milk with some Ni(NO$_3$)$_2$ added as a matrix modifier) with those obtained by ion chromatography coupled to amperometric detection. The latter technique involved significant sample preparation, initial heating for homogenization of fat, curdling

by addition of acid and filtration, centrifugal ultrafiltration of the filtrate and final processing through a C-18 cartridge prior to chromatography. The ISE method showed 87-114% recovery compared to 91-100% recovery for IC. The results for the samples exhibited a coefficient of determination (r^2) of 0.84-0.85 but interestingly the ISE results were biased high. One would have thought that if major sample preparation steps (as involved in the IC measurement) can release some of the protein bound iodine as iodide, the ISE results would be lower than the IC results but this was not the case.

The iodide ISE has also been used for measuring iodine in plants and feeds.[119] Almeida et al.[120] have described a tubular custom made AgI/Ag_2S based ISE as a detector in IC for the analysis of urine and serum samples. A background level of iodide was required in the column effluent to optimize performance. The detection limit was 1.47 μg L^{-1} and the linear range was 5-400 μg L^{-1}.

Commercial iodide ISEs are similarly based on insoluble silver salt membranes and do respond to high levels of other anions that form insoluble silver salts, notably other halides and pseudohalides. In recent years much effort has been devoted to synthesizing iodide selective ionophores that should have greater selectivity than silver salt based ISEs; these efforts were covered in a 2005 review.[121] LODs as low as 10 nM were reported. However, such ISEs have not been significantly used yet.

Electrochemical detection in general and amperometric detection in particular are popular for iodide determination because of the fast response time, sensitivity, and selectivity for the analyte of interest. A silver working electrode is most commonly used. As iodide contacts an appropriately anodically poised Ag electrode, a current flows with the concomitant precipitation of silver iodide on the electrode surface.[74,122-124] An LOD of 40 nM and a linear range of 0.2 – 1.6 μM was found in an ion-pair reverse phase

HPLC[122] assay of urine samples – good correlation (r = 0.96) with autoanalyzer-based S-K assay incorporating digestion was observed.

Comparison of HPLC-amperometric detection with ICP-MS shows good agreement although ICP-MS provides better LOD, greater linear range and greater sample throughput rate.[74] A silver electrode can only be used a certain number of times before it must be replaced because of the AgI deposits. Disposable printed electrodes on polymer substrates have recently been commercially introduced.[125] A negative dip in the signal after analyte elution is observed when using silver electrode amperometry;[123] this makes quantification difficult.

To overcome this dip-tailing issue and the progressive loss in sensitivity from AgI deposition, pulsed amperometric detection (PAD)[124] and the use of other electrode types[123,126-129] have been studied. In PAD, a multistep waveform is used such that the signal is measured under anodic conditions and then the electrode is cleansed under cathodic conditions. Compared to conventional DC amperometric detection, PAD shows no dip tailing and an improved LOD of 20 ng L^{-1}.[124] The electrode, however, still must be replaced after ~2 days of continuous use. The method was used for the measurement of iodide in surface waters and absorbable organic iodide.

Cataldi et al.[123,126] compared the performance of silver, gold, and modified platinum electrodes. The gold electrode had no dip tailing but rapidly lost sensitivity. The modified platinum electrode consisted of platinum with an iodide coating continuously regenerated by injection of potassium iodide.[126] An LOD of 0.5 µg L^{-1} and a linear range up to 6 mg L^{-1} were attained.

Other electrodes have been used. Boron-doped diamond (BDD) in thin film form[127] exhibited a limit of detection of 10 nM and was linear up to 200 µM. Silver-containing carbon paste[128] electrodes were used in IC and allowed an LOD of 0.47 µg L^{-1}.

23

This electrode was usable for 14 days of continuous use before needing regeneration. Dip-tailing was, however, observed above concentrations of 25 µg L^{-1}. It was applied to the determination of iodide in skim milk, table salts, and distillate of seaweeds. A gold nanoelectrode ensemble[129] exhibited reduced background compared to its macro scale counterparts and reduced adsorption of iodine. It was applied to the direct determination of iodide in pharmaceutical ophthalmic solutions and table salt. An order of magnitude improvement in the LOD, down to 300 nM compared to macroscale gold electrodes, was observed.

Large amounts of hydroxide left after alkaline ashing is not conducive to IC analysis. Iodide also elutes late as a broad peak compared to iodate which elutes early as a sharp peak. An electrochemical oxidation-neutralization device was developed to facilitate suppressed conductometric IC analysis; after alkaline ashing, the samples are run through this device in which iodide is oxidized to iodate and hydroxide is oxidized to water and oxygen[130]. Iodate could be determined in the range 0.1-10 mg L^{-1} with a limit of detection of 20 µg L^{-1}

1.10 A Platform for Experimenting With Novel Detection Approaches: Flow Injection Analysis (FIA).

Flow injection and related approaches represent versatile experimental platforms. It is not surprising that much iodine measurement experimentation have been conducted on such platforms.

1.10.1 Elemental Iodine.

Reaction of iodine with starch to form a blue color is well known. Amylose and amylopectin[131] are good forms of soluble starch to use in this reaction. The complex with

24

amylase has a λ_{max} at 560 nm and that with amylopectin at 630 nm. Elemental iodine

can be measured respectively with throughput rates of 140 and 220 samples h^{-1}. The

reaction with amylose was more sensitive, an LOD as low as 40 μg L^{-1} could be reached.

The reaction is catalyzed by the presence of iodide. The described system used relatively

high sample volumes and flow rates compared to current practice; elemental iodine in

sea water and salt was determined.

The same authors had earlier looked at the use of polyvinyl alcohol as a reagent

for elemental iodine[132]. The color of the product varies depending on how completely

polyvinyl acetate has been hydrolyzed to the alcohol. With the fully hydrolyzed polymer,

a blue product is formed. As in the case of amylase/amylopectin, I_3^- rather than I_2, is

likely involved. The response is nonlinear as a function of concentration; an LOD of 60

μg L^{-1} and a throughput rate of 140 samples h^{-1} were reported.

1.10.2 Sandell-Kolthoff Assay With On-line Digestion.

A FIA method incorporating on-line digestion and the S-K reaction terminated

with brucine and followed by absorbance detection was reportedly capable of a

throughput of 70 samples h^{-1} at a cost of \$0.01/sample and a capital investment of

\$2000.[50] There was minimal interference from thiocyanate and mercury. Although the

authors reported good comparability with results obtained with samples that underwent

alkaline ashing prior to injection, validation with another independent established method

was not reported. The LOD was 39 nM with a determination range up to 7.88 μM.

1.10.3 Another Catalytic Assay in a Sequential Injection Format.

Tetrabase (4,4'-methylenebis(N,N-dimethylaniline) is oxidized by Chloramine-T

to form a blue product that can be monitored at 600 nm. The uncatalyzed reaction rate is

very slow and iodide exerts a remarkable catalytic effect on this reaction. Using a

sequential injection setup, adjacent zones of sample, tetrabase and Chloramine-T are

stacked and then propelled through a reaction coil into a detector. An LOD of 50 ng L^{-1}, a

linear range of 0.1-6.0 μg L^{-1} and a throughput rate of 80 samples h^{-1} were reported. A

100-fold presence of Fe(II) interfered but operation at 30 °C reduced this interference

such that intended samples (pharmaceutical preparations/supplements/multivitamin

tablets) could be successfully analyzed[133].

1.10.4 Chemiluminescence (CL) - Based Assays.

Tris(bipyridyl)Ru^{3+} exhibits orange CL when reduced by a number of reducing

agents, the divalent Tris(bipyridyl)Ru^{2+} ion is initially formed in an excited state. The

Tris(bipyridyl)Ru^{3+} is generated *in-situ* by passage through a PbO$_2$ packed column and

then merged with a stream containing the reduced form of nicotinamide adenine

dinucleotide (NADH). The light emission is greatly affected by the presence of iodide; on

this basis, an LOD of 1 nM with a linear range of 10-500 nM, and a throughput rate of 60

samples h^{-1} were attained.[134] Applications to simple pharmaceuticals and salt were

demonstrated. Reducing/chelating agents, e.g., ascorbic acid, oxalic acid, and sulfite

interfere.

The same group had earlier looked at the iodide catalysis of the CL reaction

between formaldehyde and acidic KMnO$_4$.[135] The LOD was 1 μM. Nitrite and Fe(II)

seriously interfere and must be removed prior to analysis. Only iodized salt samples

were measured with a throughput of 120 samples h^{-1}.

Luminol is by far the most common reagent used in CL reactions and iodine can

be used as an oxidant to elicit luminol CL. CL-based assays based on such reactions are

described in the following section.

1.10.5 Vapor Transfer. Head Space, Pervaporation and Gas Diffusion.

All these techniques result in isolation of the analyte from the sample matrix that in turn provide for elimination/reduction of interferences. Burguera et al.[136] described a headspace sampling procedure where iodine is liberated from an acidic solution by dichromate and the headspace vapor at an elevated temperature is transferred to a trapping vial containing KI. The trapped iodine reacts with simultaneously introduced luminol and Co(II) as catalyst while the CL signal is monitored. Luminol reacts with molecular I_2 but not I_3^-, as such I^- concentration in the trapping solution must be kept minimal. The LOD was 10 µg L^{-1} with good spike recoveries (101-103%). Presence of extraneous salt in the sample increases the signal because iodine is more easily transferred to the head space due to salting out effects. Salts present normally in urine thus help increase the signal. Standards were prepared to contain a similar amount of salt. Urine samples were measured and the results were in good agreement with those from the S-K method.

Iodine can be liberated by oxidants and then made to diffuse across a porous PTFE "gas-diffusion" membrane. A KI solution is used to capture the iodine; this is then measured by luminol CL.[137] This configuration suffers, however from memory effects because of strong sorption of I_2 on PTFE. While the authors did find some ways to ameliorate the problem, overall a more satisfactory solution was not found until two years later when they were able to adapt the method to a pervaporation system where there was no direct contact between the sample steam and the PTFE membrane.[138] Emergency KI pills (large doses of KI designed to flush any ^{131}I from the body in the event of a major nuclear fallout) were analyzed directly. In multivitamins, ascorbic acid had to be first removed; this was accomplished with an anion-exchange resin column.

Iodide was used in the carrier stream to reduce negative effects due to I_2 adsorption. The calibration curve was nonlinear presumably due to I_2 adsorption. Recoveries ranged from 81.3 to 117%; the LOD was 0.5 mg/L with a short linear range of 1-10 mg/L.

1.10.6. Electrochemical Detection.

The BDD thin film electrode mentioned previously has been used in a FIA configuration with a linear range of 0.8 to 200 μM.[127] Nikolic et al.[139] have provided a new iodide catalyzed reaction between Mn (III) (produced by mixing Mn(II) and MnO_4^-) and As(III), the response was followed amperometrically at a Pt electrode. An LOD of 5 nM and a linear range of 0.5-100 μM were attained. They successfully analyzed samples of waters, salt, fodder, organic substances, blood sera; results compared favorably with standard procedures.

1.11 Gas and Liquid Chromatographic Methods.

After appropriate derivatization, iodine-bearing derivatives can be separated by gas chromatography (GC) and detected using electron capture detection (ECD).[140-142]

Following alkaline ashing of foods, iodide was oxidized to iodine by acidic dichromate. 3-pentanone is added to the same mixture whence it forms 2-iodo-3-pentanone.[140] This was then extracted into hexane and subjected to GC-ECD analysis. The LOD was 50 ng g^{-1}.

The use of iodine containing disinfectants is common. Blood iodine levels of burn patients treated with iodine containing disinfectants were determined by taking a blood sample, dilution with water, heating to boiling, allowing to cool before the addition of $ZnSO_4$ and $Ba(OH)_2$, and centrifugation. The supernatant was acidified, methyl isobutyl ketone (MIBK) and nitrite are added. The liberated iodine was reacted with MIBK

to form both the 1-iodo and the 3-iodo derivative which was then extracted with hexane before GC-ECD analysis.[141]

For the determination of iodide in milk, the sample was acidified strongly with sulfuric acid, allowed to stand and filtered. The filtrate was treated with iodate and acetone when iodine was liberated and formed iodoacetone. Determination of iodine already present as elemental iodine (the author referred to this as inorganic iodine) required no addition of iodate. A hexane extract was analyzed by GC-ECD.[142] More aggressive initial sample treatment was conducted to determine total iodine. Reported LODs were 0.03, 1, and 4 μg L^{-1} for inorganic iodine, iodide, and total iodine respectively.

Among liquid phase separation techniques several ion chromatographic and ion pair revered phase HPLC techniques have already been mentioned.[47,76,78-80,120,122,123,126,128,130] In another interesting and unusual technique based on size exclusion chromatography[143], iodide was converted to iodine, then sequestered with starch, and the resulting adduct was separated from the matrix using size exclusion chromatography with absorbance detection at 224 nm. The linear range was 1-100 μg L^{-1}(r^2 = 0.9992) with an LOD of 0.2 μg L^{-1}. The method was successfully applied to the determination of iodide in seawater and urine with recoveries of 92-103% with 1.5-3.7% rsd.

Pantuckova and Krivankova[144] explored several capillary electrophoretic approaches for the separation of iodide from other macro- and microcomponents in real sample matrices. The best results were obtained by adding α-cyclodextrin or polyethylenimine. Comparable resolution and sensitivity were observed in both cases. Cost considerations led to a focus on polyethylenimine. A simple procedure to determine iodide in untreated human urine, serum, cooking salt, and seawater was developed. Polyacrylamide coated capillaries, with negligible electroosmotic flow were used with the optimized background electrolyte composed of 20 mM KH_2PO_4 and 0.7% w/v

polyethylenimine and UV detection at 200 or 230 nm. For samples injected for 20 s at

0.5 psi, LODs attained were 0.14 μM for human urine, 0.17 μM for human serum, 0.17

μM for seawater, and 89 nM for salt. Relative standard deviations of iodide peak area

and height in the different matrices ranged from 0.93 to 4.19%.

1.12 UV Visible Spectrometry

Iodine is an oxidant. There are many chromogenic substrates that can be

oxidized to intensely colored products. The trick of course is to retain the iodine in a form

where the iodine-derived species is the only oxidant. The unique chemistry involving the

formation of iodate and its behavior as a pH-sensitive oxidant as well as the inherent 6-

fold redox equivalent amplification when an iodide ion is converted into an iodate ion (the

iodate can be used to generate iodine, extracted from the matrix, reduced back to iodide,

and subjected again to 6-fold amplification, see e. g.,[145]) makes this particularly possible.

The 6-fold amplication process proceeds as illustrated in the scheme below. All

iodide is oxidized to iodate, iodide may be added to generate iodine which can then be

oxidized to iodate by a suitable oxidant such as bromine water and further amplification

continued as necessary:

$$I^- + 3\ Br_2 + 3\ H_2O \rightarrow IO_3^- + 6\ H^+ + 6\ Br^-$$

or

$$I_2 + 5\ Br_2 + 6\ H_2O \rightarrow 2\ IO_3^- + 12\ H^+ + 10\ Br^-$$

$$IO_3^- + 5\ I^- + 6\ H^+ \rightarrow 3\ I_2 + 3\ H_2O$$
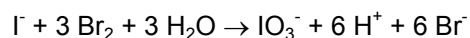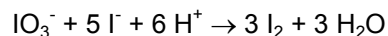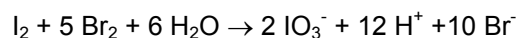
Both Ahmad[146] and two decades later, Kesari et al.[147] chose leuco crystal violet

(LCV) as the chromogenic substrate that forms intensely colored crystal violet (CV) upon

oxidation by iodine. Ahmad wet-ashed milk to form iodate and then liberated iodine and

distilled the iodine, collecting it as ammonium iodide. He oxidized the iodide to hypoiodous acid by N-chlorosuccinimide and used the HOI to oxidize LCV. Kesari et al.[147] oxidized iodide in pharmaceuticals, table salt, sea water, tap water, and soil samples to iodate by bromine water (0.04-36 mg I L^{-1}). Excess bromine was removed by adding formic acid. The iodate was then reacted with KI to form I_2 which then oxidizes LCV to CV, measured at 591 nm.

Starch has long seen practical use as both as a reversible indicator for iodine and as a direct measure of iodine concentration based on absorbance. Divrikli et al.[148] ashed urine samples, ensured conversion of iodine to iodate and liberated iodine before addition of starch and measurement at 590 nm. The LOD was 2.3 µg L^{-1} with a linear range up to 250 µg L^{-1}.

In their review of methods for determination of iodine in urine and salt (with a view to determining iodine nutrition of a population), Jooste and Styrdom[149] list starch indicator based iodine determination of salt by titration with thiosulfate ahead of all other methods. Over much of the world, where the iodine vector in salt is iodate, it is sufficient to acidify iodate-containing salt to generate molecular iodine for analysis. For countries where iodine is added in the form of iodide, as in the U.S. and Canada, the iodide is first converted to iodate by bromine water and excess bromine removed prior to iodine generation and titration.

Instead of titration, iodine can be liberated as above and starch added to form a color, the color intensity can then be read by a light emitting diode based colorimeter. Such an instrument provides data that compare well with titrimetric results[150].

Atomic absorption of iodine, as stated before, is not widely practiced because the most useful absorption lines are in the vacuum UV. However, certain molecular iodine species derived from inorganic salts and generated using graphite furnace atomic

absorption spectrometers absorb intensely in the visible. Huang et al.[151] studied the

absorption spectra of the diatomic species AlI, GaI, InI, TlI, MgI, CaI, SrI and BaI,

generated in a graphite furnace using a high-resolution spectrometer. BaI exhibited

intense absorption bands around 538 nm and 560 nm, each of them consisting of a

series of well-resolved rotational lines with half-widths of about 40–50 pm. The strongest

BaI line at 538.308 nm was used for the determination of iodine. Aside from high levels of

chloride, fluoride, iron, potassium and sodium, all of which significantly reduce the BaI

signal, there were no interferences. Different chemical forms of iodine produce identical

response with an LOD of 600 pg, and a linear range up to 250 ng I. Good agreement was

observed with standard methods for pills containing iodide and thyroxine. The rsd for 60

μg L^{-1} samples was 2%.

Burakov et al.[152] proposed an intracavity laser spectroscopy method where the

iodine vapor over the headspace of a heated sample was measured. The sample was

chemically treated to convert all forms of iodine into elemental I_2. A pulsed dye laser (5

μs pulse width) was used as the probe; the equivalent pathlength was 1 km. With urine

samples, a LOD of 15 μg L^{-1} could be achieved. The basic process is similar to

continuum source atomic absorption spectrometry but because of the increased

pathlength provided by the intracavity spectroscopy, it is several orders of magnitude

more sensitive. This method requires the use of a high resolution monochromator based

spectrometer. No components in urine were found to have an interfering effect on the

measurement of iodine.

1.12.1 Other Colorimetric Catalytic Reaction Methods.

Besides the S-K reaction, several other methods utilize the catalytic effect of

iodide. Arsenic (III) has been replaced with Sb(III) for the reduction of Cerium(IV).[153]

32

This was applied to the detection of IgG using iodine labeled antibodies and compared to the S-K method as well as enzyme linked immunoassay methods. All three methods agreed well. While the immunoassay provided the lowest LOD, both the S-K and the analogous Sb(III) based method provided greater useful assay range.

Iodide also catalyzes the oxidation of chlorpromazine by H_2O_2.[154] In this case the system reaches a maximum absorbance that directly depends on the concentration of iodide present then decays slowly. Urine or foods were digested with perchloric and sulfuric acids. The digest was mixed with chlorpromazine and hydrogen peroxide and the maximum absorbance (reached within 20-30 s) was measured at 525 nm. Negative and positive interferences were reported for Hg(II) and Fe(III), respectively. Iron can be corrected for by (a) measuring total respo0nse and (b) making a subsequent measurement after removing the iodide with Hg(II) and (c) subtracting b from a. The LOD was 1.6 ng I.

1.12.2 Visual Colorimetric Comparison.

A rapid iodine test kit for the determination of UI that relies on the iodide catalyzed oxidation of 3,3',5,5'-tetramethylbenzidine by peracetic acid and H_2O_2 has been developed and is available from Merck.[155] Urine samples were run through charcoal columns to remove interfering substances. After adding the reagents to the sample in a test cup (part of the kit), the color is compared after 30-60 s to a provided color chart that has 3 ranges: <100, 100-300, and >300 μg L^{-1}. An HPLC based method was used for comparison. It was found that the median iodine level can be estimated with sufficient accuracy. A single technician can process up to 60 samples h^{-1} at a cost of $.50-$1.00/ sample. Possibly because of urea to ammonia conversion in urine as it ages, and likely

interference from ammonia, the test can only be used with fresh urine samples. It was also found that only iodide responds in this reaction.

1.13 X-ray Fluorescence

X-ray fluorescence and X-ray absorption has been explored for iodine determination but the LOD is not adequate for trace determinations.[92,156] Using total reflection x-ray fluorescence (TXRF) a detection limit of 0.18 mg L^{-1} was achieved (data collection time 1000 s, samples digested in 25% NH_4OH). The chemistry of iodine in soils was monitored using K-edge x-ray absorption near-edge structure (XANES). Naturally occurring levels of iodine could not be seen by the method, significant levels of iodide or iodate had to be added to follow their fate.

1.14 Radiotracer Analysis by Scintillation Counting.

^{131}I is widely used in clinical medicine and for laboratories measuring ^{131}I routinely, this method of I determination in urine and water may be convenient.[157] ^{131}I, including any carrier iodide is added to the sample and a substoichiometric amount of silver ion is added as $AgNO_3$. AgI is precipitated. The ^{131}I to ^{127}I ratio in the AgI is identical to that in the original sample. Precipitated AgI is separated from the rest of the solution which bears excess ^{131}I; the authors used paper electrophoresis but other methods should be feasible. The isolated AgI is removed and the ^{131}I therein is counted with a scintillation counter using standard procedures. The response curve obtained has a negative slope because as the sample contains more nonradioactive iodide, less ^{131}I is precipitated as AgI. The LOD was 1 μg L^{-1} and the linear range extended from 7-7500 μg L^{-1}.

1.15 Quartz Crystal Oscillator.

A method based on a quartz crystal microbalance (QCMM) has been proposed for the determination of iodine in foods.[158] Following oxygen flask combustion, the iodine is trapped in an alkaline absorbing solution. After free molecular iodine is liberated, the I_2 adsorbs on the gold electrode of the QCMM. The decrease in resonant frequency of the crystal is directly dependent on the mass of I_2 adsorbed. The LOD is 0.5 μg L^{-1} and only interference seen is from bromine. The response is linear from 10-500 μg L^{-1}.

1.16 Conclusion:

Many of the methods here meet the criteria to be effective for the determination of iodine in urine including low cost, rapid analysis, accurate, free of interference and capable of being able to measure even severe iodine deficiency(UI <20 μg L^{-1}). Few, however, can be carried out without involved sample pretreatment. Low cost methods that can reliably measure UI without little or no pretreatment would be a boon. Extensive application would likely require the endorsement of the WHO or similar other bodies before such methods are adopted.

In virtually all other sample matrices, extensive sample pretreatment, if not complete digestion, is needed for virtually all methods other than INAA; XRF can also do this in principle but typically is not sufficiently sensitive. Sample preparation thus constitutes the bottleneck and few laboratories are actually equipped for perchloric acid digestion. Simple procedures to reliably measure iodine in milk will be a major advance. The cost effectiveness and simplicity of such techniques will be critical in determining how well they are used in determining regional nutrition especially in developing countries where the average diet may vary even within relatively short distances. Thus there

remain opportunities to greatly contribute to this arena, especially towards facile sample preparation.

1.17 Acknowledgment

Chapter 2

Fenton Digestion of Milk For Iodinalysis

2.1 Introduction

Iodine is an essential micronutrient. The evaluation of iodine nutrition is of great importance, especially in infants; neurodevelopment is governed by iodine-containing thyroid hormones.[159] In a newborn, the thyroid holds only a 24 hour reserve of the necessary iodine;[160,161] fresh supplies must be replenished by the feed. Recently, concerns have arisen about U.S. infant iodine nutrition.[162,163]

We have been particularly interested in infant iodine nutrition.[164,165,166] In adults, measurement of urinary iodine (UI), preferably 24 -hour iodine excretion, is the benchmark measure of iodine status;[167] creatinine adjustments of spot samples are not always reliable.[168] Our own experience indicates that collecting urine in infants is a significantly more difficult task. Aside from obvious displeasure of the subjects, the success rate tends to be low and gender-biased. Many baby care products, from diaper rash ointments to baby wipes, also contain significant concentrations of an iodinated antifungal compound, 3-iodo-2-propynyl butyl carbamate (IPBC, see ref. 169 for a partial listing of baby care products containing IPBC). Elemental iodine analysis, as in inductively coupled plasma mass spectrometry (ICP-MS), often practiced for iodine determinations,[170] can be affected by contamination of the urine with IPBC present on the skin, complicated by the fact that IPBC readily penetrates through the skin.[171] The determination of iodine in breastmilk or formula given to an infant provides an alternative, allowing facile uncontaminated sample collection.

Most laboratories use one of two methods for Iodinalysis of biological samples.[172] The Sandell-Kolthoff (S-K) method[173] relies on the catalytic effect of the iodide ion on the

decolorization of yellow Ce^{4+} by As^{3+}. There can be interferences; digestion to mineralize these is essential prior to analysis.[173,174] The other method is ICP-MS, typically conducted in the isotope dilution mode with [129]I as the isotopic tracer.[170] For urine samples, simple dilution and tracer addition is sufficient for ICP-MS. For milk samples, digestion or sample preprocessing is needed.

2.1.1 Sample Digestion Methods and Alternatives.

An alkaline digestion procedure[175] to measure protein bound iodine has been much used. The protein is precipitated as the Zinc conjugate,[176] excess alkali added and slow overnight evaporation to dryness conducted at 85-95 °C. The sample is then ashed (2.5 h@600 °C) and extracted with dilute HCl. Pre-ashing thermal losses are minimized by vessel design and using KOH as the base.[177] But glass vessels are etched during ashing and cannot be reused due to iodine loss on the surface.[177] More recently, the use of tetramethylammonium hydroxide has been advocated for alkaline ashing; such methods are still to be widely adopted.[178] Acid digestion procedures have a different problem: losses as HI or I_2 must be avoided. Fortunately, oxidation to HIO_3 occurs readily with oxidizing acids. In traditional perchloric acid digestion (H_2SO_4, HNO_3, $HClO_4$[179] or HNO_3 and $HClO_4$[180]), radiotracer studies show that iodine loss is <20%.[180] Traditional $HClO_4$ digestion[179] was later updated[181] by a procedure that involves overnight HNO_3 digestion followed by conc. H_2SO_4 - 70% $HClO_4$ digestion and is the method used by the US Food and Drug Administration.[182] Perchloric acid digestion does require special hoods and special precautions; it cannot be safely performed in standard fume hoods.

Earlier, chloric acid ($HClO_3$, prepared by stoichiometric addition of $HClO_4$ to $KClO_3$ and precipitating $KClO_4$) has been used to oxidize iodine to iodate.[183] This

procedure was adopted for a variety of biosamples.[184] Some other chloric acid

procedures additionally use perchloric and chromic acids;[185,186] appropriate precautions

must be taken. Pino et al.[187] developed a procedure in which ammonium persulfate (AP)

is used to digest urine. The simple procedure takes only 30 min and was validated

against automated acid digestion in a Technicon autoanalyzer[188,189] and reversed phase

ion-pair liquid chromatography.[188] Results obtained by the S-K method after AP digestion

have also been compared with parallel ICP-MS analysis.[190] For UI, on-line digestion with

acidic permanganate or dichromate is also viable.[191] But AP digestion has never been

validated for milk samples. Potential problems with AP digestion of milk and subsequent

S-K analysis are discussed later. AP digestion is not particularly compatible with ICP-MS

due to the high salinity of the digest.

Oxygen flask combustion methods have been described[192,193] but are impractical

with a large number of samples. In pyrohydrolysis, a complex apparatus is used to heat

the sample to 1200-1300 °C while water vapor/steam and O_2/air are passed over it; large

numbers of samples cannot be digested in this fashion.

Thus sample preparation for analysis represents a singular bottleneck that

makes iodinalysis of milk (and similar samples) particularly tedious. In some methods, if

digestion is conducted with multiple samples in a closed system, some iodine escapes

into the gas phase from high concentration samples and is reabsorbed by other

samples.[194] Very little is presently known regarding the forms of iodine present in milk.

Based on the general belief that iodine is almost exclusively present as ionic iodide we

had earlier developed and used a procedure where milk samples are spiked with a

(isotopically labeled) tracer and centrifuged to remove lipids. The resulting liquid was

placed in a disposable centrifugal ultrafilter (molecular weight cutoff of 10 kDa), and

centrifuged. Some 25-50% of the original sample, depending on the fat content, filters

through as a clear liquid, which we have analyzed.[195] A study by size exclusion

chromatography reports that while the whey obtained after centrifugation of the fresh milk

or reconstituted milk powder contained 95% of the total iodine. However, with infant

formulae, as much as 85% of the iodine was *not* in the whey and was mostly in a large

molecular weight (>1000 kDa) fraction. The presence of any significant amount of iodine

that will be retained by a 10 kDa filter will clearly lead to an underestimation of iodine.

In specific cases, iodine can be liberated from organoiodine compounds and the

resulting iodide determined by the S-K method.[196,197] Bromine[198] or chlorine[199] addition

procedures may be broadly applicable to specific organoiodine compounds. Without

specific knowledge of forms of iodine and without purification, such methods are of little

value. Simplified procedures often fail: Substituting on-line dialysis for digestion to

measure UI[200] causes thiocyanate to be transported and produce high UI values.[174] A

priori assumptions often fail: Iodide selective electrodes (ISEs) have been long used in

milk,[201,202] they may not measure protein bound iodine, but the assumption is an ISE

gives the lower limit of the iodine content. More recent studies[203] show that even after

extensive sample preparation (that will likely release iodide from protein bound forms)

used with ion chromatographic (IC) analysis, ISE results are always higher because

thiocyanate interferes in ISE measurements.

The Fenton reaction,[204] now nearly 120 years old, is still continually being

rediscovered and reviewed, especially as an advanced oxidation technique.[205] In this

paper, we explore the successful adaptation of Fenton digestion (FD) for iodinalysis of

milk samples.

2.2 Experimental Section

2.2.1 Samples.

Breast milk samples from 5 healthy subjects (~25 mL ea), collected under the guidelines of the Institutional Review Board at the University of Texas at Arlington and three formula samples (Similac Advance, Similac Soy Isomil and Enfamil Premium Infant, ~50 mL ea., prepared according to manufacturer's directions) and in addition the first two formula samples spiked to contain an additional 10 mg/L iodide (spike level blind to FDA researchers) were shipped to the Kansas City District Laboratories of the FDA. Two of the breastmilk samples were *foremilk* (first portion of the feed) and three were *hindmilk* (greater in fat content).[206] As previous experience had indicated that digestion/difficulties in analysis increases with fat content, for bovine milk we chose to analyze full fat content whole milk. FDA researchers locally bought the following branded whole milk in ½ gallon containers: Lactaid (lactose removed), Horizon (Organic), Anderson Erickson, Roberts and Great Value. UTA researchers retained portions of the same breastmilk and formula samples; FDA researchers shipped aliquots of the whole milk samples to UTA.

2.2.2 Sample Digestion and Analysis at FDA.

All 15 samples were analyzed for iodine according to Kan-Lab-Met.95.[182] Each sample was analyzed in duplicate, and spiked with an additional 500 μg/L iodide. The two formula samples already received fortified were not further spiked and were only analyzed in duplicate. The spiked sample results (Supporting Information gives detailed data and is found in Appendix B) are denoted by a suffix S. One exception to the FDA's standard reporting practice was reporting the results in w/v, rather than w/w units. To

accommodate this change, 1.00 mL of each milk sample was pipetted directly into a 100 mL Kjeldahl flask using a 2.5 mL electronic pipette (EDP3, www.rainin.com).

The frozen breastmilk and formula samples were allowed to thaw in a refrigerator; each sample was vortexed for 1 min after thawing to ensure homogeneity prior to pipetting. Store-bought whole milk samples were thoroughly shaken in their original containers prior to pipetting. Briefly, 10 mL Conc. HNO_3, 20 mL of 70% $HClO_4$ and 5.5 mL of conc. H_2SO_4 were added to each flask, covered and the samples were allowed to stand overnight before digestion was carried out the next day. Iodide was assayed by a continuous flow analyzer based S-K procedure. Aliquots of all perchloric acid sample digests in duplicate were shipped to UTA. All samples and digests were shipped either way on dry ice and received within 18 h.

At the FDA, digestion and analysis were deliberately conducted by different personnel. Researcher A prepared samples for digestion in two batches (breast milk/formula and whole milk). Researchers B and C respectively carried out the digestion of the two batches, each of which also included 3 blanks, 1 dilution solution, a set of standards and 1 portion of NIST1849 infant/adult nutritional formula standard reference material.[207] Researcher D carried out the S-K assay. The infant formula digests containing 10 mg/L spikes were found to be outside the calibration range and were reanalyzed after 10x dilution.

2.2.3 Sample Digestion and Analysis at UTA.

Fenton digestion of the same sample set was carried out as follows: To 0.5 mL of sample pipetted in to a 15 mL screw-cap centrifuge tube, 50 μL of 1 μg/mL [129]I tracer (as KI, carrier free, www.isotopeproducts.com) was added, resulting in a tracer concentration of ~100 μg [129]I/L milk. Next added was 1.5 mL of 30% H_2O_2, followed by

50 μL 0.1 M Fe(NH$_4$)$_2$(SO$_4$)$_2$ (both: www.vwrsp.com, stock solutions were refrigerated).

The centrifuge tubes were loosely capped. Several samples and standards were put in

batchwise in an oven overnight at 60 °C. After allowing to cool to room temperature, 950

μL water and 2 mL conc. NH$_4$OH were added to precipitate Fe(OH)$_3$. This results in a

total volume of 5 mL and a 10-fold dilution of the original sample. Because our

measurement relies on an isotope ratio measurement, attainment of a known volume is

not critical. The tube is then vortexed and centrifuged (3000 g @ 2 °C, 15 min). In early

experiments, the supernatant was filtered through a 0.45 μm pore size nylon syringe filter

prior to aspiration by the ICP-MS (*vide infra*); later studies indicated that if carefully

decanted, the supernatant can be used without further filtration.

Nominally known concentrations of triodothyronine (T3) and thyroxine (T4, both

USP grade, www.sial.com) were prepared and the exact iodine content assayed by ICP-

MS, using a known amount of [129]I added as a tracer. Store bought whole milk samples

were prepared with spikes of T3, T4, and KI of known concentrations and these samples

were also analyzed after FD by ID-ICP-MS). The isotopic tracer was also similarly added

to HClO$_4$ digests from the FDA prior to ICP-MS analysis. The ICP-MS and Ion

chromatography (IC) operating details are given in the SI found in Appendix B.

2.3 Results and Discussion

2.3.1 Utility of the Fenton Reaction for Sample Processing and Analysis.

Although the Fenton reaction has been known for over a century, it was not until

the 1960s that this process had been seriously considered for degradation of organics

and other waste.[208] While the hydroxyl radical is undoubtedly produced during the

Fenton reaction, it is likely that the active species involved in the oxidation of organics is

43

a peroxo-Fe(II) complex that in turn produces a transient Fe(IV) oxidant.[209] *Web of Science* produces over 4000 citations on *Fenton reaction* but analytical chemistry papers are few. Others have previously examined the analytical merit of exploiting the differences in degradation rates of different compounds in the Fenton process.[210] Among the few interesting analytical uses of the Fenton reaction are chemiluminescence (CL) reactions; CL is generated when (a) certain Schiff bases from amino acids and amines are subjected to FD,[211] and (b) when tetracyclines are Fenton-digested in the presence of Eu(III) to which energy transfer occurs.[212] Determination of trace H_2O_2 has long been important[213] and H_2O_2 determination via FD, by (a) production of phenol from benzene and its fluorometric measurement,[214] and (b) the aggregation of single-stranded DNA-conjugated gold nanoparticles,[215] have been studied. However, FD has made a far greater impact in waste treatment, from bakeries[216] to olive oil presses[217] to more efficient production of biogas from biosolids.[218] Even magnetic fields ere explored to improve FD in processing dairy waste.[219] We posit that FD can potentially make a major impact in sample digestion procedures for analysis.

In 1989, one of us described Fenton mineralization of mercury in urine prior to elemental Hg generation for measurement. While $Fe(OH)_3$ does precipitate, it is readily redissolved in acid and cleanup of a batch reactor system is easily automated.[220] Since that time we know of only one effort, FD of waste water prior to the determination of lead.[221] Interestingly, this was not done so much to release lead from bound forms, it was intended to remove organics that foul the electrode. Trace phosphorus in wastewater is usually measured after digestion to phosphate.[222] Fenton oxidation of a few phosphites and hypophosphites to phosphate has been shown[223] but demonstrated applicability to a broader suite of phosphorus compounds is needed. Fenton digestion

using ferrous iron or even elemental iron[224] has much potential in general sample digestion for inorganic analysis.

2.3.2 Sandell-Kolthoff Assay: Ammonium Persulfate Digestion Is Effective for Urine But Not for Milk.

Pearce et al[225] measured iodine and perchlorate concentrations in breast milk and urine in Boston area women. The milk was digested by the AP method prior to S-K analysis (Pino, S. Personal communication, August, 2008). We had also made similar studies on a different population, the sample processing and analytical methods were totally different; the results were compared.[166] At 110 μg/L the median urinary iodine concentration was not only identical between the two studies, it was identical to the median UI for a comparable population group reported in the 2001-2002 NHANES study.[226] But the median breast milk iodine found by Pearce et al[225] was 140 μg/L, compared to 35, 56 and 43 μg/L found in our studies.[164-166] Since neither method was validated and each looked at different population groups, validity of neither method could be determined. The AP digestion is simple. Therefore we first studied the use of AP digestion and S-K assay. Details are given in the text and Figure B - 1 - Figure B - 18 and Table B - 1 in the SI. Although clear digests are produced by AP digestion conveniently and rapidly (30 min @ 95 °C), S-K assays do *not* proceed in a straightforward fashion with these digests. Urine AP digests, like calibration standards, exhibit single exponential decay of the Ce(IV) absorbance. But milk digests show a double exponential decay. One possible explanation is that some oxidizable moiety remains and contributes to the initial accelerated rate. After these substances are fully oxidized, the terminal kinetics reflect single exponential decay. Assuming this latter rate better reflects the iodide catalyzed reaction, we examined several breastmilk samples

both as such and with spikes added. Interpretation of the data with standard curves

produced substantially higher results than the best known values while spike recovery

was as low as 50%.

2.3.3 Recoveries of Iodide, Triiodothyronine and Thyroxine Added to Milk.

All of the following were conducted using [129]I as a tracer, with 10 μg/L [129]I in the

final measurement solution. T3 and T4 added to milk bind to specific proteins.[227] Using

an independently prepared calibration curve, we analyzed individual solutions of iodide,

T3, and T4 that nominally contained 100 μg/L iodine (Figure 2-1); the T4 obviously had

lower MW iodine-bearing impurities and its iodine content measured discernibly higher
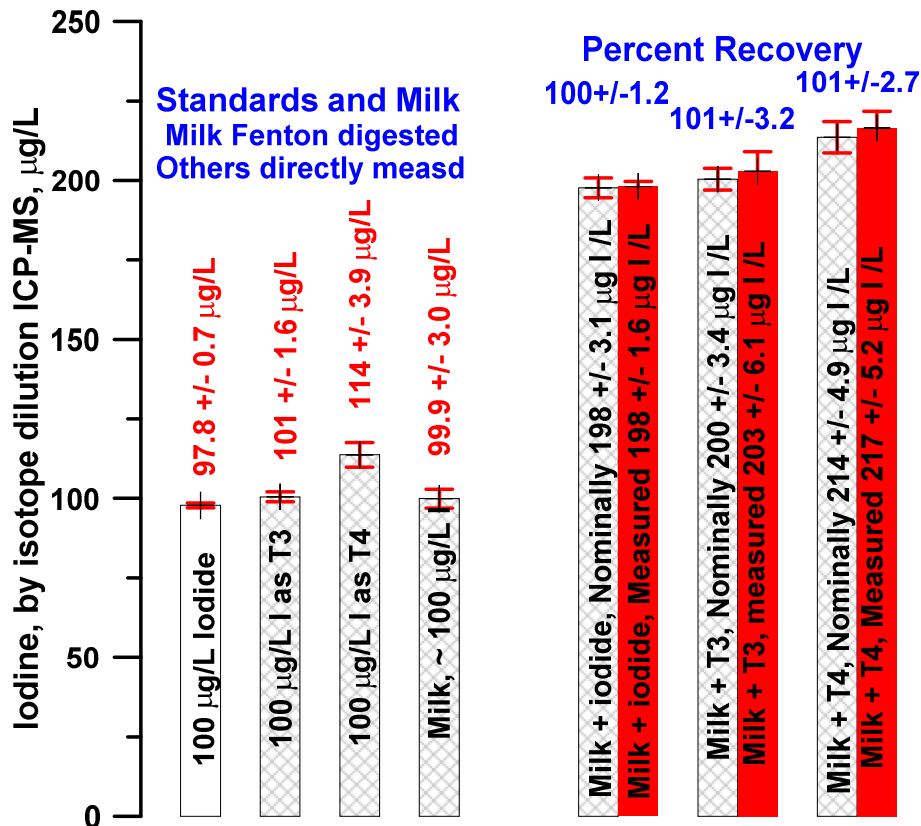
Figure 2-1. Good recoveries are obtained for I⁻, T3 and T4 from

breastmilk following Fenton digestion.

than the nominal value. As we had a significant number of breast milk samples analyzed

by various methods, we deliberately picked one that had previously been measured to be

~100 μg/L by a number of methods. Fenton Digestion and ID-ICP-MS analysis for this

sample yielded a value of 99.9 $\pm$ 3.0 μg/L. The same milk sample was spiked in triplicate

with nominally 100 μg I/L levels of iodide, T3 and T4, individually and measured after FD.

The results are shown in Figure 2-1. The recoveries were excellent (100-101%).

2.3.4 Fenton Digest by ICP-MS vs. Perchloric Acid Digest by ICP-MS vs. Perchloric Acid

Digest by S-K Method.

Because available breast milk sample volumes were limited, 5-fold dilution was

used before replicate Fenton digestion. Figure 2-2 shows the results of these

comparisons, respectively as panels (a) and (b), using the ICP-MS results of the $HClO_4$

digests as the independent variable. In both cases the intercepts were statistically

indistinguishable from zero. Further, since all the methods were already blank corrected,

the regression was forced through zero. Duplicate measurements for $HClO_4$ digests and

triplicate measurements for Fenton digests were made. Detailed data are presented in

Table B - 2 to Table B - 5 in SI. For the ICP-MS analysis of the perchloric acid digest and

the Fenton digest, regardless of the sample type, the results are almost statistically

indistinguishable (y = 1.029 $\pm$ 0.024 x). The Sandell-Kolthoff data tend to be slightly

higher than the corresponding ICP-MS data (y = 1.057 $\pm$ 0.016) x), but the difference is

small.

2.3.5 What Form is Iodine Following Fenton Digestion?

Iodate[228] and Iodide tend to be the two most stable forms in which iodine is

present. Iodate is poorly retained on any anion exchanger and elutes with other poorly

retained material. In the Fenton digest of milk, some organic acids that elute early will

always be present. This makes unequivocal identification of iodate in a Fenton digest by

conductometric ion chromatography (IC) difficult. We therefore used IC-ICP-MS for post-

FD iodine speciation. Three samples were subjected to FD and then made up to 5 mL

with 2% NH_4OH and centrifuged to remove $Fe(OH)_3$. A small amount of MnO_2 was added

to catalytically remove excess H_2O_2 as large amounts of H_2O_2 are detrimental to IC

columns. (We verified that the addition of MnO_2 will not affect any iodate formed (Figure

B - 19)). Samples were then filtered through a 0.2 µm syringe filter and analyzed by IC-

ICP-MS.
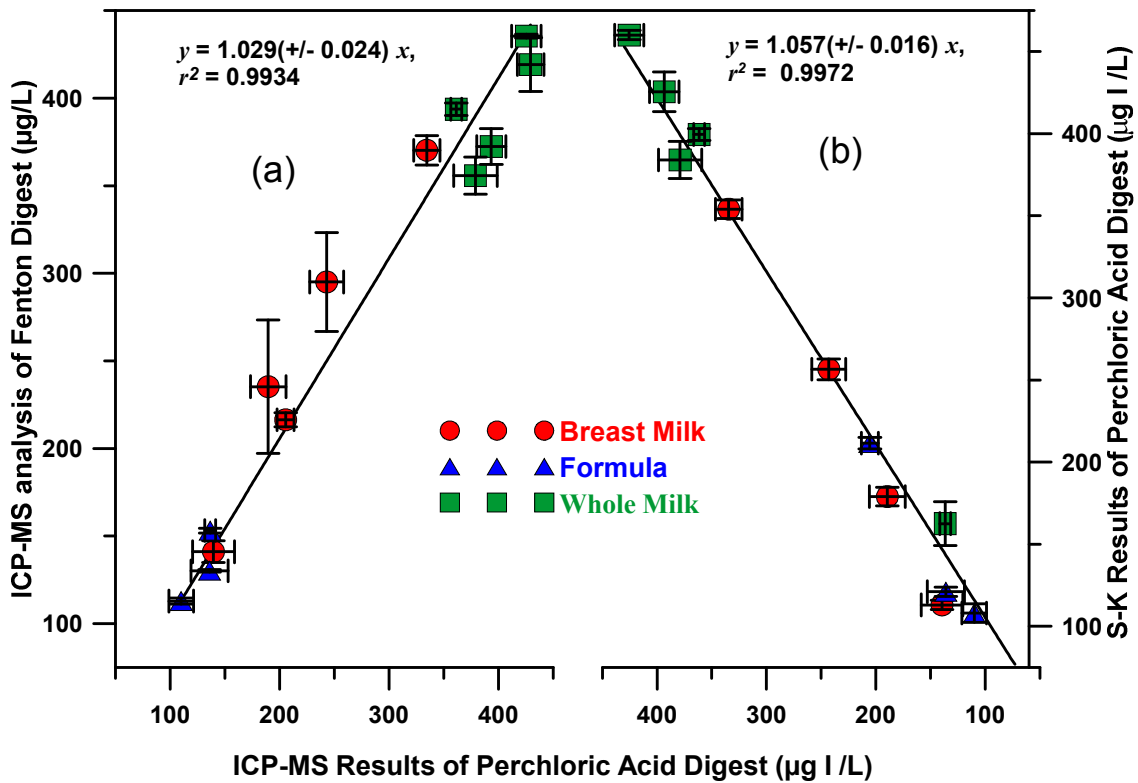
Figure 2-2. Comparison of replicate measurements of various milk and formula samples (a)

Perchloric acid digests analyzed by 129I isotope dilution ICP-MS vs. same analysis of the

corresponding Fenton digests; (b) Perchloric acid digests analyzed by 129I isotope dilution ICP-MS

vs. same analysis vs. Sandell-Kolthoff Analysis of the same digests. See text for details.

48

There was no iodate to be found in Fenton digest of the milk samples, the Iodine was present as Iodide (Figure B - 20).

2.3.6 Extent of Iodine Loss During Fenton Digestion.

Iodine is volatile and iodine loss during sample digestion is common. Discernible iodine loss may also occur in $HClO_4$ digestion.[180] Adding an isotopic tracer to the sample not only accounts for changes in ionization efficiency etc. from one sample to another, pre-digestion addition of the tracer to the sample can account for any loss of the analyte during sample processing. We explored the loss by adding [129]I before and after FD of different aliquots of the same sample. The difference between the isotope-ratioed pre-FD-spiked and post-FD-spiked data indicated the extent of the loss. For several representative milk sample types there was indication of loss: post-FD tracer addition analytical values are consistently lower (from 12±12 % for soy-based formula to 22.8±4.2 % for whole milk) relative to pre-FD tracer addition analytical values (Table B - 6). While ID-MS can account for processing losses, this is not possible with S-K or other assays. For general use, the losses must be minimized. The causes were investigated.

2.3.7 Effect of Sample to Fenton Reagent Volume Ratio on Iodine Loss.

Our base procedure used 0.5 mL sample, 1.5 mL 30% H_2O_2 and 50 µL 0.1 M Fe(II). We examined if the sample to digestion reagent ratio affects loss during FD by reducing the sample amount in steps to 25 µL, affecting a 20-fold change from the original sample to digestion reagent ratio. The sample was pre-spiked with [129]I. The tracer data indicated that increasing the oxidant reagent to sample ratio monotonically decreased the tracer recovery (Figure B - 21). If the loss occurs as I_2, an excess of oxidant and the concomitant evolved gas that helps carry volatiles will indeed increase

losses. (It is interesting to note that if the ^{127}I results are corrected for by isotope dilution, the analytical data remain unchanged for 100-500 μL sample volumes. At even lower sample concentrations, the low tracer counts cause standard deviation to increase and results to become unreliable (Figure B - 22)). Decreasing the sample to digestion reagent ratio is therefore not a solution to prevent iodine loss; increasing it further relative to the base conditions may in fact be better.

2.3.8 Possible Loss by Adsorption on Fe(OH)$_3$.

To determine if loss occurs by adsorption on Fe(OH)$_3$, identical sample aliquots, pre-FD and post-FD ^{129}I spiked, were used. Three subsets within each set were diluted with an equal volume of 2% NH$_4$OH, or DI water, or 2% HCl prior to ICP-MS measurement. Addition of HCl keeps the Fe in solution. For the pre - digestion ^{129}I spikes, all results were statistically identical. Comparing the pre- vs. post-digestion spikes, NH$_3$ addition showed the least loss but also exhibited the greatest variability. Addition of water or HCl both led to about the same loss and it was greater than with ammonia. Obviously, the loss is not due to adsorption on Fe(OH)$_3$ (Table B - 7).

2.3.9 The Role of the pH During Digestion.

It Is interesting that despite the strongly oxidizing conditions, the final solution contains iodide and not iodate. The oxidation of iodide by H$_2$O$_2$ is strongly pH-dependent.[229] In all but strongly acid conditions (when iodine and thence iodate may be produced),[229] iodide catalyzes the decomposition of H$_2$O$_2$ in a cyclic reaction in which IO$^-$ is involved; this is a popular pedagogical experiment.[230] Assuming that loss occurs as I$_2$, any free remaining I$_2$ will convert to I$^-$ and IO$^-$ upon the addition of ammonia. IO$^-$ will oxidize excess H$_2$O$_2$ present to O$_2$ and itself be reduced to I$^-$.[72] (In practice, even without

50

the presence of H_2O_2, the only I species we were able to detect in a dilute ammoniacal solution of I_2 was I^-.)

Our base case experimental protocol with milk or formula samples result in a post-digestion pH of ~2-2.6 (breast milk 2.0-2.2, Formula: 2.4, Soy Formula 2.3, whole milk 2.6), prior to NH_3 addition. The acidity originates from the oxidative hydrolysis of the Fe(II) salt with contributions from organic acids formed and not completely degraded during FD. We wanted to determine the effect of changing the pH during the FD step on iodine loss. We also increased the sample to oxidant ratio at this time to help reduce iodine loss (*vide supra*). This required that we verify that the samples are still fully digested. We used first a whole milk sample; these have the most fat and are the most difficult to digest. This particular sample was determined by pre-spiking with [129]I and the standard ID-FD-ICP-MS procedure to have an iodine content of 368.3±9.5 μg/L. In triplicate experiments, 0.5 mL of 30% H_2O_2 was added to 0.5 mL sample, followed by 50 μL of 0.1 M $Fe(NH_4)_2SO_4$. Prior to putting in the oven for digestion, to one set was added 5, 10, 25, 50, and 100 μL of 5 M HCl and to another the same volumes of 0.1 M NH_4OH. After overnight digestion at 60 °C, the pH of the resulting digests were measured. The samples were then spiked with [129]I and immediately diluted to 5 mL using 2% NH_4OH, this solution contained 10 μg [129]I/L.

The concentrations as determined by ICP-MS are shown in Figure 2-3 as a function of digestion pH. Below pH 2.5, increasing loss occurs likely as I_2. However, in the most acidic condition tested (~pH 0.64), the extent of loss begins to decrease again, either due to iodate formation,[229] or the stabilization of iodine as the chlorocomplexes[231] I_2Cl^- or ICl_2^- because of the greater chloride content from the addition of HCl (further discussion of the composition of this digest appears in the SI along with Figure B - 23). However, the overall recovery here is still only ~70% (the data, in terms of % recovery is

51
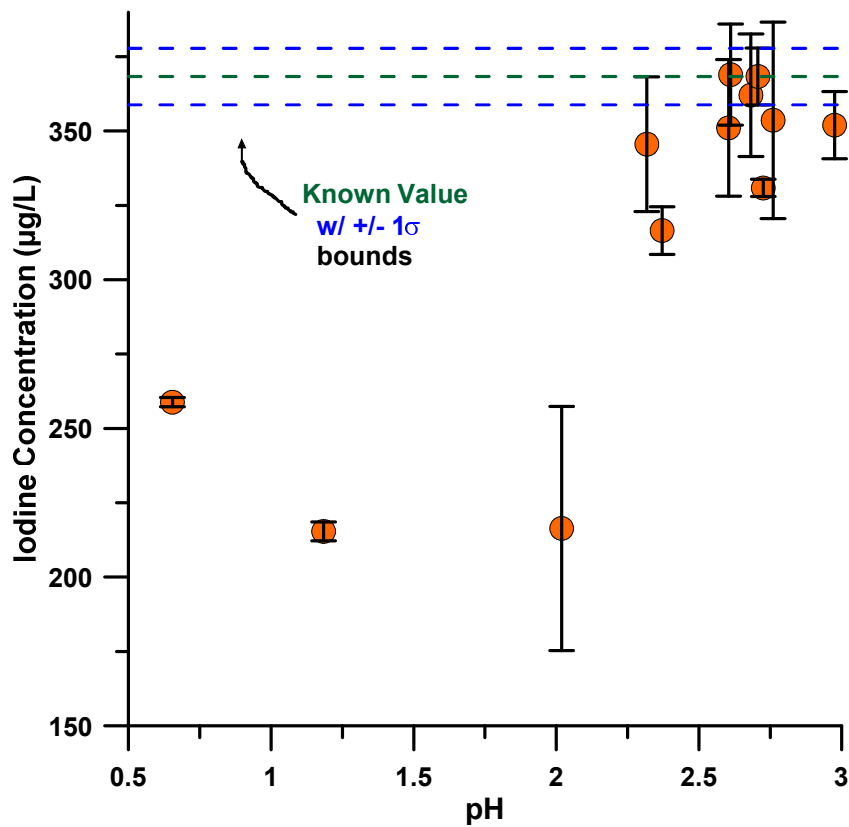
Figure 2-3. Concentrations determined by ICP-MS after Fenton digestion at varying pH. The concentrationed determined by pre-digestion spiking is taken to be the true value and is shown by the horizontal lines with ±1 standard deviation error bounds

depicted in Figure B - 24in the SI). In addition, specifically for milk, prior acidification at this level leads to curdling – this does not facilitate digestion. In contrast, good recoveries are observed above digestion pH values of 2.6 with an average loss of 3.7% and a worst case loss of <10%. Clearly, control of digestion pH can lead to a low loss digestion procedure. Very similar results were then observed for breastmilk samples (Figure B - 25 in SI).

2.3.10 Extent of Volume /Mass Loss during Digestion.

While evaporation losses leading to mass or volume change is inconsequential in ID-MS, such losses will have to be accounted for in other assays to obtain accurate results. As a significant amount of gas (O_2) is evolved, the digestion vials cannot be sealed. In a blank digest, if all the oxygen from the added H_2O_2 (30% w/v, 1 mL) is liberated and this escaping gas is saturated in water vapor at 60 °C, the estimated mass loss is 212 mg. This is likely an overestimate because (a) some of the oxygen must end up in oxidation products and (b) some of the oxygen is evolved at lower temperatures, before the mixture is put in an oven. On the other hand, mass loss may exceed this estimate when volatile materials are present or formed as a result of oxidation. For several types of milk and formula samples the loss averaged 131±18 mg, amounting to 5.9±0.9% (Table S6). The average blank digest loss was 272±3.8 mg, amounting to 12.2±0.1%. Because of the relative uniformity of this loss, a uniform correction factor will be permissible. Of course, the option of weighing all sample vials before and after digestion and performing custom corrections always remains.

2.3.11 Parametric Effects. Nature of Fe(II) Catalyst, Time and Temperature.

We are not aware of any reports in the literature that the form in which Fe(II) is added can affect the Fenton reaction. Adding an organic salt of Fe(II) like $Fe(OAc)_2$ may be potentially advantageous if IC analysis of inorganic anions in the digest is carried out, because acetate will itself be partially degraded. Further, it has poor affinity for anion exchangers, any residual acetate will elute early. While equimolar $Fe(NH_4)_2(SO_4)_2$, or $FeCl_2$ worked equally well, $Fe(OAc)_2$ appeared to oxidize rapidly in air and digestion appeared incomplete. Powdered elemental iron[224] in 1-2 g amounts per sample also produced clear digests and may be attractive for inorganic anion analysis, or in high

purity form for metals analysis; we hope to report on this in the future. Presently we chose $Fe(NH_4)_2(SO_4)_2$ because of its relatively greater stability in air and greater solubility than $FeCl_2$.

It is desirable in ICP-MS to reduce total salinity to minimize ionization suppression and thus minimize the amount of the $Fe(NH_4)_2(SO_4)_2$ used as catalyst. Using a 1:1 ratio of sample : 30% H_2O_2 we varied the volume ratio of 0.1 M $Fe(NH_4)_2(SO_4)_2$, from 0.05 to 1 and examined the FD of triplicate samples of whole milk. At the high end, the digestion proceeds rapidly and completes within 1-2 h at 60 ^{o}C; some foaming is observed and a $Fe(OH)_3$ residue is observed on the surface of the glass tubes. For overnight digestion, only the sample with the smallest amount of $Fe(NH_4)_2(SO_4)_2$ retains a turbid appearance. We henceforth chose a ratio of 1:1:0.1 ratio of sample : 30% H_2O_2 : 0.1 M $Fe(NH_4)_2(SO_4)_2$. A photographic image of the digests obtained under different conditions is in Figure B - 26 in the SI.

2.3.11.1 Peroxide.

As previously observed, a high sample: H_2O_2 ratio helps reduce iodine loss. But the highest ratio at which complete digestion will occur is also important. With a volume ratio of 1:x:0.1 for sample:H_2O_2:$Fe(NH_4)_2(SO_4)_2$, we varied x from 0.5 to 4 in steps of 0.5. x = 1 was the minimum value of x for complete digestion. Photographic images of the digests are shown in Figure B - 27.

2.3.11.2 Temperature.

The experiments were conducted with 1:1:0.1 volume ratio of sample:H_2O_2:$Fe(NH_4)_2(SO_4)_2$. Although FD processes are widely believed to be radical reactions that should be little affected by temperature, the digestion clearly proceeded at

a much accelerated rate at elevated temperatures. Figure B - 28 shows a photographic

comparison of samples allowed to react at room temperature for 12h (overnight)

compared to those at 60 ^{o}C using varying amounts of catalyst. Samples at room

temperature are never fully digested; in contrast, samples at 90 °C are rapidly digested

(Figure B - 29). Although 90 °C may not be practical for iodinalysis due to increased

losses, for many other analytes this may be useful. Presently, choice of 60 °C also

allowed us the use of inexpensive disposable polypropylene tubes.

2.3.12 Appearance of Digest.

Following digestion, addition of ammonia and centrifugation, the supernatant is

generally totally clear. Occasionally a barely cloudy appearance was observed, with or

without the familiar brownish tint of ferric hydroxide. This cloudiness (likely due to iron

hydroxide colloids) remained even after filtration through a 0.45 μm membrane filter. In

alkaline solutions, these colloids should be negatively charged and the addition of a

cationic surfactant such as hexadecyltrimethylammonium chloride (HTMAC) may help

remove the colloidal material as an adduct. Although this does not affect analysis by

ICP-MS, we explored removal of this cloudiness in those samples in which this was

observed. While coagulation was observed (the coagulated material floats to the top, the

clear liquid below is easily aspirated) but some samples required as much as 0.1%

HTMAC in the final solution; this was not pursued further. The surfactant marginally

increased the sensitivity (6-15% from 0.001 to 0.075% HTMAC), possibly due to better

efficiency of atomization of the negative iodide ion being forced to the droplet surface;

this would have required calibration in the presence of the surfactant for accurate

analyses.

An idea of the extent of digestion of the samples can be gleaned simply from the optical clarity, e.g., by comparing the visible absorbance (400-700 nm) of the 100-fold diluted original samples vs. that of the undiluted digests (Figure B - 30 and Figure B - 31). The tail of an absorbance peak, due to ferric iron, which pretty much goes to baseline by ~500 nm, is seen in all the digests, including a blank digest of water. However, the baseline is somewhat higher with the samples due presumably to complexation by carboxylic acids formed. The similarity between all the digests indicate that despite differences in their original composition, these samples are all nearly quantitatively mineralized.

The Fenton reaction has proven to be an effective means of digestion for milk samples prior to analysis by ICP-MS. Our preliminary work shows that clear digests are produced with a variety of other samples from general dairy products to hair. The recommended final recipe for digesting different milk and formula samples are given in the supporting information. We expect in the near future to report on the general application of trace metal analysis following FD.

2.4 Acknowledgement

Chapter 3

Breastfed Infants Metabolize Perchlorate

3.1 Introduction

Perchlorate is a common contaminant of food and drinking water.[232] The toxicity

of perchlorate and its regulation have been the focus of considerable controversy in the

US.[233-236] Perchlorate is an endocrine disruptor. Adequate iodine uptake, especially in

infants, is critical. Perchlorate competitively inhibits uptake of iodine into the thyroid

gland, potentially reducing production of thyroid hormones, thyroxine (T4) and tri-

iodothyronine (T3). It thus acts as a potential neurotoxicant as these hormones are

essential for neurodevelopment.[237] The sodium iodide symporter (NIS) is a glycosylated

90-97 kDa protein that is responsible for shuttling iodide to the thyroid for the

biosynthesis of the thyroid hormones. Perchlorate inhibition of iodide transport arises

because the NIS actually has greater affinity for perchlorate than it does for iodide.[238]

The NIS is well-expressed in the mammary glands during lactation and serves to

transport essential iodine to the young.

While in hindsight, the presence of perchlorate in milk is not surprising, our

original report of perchlorate in bovine[239] and later human milk[240] generated much

skepticism. Determination of perchlorate in complex matrices may have been initially

challenging to us,[241-246] but chromatography-tandem mass spectrometry has become

more affordable and sensitive over the intervening period and is now routine. Perchlorate

has been used as an ingredient in solid fuel rocket propellants, explosives and fireworks.

It also occurs naturally, appearing in Chilean mineral deposits (Chilean nitrate has been

widely used as fertilizer), rain water, and some soils and groundwater. The origin of

natural perchlorate was also of interest.[247,248]

We noted that perchlorate excretion in human milk can be highly variable between subjects and in the same subject at different times.[249] Relative to either iodide or thiocyanate, a greater fraction of perchlorate was present in milk compared to the ratio of the same species in the urine of lactating mothers.[250] Concerns about perchlorate aside, milk iodine concentrations (MI) of many mothers were very low. Iodine nutrition of infants of such mothers would be in jeopardy regardless of the concurrent presence of perchlorate.

Perchlorate at low levels is pervasive in our environment. Remedial measures are not likely to remove all or even the major sources of perchlorate anytime soon. Given limited resources, if a choice is to be made between *more iodine or less perchlorate*[251] to improve iodine nutrition, one of us concluded[252] that we should concentrate on the former. The same sentiment was echoed later in a report by the EPA Office of the Inspector General;[253] this may not, however, be a universally shared opinion, even among the present authors.

Present wisdom holds that ingested perchlorate is not metabolized in humans[235,254] and passes through with a relatively short clearance time.[255-257] Perchlorate is known to be reduced in the rumen of ruminant animals,[258] although plants are more practical bioremediation means than cows. While perchlorate is translocated and not really reduced in lettuce,[259] other plant systems, e.g., Poplar trees, do reduce perchlorate.[260] Even with plants, microbially mediated rhizodegradation is likely more important than phytodegradation.[261-264] A considerable variety of bacteria can reduce chlorate and perchlorate (often denoted as (per)chlorate) as well as nitrate, given suitable oxidizable substrates (this includes a great variety of organic anions).[265]

Despite conventional wisdom, fermentation similar to that occurring in the rumen is known to occur in the large intestine.[266] Facultative anaerobes are essential intestinal

flora in both infants and adults. Nature has been making perchlorate for eons.[267] Natural

perchlorate has thus appeared at significant concentrations in some regions in water

used by humans for time immemorial, in much the same way as it does today.[268] In

Chilean cities near the Atacama Desert where perchlorate content in water and in

mother's milk is relatively high, no unusual neonatal thyroid problems have been

reported.[268,269] Some of the effects of perchlorate in such populations may be

ameliorated by co-occuring high iodine levels; however, one cannot help but wonder if

that is the sole reason that these infants can handle breast milk perchlorate

concentrations (MPC) in excess of 100 μg/L without obvious effect on thyroid

development.

In this paper we first show that *bifidobacteria,* facultative anaerobes that

constitute the dominant bacteria in the digestive system of breastfed infants, can reduce

perchlorate in a milk matrix *in-vitro*. Metabolization of perchlorate[258] by cattle was proven

by deliberately feeding significant concentrations of perchlorate to the animals and

following its concentration in various body fluids/excreta. Given the known effects of

perchlorate, such an experiment cannot be ethically conducted with human infants. We

rationalize why iodine can be used as a conservative tracer and thus devise a means to

determine if any of the perchlorate ingested by infants through breastmilk or formula is

metabolized. The evidence indicates that perchlorate must be significantly metabolized

in breastfed infants.

<div align="center">3.2 Experimental Section</div>

3.2.1 Bacterial Cultures and Analysis for Perchlorate.

All bacterial experiments were conducted with store-bought Pasteurized skim

milk purchased locally and except as stated, spiked to contain nominally 1 mg/L ClO_4^-. (A

more limited set of experiments were conducted with milk samples spiked nominally with 100, 250, 500, and 5000 μg/L ClO_4^-.) Ten milliliter aliquots were pipetted into 15 mL screw-cap culture tubes. All experiments were conducted in triplicate; commercially available probiotic supplements, stated to contain live bacteria were added to the spiked skim milk. To each tube was added the contents of one capsule of *Align*[TM] (*bifidobacterium infantis* 35624, Procter and Gamble, each capsule contains 4 mg of the bacterial mass, labeled to contain 10^9 colony forming units (cfu) when packaged, plus other material[270]). As a point of reference, the bifidobacterial count in the feces of one-month old breastfed infants has been reported to be 200 x 10^9 cfu/g.[271]

To another similar sample set was added a probiotic blend (Advanced Probiotic 10, Nature's Bounty, Inc.). This product is labeled to contain 10^{10} cfu's/capsule of a bacterial mixture consisting of *lactobacillus plantarum*, *bifibacterium bifidum*, *lactobacillus rhamnosus*, *lactobacillus bulgaricus*, *lactobacillus salivarius*, *lactobacillus brevis*, *lactobacillus acidophilus*, *bifidobacterium lactis*, *lactobacillus paracasei*, and *lactobacillus casei* in an unspecified ratio.

The tubes were capped and placed in a 37 °C bath. Over a period of 2 days, 50 µL sample aliquots were taken in triplicate of each sample at logarithmically spaced intervals (sampling was more frequent early in the culture process). The tube was vortexed for homogenization prior to sampling. The samples developed a sufficiently gelled growth at the bottom of the tubes after 24 h; homogenization of the samples by vortexing could not necessarily be assured. If the sample aliquot thus contained more of the free liquid portion, it would be biased towards containing more perchlorate (a soluble anion), rather than less perchlorate than the sample as a whole. Samples were pipetted into 1.7 mL capacity graduated polypropylene microcentrifuge tubes (www.midsci.com) and subjected to a modified Fenton digestion method.[272] To the sample in the

microcentrifuge tube 50 µL of 150 µg/L $^{35}Cl^{18}O_4^-$ (as NaClO$_4$, 95% isotopic purity,

www.iconisotopes.com), 200 µL 30% H_2O_2, and a small spatula tip (7$\pm$3 mg) of iron

powder (P/N 00170, 99.9+% metals basis, <10 µm spheres, www.Alfa.com). Ferrous

salts are typically used in conventional Fenton oxidation; the reaction is fast but results in

incorporation of the anion associated with Fe(II). For small samples that are not

preferably diluted by large amounts, elemental iron provides an alternative; the reaction is

slower but anion contamination is avoided.[272,273] The samples were digested in a 60 °C

convection oven for 3 days to ensure complete digestion, which is slower because of the

surface area and diffusion limitations of the iron powder. DI water was added to make up

for water loss each day and to rinse the walls of the tube. After 3 days, 50 µL of 4 M

KOH was added to precipitate any dissolved iron and a small spatula tip full of MnO$_2$

(2.4$\pm$0.8 mg) was added for the catalytic removal of unreacted H_2O_2. Samples were then

diluted to 1.5 mL, centrifuged at 2000g, filtered through 0.2 µm nylon syringe filters into

autosampler vials, capped, and analyzed by Ion Chromatography–tandem Mass

Spectrometry (IC-MS/MS) with isotope ratio based quantitation (*vide infra*).

3.2.2 Human Subject Recruitment and Sample Collection.

Our protocol, approved by the Institutional Review Board at the University of

Texas at Arlington, called for the recruitment of mother-infant pairs where the infants are

below 7 months of age and are either exclusively breastfed or exclusively formula fed (no

water, juice, or solid foods). Breastfed infant ages ranged from 1.3-7.0 mo. old at the

time of sampling with an average age of 3.5 ± 1.6 mo. Formula fed infants ranged from

4.3-6.2 mo. old with an average age of 5.5 ± 0.7 mo. The mother was to collect (a) at

least three and up to five breastmilk or formula samples ($\geq$ 5 mL), alternating between

immediately before and immediately after feeding the infant (in the case of formula,

collecting an aliquot from the same batch fed to the infant), (b) at least three and up to

five infant urine samples ($\geq$ 5 mL) that represented the first micturition $\geq$ 15 min after the

above feeding, (c) a corresponding number of maternal urine samples (only for

breastfeeding mothers) collected at a time proximate (before or after) the feeding; for

some volunteer breastfeeding mothers, 24-h urine samples were also collected. The

maternal urine data are not used in this paper and are not further discussed. The

samples were stored refrigerated by the mother until the requisite number was collected.

Either the investigators picked up the sample or it was delivered to our laboratory on ice.

Once in the laboratory, the samples were stored frozen at -20 °C until analysis, typically

in a few weeks. The only exclusion criteria was known thyroid disease/impairment for

either mother or infant and any recent medical procedure that involved the use of contrast

media (which frequently contains iodine).

      While infant urine collection bags are routinely used in a hospital setting, the

successful use of such bags in a home setting by mothers proved far more difficult.

Many mothers found it frustrating that leakage occurred or an adequate volume was not

collected, compounded by the obvious displeasure of the subjects, especially when the

bag was fastened tightly to prevent leakage. Primarily for this reason, the dropout rate

after recruitment was nearly 50%. We had thirteen breastfeeding mother-infant pairs and

five formula fed infants successfully complete the study; two of the latter were fed soy-

based formula.

3.2.3 Iodinalysis.

      Recently we developed a new digestion procedure based on the Fenton

reaction.[272] The method was validated in comparison to a method used by the FDA that

uses perchloric acid digestion and Sandell-Kolthoff colorimetry. Several of the breast

milk (that were submitted with sufficient volume) and the formula samples from this study were in fact part of the above intercomparison.[272]

Briefly, to 0.5 mL of a milk or formula sample pipetted into a 15 mL screw-cap polypropylene centrifuge tube, 50 μL of 1 μg/mL ^{129}I tracer (carrier-free KI, www.ipl.isotopeproducts.com) was added. 0.5 mL of 30% H_2O_2, followed by 50 μL of 0.1 M $Fe(NH_4)_2(SO_4)_2$ were then added. After ~15 min, 25 μL of 2% NH_4OH was added. The centrifuge tube was loosely capped but not screwed shut. Fenton digestion was carried out in a convection oven overnight (12+ h) at 60 °C. After allowing the digest to cool to room temperature, the digest was diluted to 5 mL with 2% NH_4OH to precipitate $Fe(OH)_3$. The tubes were then vortexed and centrifuged (3000g at 2°C, 15 min). The supernatant was directly subjected to Induction Coupled Plasma Mass Spectrometry (ICP-MS) analysis as detailed below. Urine samples were simply diluted prior to ICP-MS analysis, typically by 10x. Some required further dilution after the initial analysis to be within calibration range.

An X Series II ICP-MS (www.thermo.com) was used in the direct infusion mode. The peristaltic pump built into the ICP-MS was used to prime the sample into the Peltier-cooled (3 °C) nebulizer at 1.6 mL/min for 45 s and then continuously aspirate the sample into the nebulizer at 0.8 mL/min. Each measurement cycle consisted of a 20-s qualitative mass survey scan followed by three 32-s long quantitative mass scans. Between samples, 1% NH_4OH was used for a monitored washout up to 4 min to eliminate effects of any carryover between samples. After analysis was complete, the autosampler probe was washed in the same wash solution before storage and reuse.

3.2.4 Determination of Perchlorate.

For urine samples, 2.5 mL of the sample was spiked with 12.5 µL of 1 mg/L $^{35}Cl^{18}O_4$ as the internal standard. Strong acid type H^+-form cation exchanger macroreticular resin (Dowex HCR-W2) was washed sequentially with methanol and water. Excess moisture was purged with air, without drying the resin. An aliquot of the resin (~250 mg) was added to the urine sample, vortexed, allowed to stand for 15 min, filtered through a 0.20 µm syringe filter into a sample vial and capped and loaded onto the autosampler.

To 5 mL of formula or milk (if sample availability was limited, the sample was diluted beforehand and the diluted sample used), 25 µL 1 mg/L $^{35}Cl^{18}O_4^-$ was added and the mixture was then centrifuged (3000g, 15 min, -2 °C). The casein, whey, and fat separated. 2.5 mL of the whey (avoiding the fat and the casein) was pipetted into a 10 kDa centrifugal filter (Vivaspin 6, www.sartorius-stedim.com). The whey was then centrifuged (10000g, 90 min, 2 °C on a 25° fixed angle rotor). To the filtrate, approximately the same mass fraction of the aforementioned cation exchange resin was added (~100 mg /mL filtrate). The sample was then vortexed, allowed to stand for 15 min, filtered through a 0.20 µm syringe filter into a sample vial and capped and loaded onto the autosampler.

The IC-MS/MS analysis protocol used an IC-25 isocratic pump with an EG40 electrodialytic eluent generator, 2 mm bore AG21/AS21 guard and separation column sets housed in a LC30 temperature controlled oven (30 °C), ASRS-Ultra II anion suppressor in external water mode, and a CD-25 conductivity detector, all from ThermoFisher/Dionex. Around the elution window of perchlorate (t_R ~9 min), 6-10 min after injection, a diverter valve directed the CD25 effluent to a tandem mass spectrometer (Thermo Scientific Quantum Discovery Max with a heated ESI probe and enhanced mass

resolution). Eletrodialytically generated high purity KOH eluent was used isocratically at a concentration of 15 mM and a flow rate of 0.35 mL/min. Eluent generation, sample injection (2 μL), electrodialytic suppression, autoranging conductivity detection and data acquisition were all conducted under Excalibur/Chromeleon software control. Perchlorate was quantified by the -99 $\rightarrow$ -83 Th (m/z) transition ratioed to the -107 $\rightarrow$ -89 Th internal standard transition. All data were interpreted in terms of a 5-point calibration with check standards run daily. Any sample falling outside the calibration range was reanalyzed after appropriate dilution. All samples were minimally analyzed in duplicate.

The limits of quantitation for iodine and perchlorate were 0.3 and 0.015 μg/L, similar to those reported previously.[250] Concentrations of both analytes in all of the analyzed samples were substantially above the limit of quantitation of the methods.

3.3 Results and Discussion

3.3.1 Microbial Perchlorate Reduction.

A number of perchlorate-reducing bacteria have been isolated and used in bioremediation of perchlorate-contaminated soils, sewage, and water systems.[274] Reduction of (per)chlorate typically occurs under anaerobic conditions, and the released oxygen is then used for respiration. All living systems that reduce perchlorate do so with the help of an enzyme *perchlorate reductase,* the same enzyme also reduces chlorate and nitrate. In fact, all bacteria that reduce perchlorate preferentially reduce nitrate if both are available.[274-276] The enzyme *perchlorate reductase* is a member of the Type II DMSO family and is closely related to *nitrate reductase*. Enzymes in this family all use a common molybdenum cofactor, [bis(molybdopterin guanine dinucleotide)-

molybdenum].[277,278] The dominant pathways for metabolism of perchlorate in plants and animals are both likely mediated by microorganisms.[261,262]

Bacterial populations present in the human intestine are diet-dependent. Populations and ratios vary over the course of a lifetime, and also among populations of humans.[279] There are numerous studies that show that the intestinal bacterial population is distinctly different for breast-fed vs. bottle-fed infants. In breastfed infants, *bifidobacteria* far outweigh other bacteria;[280-282] another important group of anaerobic bacteria, *Ruminococci,* are also present in breast-fed infants.[283,284] In bottle-fed infants the *bifidobacteria* concentrations are lower and can sometimes be below the culture threshold limit (10^4 cfu/mL) although detection by PCR methods is possible.[285] Even under conditions when bifidobacteria become the dominant intestinal bacteria in bottle-fed infants, their number count remains an order of magnitude lower than those in breastfed infants.[271] Interestingly, infant intestinal *bifidobacteria* counts are higher for infants of breastfeeding mothers with no allergies compared to those with documented allergy problems.[286] Bifidobacterial diversity has been suggested as an index of systemic immune responses.[287] *Bifidobacteria* are routinely sold as supplements[288] and there are ongoing studies to devise additives to infant formula that will have a bifidogenic effect.[289]
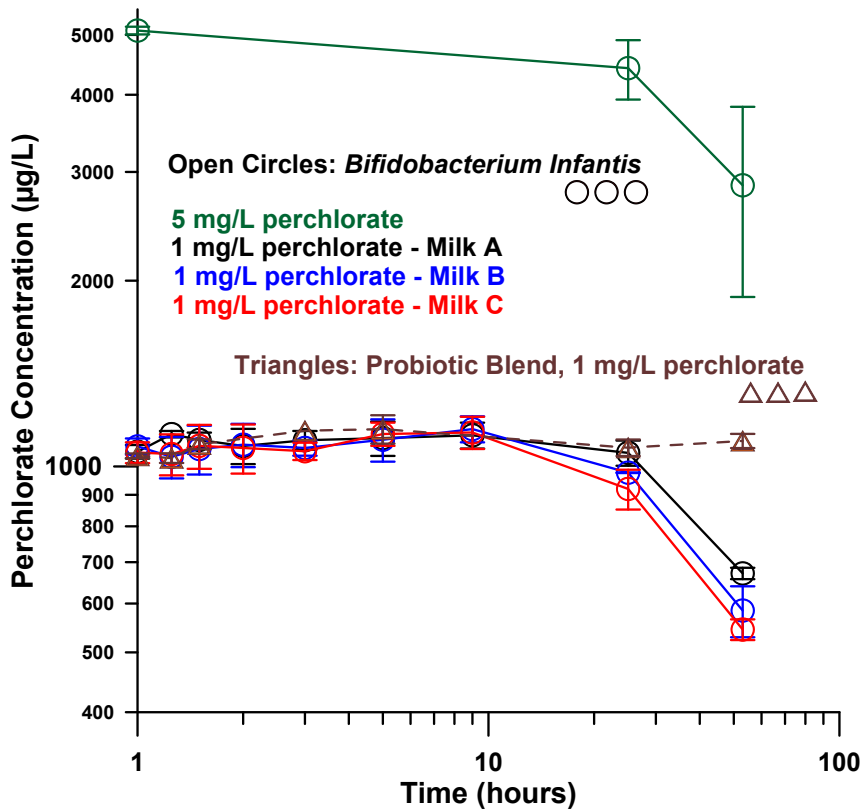
Figure 3-1. Perchlorate concentration in bacteria inoculated

perchlorate spiked milk samples monitored up to 52 hours after

bacterial addition; hour 1 represents analysis immediately after

inoculation. Error bars represent one standard deviation

It is well established that *bifidobacteria* can reduce nitrate[290,291] but no direct

experiments have ever shown that *bifidobacteria* can reduce perchlorate. However,

inferred pathways for the taxon *Bifidobacterium bifidum* and its descendants include

perchlorate reduction via *perchlorate reductase*.[292] Below we describe the results of *in-

vitro* experiments do determine whether *bifidobacteria* can reduce milk spiked with

perchlorate.

3.3.2 Perchlorate Temporal Profile in Perchlorate-spiked Milk Inoculated with Bifidobacteria.

The supplement preparations contain other insoluble (and soluble) material aside from the bacterial mass. Conceivably these may remove perchlorate by adsorption or ion exchange. A two-point measurement (before and some fixed point after inoculation) is therefore inadequate as any removal by the solids in the supplement will be unaccounted for. Therefore, time based measurements were carried out. The results are shown in Figure 3-1. It will be noted that there is really no statistically significant reduction of the perchlorate content over the first 8 h. (Note that relative to adding no inoculum, the standard deviation of replicate sample analysis always increases significantly after adding the inoculum, possibly due to the intrinsic variability of any biological process). A small but statistically significant reduction is seen after 24 h and an obviously large reduction occurs after 52 h of incubation. Unlike a real digestive system, we do not have a system at steady state; our experiments start out in a clearly oxic condition and doubtless contains other reducible substrates like nitrate that may be preferentially reduced. A similar lag period in microbial perchlorate reduction has been reported by others.[293] As was noted in the experimental section, significant part of the culture medium gels/solidifies after ~24 h and homogenization cannot be assured by vortexing. Any intrusive mechanical homogenization was avoided to preclude contamination by other adventitious species that will compromise the utility of the subsequent samples. There is however, no significant volume increase associated with the yogurt formation that will create an analytical bias on volume based analysis. To preclude any possibility that perchlorate is somehow preconcentrated in the solid, we carried out analysis of the solid portion per unit mass basis for the 5 mg/L sample. No preferential concentration of perchlorate in the gel phase over the original concentration per unit mass was found.

Perhaps most importantly, the other inoculum with the "Probiotic Blend", which we expected to behave in the same fashion, did not; rather it served as a useful control. Gelling/yogurt formation was observed after about the same length of time, but as Figure 3-1 shows, there was no reduction of perchlorate concentration in this case even after 52 h. Whether the specific species of *bifidobacteria* present in the blend are not as effective for perchlorate reduction or the absolute *bifidobacteria* content are not nearly as high, is not known.

Finally, we show the fraction of perchlorate lost after 24 h as a function of perchlorate concentration in Figure 3-2. Granted that the uncertainties are very high, the fraction of perchlorate reduced after 24 h monotonically increases with increasing $[ClO_4^-]$. The fraction of $[ClO_4^-]$ consumed should be proportional to $(K_c[ClO_4^-]/(K_R[R] + K_c[ClO_4^-]))$ where [R] is the concentration of competing reducible substrate and the K-terms are a composite representation of the binding constant to the substrate and the rate constant for its reduction. It will be obvious that for $K_R[R] >> K_c[ClO_4^-]$, the value of the overall expression will essentially linearly increase with $[ClO_4^-]$. The solid line in Figure 2 represents a best fit line that fits the expression $(a/(1+b/[ClO_4^-]))$ where a and b are constants, concordant to the expression given above in terms of [R] and $[ClO_4^-]$ at constant [R].
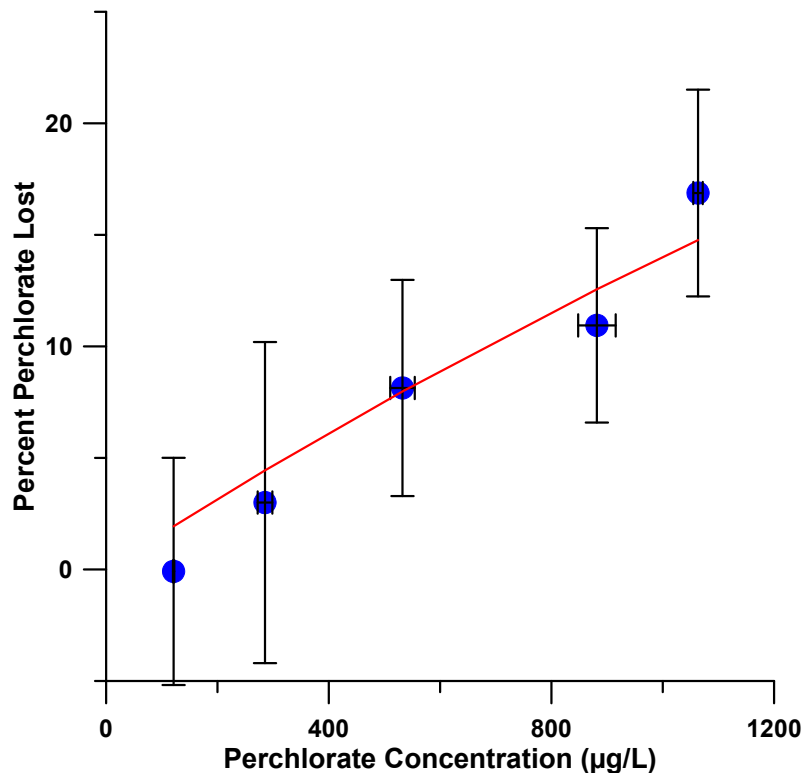
Figure 3-2. Percent perchlorate lost after 24 hours in milk samples

spiked with various concentrations of perchlorate and incubated

with bifidobacterium infantis. The solid line is the best fit to the

model: Percent Perchlorate Loss = $(1/1+b/[ClO_4^-])$

It should not be construed that the precise dependence of the extent of

perchlorate reduction on the absolute concentration observed in these in-vitro

experiments is quantitatively extrapolatable to infants. Neither the complete composition

of the microflora, nor the precise redox conditions in the infant intestine are the same as

that in a culture tube. In a real digestive system there are very likely other agents that

metabolize competing oxidants like nitrate, without *bifidobacteria* derived *perchlorate*

reductase pathway being the only agent for removal of such oxidants. In addition, the

digestive system already contains a very large number of *bifidobacteria* at steady state

(fecal count in a month –old breast fed infant is 2×10^{11} cfu/g,[271] compared to 10^8 cfu/mL

at the beginning of our incubation); we therefore expect perchlorate reduction to be more efficient *in-vivo.*

3.3.3 Does Bifidobacteria Reduce Perchlorate in Infants?

Since deliberately feeding infants perchlorate, isotopically labeled or not, in whatever amount above background levels, was not an option, we devised an approach that utilizes iodine (regardless of its chemical form), as a conservative tracer. Our null hypothesis is that perchlorate is not metabolized; it is also conserved. In solely breastfed or formula-fed infants, breastmilk or formula is the only input. If the only output occurs via urinary excretion, the ratio of concentrations of an analyte in urine to that in milk will be the same for all conserved species.

For this framework to be valid, the following will have to be true:

(a) Iodine is conserved. While there is net daily accumulation of iodine in an infant because its thyroid is growing, the daily increment of this accretion is negligible relative to daily iodine intake and excretion.

(b) For infants, urinary excretion is by far the principal mode of iodine excretion. The same must be true for perchlorate.

(c) Neither intake nor output is continuous; both are discrete events. As a constant time interval between intake and output cannot be assured, the rate of clearance of perchlorate and iodine must be comparable to draw conclusions from a finite set of data.

3.3.3.1 Urine to Milk Concentration Ratio (UMCR) for a Conserved Species.

The following are norms for infant milk intake: formula fed infants consume a greater volume; Goellner et al.[294] report average intake volumes of 657, 998, 935, and

1128 mL/d, respectively for 0-1, 1-2, 2-4 and 4-6 mo. olds, averaging 930 mL/d for 0-6 mo. olds. The same respective age groups have urinary outputs 378, 556, 496 and 505 mL/d amounting to an average urinary output of 484 mL/d for the age group. These data correspond to an intake/urine output volume ratio (the same as UMCR) of 1.7-2.2. For breastmilk, the intake volume is lower. The Child-Specific Exposure Factors Handbook[295] suggests that the mean value for a 1-3 month old is 690 mL/d, while that for a 3-6 mo. old is 770 mL/d. No data are available for urinary output volume for breastfed infants. Because there is no reason to believe that the loss of water, which takes place through breathing, sweating, feces, etc. is going to be different for breastfed vs. formula-fed infants, the UMCR for breastfed infants will be higher. Goellner's data allows us to estimate non-urine water loss for 1-3 and 3-6 mo. olds to be 440 and 531 mL/d; this will lead to respective estimates of 2.8 and 3.2 for UMCR of breastfed infants of these age groups.

The above provides approximate guidelines as to what UMCR value can be expected for a conserved analyte both for breastfed and formula-fed infants. If a particular analyte is known to be conserved, the UMCR for it can be used as a benchmark for that subject and the UMCR for another analyte can be compared to it. If the latter UMCR is significantly smaller than the benchmark UMCR, the latter species is not conserved. Regardless of the validity of these arguments, there is considerable temporal variation of perchlorate and iodine in the infant intake for a breastfed infant, as changes in the mother's diet from one meal to the next are reflected in breastmilk composition.[249] Multiple samples per subject must therefore be analyzed.

Thus if iodine is conserved, we can take its UMCR (hereinafter called the iodine concentration factor (ICF)) as the benchmark. If UMCR for perchlorate, the perchlorate concentration factor (PCCF), is statistically indistinguishable, the null hypothesis is

proven. If PCCF, however, is statistically less than ICF, the null hypothesis does not hold and perchlorate is being lost in the system.

Now we rationalize the assumptions a -c outlined above.

3.3.3.2 Iodine is Conserved.

Incremental Daily Intrathyroidal Iodine Accumulation in an Infant is Negligible Relative to Daily Intake. A full-term neonate at birth has a total thyroid weight of ~1.5 g,[296,297] and based on post-mortem data, contains ~200 μg of iodine.[298] The total iodine content of a neonatal thyroid increases essentially linearly with body weight and gestational age,[298] presumably this trend continues for several months after birth. But in a euthyroid child, the thyroid does not increase in weight beyond the age of 15.[298] However, the reported iodine content of the adult thyroid for a euthyroid population varies markedly. Zabala et al.[299] report a median value of 15±8 mg in Caracas, Venezuela. Milakovic et al.[300] report a mean value of 5.2 mg in Göteborg, Sweden. Zaichick and Zaichick[298] also report an intrathyroidal iodine content of ~5 mg for 16-25 year olds in Moscow. If we assume that from birth to 6 months, the birth weight doubles (according to the Child-Specific Exposures Factors Handbook, at 6 mo., the average weight is somewhat less than twice the birth weight), and the intrathyroidal iodine content doubles, the daily accumulation rate will be <2 μg/d. A linear accumulation of intrathyroidal iodine of 15 mg over 15 years also suggests a comparable figure, 2.7 μg/d. Relative to adequate iodine intake of 110 μg/d for 0-6 mo. olds or even recommended daily allowance of 90 μg/d for 1 year olds,[301] these daily accretion rates are negligible. In fact, circulating iodine (99% of this is total thyroxine, T4) is much larger than this; at ~560 nM as iodine,[302] assuming a 0.55 L blood volume for a 7.7 kg 7 month old, this represents 39 μg I.

3.3.3.3 Principal Iodine Excretion is Through Urine.

To trace nonselective loss of iodine, the routes to loss of water also need to be considered. One major route for moisture loss is through exhaled breath. As iodine is not present in the elemental form, it is not likely that significant amounts of iodine in the vapor phase are lost through this route.

The loss of water through feces is ~5 mL/kg bodyweight/ day,[303] amounting to ~37 mL for a 3-6 mo. old, compared to 505 mL urine volume per day (for a 4-6 mo. old). If the iodine content per unit water content is the same in urine and feces and urinary and fecal iodine excretion are the two major routes of iodine excretion, then 90% of excreted iodine is in the urine. The same conclusion has been drawn by others,[304,305] albeit there are relatively few direct measurements of iodine in feces.[306,307]

In athletes undertaking strenuous exercise and thereby generating a large amount of sweat, the amount of iodine loss through sweat can be significant.[305,308,309] However, this is not the case under other conditions. Estimates of transdermal loss of water (sweat, evaporation) for infants vary. Sharma et al.[303] estimate that this can be as large as twice that through feces). This is consistent with the measurements of Ariagno et al.[310] who report a normothermic evaporative loss in full-term healthy infants of 0.02 $mg/cm^2/min$ and the estimated body surface area is 0.064 ± 0.011 m^2/kg for 0-2 year olds according to the Child-Specific Exposures Factors Handbook. Even if iodine loss in sweat is twice that in feces, urinary excretion will remain by far the dominant route of iodine excretion. This is consistent with Mao et al.'s observation[308] with soccer players in
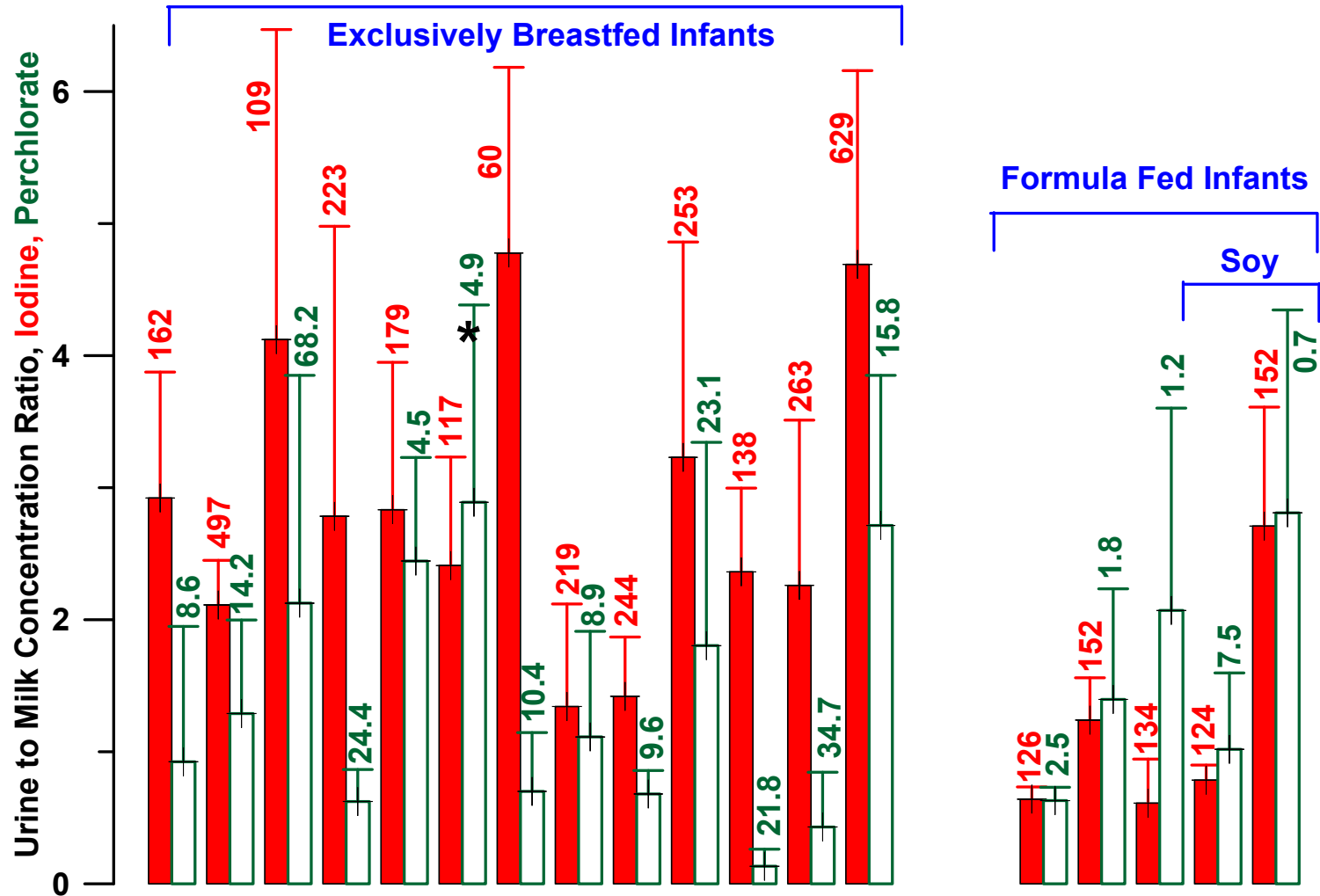
Figure 3-3. Iodine concentration factor, ICF, (C_{urine}/C_{Milk}) and Perchlorate concentration factor, PCCF shown as solid and crosshatched bars with 1 sd error bars for each mother-infant pair. Breastfed babies represent the group on the left, formula-fed babies on the right. For all but the asterisked subject in the breastfed group ICF exceeds PCCF while in none of the formula-fed subjects ICF exceeds PCCF. The average milk iodine and perchlorate concentrations in μg/L are noted on top of each bar. Given the ratio, the corresponding urinary values can be readily evaluated.

a hot humid environment that urinary iodine excretion still outweighed iodine loss through sweat by 2:1 on the average.

There may be some water loss due to regurgitative "spit-up". We were unable to find any quantitative data in the literature. It is highly unlikely that this represents either a significant amount of liquid output compared to urinary output or a significant route of iodine and perchlorate loss.

3.3.3.4 Iodine and Perchlorate are Cleared at Comparable Rates.

The clearance rate for neither perchlorate or iodine has been measured for small infants. Clewell et al.[311] have evaluated available adult data in constructing pharmacokinetic/pharmacodynamic models across life stages and suggest that the best values to use for urinary clearance are 0.1 and 0.13 L h^{-1} kg^{-1}, respectively, for iodine and perchlorate, reported for adults. It is in fact more than comparable, within the limits of significant figures, they are the same. We do not therefore expect our findings to be biased by dramatic differences in clearance rates.

3.3.4 Observed Iodine and Perchlorate Concentration Factors.

The results for each subject, including 1 standard deviation as error bar are plotted in Figure 3-3. The 13 breastfed infant-mother pairs provided 43 milk samples and 39 infant urine samples, the 5 formula-fed infant-mother pairs provided 21 milk samples and 21 infant urine samples. The data were analyzed after pre-processing in 3 steps: (1) The within-subject measurements of each of the 4 variables were averaged and the standard errors of the averages were computed. (2) These averages were used to compute ICF and PCCF and also their standard deviations using the method of propagation of errors for a ratio. (3) The ICF-PCCF difference and its standard deviation

76

for each subject were computed. These differences were analyzed by fitting the linear model:

$$d_{ij} = \mu_j + e_{ij}, \; i = 1, 2, \ldots, n_j, \; j = 1, 2 \quad \ldots(1)$$

A weighted least-squares fitting was used, with the weight of d_{ij} taken as the reciprocal of the square of its standard deviation computed above. In this model, d_{ij} denotes the ICF-PCCF difference from the ith subject in the jth group, μ_j is the mean difference of the jth group, and e_{ij} is the random error term. Here, $n_1 = 13$, $n_2 = 5$. The model was fit using the "lm" function in the statistical software package R.[312] The fitted model was significant (p-value = 0.0004). It had a residual standard error of 1.53 with 16 degrees of freedom, and its R^2 value was 0.615. The standard model diagnostics showed that this model fit to the data was acceptable. The resulting estimates for ICF-PCCF mean differences in the two groups are summarized in the following table:

Table 3-1. Summary of results for ICF-PCCF mean difference in each group

Group	Estimate	Standard error	t-value (d.f. = 16)	p-value	95% confidence interval
Breastfed	1.189	0.236	5.038	< 0.001	(0.69, 1.69)
Formula-fed	-0.054	0.127	-0.424	0.677	(-0.32, 0.22)

These results show that there is a statistically significant difference between the ICF mean and the PCCF mean (p-value < 0.001) in the breastfed group. The ICF mean is higher than the PCCF mean (95% confidence interval for mean difference = [0.69, 1.69]). On the other hand, the difference between the two means in the formula-fed group was not significant (p-value = 0.68).

These data then suggest that perchlorate is lost in the breastfed infants but may not be lost in formula-fed infants. The mean PCCF and ICF values for breastfed infants are 1.37 and 2.87, respectively. If iodine is conserved, one can estimate that on an average some 52% (= (2.87-1.37)/1.37) of the perchlorate is unaccounted for. We duly note that we are not the first to report this discrepancy. In a recently published study, based on urinary perchlorate concentrations, Valentín-Blasini et al. [313] calculated the daily average dosage for breastfed infants to be 0.42 μg/kg. They did observe that breast milk perchlorate concentrations as reported in a previous study would have suggested a significantly higher daily dosage of 1.1 μg/kg. They chose to attribute this difference to diet, geography and small size of the studies but this difference could be just as easily interpreted if 62% of the perchlorate ingested via milk was metabolized before urinary excretion.

It is important to note that in our study formula-fed infants do not serve as controls for breastfed infants. Rather, each is an independent experiment with ICF serving as a control benchmark to determine if PCCF indicates whether perchlorate is lost. Based on volume of milk intake and urinary output we computed that the UMCR of a conserved species should be in the range of 2.8-3.2 for breastfed infants, an average ICF of 2.9±1.1 is consistent with iodine being conserved. Similarly for formula fed infants, the UMCR for a conserved species is computed to be 1.7-2.2, an ICF value of 1.2 ±0.9 is not statistically significantly different. On the other hand, the PCCF value is statistically significantly lower for breastfed infants than their ICF values, voiding the null hypothesis on perchlorate being conserved.

Note that the absolute intake of perchlorate is much lower in formula-fed babies (as has been noted also by others already[313]) and if there is any similarity to what we observe in *in-vitro* experiments, even if perchlorate is reduced at all, the extent will be

78

much lower. In any case, whether or not any reduction of ingested perchlorate occurs with formula fed infants is of less importance as the absolute perchlorate dosage is much lower.

In retrospect, it may not be surprising that perchlorate can be metabolically reduced in the digestive systems of breastfed infants. Most processes in nature have evolved due to need. The occurrence of perchlorate in the Chilean nitrate deposits[314] has been known since the 1800's,[315] and there is strong evidence that this perchlorate was atmospherically formed.[316] Perchlorate is routinely detectable in rainwater[247,317] and traces of perchlorate have been measured in Pleistocene and Holocene groundwater.[267] Perchlorate is not a new entity in nature; it is logical that a natural defense to its strong iodide transport inhibiting properties would have evolved to protect the newborn, the most vulnerable life stage.

Nevertheless, we hasten to add that whether this defense is adequate to handle the presence of anthropogenic perchlorate that has appeared in a population in the short term, often at much greater concentrations than the natural background, is an altogether separate question. In this limited study, we observed no correlation (r =0.16) between the fraction of perchlorate lost as a function of the breastmilk perchlorate concentration. Maternal bacterial population also affects infant intestinal microflora.[286] It should not be overlooked that a large fraction of the perchlorate is excreted unchanged, nor should it be inferred that ingested perchlorate has no effects on infant iodine nutrition, especially since some absorption of perchlorate may take place before metabolization occurs. It is not our intent to suggest one should be complacent about perchlorate intake of infants.

Nevertheless, in formulating public policy, the metabolism of perchlorate by infants will need to be taken into account. Aside from reducing the steady state perchlorate concentration in the gut and thus reducing intestinal absorption, it has long

been known that renal reabsorption of many anions, including iodide, occurs.[318] Logically, renal reabsorption of perchlorate must also occur. Pendrin is a membrane protein strongly expressed in the kidney;[319] it is among the known transporter of anions responsible for anion reabsorption.[320] It behaves much like an anion exchanger[321] and if so, it may provide transport/reabsorption of perchlorate even more efficiently than iodide. Intestinal metabolism may thus reduce reabsorption that will need to be considered.

3.4 Acknowledgement

Chapter 4

Iodine Measurement by Gas-phase Preconcentration and Microplasma Atomic Emission

Spectroscopy

4.1 Introduction

Iodine is an essential element, necessary for the production of the thyroid

hormones tri and tetraiodothyronine (T3 and T4). These thyroid hormones are essential

for proper metabolism and are especially important for the developing brain.[322]

Insufficient Iodine uptake will manifest itself in a host of symptoms (broadly known as

Iodine deficiency disorders, IDD) such as goiter, hypothyroidism, impairment of

neurodevelopement, and in the severest cases, cretinism.[323] In moderately deficient

regions, low iodine has been linked to attention deficient hyperactivity disorder[324] and

lower intelligence.[325,326] It is estimated that nearly one third of the world's population (2

billion people) are at risk of developing IDD's.[327] For this reason regular screening of a

population is performed. Currently more than 91% of the global population in some 130

countries are routinely surveyed for their iodine nutrition status as well as salt iodization

(the most common vector for prophylactic treatment for low iodine). Populations are

categorized based on median urinary iodine (UI) levels as severely deficient (<20 µg/mL),

moderately deficient (20-49 µg/mL), mildly deficient (50-99 µg/mL), adequate (100-199

µg/mL), above requirements (100-199 µg/mL), and excessive (>300 µg/mL). Excessive

iodine use can lead to hyperthyroidism and thyroid autoimmune disorders. However, the

best available data suggest that consumption between 1000-5000 µg/d (approximately

670-3300 µg/L urinary iodine excretion) may be safe for most people for years.[328] From

the years 1993 to 2006 the number of countries in which iodine deficiency was a

recognized public health problem decreased from 123 countries to 47.[327]

The U.S. Institute of Medicine (IOM) recommended daily allowance (RDA) or adequate intake (AI) of iodine for various populations are as follows (in µg/d): 0-6 mo: 110 (AI), 7-12 mo: 130 (AI), 1-8 yr: 90 (RDA), 9-13 yr: 120 (RDA); >14 yr: 150 (RDA), pregnant women: 220 (RDA), lactating women 290 (RDA).[329] A mean urinary iodine volume of 1.5 L/d of a healthy adult may be used to correlate values to expected UI levels. The UI for non-pregnant, non-lactating adults should be ≥100 µg/L, equivalent to the lower limit of the adequate nutrition category proposed by the WHO.[327] In the United States, Iodine nutrition (monitored through National Health and Nutrition Examination Surveys; NHANES) has shown a decline over the last several decades.[330] According to the most recently available data (NHANES III), white lactating women had a median UI of 106 µg/L (well below the ideal ~190 µg/L proposed by the IOM), and lactating Hispanic women had a median UI of 50 µg/L.[331]   This decline in median UI has also been associated with rising rates of congenital hypothyroidism.[332]

Currently, there are no convenient and inexpensive ways for gauging iodine status of an individual. Iodine measurements, including those for epidemeological studies, are performed using one of two techniques. The first is based on the now more than 75 year old kinetic photometric assay known as the Sandell-Kolthoff (SK) method[333] and the second is inductively coupled plasma mass spectrometry.[334,335] The SK method measures the time dependent decay of the Ce^{4+} absorbance as it is reduced by As^{3+}. This normally slow reaction is catalyzed by iodide so that the rate of decay is a direct measure of the iodide present.[333,336] Two time point measurements are adequate but provide less information than a more extensive kinetic profile. The SK method requires complete sample digestion prior to analysis to remove any oxidizable material or interfering substances. Use of a kinetic profile can identify whether digestion is complete as shown in Appendix B.   ICP-MS allows direct analysis of some samples, notably urine,

following a simple dilution without digestion, but is optimally performed using an internal standard, preferably a low abundance isotope such as [129]I.[334] Use of ICP-MS requires expensive instrumentation, skilled personnel, and involves significant running cost, while SK requires extensive sample treatment making both methods inconvenient for infrequent analysis.

We have previously reviewed methods for measuring iodine in biological samples, and while there are numerous techniques that provide adequate sensitivity and are relatively inexpensive, we concluded that most often the limiting factor in developing a high throughput method is the sample treatment step.[337] Digestion may be circumvented if Iodine can be selectively isolated from urine and measured. In inductively coupled plasma atomic emission spectroscopy (ICP-AES), sensitivity is hampered due to the low transfer efficiency of the analyte to the gas phase. One of the most common methods for improving sensitivity in AES is by using chemical vapor generation. Iodine is predominantly in the form I$^-$ in urine which can be readily oxidized to the volatile species I$_2$. Such a scheme has been used frequently using direct sample nebulization[338-341] or gas-liquid separation prior to analysis.[342-349]

ICP-AES however, is not easier to use than ICP-MS. Use of gas liquid separators however greatly reduces the solvent load of the plasma. This allows alternative, miniaturizable plasma generation techniques to be used instead of the traditional high power ICP[350,351] (where the typical power consumed is in the kilowatt range). One such type of plasma is the dieletric barrier discharge[352] (DBD). DBD's use a layer of dielectric to separate one or both of the electrodes from the plasma. DBD's have been operated anywhere from line frequency to 10 MHz. As the voltage changes, a charge develops at the gas-dielectric interface. Eventually the voltage at the surface reaches the breakdown voltage of the gas. A microdischarge is formed that carries a

83

total charge proportional to the permittivity of the dielectric and inversely proportional to the thickness. As the microdischarge propagates, a localized electric field develops opposing the applied field and terminates the plasma at that point. Because these microdischarges only last on the order of 10 ns, a sustained arc is not formed and very little energy goes into heating of the gas. A nearly uniform discharge may be obtained if fast rising voltages, preferably from a square wave source, are used to generate a multitude of microdischarges across the whole dielectric face. Because the current allowed to flow through the plasma is limited, a the plasma never reaches thermal equilibrium; the temperature of the electrons and the gas are not the same Excitation energies, expressed often as electron temperature, are comparable to or higher than modern microwave induced plasmas or ICP's[353] while gas temperatures can be maintained at just above room temperature to 1000 K.[352]

DBD's have been used successfully to measure mercury;[354-356] sodium, potassium, zinc, and cadmium;[357] bromate and bromide;[358] Arsenic;[359,360] and as detectors for gas chromatography.[361,362] Recently, a sequential injection method was reported for online oxidation, volatilization and measurement using a DBD coupled to a fiber optic spectrometer.[363] This method showed acceptable results in the high μg/L range. Further sensitivity could be gained by use of an anion exchange concentrator prior to elution and measurement,[364,365] but because I_2 volatility is affected by the salts in solution, this may not be a reliable method for matrices that have inconsistent salt content such as urine. Additionally, water vapor present may quench the plasma or cause signal instability, reducing the sensitivity,[354,355] but may be compensated for using a neighboring emission line of the plasma as reference.[363] Preconcentration of gas-phase I_2 allows complete separation from the matrix and measurement absent of water vapor. A gold plated tungsten filament has been reported for the selective preconcentration of

84

mercury.[356] The low thermal mass of the tungsten filament allowed rapid resistive

heating and desorption of the mercury from the gold surface following the

preconcentration step. Use of alternative coatings can be used for other analytes, or

nonselective absorbing materials if no interference is obtained at the emission

wavelength of choice. Here we have thoroughly analyzed the capability of a DBD

microplasma for the measurement of I_2 at levels necessary for diagnosing severe iodine

deficiency (<20 µg/L), as well as developed a preconcentration capable of absorbing

iodine prior to measurement.

4.2 Measurement of Iodine in a Dielectric Barrier Discharge

Several geometries were explored for DBD atomic emission devices. The most

effective device, shown in Figure 4-1, consisted of a glass or quartz tube (I.D. = 2 mm,

O.D. = 3.15 mm)) with three ring shaped electrodes external to the tube (alternative

designs are provided in Appendix C). The electrodes were made of aluminum tape and

were approximately 7 mm wide. The middle electrode was attached to the plasma power

supply high voltage output (information unlimited, GRD RIV-1) which provided a square

wave excitation at a frequency of 36 kHz with a peak to peak voltage of up to 7500 Volts.

The amplitude is adjustable as a function of the input voltage. The supply also provided

duty cycle control as a means of adjusting power output (The duty cycle here refers to the

time the excitation source is applied, not the excitation waveform itself) For these
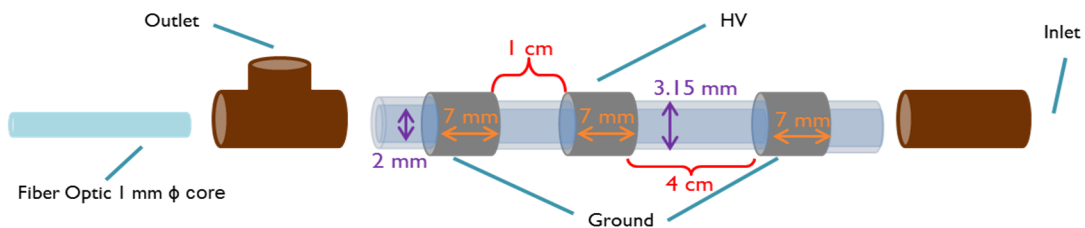
Figure 4-1. Dielectric Barrier Discharge Design for measurement of Iodine

experiments 100% duty cycle was used. The two other electrodes were grounded on either side of the excitation electrode. The spacing between the excitation and ground electrodes are not identical. Near the exit of the discharge cell, the excitation and ground electrodes are only 1 cm apart, while the ground electrode near the entrance is separated from the excitation electrode by 4 cm. This results in the most intense portion of the plasma being near the exit of the device. The third electrode near the entrance is not necessary, but it was observed the plasma was traveling through the inlet gas line, so as a safety precaution a third grounded electrode was introduced to terminate the plasma. At the exit of the discharging device, a polyetheretherketone (PEEK) tee (www.upchurch.com) is used to couple the device to a 1 mm ϕ core silica fiber optic, while still providing an outlet for the gas (www.polymicro.com). The inlet of the device was coupled to the rest of the system by using a PEEK union. The advantage of this design over others (Appendix C), is that coupling of detection and system are facile, requiring no additional machining, no electrodes are in contact with the plasma, and there is no obstruction of viewing the plasma as occurs in Figure C - 2. Because there is no barrier between the electrodes external to the device, only plasma gases with breakdown voltages less than air, e.g. Helium, may be used internal to the cell otherwise an arc will form between the electrodes outside the tube (An image of the plasma is shown in Figure 4-2). It is possible however, to encapsulate the exterior and seal after creating a vacuum to prevent. All gas lines after the mass flow controllers were made of polytetrafluoroethylene (PTFE) tubing.

Figure 4-3. Helium plasma in a dielectric barrier discharge.

Atomic emission spectra, between 200-1100, nm were taken using an ocean optics QE65000 CCD spectrometer equipped with a 5 μm slit.   Nitrogen, Argon, and Helium were explored as possible carrier gases. Iodine spectra were acquired in the carrier by passing the gas though a PTFE tube filled with iodine crystals. The helium and iodine spectra are shown in Figure 4-3. Nitrogen and Argon spectra are provided in Figure C - 3 and Figure C - 4. Several predominant features were observed for iodine emission. A broadband, though relatively weak molecular fluorescence was seen spanning from ~425-550 nm, an intense excimer emission that tails into shorter wavelengths at 341 nm, and several atomic emission lines including the dominant lines at
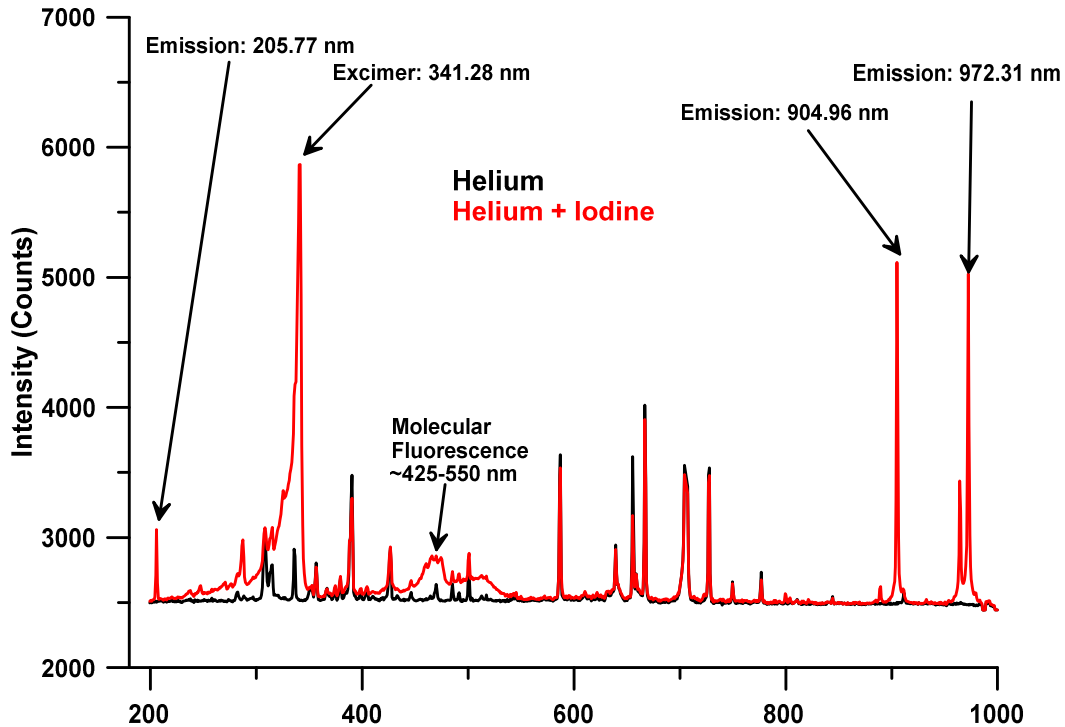
Figure 4-2. Atomic emission spectrum of helium and iodine

206, 905, and 972 nm. The excimer emission is known to involve a multiatom collision process for iodine[366] and may be expected to behave nonlinearly at low gas phase concentration. Additionally, numerous background lines exist in this region for all gases tested. In argon, there is little background in the region of 450-550 nm where iodine fluorescence is a maximum. This area can be measured sensitively using a photomultiplier tube equipped with an interference filter, but it was observed that at low concentrations of iodine, the background plasma emission is initially partially quenched before iodine fluorescence is observed at higher concentrations (Figure C - 5). This limited measurement to atomic emission lines at 206, 905, and 972 nm.

4.2.1 Gaseous Iodine Calibration Source

A gas phase calibration source was prepared for iodine as shown in Figure 4-4. A permeation tube was constructed of low density polyethylene. The tubing was approximately 2.5 mm in diameter with a wall thickness of 0.5 mm. A 5 cm portion of tubing was used. One end was melt sealed by placing the end in the tip of a propane torch flame till the LDPE became soft and was then pressed shut with pliers. The tube was then filled halfway with iodine crystals. The other end was melt sealed in the same fashion. The tube was kept thermostatted at 30 °C and continually purged with air. The
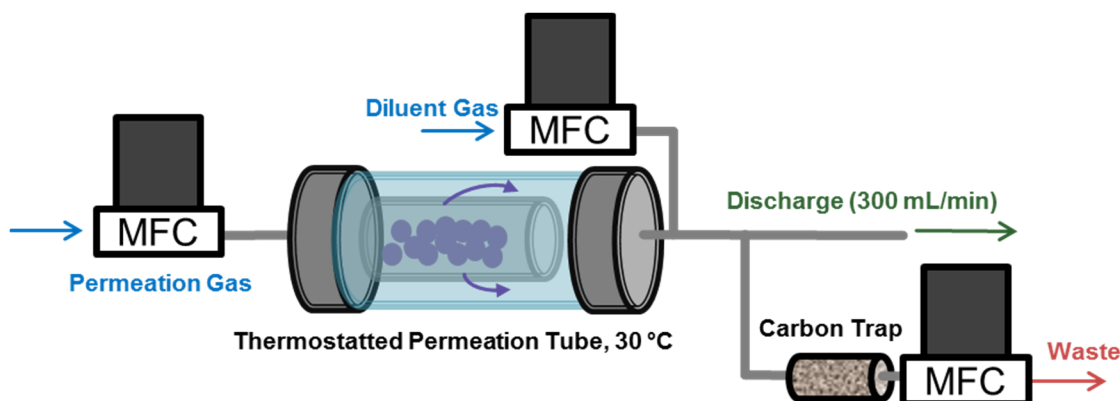
Figure 4-4. Permeation Tube Setup

permeation rate was measured by weighing the tube minimally on a weekly basis. Iodine

permeates through the wall of the tube at a constant rate, so long as the temperature is

constant and the concentration gradient is maintained constant by continuously purging

the exterior.[367]

Controlled concentrations of iodine could be introduced into the plasma using

three mass flow controllers (MFC). The first MFC was used to introduce a controlled flow

of gas (the same gas used for the plasma) through the permeation cell.. The gas passed

through a length of PTFE tubing to equilibrate it to the temperature of the permeation

tube. Dilution gas was introduced after the permeation cell to control the iodine

concentration. A third MFC was used to vent the excess flow through an activated

carbon trap to prevent corrosion of the MFC and maintain a constant flow through the
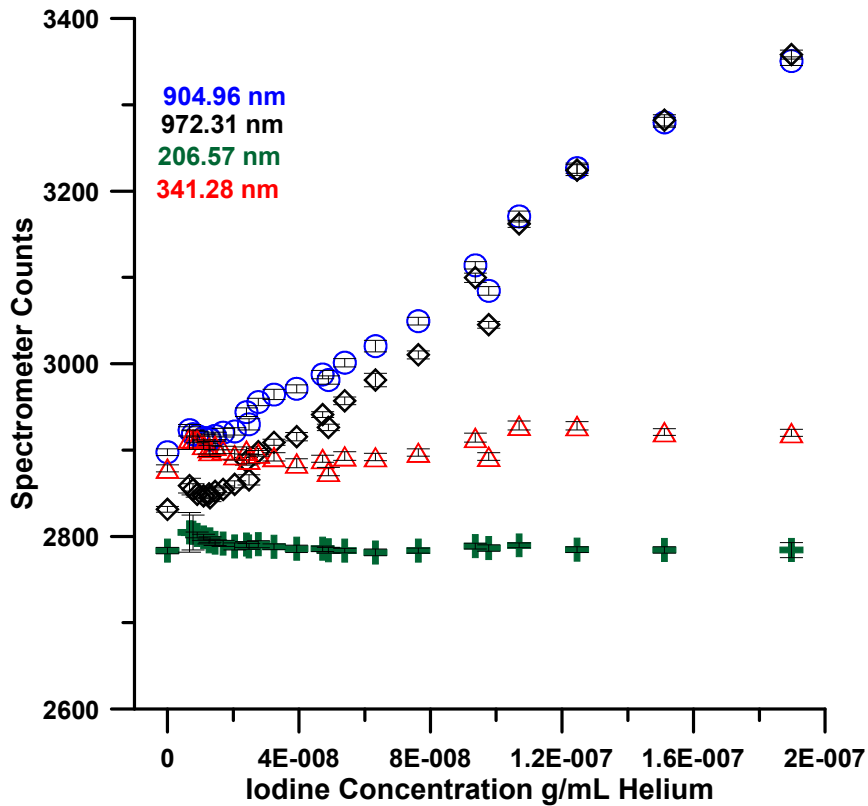
Figure 4-5. Emission intensities of several iodine emission lines

discharge cell. Plasma intensity is sensitive to pressure internal to the dieletric cell as well as flow through the cell, and it was found the current setup provided the most consistent results if gas flows must be changed.

The emission intensities of iodine at 206, 341, 905, and 972 nm were recorded using the CCD spectrometer from gas phase concentrations of iodine (in helium) in the range 5-200 ng/mL as shown in Figure 4-5. As expected, the excimer emission at 341 nm, though the most intense peak at high concentration, produces no effective response at low concentrations. The spectrometer was also not sufficiently sensitive in the deep UV to measure the 206 nm emission at these levels. The emission lines at 905 and 972 nm, had similar response, but the background at 972 nm is significantly lower than that at 905. For this reason the 972 nm line was selected for future studies.
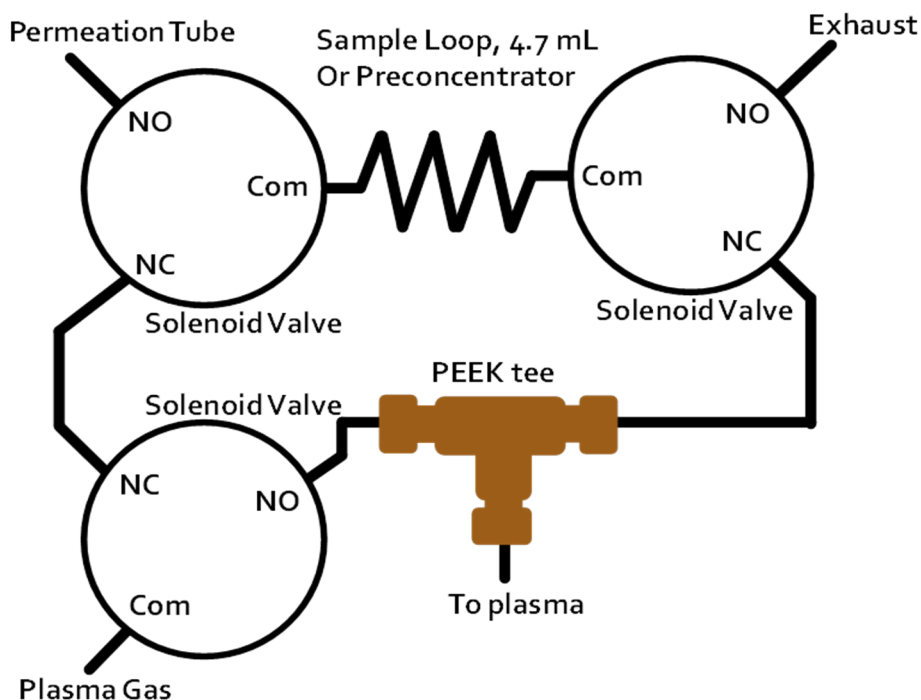
Figure 4-6 Three solenoid valve injection loop setup

4.2.2 Sample Loop Injection With an Avalanche Photodiode Detector

To improve sensitivity, and reduce the cost of the overall instrument design, a

designated detector was implemented. The detector is a Hamamatsu C4777-01

avalanche photodiode module, with a TEC cooled chip equipped with a 970 nm

interference filter with a 10 nm full width half maximum bandwidth (www.intor.com).

Three PTFE, 3 port solenoid valves (Neptune Research) were configured as

shown in Figure 4-6. NC and NO stand for normally open and normally closed,

respectively. Com is the common port. During the loading time, the valves are in the

normally open position. Plasma gas flows through the lower left solenoid valve to the

DBD to sustain a background plasma. The same gas is also routed through the

permeation tube setup to generate a controlled concentration of iodine. This travels
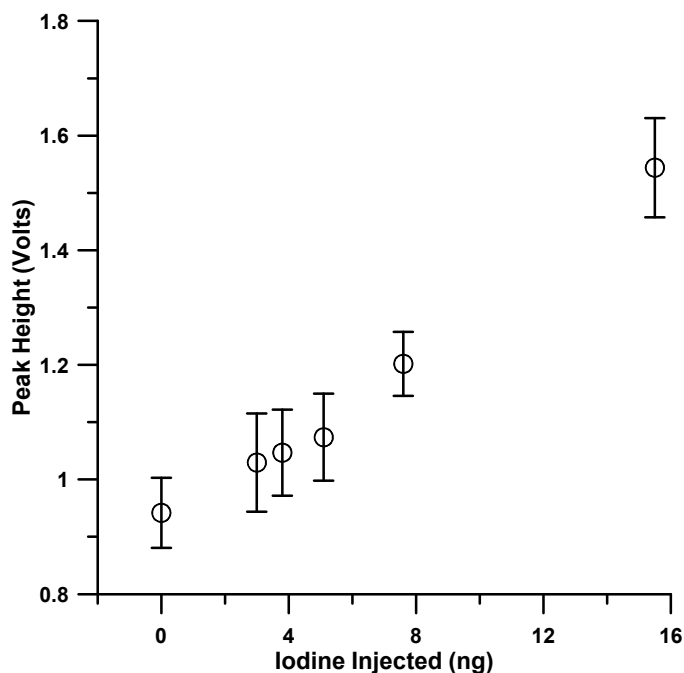
Figure 4-7. Loop injection of iodine

through the loop and is vented to the atmosphere. The valves actuate and the iodine in the loops is injected into the DBD as a sharp spike. The injection loop volume, including the valves, was measured to be 4.7 mL. The loop is replaced with a preconcentrator in subsequent experiments described later.

Using the loop injector, single digit nanogram levels of iodine are clearly measurable, Figure 4-7. If all the iodine present in a 1 mL sample of urine were concentrated, the present setup would provide more than adequate sensitivity for diagnosing severe deficiency.

4.3 Preconcentrator for Iodine

Preconcentrators were made from quartz-halogen lamps (Figure 4-8). The tungsten filament was of coiled-coil design. First, the glass envelope was removed using a diamond blade saw, near the base of the bulb (l'il trimmer, www.lapcraft.com). A Lapcraft 2 mm diamond drill bit was then used to drill ports into the base as well as through the tip of the device to fit 2.1 mm O.D. glass tubing (1 mm I.D.). One end of the glass tubing was slipped into PTFE tubing (14 gauge, standard wall) which could be coupled using ¼-28 PEEK fittings to the PTFE solenoid valves of the injection loop setup. The other end of the glass tubing was cemented into the quartz bulb using Resbond 940 LE ceramic adhesive (www.cotronics.com). Inactive portions of the filament (e.g. support struts) were coated with nail polish and allowed to dry, then the filament was coated with absorbing material (*vide infra*). Nail polish was subsequently removed with acetone. The base and the envelope were then sealed back together using the ceramic adhesive. The ceramic adhesive did not form an air tight seal, so the joints were then encased in a layer of JB Weld high temperature epoxy.
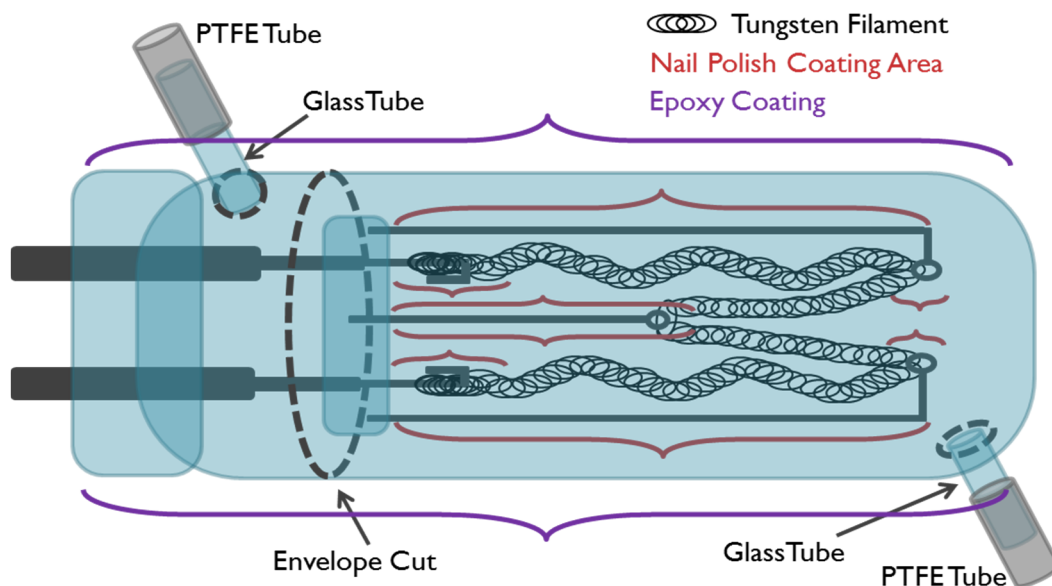
Figure 4-8. Iodine preconcentrator design

Several sorbents were tested as concentrators for iodine. Palladium was found to be the most suitable (See appendix C for other sorbents used). Palladium is known to be quite iodophilic.[368] Iodine binds to palladium through a chemisorption process and is not released until high temperatures. Palladium was electroplated using a slightly modified version of a plating solution described by Way et al.[369] In a 50 mL volumetric flask, 10 mg of palladium was dissolved in 30 mL of deionized water and 0.3 mL of 36.5-38% HCl (Macon). The flask was then filled up to the mark (~20 mL) with 28-30% NH_4OH (BDH). The tungsten filament was placed into 5 mL of the plating solution. The cathode was attached to the terminal of the bulb. The anode consisted of a platinum wire that was placed in the solution parallel to the filament. The plating solution was agitated using a magnetic stir bar. The voltage was raised till a current of 0.2 mA was flowing through the circuit. The solution was allowed to plate at this current for 10 minutes. After 10 minutes the voltage was raised slowly over ~20 seconds till a current of 40 mA was
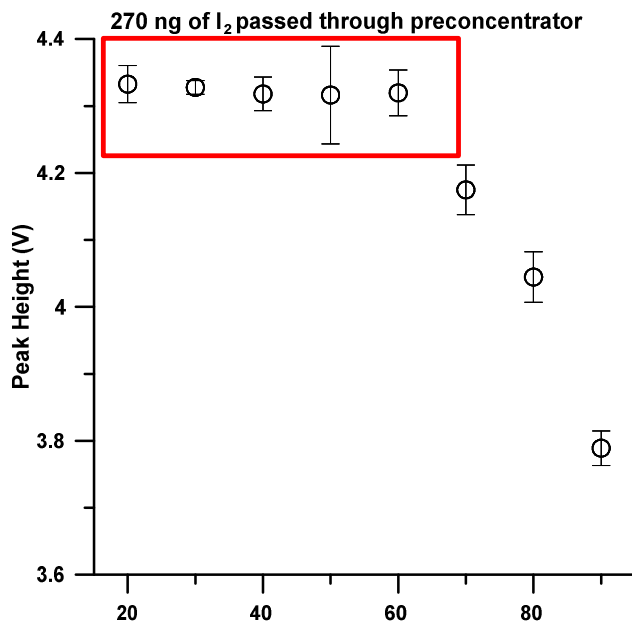
Figure 4-9. Effect of flow rate through the preconcentrator on the amount of
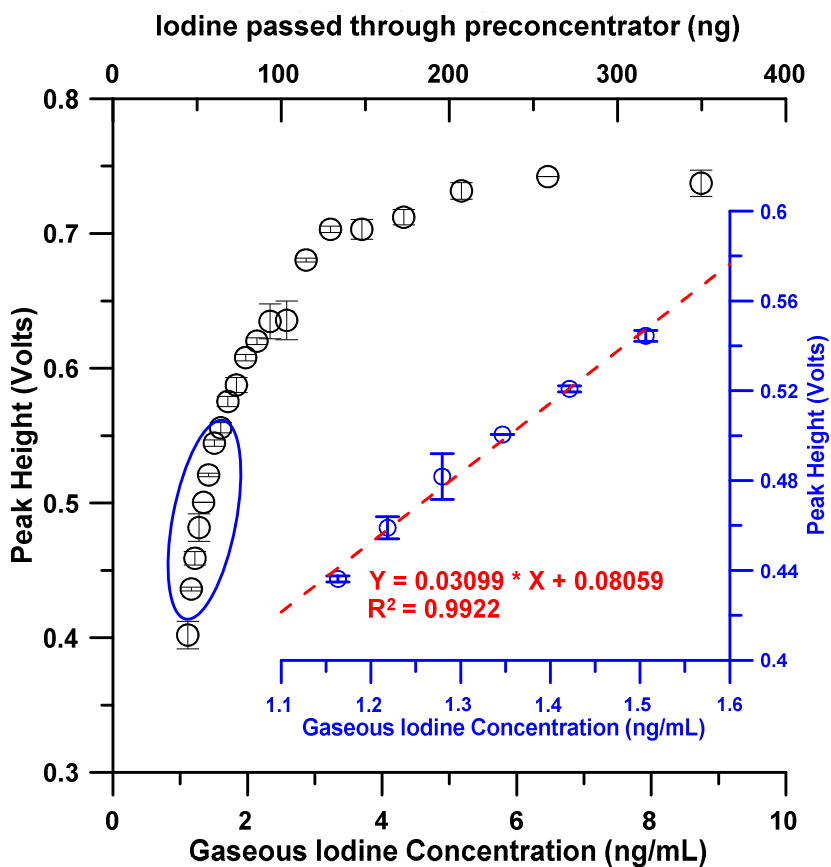
Figure 4-10. Ability of the preconcentrator to concentrate iodine at different concentrations of

gaseous iodine. The inset contains a magnified view of the low level injections to show the

device behaves linearly

94

reached. The solution was allowed to plate for another 30 minutes before being removed and rinsed with water and acetone to remove the nail polish. This plating scheme provided a high surface area , fine particle coating, apparent from the fact the metal appears black rather than lustrous.

The preconcentrator was evaluated using the injection loop setup described in Figure 4-7, but with the concentrator replacing the loop. The preconcentrator was first evaluated for iodine extraction efficiency as a function of flow rate (Figure 4-9). The flow rate through the system was altered from 20-100 mL/min, and the sample time adjusted accordingly so that the same amount of iodine passed through the concentrator regardless of the flow rate. It was found that at flow rates greater than 60 mL/min the peak height decreased significantly, indicating the there is a loss in capture efficiency at these flow rates. A plateau region (shown in red) below 60 mL/min is observed and is indicative of 100% extraction efficiency. A flow rate of 40 mL/min was selected for all future experiments to allow for compete extraction of iodine from the gas.

The preconcentrator was additionally evaluated for its linearity. The iodine concentration was adjusted using the mass flow controllers. The gas flowed through the preconcentrator at 40 mL/min for 1 min. As can be seen in Figure 4-10, the system behaves linearly up to 70 ng, at amounts higher amounts the capacity of the filament is reached. This particular concentrator was an early version and had low capacity due to the uniform plating current, subsequent versions made using the stepped plating current procedure described had capacities exceeding the measurable limit of the system. Figure 4-11 shows the a small amount of iodine measured using the current permeation tube setup . Only 17 ng of iodine was concentrated and still produced a peak with excellent signal to noise. As perspective, 1 mL of urine with 20 µg/L iodide contains 20 ng iodine. The system is more than adequately sensitive for diagnosing severe

deficiency cases, if all iodine present in the sample can be liberated and concentrated prior to analysis.
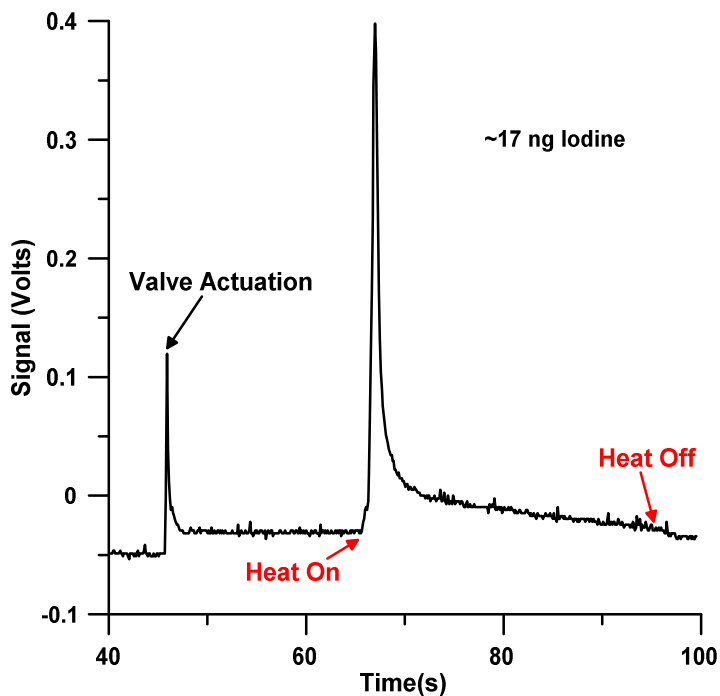
Figure 4-11. Sample measurement of low concentration iodine

4.4 Liquid Analysis

4.4.1 Setup.

A sampling system for performing liquid analyses was constructed as shown in Figure 4-12. A 5 mL Tekmar sparger with a sidearm injection port was used for purging iodine from solution in place of the permeation cell, while the rest of the solenoid valve setup remains identical to that used previously. During sampling, gas enters the sparger and passes through a porous glass frit. Iodine in solution (present as I_2) is transferred to the gas phase and is carried out of the sparger. The gas then passes through a solenoid
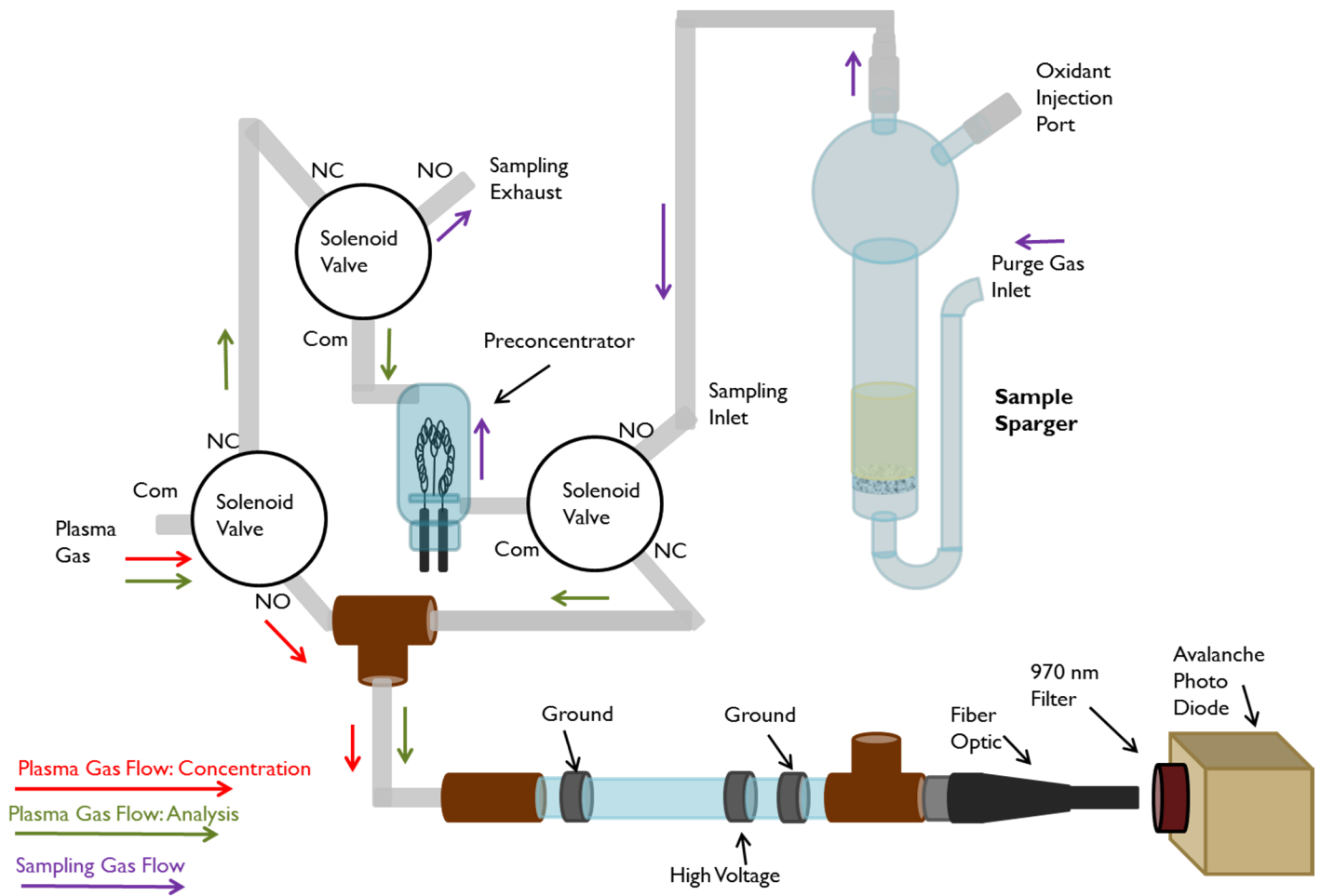
Figure 4-12. System setup for measuring iodine in liquids

valve followed by the preconcentrator where iodine is absorbed. The gas then continues

out a second solenoid valve that is vented to atmosphere. Once sampling is complete

the three solenoid valves are actuated and the plasma gas back flushes the

preconcentrator. The system is allowed to purge out water vapor and establish a stable

baseline for 30 seconds, at which point the filament is heated and iodine emission from

the plasma is measured. Colored arrows in the Figure 4-12 show the direction of gas

flow during concentration and measurement phases.

The system was optimized using 1 mL of a 500 µg/L solution of I⁻, prepared from

KI. I⁻ was oxidized using 50 µL of 30% H_2O_2 and 1 mL 2 mol/L H_2SO_4, saturated with

$(NH_4)_2SO_4$. The $(NH_4)_2SO_4$ serves as a salting out agent to improve iodine mass transfer

to the gas phase. Discussion of the salting out effect and oxidant is included in a

subsequent section. Samples were purged for 5 minutes prior to analysis. The plasma

gas flow was investigated for its effect upon the peak height between 100-500 mL/min

(Figure 4-13). A sparging gas flow of 40 mL/min was used. A drastic decrease in peak

height is observed for flow rates below 200 mL/min. Above 200 mL/min a gradual decline

in sensitivity was observed. 300 mL/min was chosen as the operating flow rate for future

experiments due to the precipitous decline in sensitivity near 200 mL/min. The collection

efficiency in the presence of water vapor was again verified. A sparging flow rate

between 20-80 mL/min was investigated (Figure 4-14). Sampling time was altered
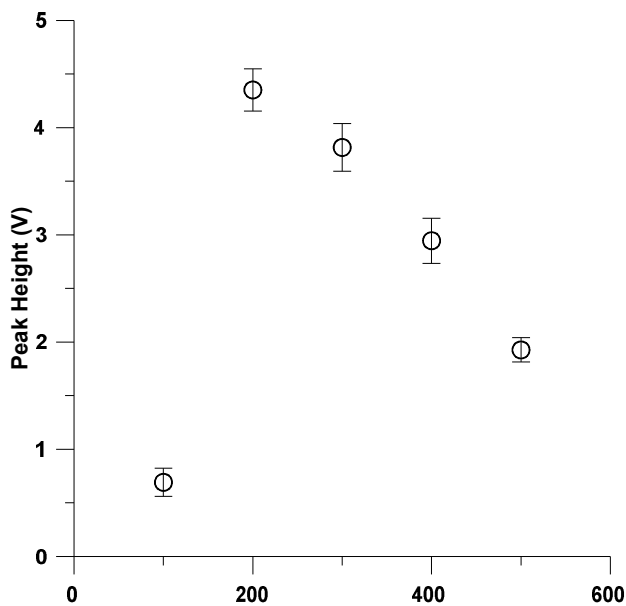
Figure 4-13. Optimization of plasma gas flow rate

between 100-500 mL/min
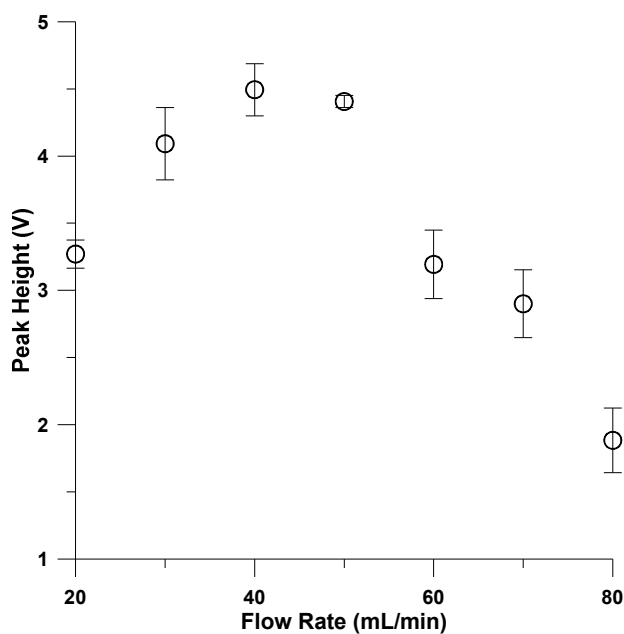
Figure 4-14. Optimation of sampling gas flow

between 20-80 mL/min

accordingly from 2.5 minutes to 10 minutes so that the total sampled air volume was the same. A peak in efficiency is observed at 40 mL/min. It is not fully understood why a decrease is seen below this value, when previously a plateau was seen to be reached when directly concentration gas phase I_2. It is possible the efficiency of purging is increased at higher flow rates. A foam develops and significant sample churning occurs, while at low flow rate no foam is formed above the liquid. The foam formed will likely improve the gas-liquid exchange and thus the efficiency of removal from the solution.

The time necessary for the complete reaction and removal of iodine from solution was also investigated. A solution as described above was purged in 2 minute intervals and the resulting peak measured. As can be seen in Figure 4-15, Iodine is easily liberated in under 4 minutes (2 samplings). No discernible amount of iodine is detected after in a third sampling, indicating a sparging time of 5 minutes is adequate for measurement of iodine in aqueous solution.
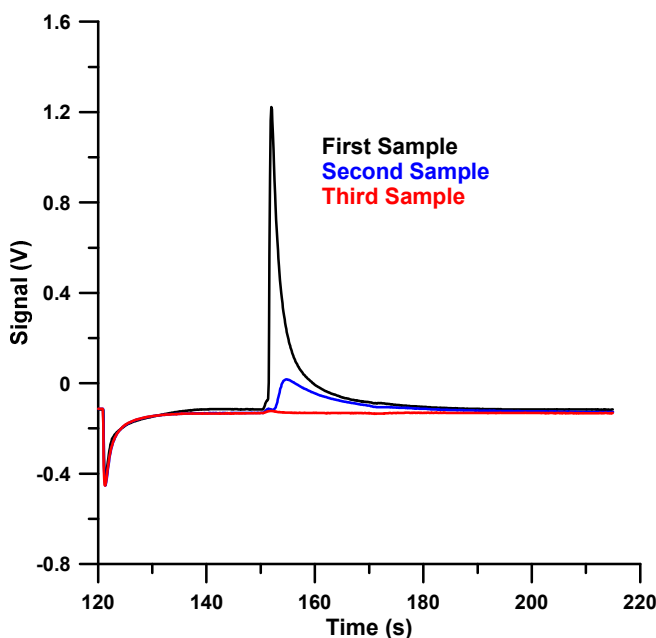
Figure 4-15. 2 minute repeative sampling of a 500 µg/L I⁻ solution

4.4.3 Synthetic Urine Matrix.

A synthetic urine matrix was prepared according to Nham.[370] To a 1 liter

volumetric flask was added 14.1 g NaCl, 2.8 g KCl, 17.3 g Urea, 1.6 mL 29.85% NH_4OH,

0.6 g $CaCl_2$, and 0.43 g $MgSO_4$. The mixture was diluted to the mark using 0.02 mol/L

HCl. This mixture was substituted for water. Use of the mixture provided poorer results

than water when using the oxidant mixture described above, as shown in Figure C - 7. A

second aliquot of peroxide was added in case the oxidant was exhausted due to

oxidation of urea in the matrix with no subsequent release of iodine. Iodine is known to

form a weak complex with Cl^- which to form I_2Cl^-.   Given the high Cl^- present, this could

potentially impede volatilization[371,372]. A measure of iodine volatility in the presence of
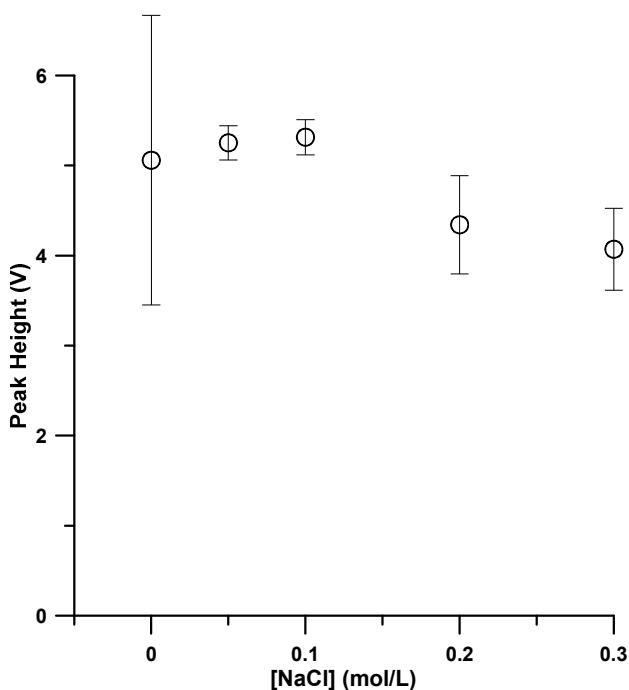
Figure 4-16. Effect of added NaCl on the volatility of

chloride was carried out to determine whether this could significantly impact iodine

volatilization. An I_2 standard was prepared by first measuring iodine crystals in a sealed 25 mL volumetric flask. Ethanol was then added to the mark to prepare a solution of approximately 990 mg/L I_2. This solution was further diluted to 50 mg/L in ethanol. To 1 mL of sample with NaCl concentration between 0-0.3 mol/L was added 10 µL of the 50 mg/L I_2 solution to provide a final concentration of 500 µg/L I_2. 200 µL of 1 mol/L H_2SO_4 saturated in $(NH_4)_2SO_4$ was added and the solution purged for 5 minutes and the iodine measured. The peak height is provided in Figure 4-16. Overall, very little impact is observed at the concentration of salt used, indicating that Cl^- complexation is not the cause for the observed behavior. H_2O_2 is a potent oxidant, capable of producing Cl_2 and HOCl from solutions of Cl^-. It was found that continued use of H_2O_2 in the presence of Cl^- resulted in eventual degradation of peak shape and reduced capacity of the preconcentrator. It was thus necessary to evaluate other potential oxidants for the production of I_2.

4.4.4 Search for an Oxidant.

The oxidants H_2O_2, Fe^{3+}, NO_2^-, and $Cr_2O_7^{2-}$ were explored primarily as potential oxidants. Ce^{4+} showed promising results initially in DI H_2O, but reacted immediately with the synthetic urine matrix as did MnO_4^-. NO_2^- has been used extensively as an alternative to H_2O_2 which has by far been used as the most frequent oxidant for iodine vapor generation.[338,342,346] Vtorushina et al.[342] conclude that NO_2^- provides the better results compared to H_2O_2 for the online vapor generation of I_2. The oxidation procedure used was adopted and used here; 300 µL of a 50 mM $NaNO_2$ / 0.5 mol/L HNO_3 solution was added to 1 mL of sample. Use of this mixture however was found to lead to rapid reduction in the capacity of the preconcentrator. Figure C - 8 shows that when 3 samples of the synthetic urine matrix are measured subsequently using a sampling time of only 30

101

seconds, less than half the peak height is obtained for the second injection as the first injection. This trend continues till there is no iodine measurable at all. The concentrator is easily regenerated upon rinsing with 2 mol/L HCl followed by water and acetone. It is possible that NOx fromed with the use of NO_2^- is adsorbed on the palladium

Fe^{3+} was explored as an ideal alternative. No volatile species are produced from the oxidant, the reduction potential is sufficient for oxidation of I^- ($E°$ for $Fe^{3+} + e^- = 0.771$ volts, $E°$ for $I_2 + 2 e^- = 0.5355$, vs. standard hydrogen electrode),[373] and there is no generation of hazardous waste. The process, however is an equilibrium and large amounts of Fe^{3+} are required to induce formation of I_2.[374] Addition of 100 µL a saturated solution of $FeCl_3$ to 5 mg/L of I^- showed that removal of I_2 is a very slow process requiring over 30 minutes to complete. It is also observed that the peak intensity increases with increasing sample measurement from 1 to 5 before decreasing again. This suggests iodine oxidation by Fe^{3+} may not be a straightforward process, requiring formation first of
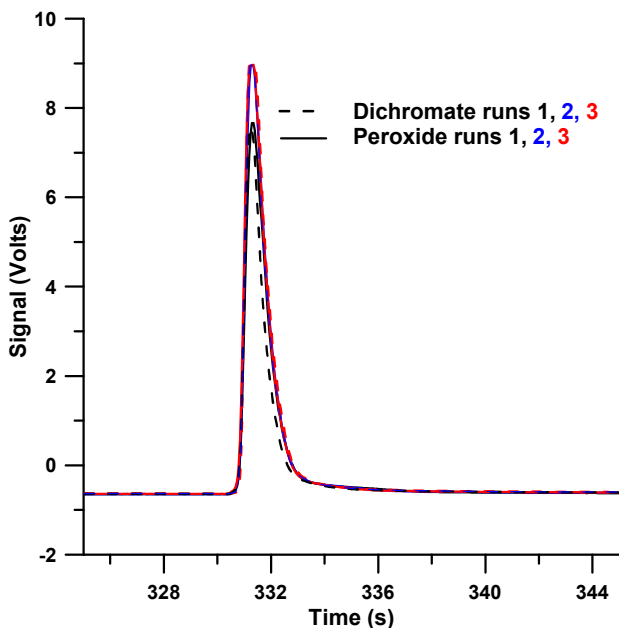
Figure 4-17. Comparision of peroxide and dichromate as oxidants using 500 µg/L I^-.

an intermediate followed by subsequent formation of I_2 as reported previously.[375] While

30 minutes is an acceptable incubation time prior to analysis, the rate of reaction with

respect to I^- is second order and to be able to measure I at concentrations below 10 µg/L,

an impractically long incubation period will be required.

$Cr_2O_7^{2-}$ was initially avoided due to its toxicity, but was explored as an alternative

to H_2O_2 to determine whether formation of the presumptive chlorine species could be

reduced while still liberating iodine. Its ability to oxidize I_2 compared to that of H_2O_2 was

examined first. A saturated solution of $K_2Cr_2O_7$ was prepared. To a 1 mL sample of 500

µg/L I^- was added 1 mL 2 mol/L H_2SO_4 saturated with $(NH_4)SO_4$. To the sample was

added 50 µL of either 30% H_2O_2 or $K_2Cr_2O_7$. Each oxidation method was run in triplicate

and is shown in Figure 4-17. $Cr_2O_7^{2-}$ produced nearly identical results to that of H_2O_2,

with average peak height and area for Cr_2O_7 only 0.28% and 3.1% less than that of H_2O_2.

Use of the synthetic urine matrix though resulted in a gradual decline in signal as

observed for H_2O_2, but the degree was significantly less than that observed previously for

H_2O_2 (Figure C - 10). The oxidation potential of $Cr_2O_7^{2-}$ is pH dependent[376] so that

adjustment of the acid concentration may in fact reduce chloride interference since I^- has

a lower oxidation potential than that of Cl^-. The rate of oxidation however is also

dependent upon the concentration of the acid, so that a balance must be struck between

reducing the interference of Cl^- while maximizing the rate of production of I_2.[377]

Experiments were carried in which the concentration of H_2SO_4 in the acid/salt solution

was adjusted from 0 to 2 mol/L. 1 mL of 500 µg/L solution was mixed with the acid/salt

solution and 50 µL $K_2Cr_2O_7$, then sampled for 5 minutes at 40 mL/min. No iodine is seen

below 0.1 mol/L of H_2SO_4 (Figure C - 11). The measured iodine signal rises rapidly going

from 0.1 to 1.0 mol/L H_2SO_4 before decreasing at 2 mol/L. The standard deviation is

greater for 2 mol/L H_2SO_4, brought about by the gradual degradation of the

preconcentrator. Use of 1 mol/L H_2SO_4 was selected for subsequent optimization of the $Cr_2O_7{}^{2-}$ solution.

Because $Cr_2O_7{}^{2-}$ is toxic, the minimum usable amount was sought after. A solution of 0.25 mol/L $K_2Cr_2O_7{}^{2-}$ was prepared. 500 µg/L of I^- in synthetic urine was used as the sample to which was added 1 mL of the 1 mol/L H_2SO_4 saturated with $(NH_4)_2SO_4$. $Cr_2O_7{}^{2-}$ was added in volumes between 5-200 µL. The liberated iodine was found to be dependent upon the concentration of $Cr_2O_7{}^{2-}$ in solution (Figure 4-18). The system shows a first order dependence with respect to the $Cr_2O_7{}^{2-}$ concentration in the final solution. At 5 minutes of reaction time, formation of I_2 is not complete. The samples were allowed to incubate prior to analysis in covered glass test tubes to determine whether complete oxidation could be obtained without loss of I_2. A 50 µL portion of $Cr_2O_7{}^{2-}$ (approximately 6.1 mmol/L in the final solution) was added to the samples which were allowed to incubate between 0-180 min before analysis. A 5 minute purging time was used. Increases in peak area are observed up until 15 minutes of incubation time, after which peak area decreases rapidly. I_2 may be lost at the longer reaction times, but
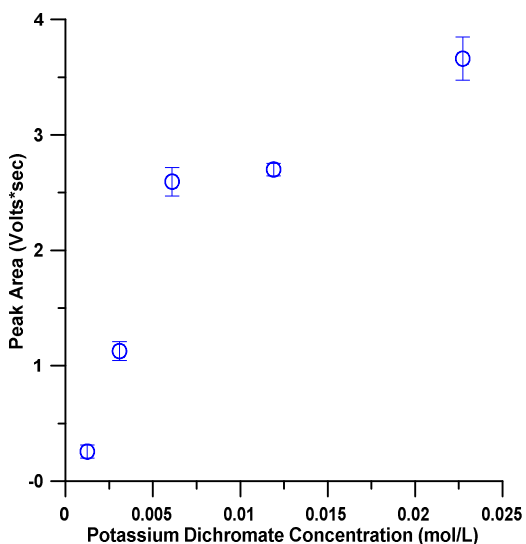
Figure 4-18. Peak area of measured iodine as a function of volume of 0.25 mol/L $Cr_2O_7{}^{2-}$
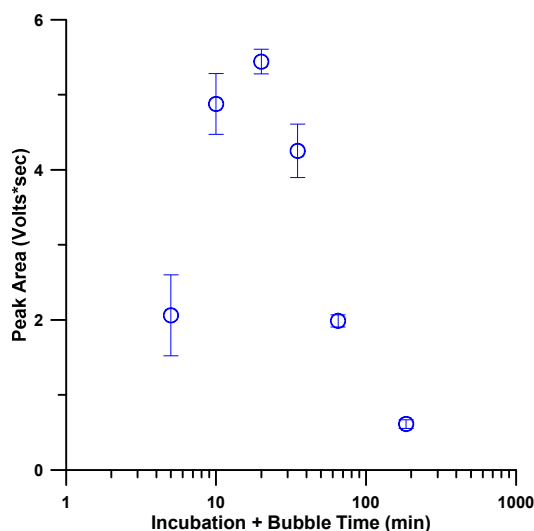
Figure 4-19. Effect of incubation time on measured iodine
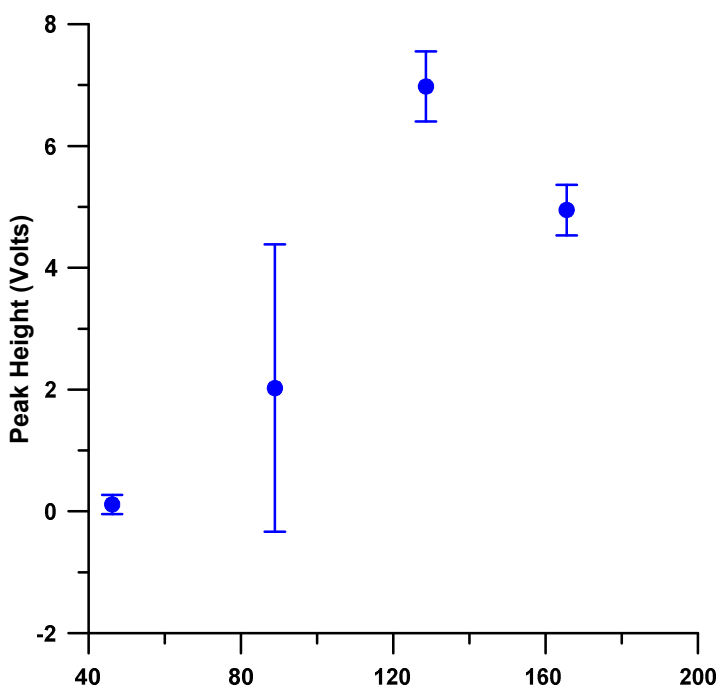
Figure 4-20. Effect of Cu^{2+} concentration on liberated iodine

it was found this decrease is irreversible indicative that chlorine species might be generated at a much slower rate and thus at longer incubation sufficient Cl$_2$ is generated that causes irreversible damage to the preconcentrator through oxidation to PdCl$_2$ which is not thermally labile.

It is well known that Cu^{2+} catalyzes the reaction between Cr$_2$O$_7^{2-}$ and I$^-$.[378,379] Based on the previous acid optimization experiment, only 0.200 mL of 1 mol/L H$_2$SO$_4$ saturated in (NH$_4$)$_2$SO$_4$ was used. 50 µL of 0.25 mol/L and H$_2$O$_2$ were explored as oxidants, using 1mL 500 µg/L I$^-$ in DI H$_2$O as a test solution. At this acid level essentially zero I$_2$ is liberated from solution when only Cr$_2$O$_7^{2-}$ is used (Figure C - 12), and even H$_2$O$_2$ liberates only a fraction of the iodine present. When however 50 µL of 1.2 mol/L CuSO$_4$ is added, I$_2$ is liberated readily. The optimum value of CuSO$_4$ was explored. Synthetic urine matrix containing 1 mg/L I$^-$ was used, with 0.2 mL of the acid solution, and 50 µL of

0.25 mol/L $Cr_2O_7^{2-}$. 1.2 mol/L $CuSO_4$ solution was added from 50-200 µL. 200 µL was chosen as the optimum value. Below 150 µL the variability greatly increased. Complexation with Cl^- may be a critical factor so that no gain is seen when Cu^{2+} is at concentrations less than the amount necessary to complex chloride. The total chloride present in the urine matrix is ~0.29 mol/L and for the formation of $CuCl_4^{2-}$, Cu^{2+} must minimally be at 0.072 mol/L. This is in agreement with the data observed where signal begins to increase at approximately 90 mmol/L. Use of higher than necessary concentrations of Cu^{2+}, does however have a slight detrimental effect; Cu^{2+} reacts with iodide in a disproportionation reaction making the insoluble compound CuI. It is likely this is as a result of a reduced reaction rate. Multiple samplings from a single standard show that when the sampling time is increased to 10 minutes (Figure C - 13), little iodine is evolved in subsequent samplings. Thus 10 minutes was selected as the optimum sampling time with the current oxidation conditions. Cu^{2+} is also known to catalyze oxidation of I^- by using other oxidants,[380-382] thus a variety of alternatives were tested to see whether improvement could be made upon addition of Cu^{2+} (Figure C - 14). No other oxidant was found to provide results comparable to that of $Cr_2O_7^{2-}$.

4.4.5 Linearity of Iodine Evolution. Calibrations were prepared using the optimized method described above. Figure 4-21 shows the best results obtained using the dichromate-copper oxidation mixture. The system is clearly nonlinear at low concentrations. Despite previous measurements of single digit nanogram levels of iodine, the current method cannot effectively distinguish standards below 50 µg/L. Once atomic I has been liberated, the formation of I_2 can intuitively be expected to be second order in the initial I^- present. Therefore, production of I_2 may be rate limited. Multiple measurements of the same sample beyond 10 minutes at the concentrations probed here, however, show essentially no iodine evolves beyond 10 minutes regardless of the concentration, in agreement with the rate study above. Confident in the ability of the system to concentrate low concentrations of iodine from solution we investigated the volatility of I_2 in the absence of oxidant or possible interfering substances in the matrix.
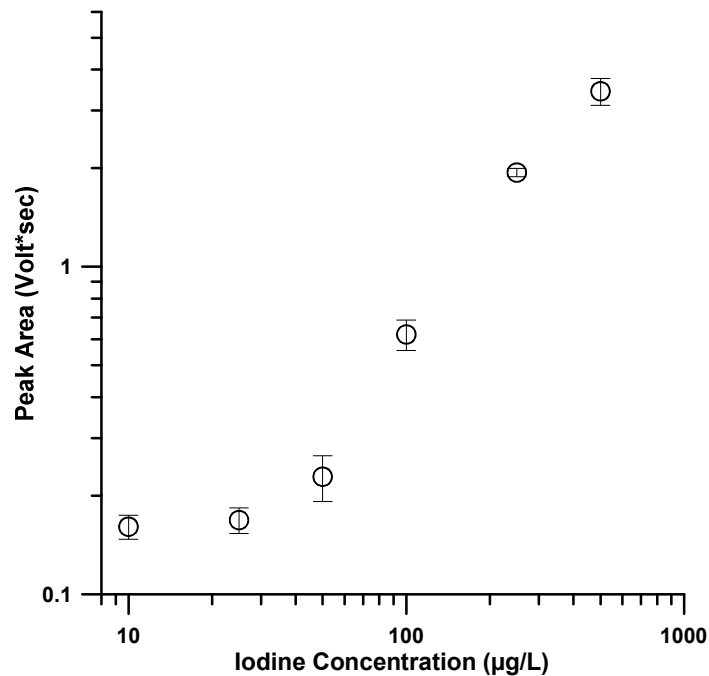
Figure 4-21. Calibration plot prepared from iodide in synthetic urine following vapor generation and preconcentration. Note both axes are logarithmic.

0.5 mL of DI H_2O was used as the matrix. Less sample volume was used to extend the range of the system to higher iodine concentration. To the water was spiked I_2, from the previously described I_2-ethanol solution, at levels from 25-1600 µg/L. 0.1 mL of H_2SO_4 saturated with $(NH_4)_2SO_4$ was added. The solution was then purged for 5 minutes prior to analysis. Results are shown in Figure 4-22. Note that the axes are in logarithmic scale. Two distinct regions are apparent adjacent to 200 µg/L. Power fits have been applied to the data to determine the dependence upon iodine. Below 200 µg/L the dependence shows an approximate square root relationship (power of ~0.5). Above this level, iodine becomes second order with respect to concentration. The nonlinearity observed here is discussed in much greater detail in chapter 5 of this dissertation. Addition of greater amounts of the acid/salt solution was explored to determine whether the volatility could be improved. It was observed (Figure 4-23), that there is an improvement at low concentrations. However, addition of more salt/acid results in a dilution of the sample solution, which results in an overall decrease in the signal given the nonlinearity of the system. The value circled in red is the amount of salting out solution used in all previous experiments.
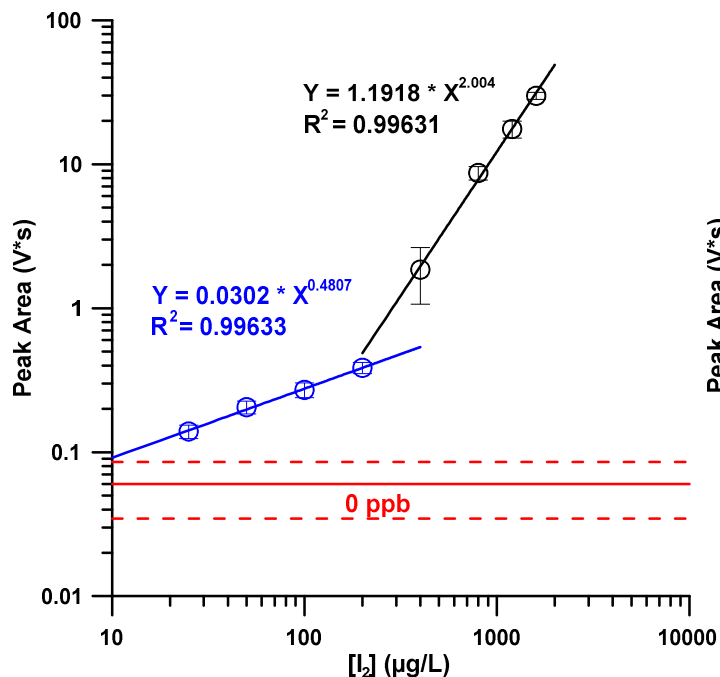
Figure 4-22. Response of I_2 purged from solution,

note logarithmic scaling used for axes
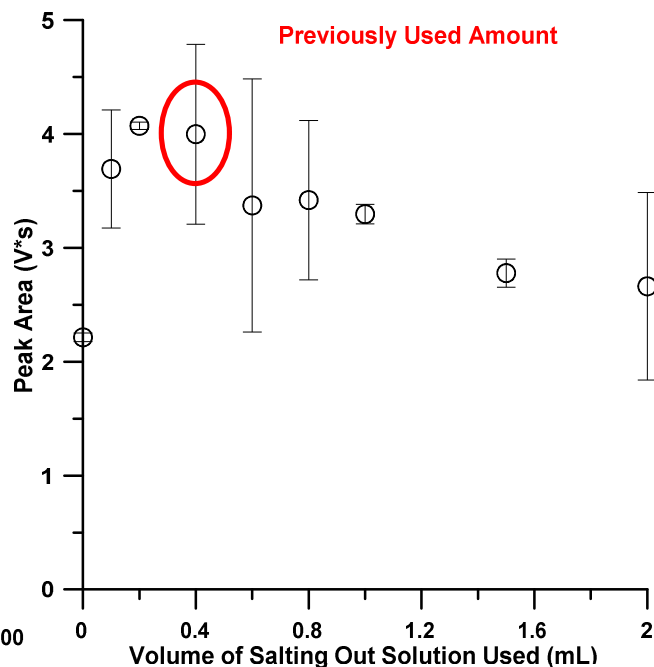
Figure 4-23. Effect of volume of "salting-out"

solution added

4.5 Alternative Approaches to Generation of I_2 Vapor

4.5.1 Complete Sample Vaporization

Due to the nonlinearities observed for solution based I_2 evolution, an alternative

approach was tested: evaporation of the entire sample solution. We had pursued the

belief that as the sample solution is evaporated, iodine in solution will concentrate and

the volatility will improve till the sample solution and thus iodine are completely removed.

The device shematic is shown in Figure 4-24. The preconcentrator and sample

apparatus were placed inside a Shimadzu GC-8A gas chromatography oven to provide

temperature control. Significant accommodations needed to be made. Due to the

increased flow rate through the preconcentrator caused by boiling of the sample solution,

a more efficient preconcentrator design was needed. The tungsten filament from two

quartz-halogen bulbs was carefully removed from the struts. The filament was coiled

around a tungsten wire (0.5 mm in diameter) with a U-shaped end to hold the filament.

Two filaments were coupled together using an S-shaped tungsten wire. The wire was

then treated as before, covering the connecting portions with nail polish and plating

palladium. The device was then strung through a glass tube (6.5 mm O.D., 4 mm I.D.).

The tube was connected to 2 PEEK crosses using ¼-28 PEEK nuts and ferrules. The
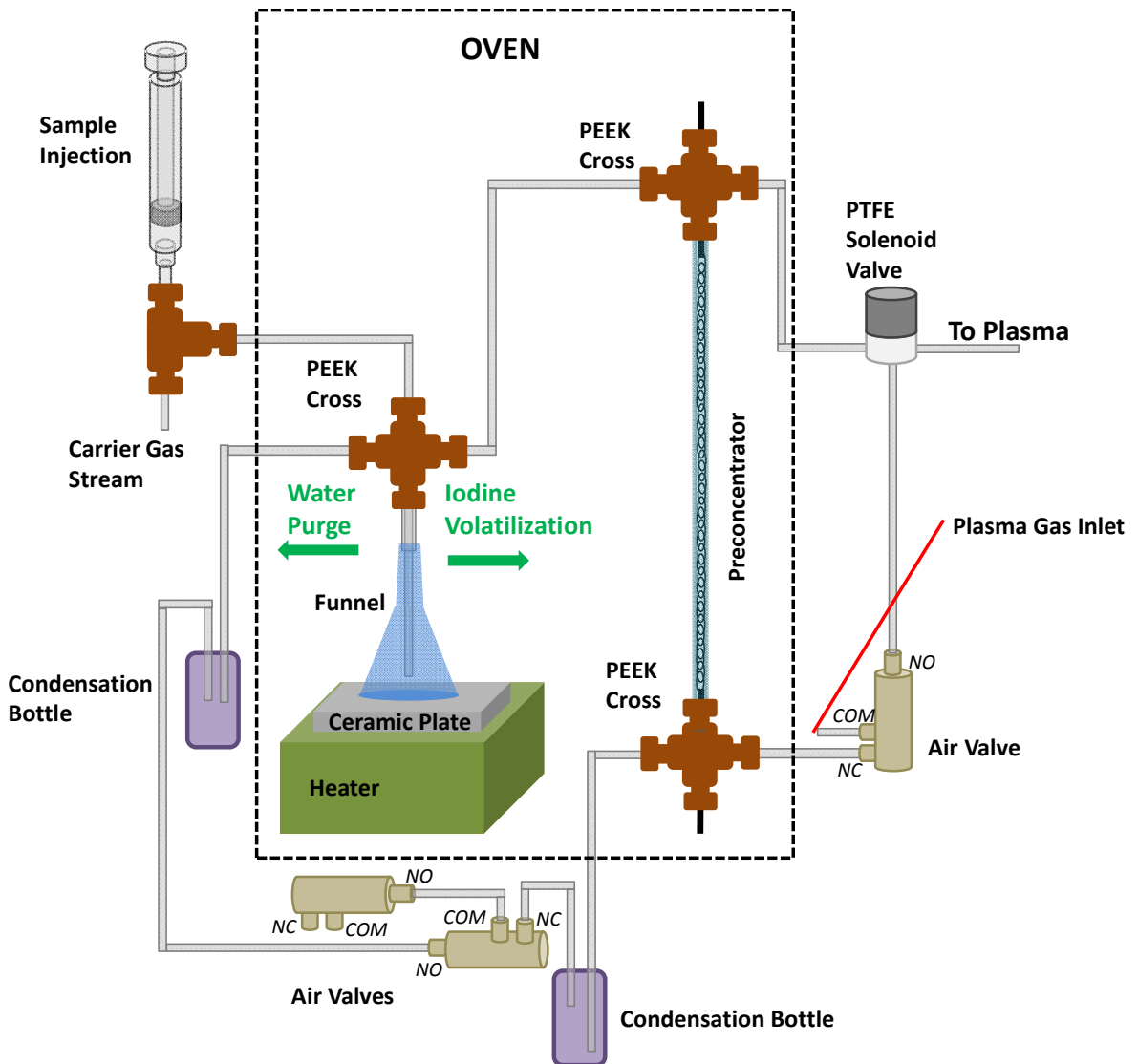
Figure 4-24. Setup used for complete sample vaporization

tungsten wires were pass through the PEEK cross. PTFE tubing and another peek nut and ferrule was used to form a seal around the tungsten wire. On the other end the tungsten wire was pulled till the filament was taught and suspended from the glass tube, then sealed using PTFE tubing and PEEK nut and ferrule. This new preconcentrator was longer with a lower empty-volume around the coil and thus improved collection efficiency.

The valves used were not rated to the temperatures reached here and needed to be kept outside the oven. The valve diagram shown was sufficient to alter gas flows w/o being internal to the oven. An additional valve was added to allow a prevaporization step. Ideally this would allow the evaporation of the bulk of the solution rapidly before addition of oxidant and a more controlled evolution and measurement. The sampling device consisted of a ceramic well plate. Each well had a maximum capacity of 1 mL. Over one of the wells was cemented a glass funnel that was inverted. Around the edge of the cement was added high temperature silicone glue to prevent gas leakage. Through the funnel tip was push fit PTFE tubing. This tubing connected directly to a PEEK cross. Through the cross was run PTFE tubing till it reached the bottom of the well. This tubing was used for introduction of sample, oxidant, and carrier gas. This tubing was then connected to a Tee, where sample could be introduced into the purge gas stream. A 77 watt heating tape (Minco) was attached to the bottom of the ceramic plate using kapton tape to allow higher temperature heating of the sample, while the oven could maintain the temperature above the condensation temperature.

The system was evaluated first using I_2 dissolved in ethanol at a concentration of 1 mg/L. The volume of this solution was changed to alter the amount of I_2 present in the system. The oven was used to evaporate the sample at a temperature of 70 ºC for 10 minutes using a sampling flow of 40 mL/min. The response as a function of total iodine injected is shown in Figure 4-25. The system performance is excellent, capable of

measuring 10 ng of I_2. When the system was evaluated, however, using I_2 spiked into DI H_2O, I_2 volatility was found to still be much less than that anticipated (Figure 4-26). Some improvement could be gained by addition of acid to the solution, but this was minimal at the levels of interest. We attribute this phenomenon, as discussed in chapter 5, to the rapid disproportionation of I2 into OI-, I-, and other higher oxyiodides. The ceramic plate could not be heated to a temperature that resulted in further liberation of iodine without first causing damage to the silicone sealant of the sampling device.
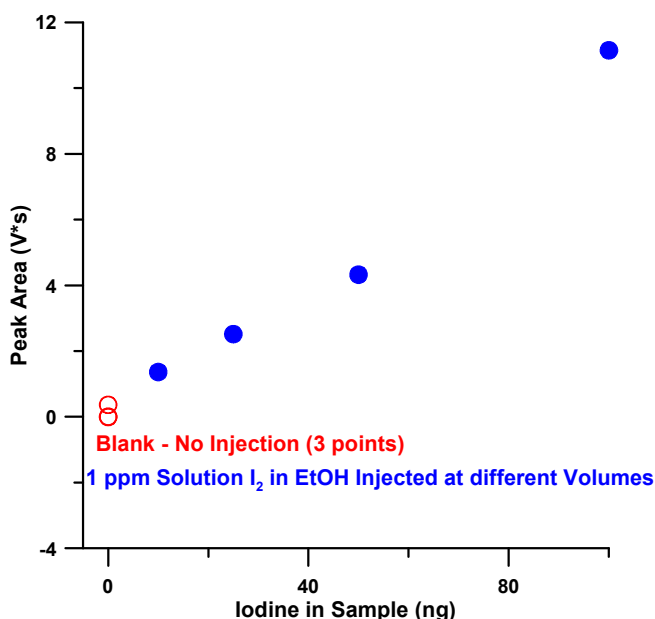
Figure 4-25. Response of I_2 dissolved in Ethanol using the vaporization apparatus
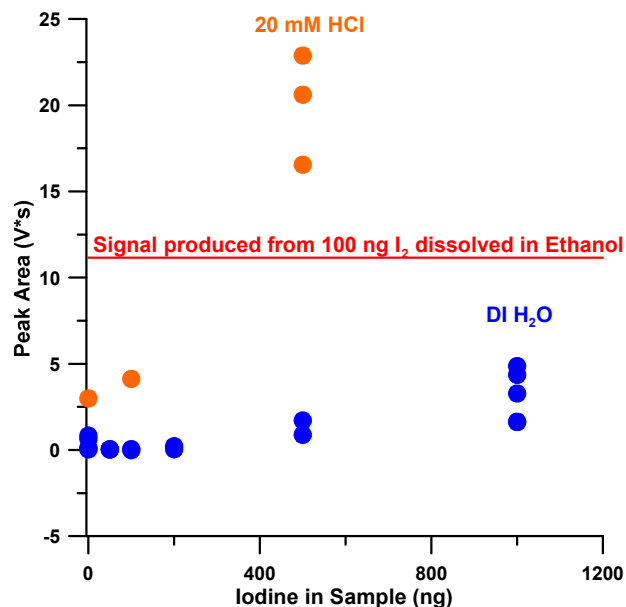
Figure 4-26. Iodine response measured from aqueous solutions of I_2

4.5.2. Measurement as CH_3I.

CH_3I is a volatile liquid in the pure form. It has a 20x lower henry's law solubility than I_2,[383] which should make it easier to remove from aqueous solution than I_2. Methyl iodide has been generated readily from iodide in aqueous solution using dimethyl sulfate[384] or UV irradiation and acetic acid.[385] Additionally, CH_3I is not as easily
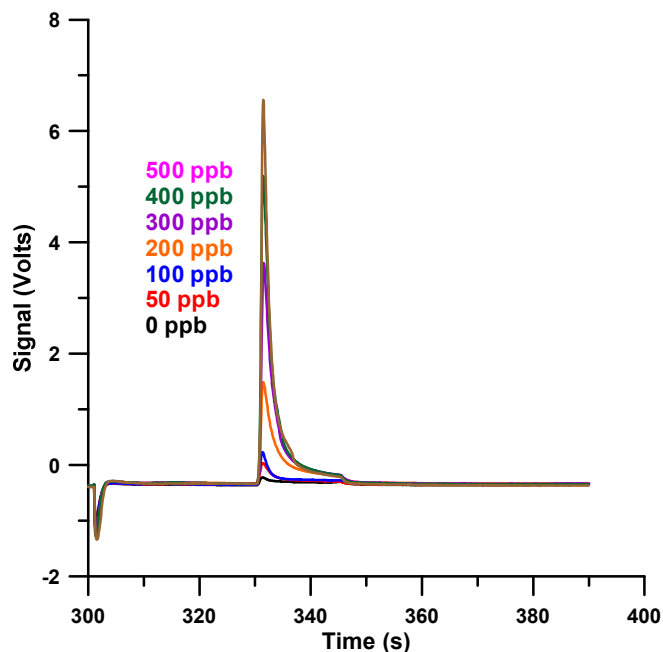
Figure 4-27. Iodine signal response of CH$_3$I decomposed and preconcentrated
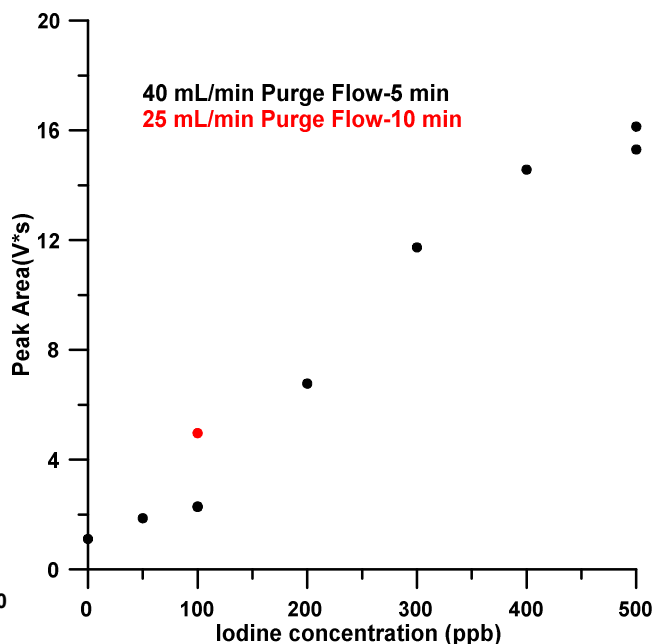
Figure 4-28. Peak area of CH$_3$I standards decomposed using UV light and preconcentrated as I$_2$

hydrolyzed in aqueous solution thus preventing the observed nonlinearity. CH$_3$I may be measured directly in the plasma, the energy is sufficient to break C-I bonds, generate atomic I, and and produce the characteristic iodine emission spectrum. Alternatively, CH$_3$I is quite labile when irradiated with UV, generating I$_2$ in situ. Figure C - 15 shows a small volume of CH$_3$I (~200 µL) stored in a sealed quartz cuvette before and after irradiation with a mercury pen lamp. The solution develops a deep maroon color from formation of I$_2$. The system in Figure 4-12 was adapted by inserting a quartz coil (length: 18 cm, coil O.D.: 1.5 cm, tubing O.D. 3.24 mm, tubing I.D. 1 mm, 50 turns), with a mercury pen lamp (length: 17.5 cm, width 6.5 mm) inserted in the annular portion in series between the sparger and the first solenoid valve ahead of the preconcentrator. A pilot test of samples between 0-500 ppb showed excellent results (Figure 4-27 and Figure 4-28). At low concentrations, deviation from linearity was observed, but this was determined to be due to the low residence time in the UV cell. When the

113
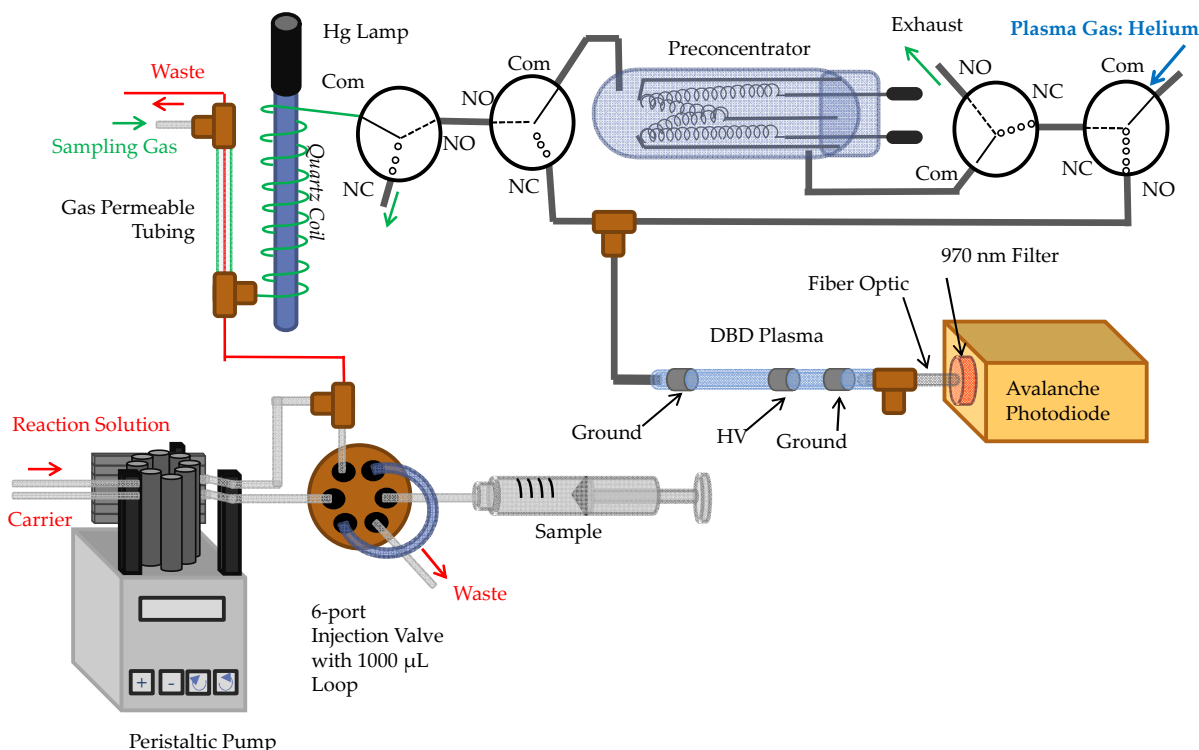
Figure 4-29. Flow injection setup for generating CH$_3$I followed by

photodegradation and preconcentration

preconcentration flow rate was decreased, accompanied by a simultaneous increase in

preconcentration time, the signal was improved. Using CH$_3$I the sensitivity of the system

is finally realized; 50 ng of iodine produces more than 1 volt in peak height.

Because CH$_3$I is easy to remove from solution, active sparging from solution is

not required. A system was constructed to utilize silicone rubber tubing as a gas liquid

separator as shown in Figure 4-29. A peristaltic pump is used to pump carrier solution

through a 6 port injection valve and to a PEEK tee, where the sample and carrier are

mixed with a reaction solution to be used for the generation of CH$_3$I. The solution then

flows through a gas liquid separator (GLS). The GLS consists of 12 cm of silicone rubber

tubing (0.02" I.D. 0.03" OD). 2 lb nylon fishing line is fed through the tubing. The fishing

line is then fed through 20 cm of 28 gauge standard wall PTFE tubing on one side, and

80 cm on the other with excess fishing line on each end. The silicone rubber tubing was

then slipped over the PTFE tubing to a length of approximately 1 cm on each end. The

silicone tubing was securely sealed around the PTFE tubing. The remaining active

length of silicone tubing (10 cm) was stretched to 60 cm. The silicone tubing adjacent to

where it joined the PTFE tubing was pinched. Slowly, the tension of the silicone tubing

was released while still pinching. The pinching prevents the nylon fishing line from

evacuating the silicone tubing. Once tension is released, a self assembled helical coil

exists inside the silicone tubing (Figure C - 16). This coil serves to disrupt laminar flow

and improve mass transfer to the wall of the tube.   A 0.5 mL sample was injected onto

the system using a carrier flow rate of 0.5 mL/min. The system was allowed to sample

for 5 minutes to allow the line to be completely cleared of CH_3I before analysis. A sample

injection is provided in Figure 4-30. 250 µg/L I, present as CH_3I is injected onto the

system. Excellent response is obtained; this would approximately correspond to the total

iodine present in a 1 mL urine sample of a healthy individual.
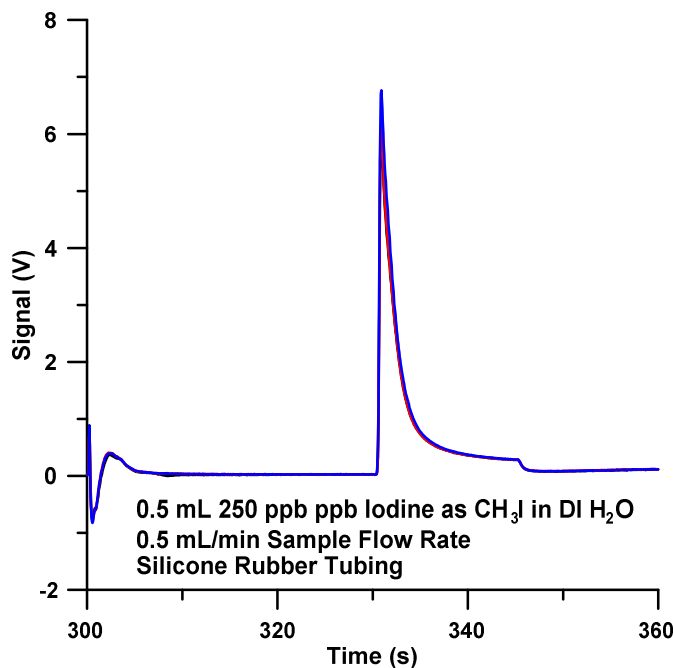
Figure 4-30. Iodine peak using gas permeable tubing to separate

CH_3I from aqueous solution

Grindberg and Sturgeon have previously reported generating CH_3I using a mercury source and acetic acid using a mercury lamp built into the spray chamber of a pneumatic nebulizer[385]. We attempted to use a similar method using a second mercury lamp and reaction coil ahead of the gas-liquid separator. We found that, the method does produce CH_3I, but the reaction is quite inefficient (Figure C - 17). It is likely a steady state will eventually be reached in which the rate of degradation of the product CH_3I will equal it's formation. Complete reaction is unlikely to be possible. No other chemistries have yet been explored for the generation of CH_3I.

4.6 Conclusions and Future Work

We have developed a system using a palladium based preconcentrator coupled to a microplasma atomic emission device for the measurement of trace iodine. The system has achieved the requisite sensitivity for measuring iodine of epidemiological interest. However, the chemistry of iodine at the trace and ultra-trace level is not yet well understood and is the subject of the following chapter. Use of CH_3I as an alternative to I_2 is promising. To date only UV photochemical reaction technique has been attempted for the production of CH_3I. Future work will likely focus on use of methylating agents which have been used previously for the formation of CH_3I with success at the level of interest.[384] It will be necessary to verify no interference is caused by other halomethanes.

Chapter 5

Nonlinearity of Iodine Purging from Aqueous Solution

5.1 Introduction

Iodine is an essential element necessary for the production of thyroid hormones. Insufficient iodine nutrition can lead to a number of diseases commonly grouped together as iodine deficiency disorders (IDD's). Extreme deficiencies lead to deformities such as goiter or cretinism.[386] Even mild iodine deficiency has recently been linked to lower IQ[387-389] and ADHD.[390] The developing brain is highly susceptible to low iodine levels with deficit and timing critically affecting the outcome.[391] As of 2009 nearly a third of the world population is estimated to be iodine insufficient,[386] so it comes as no surprise then that iodine deficiency is the most common cause for cognitive impairment,[392] which is entirely preventable through prophylactic iodine supplementation, most commonly carried out through salt.

Urinary iodine serves as the epidemiological marker for iodine nutrition in a population. The iodine nutrition status of the population of 130 countries, representing more than 91% of the global populace, is routinely surveyed. Populations are characterized based on median UI levels as severely deficient, moderately deficient, mildly deficient, adequate nutrition, above requirements, and excessive intake at <20 ng mL^{-1}, 20-49 ng mL^{-1}, 50-99 ng mL^{-1}, 100-199 ng mL^{-1}, 200-299 ng mL^{-1}, and >300 ng mL^{-1} respectively[392]. Routine measurement is dominated by two techniques: a spectrophotometric kinetic assay based on the iodine catalyzed oxidation of As (III) by Ce (IV) known as the Sandell-Kolthoff method,[393] and inductively coupled plasma mass spectrometry (ICP-MS). ICP-MS is preferentially performed using an isotopic standard[394,395] such as ^{129}I and only requires dilution of the urine prior to analysis. The

Sandell-Kolthoff method is prone to interferences[393,396] however, and requires complete sample mineralization prior to analysis to remove any oxidizable material present. To date individual iodine nutrition assessment is not practical. This is in part due to the high cost of ownership of ICP-MS, but as we conclude in a 2011 review on iodine quantitation in complex matrices,[397] the major bottleneck in many methods is sample digestion/pretreatment.

There have been numerous efforts to circumvent the necessity to digest samples prior to analysis. This is most often accomplished by generation of a volatile species readily isolated from aqueous solution. In urine, iodine is almost entirely present as I^-. It's well known that oxidation of I^- in acidic media results in the volatile species I_2. I_2 can be further reacted in acidic solution with ketones to form the α-halogenated product which is readily isolated via liquid extraction and measurable by gas chromatography (GC).[398-400] Reaction with other derivitizing agents is also possible such as 2,6-dimethylphenol[401] or 2,6-dimethylanaline.[402] Alternatively, a methylating agent such has dimethyl sulfate may be used to generate CH_3I.[403] Due to the health risks associated with methylating agents, use of such techniques will likely be limited. Grindberg and Sturgeon reported a novel UV photoreaction method that generates CH_3I in situ using pneumatically nebulized ICP-MS with a Hg lamp built into the spray chamber[404,405]. Sensitivity is improved by more than 40 times.

Generation of I_2 vapor and volatilization from solution has received far more attention. Online techniques prior to pneumatic or ultrasonic nebulization are widely used particularly in plasma atomic emission spectroscopy (AES).[406-409] Use of gas-liquid separators can further increase sensitivity and in AES can reduce phosphorous spectral interference at the most sensitive iodine emission line at ~178.3 nm.[410-417] I_2 can also be reacted with luminol to produce chemiluminescence after separation using gas diffusion

membranes[418,419] or head space injection.[420] Single drop headspace microdrop

extraction was used to measure the absorbance of I_2 directly with sub ng mL^{-1} detection

limits[421,422] or reacted with 3-pentanone in the drop prior to measurement by GC coupled

to electron capture detection.[423] The headspace can also be measured directly using

intracavity laser spectrometry with a limit of detection of 15 ng mL^{-1}.[424]

Recently a method has been introduced by Yu et al. where elemental I_2 is

generated using a sequential injection setup before being transferred to the gas phase

and measured in a helium dieletric barrier discharge.[425] This method requires

inexpensive instrumentation and has the advantage of being rapid and sensitive, claiming

a detection limit of ~30 ng mL^{-1} limited largely by the sensitivity of the detector. Our own

research, however, indicates that at levels of interest for performing epidemiological

analysis, capable of diagnosing severe deficiency (<10 ng mL^{-1}), I_2 evolution from

aqueous solutions is inherently nonlinear. We have demonstrated this using the method

of Yu et al. coupled to ICP-MS and real-time evolution studies. Due to the

preponderance of supposedly effective volatilization methods we have further reviewed

these procedures to further understand iodine chemistry at trace levels.

5.2 Experimental

5.2.1 Sequential Injection Apparatus.

A sequential injection analysis (SIA) setup identical to that of Yu et a.l[425] (Figure

5-1A) was used for I_2 vapor generation prior to measurement by ICP-MS. The ICP-MS

was a Thermo Electron X-series II with concentric pneumatic nebulizer controlled using

plasmalab software. I_2 vapor generation was accomplished using two syringe pumps,

both Kloehn versa 6, and a Vici Valco Cheminert 13T-0705L 8 port selection valve. An

Advantech PCI-1760U relay board, controllable in plasmalab, was used to trigger syringe
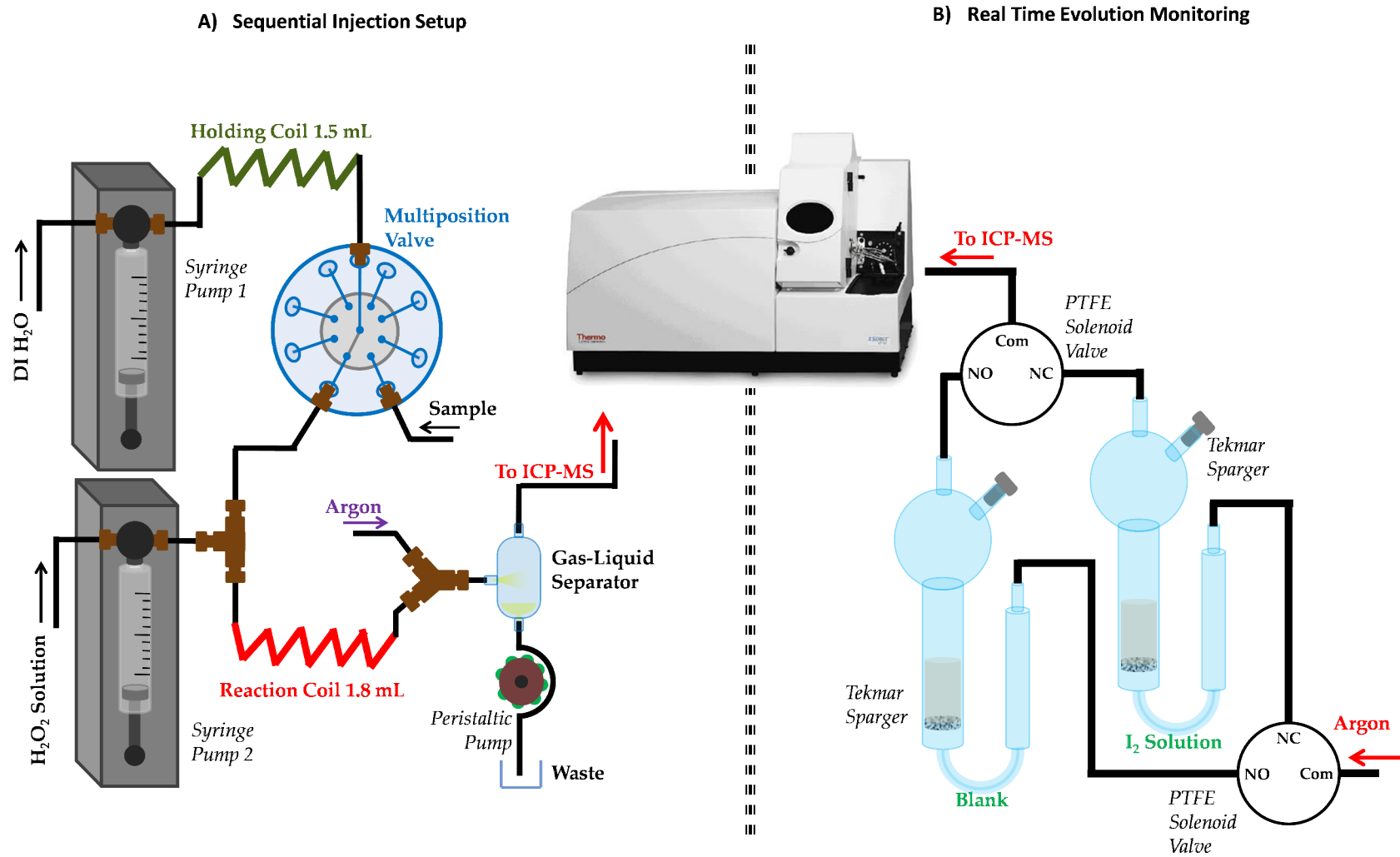
Figure 5-1. Instrumental Configuration for A) Sequential Injection Apparatus for I_2 Oxidation/Volatilization and B) Monitoring of Iodine Sparging

from solution

pump commands and valve actuation. Syringe pump 1 was equipped with a 10 mL syringe while syringe pump 2 was equipped with a 2.5 mL syringe. $1/16^{th}$ inch PTFE tubing, inner diameter 0.8 mm, was used to plumb the entire system except for the 1.8 mL reaction and 1.5 mL holding coils which were comprised of 2.1 mm i.d. PTFE tubing.

The system was operated as follows, using the parameters that Yu et al. reported as optimized.[425] Syringe pump 1 was filled with 5.2 mL Deionized water (18.3 MΩ obtained from Milli-Q system, EMD Millipore) while syringe pump 2 was filled with 0.5 mL oxidant solution. The oxidant solution was prepared by dissolving concentrated H_2SO_4 (AR 95-98%, Mallinckrodt) in 30% w/v H_2O_2(ACS, Fisher Scientific) to achieve a final concentration of 0.1 mol L^{-1} H_2SO_4. Syringe pump 1 is then used to aspirate 1 mL sample through the selection valve into the holding coil. After receiving the trigger from the ICP-MS, the selection valve actuates to the dispense port, then syringe pump 1 delivers the sample followed by 2.7 mL of DI H_2O at 12 mL min^{-1} through a PEEK tee where it is mixed with 0.5 mL of H_2O_2 solution being delivered by syringe pump 2 at 4.8 mL/min. The mixture passes through the reaction coil after which a PEEK Y-connector is used to introduce 100 mL min^{-1} argon (UHP 5.0 Praxair), delivered by a Tylan FC 260 mass flow controller, into the sample solution. The solution and gas immediately enter a gas liquid separator. Volatile I_2 (previously present as I^-) is carried from the gas liquid separator to the pneumatic nebulizer of the ICP-MS where it is then measured. A peristaltic pump was used to drain the gas liquid separator at approximately 5 mL min^{-1}.

A working stock solution of 1000 mg L^{-1} iodine as KI (AR, Malinckrodt) was prepared in DI H_2O and kept refrigerated in the dark. 10 mL of standards from 0-500 ng mL^{-1} were prepared daily upon appropriate dilution of the stock solution. To each standard was spiked 5 ng mL^{-1} ^{129}I (Eckert & Ziegler, 100 nCi) as isotopic tracer. A dwell time of 50 msec was used for ^{127}I and ^{129}I. Data was collected for 30 seconds prior to

121

initiating injection by the syringe pumps to provide a background reading. Data acquisition was subsequently acquired for another 90 seconds for a total run time of 2 minutes per sample. Standards were injected 8 times a piece.

5.2.2 Iodine Sparging From Solution.

Real time monitoring of iodine sparging from solution was carried out as well. The setup is shown in Figure 5-1B. Two PTFE 3-way solenoid valves (Neptune Research), controlled by the aforementioned relay board, separate two Teledyne-Tekmar pyrex spargers with side arm (the blank sparger has a 25 mL capacity while the sample sparger holds 5 mL). The blank sparger is filled with 10 mL of H_2O while the sample sparger is filled with 3 mL of the desired purging solution. The mass flow controller is used to deliver 40 mL min^{-1} argon as the purging gas. The blank sparger is purged for the first 30 seconds before the PTFE solenoid valves are actuated, at which point the sample sparger begins purging. Data is acquired for 10 minutes. A dwell time of 50 msec was used to monitor ^{127}I. To prepare I_2 standards, Iodine crystals (EM Science) were placed inside a sealed volumetric flask and weighed. The flask was then filled with ethanol (USP, 200 proof, Decon Labs) to prepare a 980 mg L^{-1} solution and stored in a sealed glass flask in a freezer till needed. To prepare aqueous standards, the I_2-ethanol solution was allowed to warm up to room temperature before serially diluting in ethanol before spiking DI H_2O to the desired amount just prior to analysis. 25 mL standards were prepared ranging from nominal concentrations of 0-200 ng mL^{-1} and analyzed in triplicate.

Because vapor generation greatly increases sample introduction into the plasma of the ICP-MS and the bulk of the purged iodine is released in less than a minute (as shown in Figure 5-2), large gains in sensitivity are realized. Introduction of higher

concentrations, however, risks saturation and damage to the electron multiplier in the instrument. Further, without the use of an internal standard, substantial standard deviations are observed upon integration of the data. For this reason, an offline mode was also used. 100 mL of standard solutions, ranging from nominally 0-500 ng mL^{-1}, were prepared upon dilution of the I_2 in ethanol with DI H_2O. From the fresh standard was immediately taken three 2.5 mL aliquots which were then diluted with 2.5 mL DI H_2O, 50 µL concentrated NH_4OH (29.54% ACS, Fisher Scientific), and 50 µL of 100 mmol L^{-1} of $Na_2S_2O_3$ (AR, Mallinckrodt) to reduce I_2 to I$^-$. 5 mL portions of the standard were then purged for 10 minutes at 40 mL min^{-1} with argon. 2.5 mL of the purged solution was then taken and treated as above. Standards were sparged and processed in triplicate. To each of the purged and unpurged samples was added 50 µL of 1 ng mL^{-1} ^{129}I as internal standard. Samples were then analyzed in the conventional way: The ICP-MS built in peristaltic pump was used to deliver samples at 0.8 mL min^{-1} to the pneumatic nebulizer. Dwell times of 50 msec were used for both ^{127}I and ^{129}I which were measured in the peak jumping mode. 100 sweeps were performed per main run and a total of 3 main runs were taken per sample.

Offline sparging measurements were also performed to determine the impact of pH in I_2 volatility. 1 Liter of 0.1 mol L^{-1} of NH_4NO_3 (J.T. Baker) was prepared and 100 mL portions were pH adjusted using HNO_3 (AR 68-70% Mallinckrodt) or NH_4OH to achieve pH ranging from approximately 3 to 7 in increments of 0.5, measured on an Altex 71 pH meter. NH_4NO_3 is an ICP-MS friendly salt that was used to maintain similar ionic strength between pH adjusted samples since I_2 volatility is influenced greatly by the "salting-out" effect.[420,421,423,426] Analysis was carried out in an identical fashion to the offline sparging above.
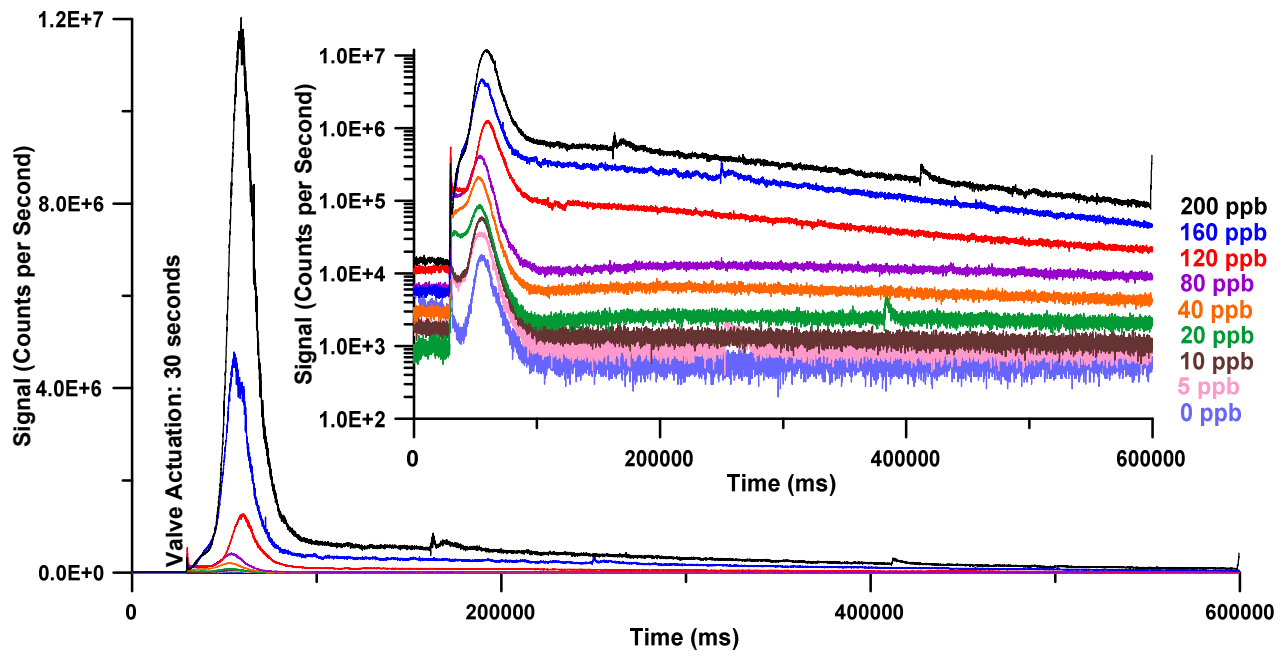
Figure 5-2. Iodine sparging evolution measured in real time. Inset uses logarithmic ordinant scale
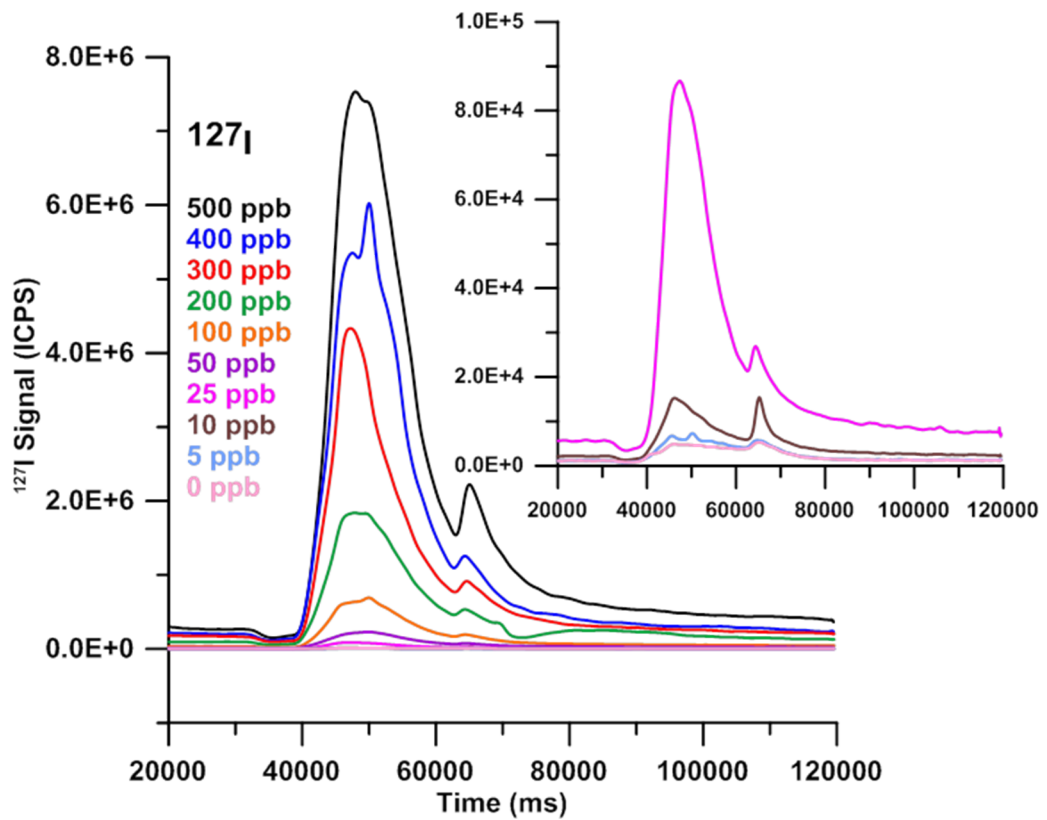
Figure 5-3. SIA sample signal, inset contains sample injections for 4

lowest concentration standards

5.3 Results and Discussion

5.3.1 Sequential Injection Analysis.

Signal data for [127]I are provided for a single injection of each standard in Figure 5-3. The lowest standards are shown in the inset. Changes in flow rate cause perturbations in the signal. This has the effect that when flow starts there is a brief dip before iodine begins to be evolved and when flow stops a small spike is observed. Peak areas are provided in Figure 5-4A for both [127]I and [129]I and response factor, (response * conc^{-1} vs conc, for [127]I) has been plotted in Figure 5-4B. In an ideal linear system, the response factor maintains a constant value (equal to the slope of calibration curve) at all concentrations or at concentrations in the range of interest. This usually has a low limit dictated by the noise of the system and an upper limit imposed by the detection method involved. Clearly the present case is nonlinear at low concentrations. The response factor is approaching an asymptote at high concentrations indicating that at levels above 500 ng mL^{-1} linear behavior may be expected. This
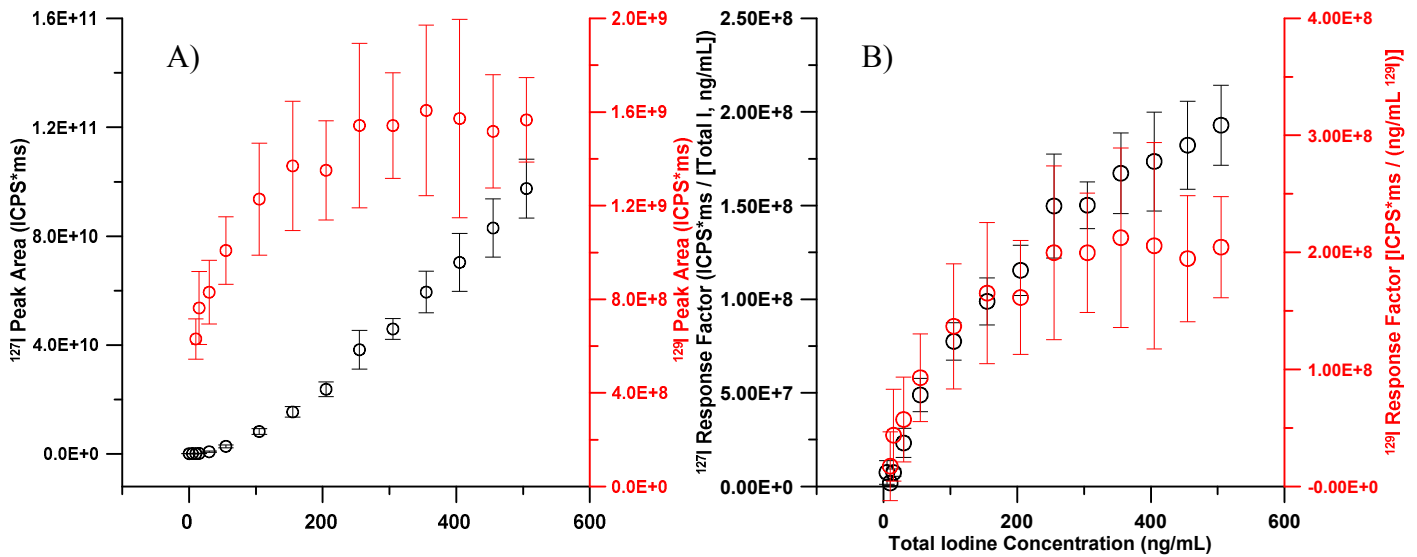
Figure 5-4. A) Response Curves for [127]I and [129]I and B) Response factors. The concentration of [129]I is 5 μg/L in all samples

125

nonlinearity is a chemical process supported by the fact that [129]I counts increase in a similar fashion despite maintaining a constant concentration in each standard. Because of this, measurement only with higher concentration standards will falsely predict much lower limits of detection those actually attainable. In the present system if the response factor for 500 ng mL^{-1} were taken to be the slope, a limit of detection of 3x the standard deviation of the blank would be 0.48 ng mL^{-1}. Conversely, neither the 5 nor 10 ng mL^{-1} standards provide signal three times the standard deviation of the blank. Measurement of sub ng mL^{-1} iodine is performed routinely by conventional direct solution introduction into the pneumatic nebulizer of an ICP-MS; vapor generation at low levels is so inefficient that it becomes actually less sensitive than solution nebulization.

5.3.2 Carryover.

Carryover may be expected to play a critical role in evaluating systems that use I_2 vapor generation. I_2 adsorbs strongly to many materials including PTFE. Our own experience has been that systems left idle for several days are more greatly affected by carryover and must be washed out with H_2O and acetone and ideally kept purged with clean air when not in use. The memory effect of I_2 can be substantial as seen in Figure 5-3. The experiement was carried out in ascending order. The individual graphs are not offset. The starting baseline perceptibly increases after each injection. The results demonstrate also the slow nature of the removal of I_2 from the system. During the optimization process, it is common to use higher concentrations of iodine. This may lead to a memory effect and given the inherent nonlinearity at low concentrations, would make lower concentrations more responsive. That would not actually be seen if one started with low concentration samples or standards.

5.3.3 The Complexity of the Iodide-peroxide-iodine system.

While it is convenient to summarize oxidation of I^- as the reaction:

$$2\ I^- + H_2O_2\ H^+ \rightarrow I_2 + 2\ H_2O$$
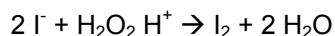
The reality is that the system is very complex. Bray and Liebhafsky[427-433] detail in a series of 7 publications the catalytic decomposition of peroxide, formation of iodate and other iodine intermediates. The work of Abel[434] suggests a steady state concentration of I_2 is reached and has been used in nuclear containment models of radioiodine, where H_2O_2 is generated upon radiolysis of water to predict iodine volatility with some success.[435]. It is acknowledged, however, that below about 1 µM (250 ng/mL), iodine shows anomalous behavior likely due to the formation of IO_3^-.[435] This is in agreement with our data where deviation from maximum response factor begins around 5 µM. Simulations of the fractions of I_2 present at various concentrations and pH using the Abel model are provided in Figure D - 1 and Figure D - 2 in the supporting information (Appendix D). It does predict that the fraction of iodine in the form of I_2, the dominant volatile species, decreases with decreasing total concentration of iodine, so that deviation at low concentrations should be expected. Since we are measuring essentially only I_2, this should follow the general trend of our response factor plot in Figure 5-4B. However, our data does not quantitatively agree with this model. The model predicts that at pH 1.0, 5 ng mL^{-1} and 100 ng mL^{-1} will have I_2 fractions of 0.55 and 0.87 respectively. Our data shows that essentially no iodine is removed at 5 ng mL^{-1} and less than half at 100 ng mL^{-1}. A kinetic limitation, however, cannot be ruled out. The residence time of the solution in the reaction coil is less than 10 seconds, and the formation of I_2 can be expected to be inherently second order with respect to I^-. Due to the complexity of the iodine-peroxide system, and the need to determine whether the nonlinearity arises from the oxidation of iodine, experiments were next carried out using I_2 spiked into aqueous solutions.
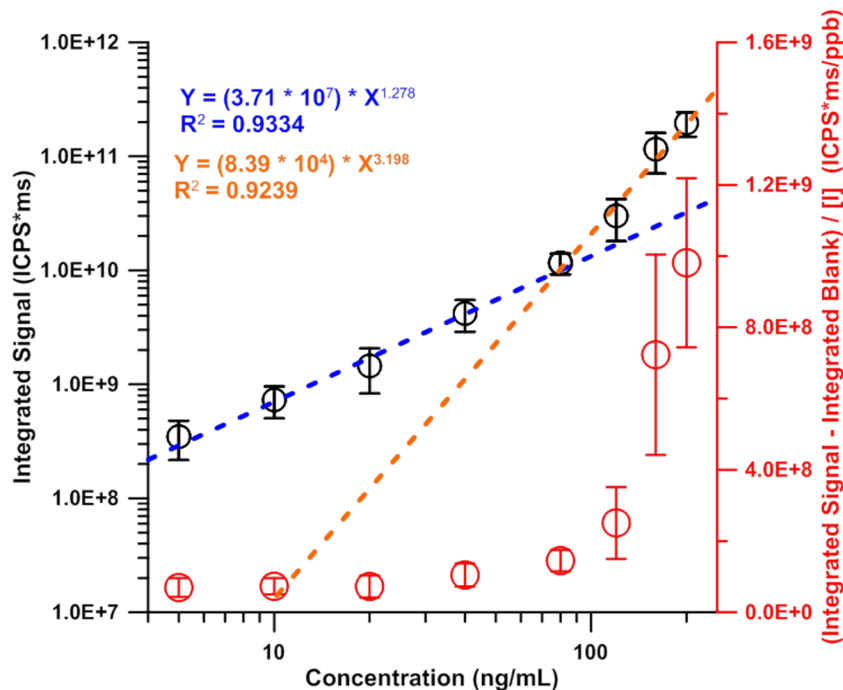
Figure 5-5. A) Integrated response of monitored I_2 purged from solution and B) Reponse Factor

5.3.4 Iodine Sparging From Solution.

The transient monitoring of iodine evolution from aqueous solution for 1 sample at each concentration is provided in Figure 5-2. Sparging has been carried out at 40 mL min^{-1} for 10 min. We had already determined that no appreciable amount of I_2 can be seen after 10 minutes. It can be seen that after the valves are actuated and the iodine containing solution begins to be purged, a relatively sharp peak is observed before settling back down to a slower removal of iodine (spikes in signal are occasionally observed and may be due to formation of aerosol). Signal integration shows that 75.2 ± 8.4 % of the iodine purged within the observed window is purged within the first 90 seconds of the valve switching. Results of the integration and response factor are provided in Figure 5-5. Below 100 ng mL^{-1}, the response factor is lower, but a log-log plot and power fits show that the response is essentially linear at this level. Conversely, above 100 ng mL^{-1} response factor is increasing and a higher order fit is obtained.

It is well known that I_2 in solution undergoes hydrolysis and disproportionation reactions. The first reaction is rapid[436] and is the direct hydrolysis of I_2 to form HOI and I$^-$:

$$I_2 + H_2O \rightleftharpoons HOI + H^+ + I^-$$
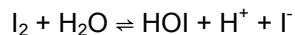
Further reactions are thought to be slower eventually leading to the formation of IO_3^{-}[437] and are generally summarized as:

$$3\,HOI \rightleftharpoons IO_3^- + 3\,H^+ + 2\,I^-$$
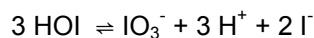
Since the solutions were prepared just prior to analysis it is logical to assume that only the initial hydrolysis reaction should play a critical role in iodine volatility. Sparging is a nonequilibrium process and should drive the formation of I_2 which can be purged easily
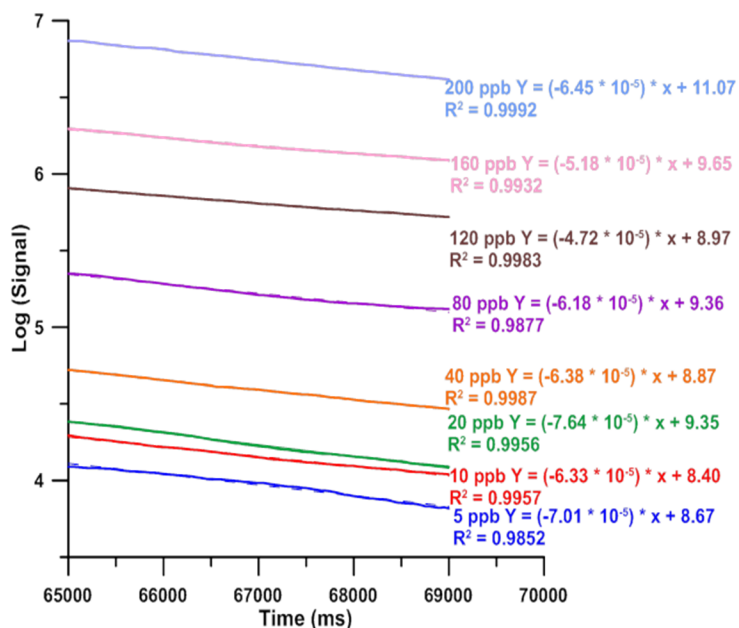
Figure 5-6. Log Signal vs. time for transient monitoring of I_2 sparging between 65-70 seconds. A 1 second smoothing filter is used to improve data appearance.

200 ppb Y = (-6.45 * 10⁻⁵) * x + 11.07 $R^2 = 0.9992$
160 ppb Y = (-5.18 * 10⁻⁵) * x + 9.65 $R^2 = 0.9932$
120 ppb Y = (-4.72 * 10⁻⁵) * x + 8.97 $R^2 = 0.9983$
80 ppb Y = (-6.18 * 10⁻⁵) * x + 9.36 $R^2 = 0.9877$
40 ppb Y = (-6.38 * 10⁻⁵) * x + 8.87 $R^2 = 0.9987$
20 ppb Y = (-7.64 * 10⁻⁵) * x + 9.35 $R^2 = 0.9956$
10 ppb Y = (-6.33 * 10⁻⁵) * x + 8.40 $R^2 = 0.9957$
5 ppb Y = (-7.01 * 10⁻⁵) * x + 8.67 $R^2 = 0.9852$

Figure 5-7. The slopes of the regression for the first order fits between 65-70 seconds. The blue and red lines are the average and ±1 standard deviation

from solution. We believe that the initial peak observed is due to the free I_2 present at equilibrium. The sparging process is first order and should be independent of concentration. Plots of log (signal) vs time (Figure 5-6) in the region 65-70 seconds show that nearly identical slopes (Figure 5-7) are obtained confirming our belief that the initial

129

spike is free iodine and its removal is a rapid first order process. After 90 seconds a slower removal of I_2 is seen which is dependent upon total iodine concentration. Visual inspection of Figure 5-2 shows this process to be essentially 0 order for 80 ng mL^{-1} and below.

Plots of log (signal) vs time from the 300-500 second region are provided in Figure 5-8. Iodine removal in this region is still first order though the rate depends upon the concentration (Figure 5-9) showing more than an order of magnitude increase from 5-200 ng mL^{-1}. This first order loss is unexpected if only a single step hydrolysis of I_2 were occurring. Equal portions of HOI and I⁻ should be formed and recombination should become a second order process. The first order rate however indicates that either HOI or
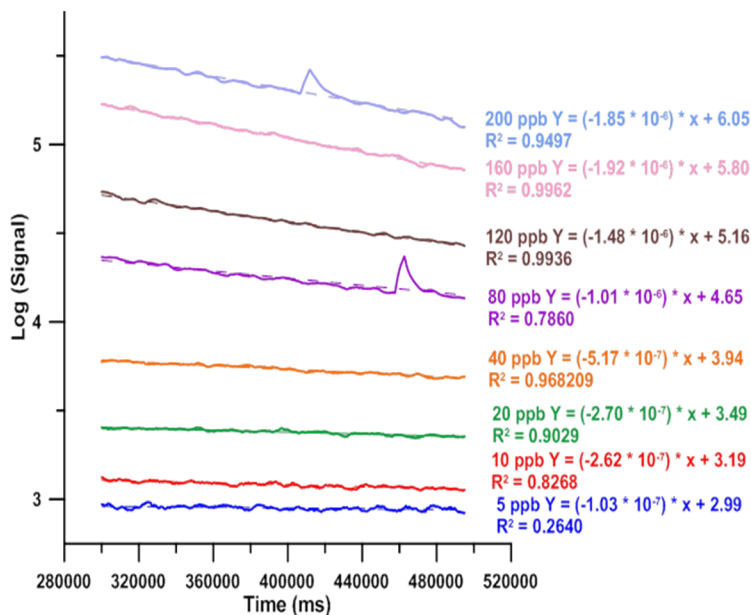
Figure 5-9. Log Signal vs time for the 300-500 sec portion of I_2 sparging.
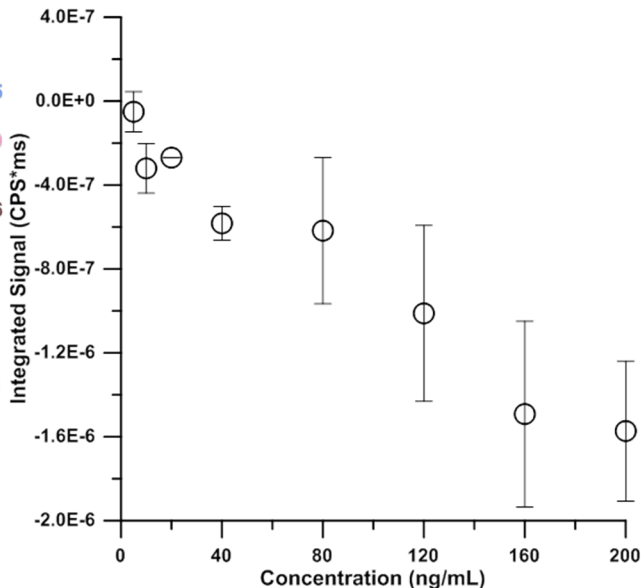
Figure 5-8. Slope of log (signal) vs time for 300-500 seconds of I_2 sparging.

I⁻ must be at significantly lower concentration than the other to produce a pseudo first order process. Since further disproportionation reactions of HOI result in I⁻ and higher valency oxyiodides we speculate that HOI must be the limiting constituent and that

reduction of higher oxyiodides by I⁻ is slow relative to that of HOI under the present conditions.

Despite the apparent completion of I_2 removal upon sparging, analysis of standards before and after sparging indicates that essentially zero iodine is removed from solutions below 200 ng mL^{-1} (Figure 5-10). This further supports our claim that iodine is rapidly disproportioning. The equilibrium constant for the first hydrolysis reaction was determined by Palmer and Lietzke[438] to be 3.13 x 10^{-13}. Figure D - 4 shows I_2 fraction curves as a function of pH and concentration. At a pH of 7.0 approximately 54% of the
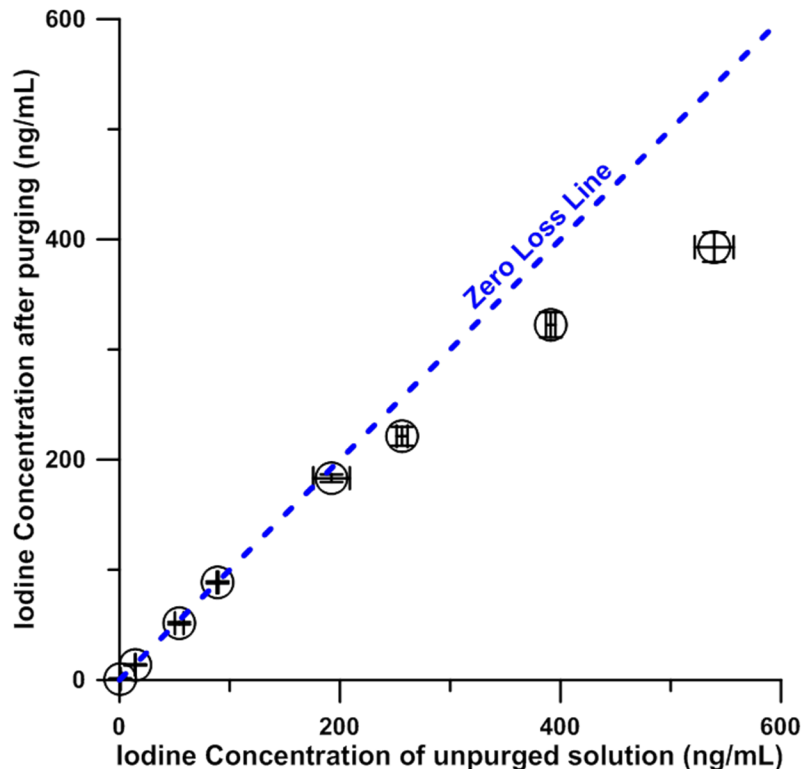
Figure 5-10. Measured concentration of I_2 in solution before

and after sparging for 10 minutes.

total iodine of a 100 ng mL^{-1} solution is expected to be in the form of I_2, while at 10 ng mL^{-1} only 17% will be present as I_2. This equilibrium alone cannot explain the residual iodine

loss due to purging calculated from the residual iodine content of a purged vs an unpurged solution with various initial iodine concentrations. Iodine loss isn't even statistically distinguishable until 300 ng mL^{-1} and is only 13.64 ± 3.6 % at that. The iodine disproportionation reaction must therefore play a role, making the iodate formed essentially unavailable for release.

Because the iodine disproportionation reactions are pH dependent and favor I_2 at low pH, experiments in which the pH was varied were carried out to determine whether more quantitative recoveries could be obtained. Samples were prepared in 0.1 mol L^{-1} NH_4NO_3 solutions in the pH range ~3-7, adjusted using HNO_3 or NH_4OH. Ammonium Nitrate, friendly to ICP-MS, was used to maintain a constant ionic strength. I_2 volatility can be considerably improved by addition of salts in solution.[420,421,423,426] A solution concentration of 200 ng mL^{-1} was chosen as this seems to be the threshold concentration at which significant I_2 release begins. The effect of pH should be more discernible at this level. The concentration of iodine measured in the standard solution before and after purging for 10 minutes was recorded. The purging efficiency as a function of pH is provided in Figure 5-11. It is clear production of I_2 is favored at lower pH's, but a plateau value is reached at 48.1 ± 1.2%. In light of the fact that I_2 removal from solution is rapid, it is clear some fraction of iodine remains as a nonvolatile component. Note that even if the rate of I_2 sparging is the limiting factor, it would take more than 30 minutes to remove 90% of the I_2 from solution, assuming a half life of 10 minutes. In contrast, various headspace techniques however show that equilibration is rapid, being complete in 1.5 – 20 minutes.[420-423] Response factor of the sequential injection method, which should be considered indicative of the relative amount of I_2 present, shows that the response factor at 200 ng mL^{-1} is 62.6 ± 5.7% of that at 500 ng mL^{-1}. As seen in Figure 5-4B, the response factor of 500 ng mL^{-1} has not yet reached a maximum and thus it can be

expected that the actual I_2 content in the 200 ng mL^{-1} level is even lass than 60%, and this is concordant with what is observed in the oxidant free purging experiments. This agreement allows us to conclude that iodine release is intrinsic to the iodine purging experiments and is not a function of the choice of oxidant or a particular system nonlinearity in the sequential injection method.

One of the more thorough models of iodine volatility in nuclear containment, at concentrations of interest[439] developed by Wren and Ball, does not predict such discrepancies. Experimental data they present is stated to follow the model, though there is little information below 1 µM. Actually the presented data often shows that gas phase iodine levels are lower than those predicted by the model; this is attributed conveniently to surface adsorption losses in the system. It is to be noted further that the reported experiments had a duration of hundreds of hours to attain equilibrium. Our own real time data show that iodine evolution does not stop, but slows considerably. Given enough time complete removal may be possible, though it would not be on a timescale of analytical interest. Experiments conducted by Ashmore et al.[440] involved monitoring of I_2
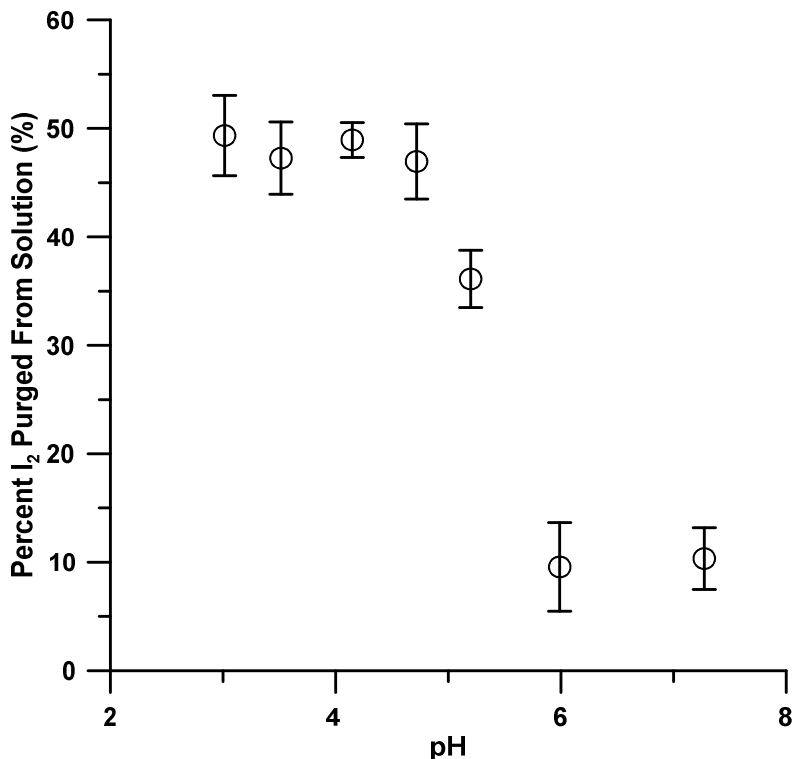
Figure 5-11. Percent of 200 ng mL^{-1} I$_2$ purged from solution as

a function of pH

evolved from I$^-$ solutions at various pH. It was observed that the rate of transfer

decreases with decreasing I$^-$ concentration. Additionally they observed that there is a

significant induction period prior to I$_2$ evolution and recovery is less than quantitative,

especially for lower I$^-$ concentrations even after sparging for 20 hours. This induction

period may be indicative of formation of oxyiodides upon oxidation prior to further

reduction to I$_2$.[429] One of the more peculiar results reported was that elevated

temperatures actually decrease iodine transfer to the gas phase. This is in contradiction

to Henry's law data[441] and other vapor phase measurement techniques that are often

carried out by heating the sample vessel.[420,412] It is also well known that heating of lewis

base solvents (such as water) results in a greater amount of free I$_2$ observable by the

change in solution color from brown-orange to purple[442]. The rate of hydrolysis of halogens however has been shown to increase at elevated temperatures[429,436] and would explain the lower yield observed.

5.3.5 Perspective on Past Methods.

Numerous methods have been presented in the past for determine of iodine following derivatization or vapor generation. As many of these methods proclaim linearity well below the threshold we have observed, our findings would then appear contradictory. We have summarily reevaluated past efforts in an attempt to better understand iodine chemistry at the level of interest.

We are not the first to observe peculiarities in iodine volatility for the purpose of vapor phase measurement.[407,408,415,418-420] Burguera et al., using a headspace sampling apparatus followed by chemiluminescence detection, observed that at concentrations above 5 μg mL^{-1} that iodine response became second order and that it was linear below that concentration down to a detection limit of 10 ng mL^{-1}.[420] Camuna et al. observed a similar effect at high iodine concentrations (up to 500 μg/mL) showing response to be exponential; they recommended the use of log-log calibration[415]. A slope of 2.6 was achieved. Note this is strikingly similar to the power ~3.2 we obtained in Figure 5 for concentrations above 100 ng mL^{-1}. Differences observed for when this nonlinearity arises may be attributed to conditions under which the experiments are performed. Clearly pH played a critical role as evident in Figure 5-11. In the headspace analysis experiment[420], a sigmoidal response curve was seen for temperatures between 105-150 °C showing an intense increase at 125 °C which may be indicative of a chemical shift towards the formation of I_2 and not just an improvement in volatility. However formation of volatile HOI cannot be ruled out, which would react with I$^-$ in the trapping solution to

136

regenerate I_2. Formation of HOI would have been detectable by our experiments using ICP-MS. The observations of Ratanawimarnwong et al. are relevant.[418] They developed a chemiluminescence based flow injection setup in which the detector stream is separated from the oxidation stream by a gas diffusion membrane. They found that iodine response decreased below 2 μg mL^{-1}. The authors attributed this to absorption to the PTFE membrane used. They attempted to condition the membrane by pumping a continuous amount (1 – 3 μg mL^{-1}) of I$^-$ in the carrier. The background signal did not increase linearly with I$^-$ concentration, and in addition, they observed that the response of the injected standards increased with the background I$^-$ concentration by 3 times in going from 1 μg mL^{-1} to 3 μg mL^{-1}. This would imply a second order response as indicated before.[415,420] Additionally, had this effect been purely due to adsorption to the membrane, considerable tailing would be observed and after conditioning this tailing should be improved. Good peak shapes were seen for all concentrations and no improvement could be observed upon addition of the conditioner. The same authors proposed a pervaporation method in which the sample stream does not contact the membrane. This increased the life of the membrane, but it was confirmed again that a background of I$^-$ must be used to measure iodine sensitively at sub μg mL^{-1} levels.[419] Similarly Fei et al.[408] have shown that measurement below 1 μg mL^{-1} was not possible, though the response at 10 μg mL^{-1} indicated otherwise! Their system involved preconcentration of I$^-$ on an anion fiber followed by oxidation, volatilization and measurement by atomic emission spectroscopy. The authors attributed this to failure of the anion fiber to adequately absorb I$^-$ from solution. This is impossible as I$^-$ is more strongly retained by most anion exchangers than Cl$^-$ which the resin was saturated in. Additionally in a background of DI H_2O, there is no competing ion to displace I$^-$ during the preconcentration phase and selectivity for an ion actually increases as the ion concentration is decreased.[443] The lack

of sensitivity then can only be attributable to losses in the system that more severely impact lower concentrations or failure to generate I_2. Dolan et al. performed a nearly identical experiment using an anion exchange membrane disc prior to ICP-OES.[407] A sigmoidal response curve was obtained, though it spanned 5 orders of magnitude with only 5 points.

Though there have been several observations of nonlinearity as mentioned above, the vast majority of analytical procedures surveyed here declare that iodine volatilization is linear and even to levels well below the deviations we have observed. It is fascinating though, that the bulk of these reports do not provide calibration graphs or data. Furthermore, none provide evidence that response factor plots or residuals plots confirmed linearity. As our data indicate I_2 evolution approaches linearity at higher concentrations; generation of calibration plots spanning multiple orders of magnitude especially at concentrations above 500 ng mL^{-1} do not predict behavior at low levels. A simple, unweighted evaluation of the linear coefficient of determination R^2 may be insufficient. Regression of the average SIA values forced through the blank provides a reasonable R^2 of 0.9802 despite the observed nonlinearity. Furthermore, it is often easier to represent data spanning multiple orders of magnitude using log-log plots.[407,410,414,415,424,445] If the data follows a power function, such representation will produce a linear fit. Figure D - 4 represents our own SIA data in such a fashion. A linear fit of the logarithmic data provides an excellent R^2 of 0.9977, though the slope which should be 1 for linearly related data is 1.63.

As it is unlikely that all past work is invalid, it is essential to understand how the production and volatility of I_2 may be improved. It is well known that hydrophobic compounds in aqueous solution may be removed more easily by the addition of copious amounts of ionic solute, often termed the "salting-out" effect. I_2 is no exception and

further partitions into the gas phase when concentrated solutions of $ZnSO_4$,[423] Na_2SO_4,[421,426] NaCl and KCl[420] are used. As described in the previous chapter, addition of saturated solutions of Na_2SO_4 or $(NH_2)_2SO4$ in 1 mol L^{-1} H_2SO_4 to a sample solution containing I_2 (typically in a 1:5 ratio) greatly improves the rate of transfer into the gas phase, but is still unable to overcome the observed nonlinearity. Additionally, we have observed that greater mixing ratios actually decrease the amount of I_2 expelled from solution. The dilution caused upon addition of such salt solutions reduces the fraction of total iodine present as purgeable I_2 and is in agreement with our hypothesis that iodine is disproportioning. While salting-out can improve I_2 transfer to the vapor phase, it is clear that addition of salt or the like, cannot induce reformation of I_2 from e.g. iodate. Although the iodate-iodide reaction in acid solution should lead to the formation of I_2, the kinetics of this reaction will be extremely slow at low levels of total iodine.[448]

Inspection of the most successful methods thus far show that the acid concentration is crucial.[406,407, 409414,416,421,423,444-446] Most methods exceed 1 mol L^{-1} which is well in excess of the acid necessary to generate I_2 from any of the oxidants used. It must however be stated that the methods of Ratanawinwrong,[418] Camuna[415], and Fei,[408] which provided nonlinear results as described above, used between 1.0-1.4 mol L^{-1} H_2SO_4 in the oxidation reaction while Burguera[420] observed second order behavior at high concentrations when using 1 mol L^{-1} HCl at elevated temperatures. It has been shown that a plateau is reached at concentrations near 2 mol L^{-1} H_2SO_4 [423,406,412]. Calzada used as much as 12 mol L^{-1} H_2SO_4 for online oxidation prior to analysis by MIP-OES,[416] and demonstrated that in the absence of oxidant no signal is detected indicating that formation of the volatile species HI does not contribute to the signal. Ahmad used nearly 5 mol L^{-1} H_2SO_4 to distill I_2 from solution using standards at concentrations as low as 250 ng mL^{-1} further diluted 24 times in the digest.[444] I_2 was distilled following addition

of phosphorous acid to the digest to reduce IO_3^- to I_2 and subsequent addition of H_2O_2 to remove excess $Cr_2O_7^{2-}$ from the digest. Recoveries were as a good as 88% after nearly 15 minutes of distillation. It was found that recoveries decreased upon addition of more concentrated H_2O_2 presumably due to reformation of IO_3^- under such acidic conditions. Use of H_2O_2 as an oxidant for vapor generation is common[407,408,412,413,415,421,423-425] and provides comparable results to NO_2^- [406,410,414] which is also used commonly. Perhaps the most extreme case is reported by Duan et al. They added concentrated sulfuric acid in a 3:1 ratio to the standard prior to measurement by atomic absorption spectroscopy.[445] Short reaction and accumulation times were necessary (< 10 sec). However, they operated at levels far greater than those relevant to urinalysis. Additionally, concentrated H_2SO_4 dessication has been used to reduce interferences from H_2O with no loss of Iodine signal.[415,416,445] Any loss then to the dessicating medium is minimal and disproportionation is likely prevented at such strong acidity. Any comment to the mechanism of this increased I_2 volatility is merely speculative. Acid requires significant hydration and can be utilized as a salting out agent, but it has been shown that addition of salt to an already acidic medium is more efficient than further addition of acid, and conversely even in highly saline media addition of acid still greatly improves iodine volatility.[420,421,423] It is also insufficient to suggest that it is a simple matter of shifting the equilibrium back towards I_2 upon addition of $[H^+]$; otherwise, a continuous increase in the amount of I_2 purged from solution would be seen below pH 5.0 instead of the plateau observed in Figure 5-11. Formation of a protonated species at such low pH may occur which is more reactive then the unprotonated form such as HIO_3 (pKa = 0.809[447], this will be the dominant species in the iodate system at the acid concentrations recommended here). A protonated species such as H_2IO^+ which has a pKa between 1-2[437] may also be restricted from further disproportionation. Dolan et al. report unusual behavior of an

anion exchange concentrator. Iodide was eluted with HNO_3[407] and the oxidatively formed I_2 was then volatilized using a solution nebulizer with ICP-MS detection. No signal was observed when less than 1 mol L^{-1} HNO_3 was used, but in going from 2 to 3 mol L^{-1} HNO_3, the observed peak height increases but it begins to tail considerably while the peak elution time is the same. One would expect elution of I^- from an anion exchanger by 2-3 mol L^{-1} NO_3^- will be immediate and there would be no change in peak shape. Peak shape should only improve at higher concentrations of HNO_3.

Work of Pena-Pereira et al. showed that measurement of I^- by headspace microdrop extraction was sensitive and effective using 2 mol L^{-1} H_2SO_4[421]. Subsequent work to measure IO_3^- was less sensitive and used only 0.2 mol L^{-1} HCl due to a high blank from H_2SO_4[422]. I^- was used as reductant, so that for every mole IO_3^- present, 3 mole I_2 is produced compared to direct oxidation of I^- which yields only half a mole I_2 per mole I^-. This should result in 6x greater sensitivity between the two methods but it was found that measurement of IO_3^- is less sensitive than I^-. Lower recoveries were speculated to be caused by formation of triodide though this is unlikely as the quantity of I^- was shown to have no impact upon the signal. This suggests that at lower levels iodine trapped as iodate is not easily recoverable, even in favored cases where a lot of iodide is being added.

The iodate-iodide reaction is a complicated process thought to involve initial formation of the species I_2O_2 (the hydrated product is $H_2I_2O_3$) which can react directly with I^- to form I_2 and IO_2^- or undergo hydrolysis to form HIO_2 and HIO.[448] Hypoiodite in acidic solution will react rapidly with I^- to form I_2 which in turn is liberated readily form solution. It has been shown at low I^- concentrations that the rate determining step for the oxidation of I^- by IO_3^- is the hydrolysis of I_2O_2. The rate of oxidation of I^- by IO_3^- has a dependence on the square of the hydrogen ion concentration. At neutral pH this process

then is extremely slow causing HOI to be only slowly depleted (as observed in Figure 5-2). As the pH is reduced, IO_3^- reacts completely with I^- to yield the intermediate I_2O_2. The slow hydration of this molecule then will account for the incomplete removal of I_2 from solution even after 10 minutes of sparging. Formation of the intermediate species I_2O_2 is additionally supported by the fact that when IO_3^- is used in acidic solution for the oxidation of I^- to I_2 prior to volatilization and measurement by ICP-AES,[410] no signal is seen, but IO_3^- can be used for the oxidation of I^- and derivitazation of acetone prior to GC anlaysis.[398] The hydration of I_2O_2 has been shown to be catalyzed by carboxylic acids, chloride, and bromide. Use of other halides may result in the formation of ICl or IBr which would be volatile and measurable by various atomic spectroscopic methods. These could also react directly with I^- to regenerate the halide and I_2. Oxidation of I^- by IO_3^- has also shown second order behavior at high I^- concentrations but is first order at low concentrations[448] in agreement with the nonlinear behaviors observed thus far, and indicates that I_2 must be disproportionating rapidly at low concentrations, and the iodine from any iodate formed is not recoverable in the analytical time scale. the I^- - IO_3^- system is known to be an integral part of the Bray-Liefhabsky peroxide reaction[448] and must be taken into consideration when H_2O_2 is used as oxidant.

5.4 Conclusion

We have demonstrated that at trace levels pertinent to performing epidemiological studies, that I_2 production and volatization in a nonlinear function dependent on the total iodine concentration. We attribute this to rapid iodine disproportionation reactions that lead to iodate formation at low concentrations from which iodine is not recovered as I_2 by the IO_3^- - I^- reaction in an analytical time scale. It is evident, however, that there is still a void in the knowledge of iodine chemistry at this

level. A review of the literature suggests this is not unknown. Using very large amounts

of acid, especially desiccating acids like H_2SO_4, may solve the problem partially, butt this

certainly does not lead to a green analytical method. Future work is in progress to

improve the removal of iodine from aqueous solution to the vapor phase.

Appendix A

Supporting Information for Chapter 1

Table A - 1. Techniques used for the quantitation of Iodine

Table A - 1

Reference	Method	Application	LOD	Linear Range	linear r²	RSD (%)	Spiked Recovery (%)	Analysis Time	Interferences/Comments
[30]	Sandell-Kolthoff (S-K)	Serum	-	0.04-1 µg L^{-1}	-	6	-	-	Measured at 310 nm, Interferences from Copper and Chromium, Ni(II), Co(II), Fe(III), Hg(II), Ag(I)
[31]	S-K	Serum	-	-	-	-	99.2-100.2 I^- 99.4-100.4 T_4	-	Measured at 317 nm, uses alkaline incineration, only requires 50 µL of serum; Total and Protein Bound Iodine
[36]	S-K: Autoanalyzer	Plants	-	100-800 µg kg^{-1}	-	3-5, N=10	93.4	-	Digested using alkaline ashing
[38]	S-K: Autoanalyzer	Soluble Foods	-	0-10.16 µg L^{-1}	-	.9, 2% milk 6.8, infant formula	97-101, milk	-	Uses mixtures of HNO_3, H_2SO_4, and $HClO_4$ for sample ashing
[40]	S-K: Autoanalyzer	Foods	0.1 µg L^{-1}	9-3360 µg kg^{-1}	-	0.031	90.3-101.3	-	Digestion carried out overnight using mixed acids.
[44]	S-K	serum	0.2 µg L^{-1}	1-17 µg L^{-1}	-	-	-	-	only requires 12.3 µL of sample
[45]	S-K	Thyroid Tissue	-	-	0.9986	5.7-9.4	94-110		10 mg of thyroid tissue required, Chloric Acid digestion
[46]	S-K: Autoanalyzer	Urine	-	17-500 µg L^{-1}	0.988	intra-assay: 7.9-10.2 inter-assay: 4-9.1	97-107	-	Ammonium Persulfate Digestion; no interferences from L-ascorbic acid or thiocyanate
[49]	ICP-MS	Urine	1 µg L^{-1}	1-1000 µg L^{-1}	-	-	97.5-99.0	-	Urine diluted 50 fold with 1% $N(Me)_4OH$ (v/v)
[50]	S-K: Flow Injection	Urine	5 µg L^{-1}	5-1000 µg L^{-1}	-	<3	92-104	<1 min	Reaction terminated with Brucine Sulphate and Absorbance measured at 480 nm
[51]	S-K	Solid Food	-	20-100 µg L^{-1}	-	-	98	-	Oxygen flask combustion used for sample mineralization
[52]	S-K	Serum	-	10-100 µg L^{-1}	-	-	-	6 min	Oxygen Flask combustion; Protein Bound Iodine
[53]	S-K	Geochemical Samples	50 µg kg^{-1}	-	-	1.09-3.87 n=7	-	-	Pyrohydrolitic decomposition using V_2O_5 as flux
[54]	S-K	Coal	90 µg kg^{-1}	290 µg kg^{-1}<	-	2.88-9.52	94.97-109.56	-	Pyrohydrolitic decomposition using quartz sand as flux; no interference from fluorine or sulfur
[56]	S-K	Serum Thyroxine	-	20-120 µg L^{-1}	-	-	-	-	T_4 and T_3 are separated from serum by column chromatography and the iodine exchanged with bromine; non-incinerative technique
[57]	S-K	Serum Thyroxine	-	15-150 µg L^{-1} T_4	-	8.5	98	1.2 min	T_4 and T_3 are separated on an anion exchange column and the iodine is exchanged with bromine before being measured in an autoanalyzer. Interferences for 19 contrast media were measured.
[58]	S-K	Thyroid Hormones	10 pmol	10-1000 pmol	-	Between days 2.8-8.2 Day to Day: 2.8-10.1	-	<30 min	Iodine containing proteins are treated with bromine in acidic media and measured colorometrically
[60]	S-K:Microplate	Iodo-amino acids	1 pmol T_1 0.5 pmol T_2, T_3, T_4	0-40 pmol T_2, T_3, T_4 0-100 pmol T_1	>0.97	intra-assay: 4.2-7.3 inter-assay: 6.5-9.2	96-99	<2 h per plate	Iodo-amino acids were eluted using HPLC and measured using a 96 well micro-titer plate
[61]	S-K: Autoanalyzer	Urine	-	50-400 µg L^{-1}	0.953	6.89	90-103	30 s	Autoanalyzer used with dialysis; Experiences interferences from thiocyanate

	Method	Sample	LOD	Linear range	R^2	Precision (RSD %)	Recovery	Time	Comments
[63]	S-K: terminated with Fe(II)	Urine	-	70-250 µg L^{-1}	-	-	-	-	The S-K reaction is terminated by the addition of Fe(II) followed by addition of thiocyanate and the resultant ferrithiocynate complex absorbance is measured at 460 nm
[67]	S-K: Microplate	Urine	13.809 µg L^{-1}	0-200 µg L^{-1}	0.986	intra-assay: 5-13 n=20 inter-assay: 7-15 n=10	103-114	-	Ammonium Persulfate digest used and measured by S-K on microtiter plates
[68]	S-K: Microplate	Urine	14 µg L^{-1}	40-400 µg L^{-1}	0.982	<10	98	<2 h per plate	Ammonium persulfate Digest then measured on microtiter plates and compared to ICP-MS. 80 samples per plate
[71]	S-K	Immunoassay for human antibodies	-	7-27 g L^{-1} IgG in serum	0.96-0.98	-	-	-	Avoids radio-labelling for determination of antibodies
[73]	ICP-MS	Urine	2.5 µg L^{-1}	25-355 µg L^{-1}	-	within-run 2.5% between-run 11.9%	90-100	5 min	Diluted with ammonia and ^{129}I is used as ISTD
[75]	ICP-MS	Food	-	-	-	0.41-0.47	95-105	-	Uses double isotope dilution to work outside radiological controls.
[76]	ICP-MS	Biological Fluids	0.01 µg L^{-1}	-	-	0.55	-	-	Magnetic sector ICP-MS is used to achieve very low limits of detection coupled with ion chromatography.
[78]	ICP-MS	Urine	.08-.22 µg L^{-1} Iodophenols	<1000 µg L^{-1}	0.999	2.3-2.9	97.8-101	7 min	Anion Exchange and Reverse Phase Chromatography is used to determine iodophenols in urine
[80]	ICP-MS	Milk	<2 µg L^{-1}	4-200 µg L^{-1}	-	1-1.9	-	-	Speciation of Iodine compounds in milk using ion exchange chromatography
[82]	ICP-MS	serum	0.08 µg L^{-1} I$^-$ 0.3 µg L^{-1} IO$_3^-$ 3.5 µg L^{-1} T$_4$ 2.5 µg L^{-1} T$_3$	-	0.9989	2.8-3.9	-	15 min	Capillary electrophoresis used for the separation and detection of iodide, iodate, T$_4$ and T$_3$
[86]	ICP-MS	Foods and solid samples	0.01 µg L^{-1} 50 µg kg^{-1}	0.01-100 µg L^{-1}	-	-	-	-	Schöninger combustion is used to digest solid samples and Iodine is absorbed in .1 mol L^{-1} NaOH
[87]	ICP-MS	Food	30 µg kg^{-1}	-	0.999	3.4 n=8	-	-	Wet ashing used in steel bombs and a small amount of methanol is used to enhance signal
[88]	ICP-MS	Food	2 µg kg^{-1}	-	-	-	>99	25 min	Samples are combusted in a pressurized oxygen bomb with NH$_4$NO$_3$ as a flux using microwaves as the source of ignition and to assist digestion. Iodine is absorbed into alkaline solution and measured
[90]	ICP-OES	water	0.4 µg L^{-1}	2-10000 µg L^{-1}	0.9991	-	-	-	I$^-$ is volatilized before being measured at 178.276 nm and CRM's are measured after separation using ion chromatography.
[92]	Total Reflection Xray Fluorescence	Kelp, water, dietary supplements	180 µg L^{-1}	-	-	<4	-	>15 min	Samples were digested with 25% NH$_4$OH before being irradiated and measured for 1000 seconds
[92]	ICP-OES	mineral tablets and kelp	370 µg L^{-1}	-	-	-	-	-	Kelp samples digested with nitric acid and measured at 178.276 and 183.038 nm but phosphorous interferes at 178.276 nm peak
[93]	ICP-OES	serum	-	15-600 mg L^{-1}	-	1.2-16 n=13	91.3-99.7	-	iohexanol clearance measured; Phosphorous correction required
[94]	ICP-OES	Alga Chlorella	3 mg kg^{-1}	0-500 mg L^{-1}	0.9659	-	89-111	-	Iodine removed from encriched chlorella with N(Me)$_4$OH, interferences from phosphorous and carbon

Ref	Method	Sample	LOD	Linear Range	R²	RSD	Recovery	Time	Notes
[95]	ICP-OES	Food	40 mg kg^{-1}	-	-	2 n=5	85-95	-	Microwave digestion with HNO_3 and H_2O_2; I^- is precipitated with Ag^+ and redissolved in NH_4OH
[97]	ICP-OES	Ground water	4.5 µg L^{-1}	-	-	-	-	5 min	Iodine is volatilized and removed from solution using a gas-liquid separator; requires larger sample volume
[98]	ICP-OES	Milk	20 µg L^{-1}	0-1000 µg L^{-1}	-	0.5-3.5 n=3	68-71	-	Alkaline ashing of milk, Iodine is then volatilized and passed through a phase separator
[99]	ICP-OES		0.75 µg L^{-1}	-	-	-	-	-	Iodide is preconcentrated on an anion exchange column, eluted, and volatilized.
[103]	INAA	Food and Biologicals	20 µg kg^{-1}	-	-	-	-	28 min	Samples are irradiated with Epithermal Neutrons and measured using anticoincidence counting
[104]	INAA	Salt	500 µg kg^{-1}	10-210 mg kg^{-1}	-	-	-	15 min	Samples are irradiated with epithermal neutrons filtered by flexible boron-carbide tubes and measured directly
[108]	INAA	Seawater, Urine, and Milk	10 ng	-	-	-	94.4-98.3	-	I^- and IO_3^- are separated on disposable ion exchange columns and irradiated. Only minor Cl interference is measured
[111]	INAA	Protein Bound Iodine	2 µg L^{-1}	12-14 X 10^5 µg L^{-1}	-	-	>98	-	After irradiation, silver iodide is precipitated and separated from the solution before counting
[114]	AAS	Milk	2.75 µg L^{-1}	11-350 µg L^{-1}	0.998	1.3-6.8	95.3-100.7	~3 min	Iodine is determined indirectly after precipitation with silver. No noticeable interferences due to halides were found up to 50 times the concentration of Iodide
[115]	AAS		3.6 µg L^{-1}	0-100 µg L^{-1}	0.995	1.2-1.3	-	-	A cold vapor mercury analyzer is used for the indirect determination of iodine.
[116]	ISE	Beverages	-	25-13 X 10^4 µg L^{-1}	-	1-4	90-120	5-10 min	The electrode develops a layer after 10-15 hours of continuous use; susceptible to changes in temperature and interferences from chloride
[118]	ISE	Milk	-	100-1 X 10^5 µg L^{-1}	>.95	-	87-114	-	$Ni(NO_3)_2$ is used as a matrix modifier and the method is validated against IC-HPLC with electrochemical detection. ISE had consistently higher results
[120]	ISE	Urine and Serum	1.47 µg L^{-1}	5-400 µg L^{-1}	0.9994	2.2	91.4-106	7 min	A crystalline tubular membrane is used as the detector following ion chromatography
[122]	Electrochemical Detection (ED)	Urine	5 µg L^{-1}	25-200 µg L^{-1}	0.98	<5 n=10	94	7.5 min	Ion Chromatography used with a silver electrode; Compared to Technicon Autoanalyzer method
[123, 126]	ED	Urine, Milk, Salt, Seawater	0.5 µg L^{-1}	0.5-6000 µg L^{-1}	0.999	-	-	-	A comparison between 3 electrodes following ion chromatography is made with a modified platinum electrode providing the best results and the lowest signal deterioration.
[124]	ED	Surface Water	0.02 µg L^{-1}	0-50 µg L^{-1}	0.998	6.2	-	-	Pulsed amperometric detection is used with a silver electrode. A constant decline in signal occurs but diptailing issues are resolved
[127]	ED	Nuclear Emergency Tablets and Multivitamins	1.3 µg L^{-1}	100-2.5 X 10^4 µg L^{-1}	0.999	2.2	-	<1 min	Amperometric detection combined with flow injection analysis using a boron doped diamond thin-film electrode.
[128]	ED	Salt, Seawater, Drugs, Milk	0.47 µg L^{-1}	0.635-63.5 µg L^{-1}	-	<3	-	-	A silver paste carbon electrode for using in ion chromatography; chloride interferes at high concentrations; dip-tailing occurs above 25 µg L^{-1}

Ref	Method	Sample	LOD	Linear Range	R	RSD	Recovery	Time	Notes
[129]	ED	salt, opthalmic drugs	40 $\mu g\ L^{-1}$	-	-	2	-	-	Gold nano ensembles are compared to macro electrodes and have enhanced limit of detection. Experiences interference at low concentrations likely due to anti-caking agents
[130]	Suppressed Conductivity	Biological Samples	20 $\mu g\ L^{-1}\ IO_3^-$	100-10000 $\mu g\ L^{-1}$ IO_3^-	-	1.5	86-98	-	Uses an electrochemical oxidation neutralization device to neutralize samples after ashing to be used with ion chromatography and suppressed conductivity detection
[131]	FIA	I_2 in seawater and salt	40 $\mu g\ L^{-1}$	-	-	0.4-9.4	96.8-101	<30 s	Amylose and Amylopectin are used to form a clathrate with elemental iodine and the absorbance is measured.
[132]	FIA	seawater, salt	60 $\mu g\ L^{-1}$	-	-	-	-	<30 s	polyvinyl alcohol is used to form a clathrate with iodine whose absorbance can be measure; Absorbance maximum is dependent upon degree of hydrolyzation and a non-linear calibration plot is formed
[133]	Sequential Injection Analysis	Pharma-ceuticals	0.05 $\mu g\ L^{-1}$	0.1-6.0 $\mu g\ L^{-1}$	0.996	2	-	<1 min	the catalytic effect iodide has on the reaction between tetrabase and chloramine-T is measured; interferences due to Fe(II) minimized by increasing temperature
[134]	FIA	salts and Pharama-ceuticals	0.13 $\mu g\ L^{-1}$	1.3-63 $\mu g\ L^{-1}$	0.999	1-2.5 n=4	-	1 minute	utilizes the chemiluminescent reaction between $Ru(bpy)_3^{3+}$ and NADH; the reaction is most sensitive to interferences from sulfite and ascorbic and oxalic acids.
[135]	FIA	salt	13 $\mu g\ L^{-1}$	130-1500 $\mu g\ L^{-1}$	0.9955	1-3.5 n=4	-	30 seconds	chemiluminescent detection with acidic potassium permanganate; interferences were removed with a chelating resin
[136]	FIA	urine	10 $\mu g\ L^{-1}$	<5 mg L^{-1}	-	1.8 n=10	101-103	<20 min	Iodine is volatilized and carried into a solution of potassium iodide and reacted with luminol and cobalt solution.
[137]	FIA	Pharma-ceuticals	-	100-1000 $\mu g\ L^{-1}$	0.999	-	-	-	Iodine is volatilized and passes through a gas diffusion membrane into a solution of potassium iodide and then measured by chemiluminescence; Iodine adsorbs strongly on the membrane and thus it is conditioned; strong interferences are present from ascorbic acid
[138]	FIA	multivitamin tablets	500 $\mu g\ L^{-1}$	1-10 mg L^{-1}	0.999	5.2	81.3-117 n=8	2 min	like [134] but Contact with the gas diffusion membrane by the sample solution is eliminated with a pervaporation technique. Ascorbic acid interferes with detection and must be removed.
[139]	FIA-ED	waters, salts, fodder, organics, blood serum	0.63 $\mu g\ L^{-1}$	63-1.3 X 10^4 $\mu g\ L^{-1}$	-	1.68-3.03 n=6	-	-	Iodide catalyzes the reaction between Mn(III) and As(III) in acid and amperometric detection is used at a Pt electrode
[140]	GC-ECD	Food	50 $\mu g\ kg^{-1}$	-	-	-	91.4-99.6	-	Samples are ashed and I_2 is liberated, then reacted with 3-pentanone to form 2-iodo-3-pentanone and extracted in hexane.
[141]	GC-ECD	Blood Iodide	-	2-40 mg L^{-1}	-	intra-assay 2.62-3.6 inter-assay 4.15-11.40	-	-	Blood Iodide is reacted with methyl-isobutylketone and extracted into hexane.
[142]	GC-ECD	Milk	I_2: 0.03 $\mu g\ L^{-1}$ I^-: 1 $\mu g\ L^{-1}$ Total I: 4 $\mu g\ L^{-1}$	-	-	I^-: 2.46 Total I: 2.64	80.5	-	I_2, I^-, and total iodine are measured in milk. IO_3^- is used to oxidize I^- to I_2 which is reacted with acetone to form monoiodoacetone in acidic solution
[143]	SEC	Seawater, Urine	0.2 $\mu g\ L^{-1}$	1-100 $\mu g\ L^{-1}$	.9992 n=6	1.5-3.7	92-103	~20 min	I^- is oxidized to I_2; sequestered with starch and separated by SEC whose absorbance is measured at 224 nm.

Ref	Method	Matrix	LOD	Linear Range	R^2	RSD	Recovery	Time	Comments
[146]	UV-Vis Spectrometry	Milk	-	200-1500 $\mu g\,L^{-1}$	-	10.3-20.6	88	-	Samples are wet ashed with $K_2Cr_2O_7$. I_2 is then liberated by addition of phosphorous acid, trapped in NH_4OH; oxidized to HIO; reacted with leuco crystal violet to form crystal violet and absorbance measured at 592 nm
[147]	UV-Vis Spectrometry	Environmental and pharma-ceuticals	-	40-360 $\mu g\,L^{-1}$	-	1.5 n=7	-	-	I^- is converted to IO_3^- with bromine water and then I_2 is liberated with I^- and the absorbance measured at 591 nm with lecuo crystal violet; no interferences from Cl^-, Br^-, SO_4^{2-}, PO_4^{3-} and NO_3^-, Hg(II) and Mn(II) positively catalyzed reaction
[148]	UV-Vis Spectrometry	Urine, drinking water	2.3 $\mu g\,L^{-1}$	<250 $\mu g\,L^{-1}$	0.9998	3 n=10	95-100 n=4	-	Urine is ashed and bromine water and potassium iodide are added to form elemental iodine which is bound by starch and the absorbance measured at 590 nm. Creatinine interferes heavily
[151]	Molecular absorption spectrometry	Iodide and thyroid hormone supplements	60 $\mu g\,L^{-1}$	60-25000 $\mu g\,L^{-1}$	0.998	<2	-	-	BaI_2 is generated in a graphite furnace and the molecular absorption spectra measured at 538.308 nm. Interferences arose from samples with high chloride content, oxidants, Na, K
[152]	Intracavity Laser Absorbance	Water, Urine	15 $\mu g\,L^{-1}$	-	-	10	-	-	I^- in urine is converted to I_2 using H_2O_2 and H_2SO_4. The laser path lies just above the surface of solution and the gaseous I_2 absorbs strongly at 585 nm
[153]	Kinetic Colorimetry	Iodine labelled Antibody	-	25-1000 $\mu g\,L^{-1}$ Human IgG	0.988	-	-	-	I^- catalyzes the reaction between Sb(III) and Ce(IV) and is non-carcinogenic compared to As(III). Compares with S-K and ELISA. Larger range than ELISA but LOD is higher than S-K
[154]	Kinetic Colorimetry	urine, food, biological material	8 $\mu g\,kg^{-1}$ 5 $\mu g\,L^{-1}$	-	-	1.6-6.8	90-102	-	Samples are wet ashed then reacted with chlorpromazine and H_2O_2; The reaction reaches a maximum absorbance based on I^- concentration before gradually decreasing; Interferences occur from both Fe(III) and Hg(II) but Fe(III) an be corrected for.
[155]	Rapid Test Kit	Urine	-	100< $\mu g\,L^{-1}$	-	-	-	1 min	Interfering substances removed by a charcoal column then I^- catalyzes oxidation of 3,3',5,5'-tetramethylbenzidine by peracetic acid and H_2O_2. Colors are matched to a chart and I^- concentration estimated. Only works on fresh urine.
[157]	Isotope Dilution	Urine, Water	1 $\mu g\,L^{-1}$	7-7500 $\mu g\,L^{-1}$	-	<14 n=3	-	-	[131]I^- is aded to solution then a substoichiometric amount of $AgNO_3$ is added to precipitate AgI which is separated on electrophoresis paper and counted.
[158]	Quartz Crystal Microbalance	Food	0.5 $\mu g\,L^{-1}$	10-500 $\mu g\,L^{-1}$	-	1.1-4.1	93.2-101.1	-	Samples are combusted in an oxygen flask or ashed with KOH and $ZnSO_4$ and then I_2 is liberated and adsorbed onto the gold electrode of the microbalance where the frequency shift is monitored. Only Br^- contributes appreciable interference.

Appendix B

Supporting Information for Chapter 4

B.1 Reagents:

Hexadecyltrimethylammonium chloride (HTMAC, 25% w/v solution, HPLC grade) Ferrous Ammonium Sulfate Hexahydrate (both from www.fishersci.com), Ferrous chloride Tetrahydrate (www.acros.com), and ferrous acetate(www.sial.com) and solid elemental iron powder (www.alfa.com) were obtained as indicated.

B.2 Final Recommended Procedure.

The final recommended procedure is as follows: To 0.5 mL of sample pipetted in to a 15 mL screw-cap polypropylene centrifuge tube add 50 μL of 1 μg/mL ^{129}I tracer (carrier free KI, www.ipl.isotopeproducts.com). Add 0.5 mL of 30% H_2O_2, followed by 50 μL 0.1 M $Fe(NH_4)_2(SO_4)_2$. Within 15 min add 25 μL 2% NH_4OH. The centrifuge tube is loosely capped but not screwed shut. Carry out Fenton digestion in a convection oven overnight (12+ h) at 60 °C. After allowing to cool to room temperature add 2 mL 2% NH_4OH is added to precipitate $Fe(OH)_3$ Addition of 950 μL water brings the total volume to 5.0 mL. Vortex and centrifuge the tubes (3000 g @ 2 °C, 15 min). The supernatant is directly subjected to analysis

.

B.3 Ammonium Persulfate (AP) Digestion method followed by the Sandell-Kolthoff Reaction.

B.3.1 Reagents.

The reagents were prepared according to Pino et al[449]

H_2SO_4, 2.5 M: Add 140 mL Conc. H_2SO_4 to 500 mL water in ice bath, then   make up to volume with water to 1000 mL.

Ceric ammonium sulfate, 15.8 mM: 1 g Ceric ammonium sulfate in 100 mL of 1.25 M sulfuric acid.

Ammonium persulfate 1 M: 22.82 g to 100 mL with water, prepared fresh at least every week.

Arsenious acid 25.3 mM: Heat 0.5 g arsenic trioxide and 2.5 g NaCl in 20 mL 2.5 M sulfuric acid until dissolved, cool and dilute with water to 100 mL.
Store in amber bottles at room temp.

Standards are prepared by preparing a stock solution A containing 1000 mg/L iodine by Dissolving 168.8 mg of potassium iodate in 100 mL water. Stock B is a 1:100 dilution of stock A and is used to prepare individual calibrators and for standard addition.

All experiments were conducted in an Agilent 8453 diode array spectrometer.

For AP digestion, to 1 mL of the milk sample (or milk sample pre-diluted with water) in a glass vial, 200 μL of AP was added. Except as noted the mixture was maintained at 95 °C for 30 min in a capped vial. Initially the AP concentration chosen was 1 M but as noted below, this concentration was increased in subsequent experiments.
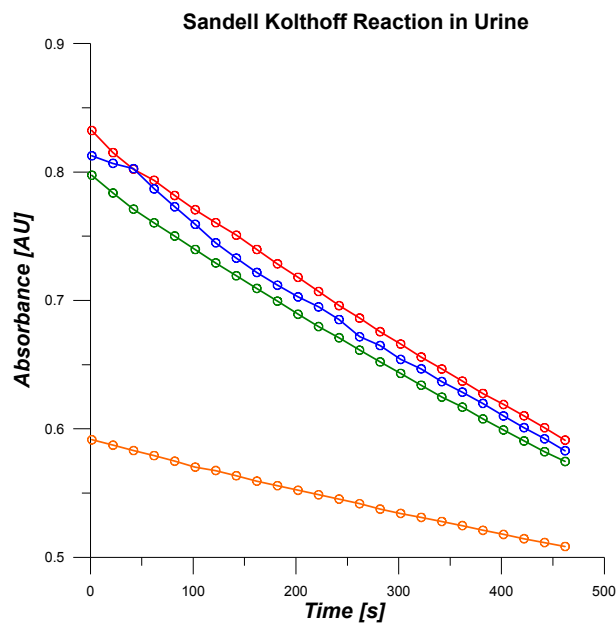
Sandell Kolthoff Reaction in Urine

Absorption data from Urine
digested with 1.1, 1.3, 1.5, 1.7 M
final concentration
Ammonium persulfate
at 410 nm

Figure B - 1
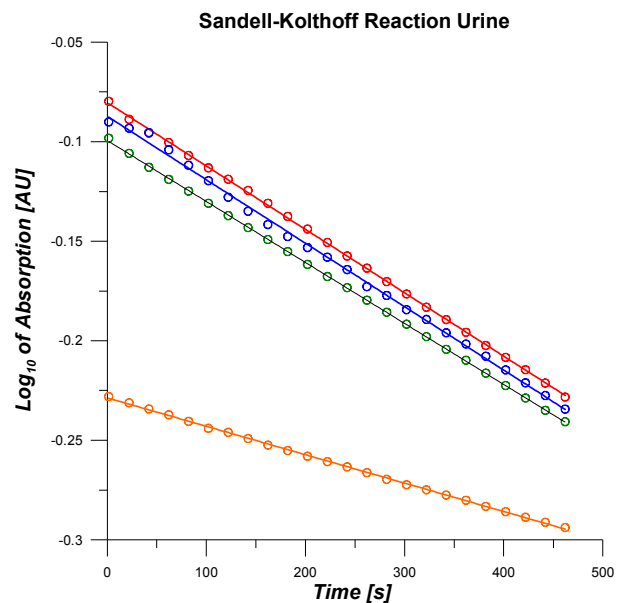
Sandell-Kolthoff Reaction Urine

Y = -0.00032 * X - 0.0804
r^2 = 0.9997
Y = -0.00032 * X - 0.0873
r^2 = 0.9983
Y = -0.00031 * X - 0.0995
r^2 = 0.9999
Y= -0.00014 * X - 0.2287
r^2 = 0.9995

Log$_{10}$ of Absorption data from Urine
digested with 1.1, 1.3, 1.5, 1.7 M
final concentration
Ammonium persulfate
at 420

Figure B - 2

B.3.2 Urine Results.

Urine data for digestion with different concentrations of AP are shown overleaf. Data conform to 1st order reaction kinetics, thus plots with log(absorbance) results in good linear r^2 values. It is to be noted that while the kinetics remain the same for digestion with 1.1, 1.3 and 1.5 M AP, there is a significant drop in the rate of the reaction when digested with 1.7 M ammonium persulfate. Ohashi et al[450] see similar effects when digestion time is extended over 70 min. Either 405 or 410 nm provides satisfactory results. Digestion of breastmilk shows best linearity in a log plot with 1.7 M concentration of ammonium persulfate.

B.3.4 Breast Milk Results.

153

In contrast to results with urine, breast milk data did not produce a linear plot in log A vs. time, especially at lower concentrations of AP; the results far deviated from a linear plot. Even at higher concentrations of AP, slopes of log A vs t was not constant with time. These figures were from a single breast milk sample but other samples experimented with produced similar results.

Sandell-Kolthoff Reaction in Breast Milk
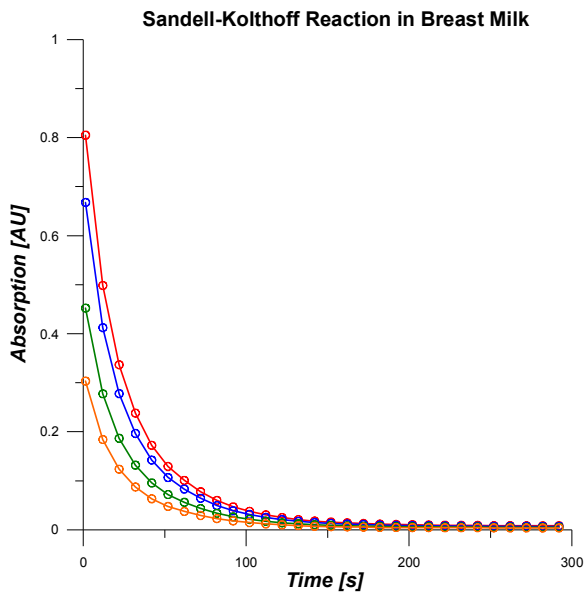
Absorption of breast milk digested with 1.1 M ammonium persulfate at 405, 410, 420 and 430 nm

Figure B - 3

Sandell-Kolthoff Reaction in Breast Milk
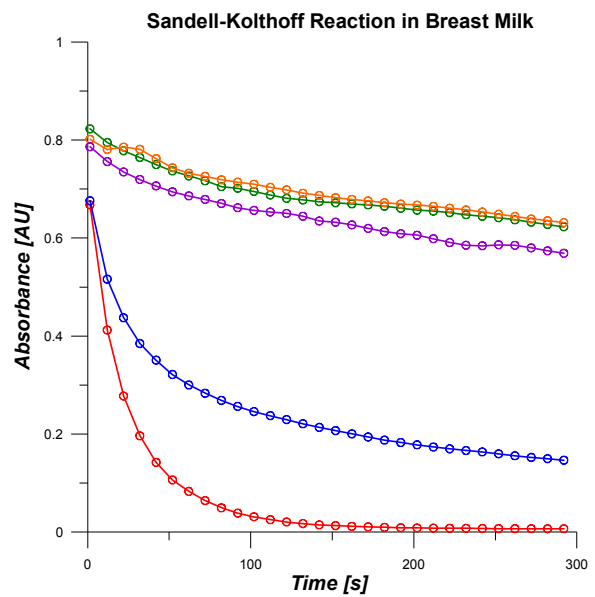
Absorption at 410 nm,
Breastmilk digested with 1,1, 1,3, 1,5, and 1,7 M ammonium persulfate
Breastmilk digested with 1.1 M ammonium persulfate and dil. 1:1

Figure B - 4

When plotted on the same plot, The higher AP data seemed to indicate comparable best fit kinetic slopes (Figure B - 5). At lower AP concentrations, the reaction seemed to be a combination of two reactions. When viewed magnified (Figure B - 6), the same seemed to be true of higher AP concentrations. We decided to explore digestions with even higher AP concentrations and picking the best digestion condition
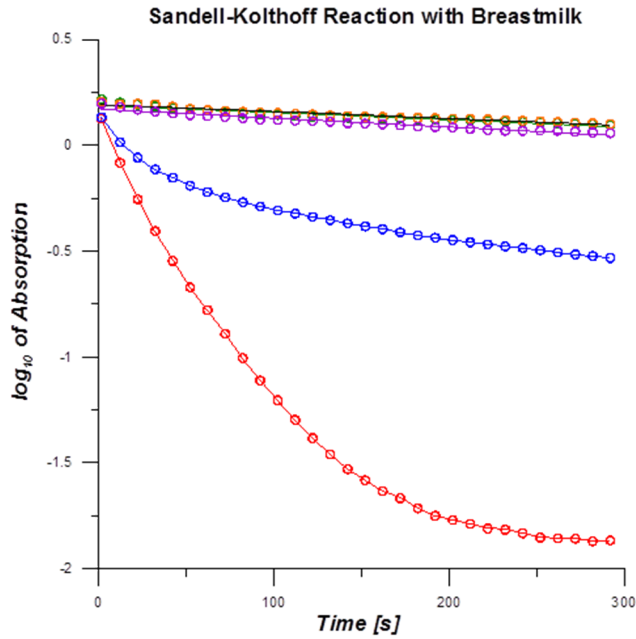
154

Sandell-Kolthoff Reaction with Breastmilk

Y= -0.00034 * X + 0.1885
r² = 0.9113
Y = -0.00033 * X + 0.1917
r² = 0.9530
Y = -0.00042 * X + 0.1693
r² = 0.9533

Log₁₀ of Absorption
of breastmilk
digested with 1.1, 1.3, 1.5, 1.7 M
ammonium persulfate
and breastmilk dig. with 1.1 M
amm. pers. and dil. 1:1
at 410 nm

Figure B - 5
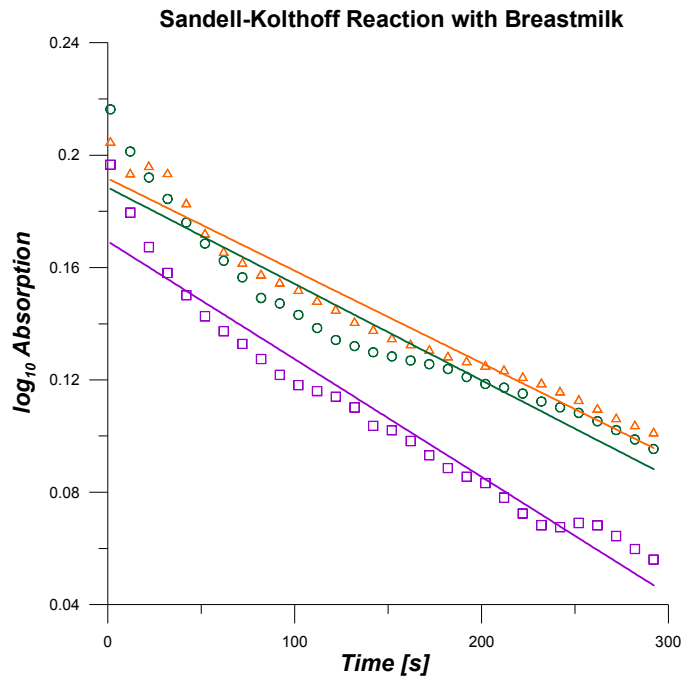
Sandell-Kolthoff Reaction with Breastmilk

Y= -0.00034 * X + 0.1885
r² = 0.9113
Y = -0.00033 * X + 0.1917
r² = 0.9530
Y = -0.00042 * X + 0.1693
r² = 0.9533

Log₁₀ of Absorption
of breastmilk
digested with 1.3, 1.5, 1.7 M
ammonium persulfate
at 420nm

Figure B - 6

Two new breast milk samples were tested, coded GBTX20 and PER. They were digested with 1.75 M, 1.97 M, 2.19 M and 2.41 M AP (95°C, 30 min). S-K kinetics were measured for 3 min at 410 nm.

The sample PER (Figure B - 7) shows better linearity in the log A vs. *t* plot and shows the best linearity and the highest slope when digested with 1.97 M ammonium persulfate. However, the sample GBTX20 (Figure B - 8) did not show a linear log A vs. t plot under any digestion conditions; obviously, there is considerable sample to sample variation.

Breastmilk, sample PER

1.75 M ammonium persulfate:
Y = -3.795*10^{-4} * X - 0.0955
r^2 = 0.9845
1.97 M ammonium persulfate:
Y = -7.031 * X - 0.2623
r^2 = 0.9863
2.19 M ammonium persulfate:
Y = -4.326*10^{-4} * X - 0.1705
r^2 = 0.9842
2.41 M ammonium persulfate:
Y = -4.983*10^{-4}* X - 0.1952
r^2 = 0.971358

Figure B - 7

Sandell-Kolthoff Reaction in Breastmilk, sample GBTX20, 10/12/07, 8:45 am

1.75 M ammonium persulfate
1.97 M ammonium persulfate
2.19 M ammonium persulfate
2.41 M ammonium persulfate

Figure B - 8

The reason for the differing behavior (Figure B - 9) is not understood. Whatever the reason is, it must be true that the sample is not fully mineralized by the persulfate to participate uninfluenced in the S-K reaction. One possible explanation is that some

Sandell-Kolthoff Reaction in Breastmilk
comparison samples GBTX20 and PER

Sandell-Kolthoff Reaction, Calibrators

1.75 M ammonium persulfate   ○○○ GBTX20
1.97 M ammonium persulfate   ●●● PER
2.19 M ammonium persulfate
2.41 M ammonium persulfate
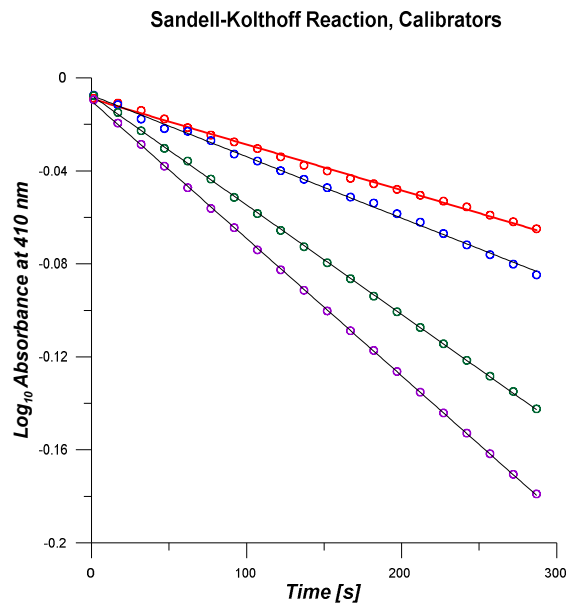
Figure B - 9

0 ppb: $Y = -1.970 \times 10^{-4} \cdot X - 0.0089$
                $r^2 = 0.9974$
50 ppb: $Y = -2.640 \times 10^{-4} \cdot X - 0.0075$
                $r^2 = 0.9981$
100 ppb: $Y = -4.710 \times 10^{-4} \cdot X - 0.0075$
                $r^2 = 0.9999$

Figure B - 10

oxidizable moiety remains aside from iodide/iodate and contributes to the accelerated

rate during the first part of the observed kinetics. When this(these) substance(s) are fully

oxidized, perhaps the terminal kinetics more correctly reflect the iodide catalyzed

reaction. With this thought, we attempted next ignoring the initial part (first 100s) of the

kinetics and following the reaction for 5 min total. Calibration curves were run and 3

different breast milk samples were digested with 1.97 M ammonium persulfate for 30 min

at 95°C. The samples run were spiked to contain an additional (a) 0, (b) 100 and (c) 200

μg/L iodine. The calibration data are shown below; Figure B - 10 shows the calibration

data for the 0, 50, 200 and 500 μg/L iodine data (relevant stats for the linear fits in Figure

B - 10), and Figure B - 12 show the reaction rate slope based calibration plot.
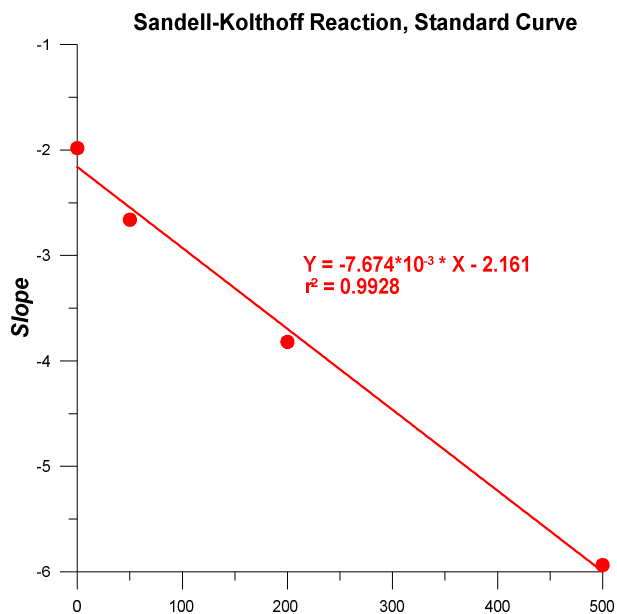
Figure B - 11
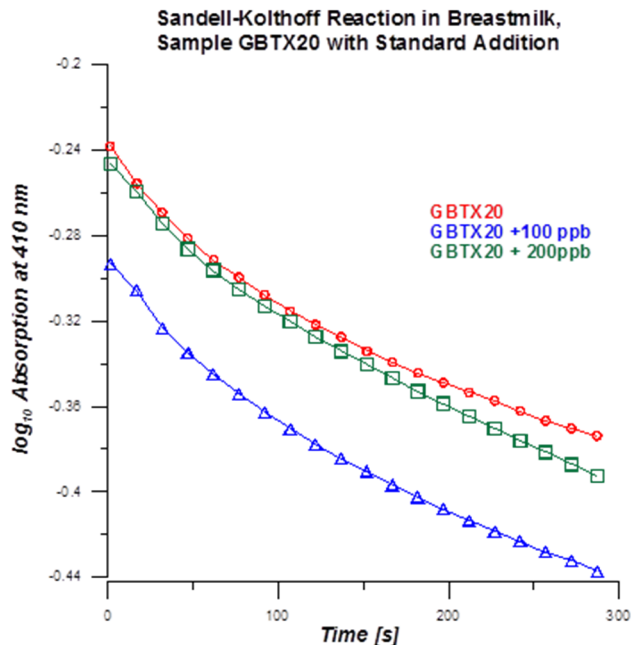
Figure B - 12

Figure B - 12 shows the data for sample GBTX20 with two spike levels as indicated. Figure B - 13 shows the log A vs. t plot where the clock is started to zero at t= 107 s. Good linearity is observed. The same is then shown for sample PER in Figure B - 14 and Figure B - 15, respectively.

Overleaf in Figure B - 16 and Figure B - 17 are similar data presented for a third breastmilk sample coded MA. In this case, only one spike level (100 μg/L) was examined. Again, a truncated data set exhibited good linearity in the log A vs. t plots. For all of these experiments (Figure B - 13, B - 15, B - 17) we translated the observed slopes to concentrations of iodine using the calibration equation depicted in Figure B - 12.

These data and percent recoveries are listed in Table B - 1 overleaf. The latter are consistently substantially below stoichiometric, as little as 50% recovery is observed. It may be observed that GBTX 20 had been processed

and measured by various techniques before with a consistent value of ~98 μg/L. The

observed value of 137 μg/L has a large positive error, possibly because whatever

residual reacting substance persists, contributes to this value, despite disregarding the

initial rate data. Any "one time point measurement" such as that often carried out in

continuous flow systems will result in gross error.

Figure B - 13

Figure B - 14

Sandell-Kolthoff Reaction in Breastmilk, Sample PER with Standard Addition

PER
Y = -3.529*10^{-4} * X - 0.204
r^2 = 0.9981
PER + 100
Y = -3.996*10^{-4} * X - 0.1599
r^2 = 0.9988
PER + 200
Y = -4.546*10^{-4} * X - 0.2121
r^2 = 0.9990

Figure B - 15

Sandell-Kolthoff Reaction in Breastmilk, Sample MA with Standard Addition

MA
MA + 100

Figure B - 16

Sandell-Kolthoff Reaction in Breastmilk, Sample MA with Standard Addition

MA
Y= -3.137*10^{-4} * X - 0.1578
r^2 = 0.9982
MA + 100
Y = -3.7013*10^{-4}* X - 0.1505
r^2 = 0.9982
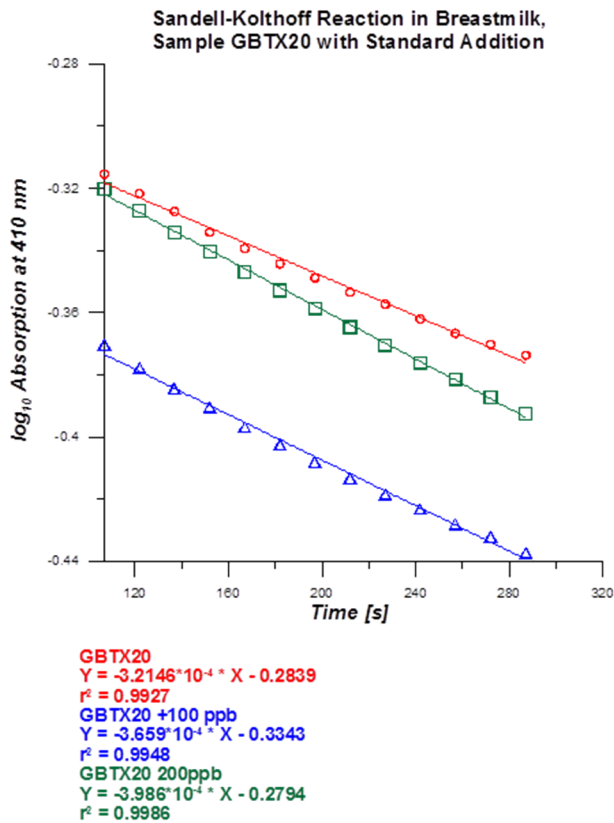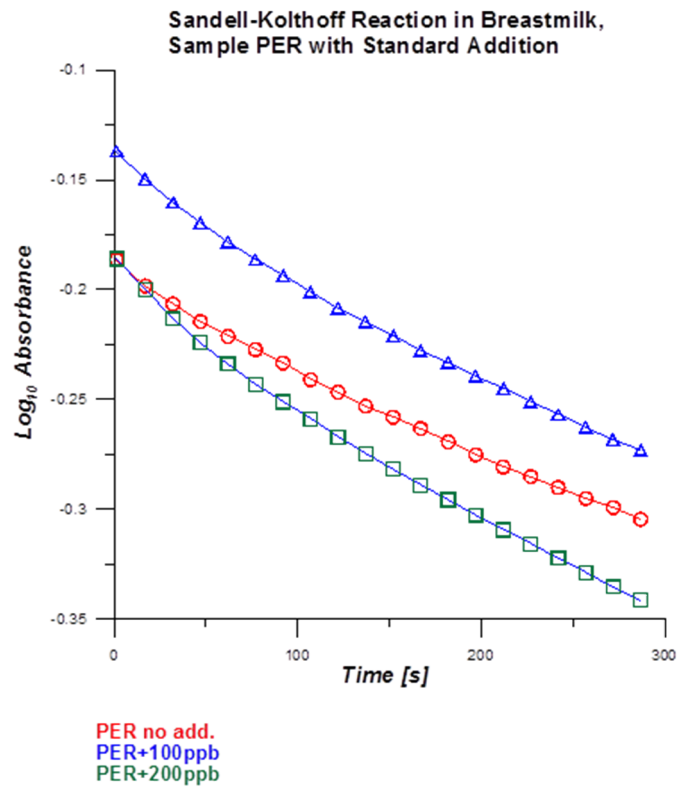
Figure B - 17

Table B - 1

Sample	slope	Calc concn, μg/L	%recovery
GBTX20	-3.215	137	
GBTX20+100	-3.659	195	58
GBTX20+200	-3.986	238	50
PER	-3.529	178	
PER+100	-3.996	239	61
PER+200	-4.546	311	66
MA	-3.137	127	
MA+100	-3.701	201	74

Figure B - 18 below shows that clear digests are obtained by AP digestion of milk samples. Nevertheless these digests do not provide reliable results in Sandell—Kolthoff Analysis. Ammonium persulfate digested breast milk sample GBTX20, Digestion temperature 95 °C, 1 mL milk sample + 200 μL 1 M AP. (1) undiluted milk, 30 min (2) undiluted milk, 45 min (3) undiluted milk, 60 min (5) 1:1 diluted milk, 30 min (5) 1:1 diluted milk, 45 min (6) 1:1 diluted milk, 60 min (7) 1:3 diluted milk, 30 min (8) 1:3 diluted milk, 45 min (9) 1:3 diluted milk, 60 min
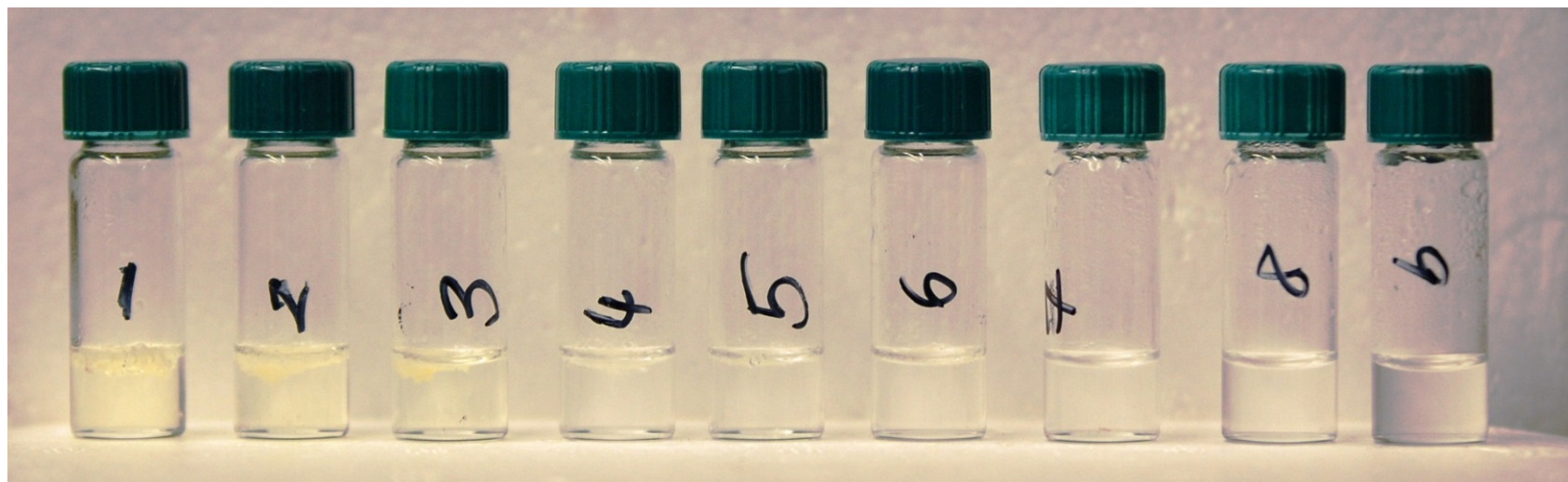
Figure B - 18

Table B - 2. . Comparison of Fenton Digestion with HClO4 digest

Sample ID	Fenton Digest Average µg/ L	SD	RSD %	FDA HClO4 Average µg/L	SD	RSD %
1-Breast Milk	235.3	38.0	16.2	189.5	16.3	8.6
2-Breast Milk	295.1	28.2	9.6	243	15.6	6.4
3-Breast Milk	370.2	8.5	2.3	334.5	12.0	3.6
4-Breast Milk	141.0	6.2	4.4	139.5	19.1	13.7
5-Breast Milk	216.4	4.0	1.9	205.5	7.8	3.8
6-Similac Advanced	130.2	0.7	0.6	136	17.0	12.5
8-Similac Isomil	112.9	1.8	1.6	110	11.3	10.3
10-Enfamil	153.1	1.3	0.9	136.5	4.9	3.6
11-Lactaid	393.7	3.5	0.9	361.5	4.9	1.4
12-Horizon Organic	372.4	10.2	2.7	393.5	13.4	3.4
13-Anderson Erikson	355.8	10.7	3.0	379	19.8	5.2
14-Roberts	435.4	1.2	0.3	425.5	13.4	3.2
15-Great Value	419.2	15.4	3.7	429.5	12.0	2.8

SUMMARY OUTPUT

Regression Statistics	
Multiple R	0.9967
R Square	0.9934
Adjusted R Square	0.9101
Standard Error	25.6
Observations	13

ANOVA

	Df	SS	MS	F	Significance F
Regression	1	1.18E+06	1.18E+06	1.80E+03	1.51E-13
Residual	12	7.84E+03	6.53E+02		
Total	13	1.18E+06			

	Coefficients	Standard Error	t Stat	P-value	Lower 95%	Upper 95%	Lower 95.0%	Upper 95.0%
X Variable 1	1.029	0.024	42.46	1.89E-14	0.98	1.08	0.98	1.08

Table B - 3. t-test for difference: Table 2 Data

Sample ID	Fenton Digest Average µg/ L	HClO4 Digest Average µg/ L	Di	Di - Dbar	Col E sqrd
1-Breast Milk	235.3	189.5	45.8	34.5	1187.6
2-Breast Milk	295.1	243.0	52.1	40.7	1659.8
3-Breast Milk	370.2	334.5	35.7	24.4	596.1
4-Breast Milk	141.0	139.5	1.5	-9.8	95.7
5-Breast Milk	216.4	205.5	10.9	-0.4	0.2
6-Similac Advanced	130.2	136.0	-5.8	-17.1	294.1
8-Similac Isomil	112.9	110.0	2.9	-8.4	71.3
10-Enfamil	153.1	136.5	16.6	5.3	28.0
11-Lactaid	393.7	361.5	32.2	20.9	435.6
12-Horizon Organic	372.4	393.5	-21.1	-32.4	1050.7
13-Anderson Erikson	355.8	379.0	-23.2	-34.6	1193.8
14-Roberts	435.4	425.5	9.9	-1.4	1.9
15-Great Value	419.2	429.5	-10.3	-21.6	466.8

Dbar =	11.32819	7082
	SD =	24.3
	t =	1.615

The tabulated t-value for a 95% confidence limit for $\upsilon = 12$ is 2.18.
Statistically the methods do not produce different results.

Table B - 4 Comparison of HClO$_4$ Digest Analyses by ID-KCP-MS vs. Sandell-Kolthoff Kinetic Colorimetry

Sample ID		ICP-MS Average, µg/ L	SD	S-K Average, µg/ L	SD
1-Breast Milk		189.5	16.3	179	5.7
2-Breast Milk		243	15.6	256.5	6.4
3-Breast Milk		334.5	12.0	354	5.7
4-Breast Milk		139.5	19.1	113	2.8
5-Breast Milk		205.5	7.8	211.5	3.5
6-Similac Advanced		136	17.0	121	2.8
8-Similac Isomil		110	11.3	108	5.7
10-Enfamil		136.5	4.9	162.5	13.4
11-Lactaid		361.5	4.9	399.5	3.5
12-Horizon Organic		393.5	13.4	425.5	12.0
13-Anderson Erikson		379	19.8	384	11.3
14-Roberts		425.5	13.4	460	2.8
15-Great Value		429.5	12.0	461	7.1

SUMMARY OUTPUT

Regression Statistics	
Multiple R	0.9986
R Square	0.9973
Adjusted R Square	0.9139
Standard Error	16.9
Observations	13

ANOVA

	Df	SS	MS	F	Significance F
Regression	1	1.24E+06	1.24E+06	4.36E+03	1.19E-15
Residual	12	3.42E+03	2.85E+02		
Total	13	1.25E+06			

	Coefficients	Standard Error	t Stat	P-value	Lower 95%	Upper 95%	Lower 95.0%	Upper 95.0%
X Variable 1	1.06E+00	1.60E-02	6.61E+01	9.60E-17	1.02	1.09	1.02	1.09

Table B - 5. t-test for Difference: Table S4 data

Sample ID	ICP-MS Average	S-K Average	Di	Di - Dbar	Col F sqrd
1-Breast Milk	189.5	179	-10.5	-42	1764
2-Breast Milk	243	256.5	13.5	-18	324
3-Breast Milk	334.5	354	19.5	-12	144
4-Breast Milk	139.5	113	-26.5	-58	3364
5-Breast Milk	205.5	211.5	6	-25.5	650.25
6-Similac Advanced	136	121	-15	-46.5	2162.25
8-Similac Isomil	110	108	-2	-33.5	1122.25
10-Enfamil	136.5	162.5	26	-5.5	30.25
11-Lactaid	361.5	399.5	38	6.5	42.25
12-Horizon Organic	393.5	425.5	32	0.5	0.25
13-Anderson Erikson	379	384	5	-26.5	702.25
14-Roberts	425.5	460	34.5	3	9
15-Great Value	429.5	461	31.5	0	0

Dbar =	11.69231		10314.75
		SD =	29.3183
		t =	1.381504

The tabulated t-value for a 95% confidence limit for υ = 12 is 2.18.
Statistically the methods do not produce different results.

Figure B - 19. Ion Chromatographic separation of Iodate treated using the Fenton digestion

To a 4 mL solution of IO_3^- standard prepared in 0.2% NH_4OH 2 mL 30% H_2O_2 was added. The final concentration of iodate was 10 μg I/L. MnO_2 was added. After effervescence subsided, the sample was analyzed by IC-ICP-MS. No observable conversion of the IO_3^- can be seen.
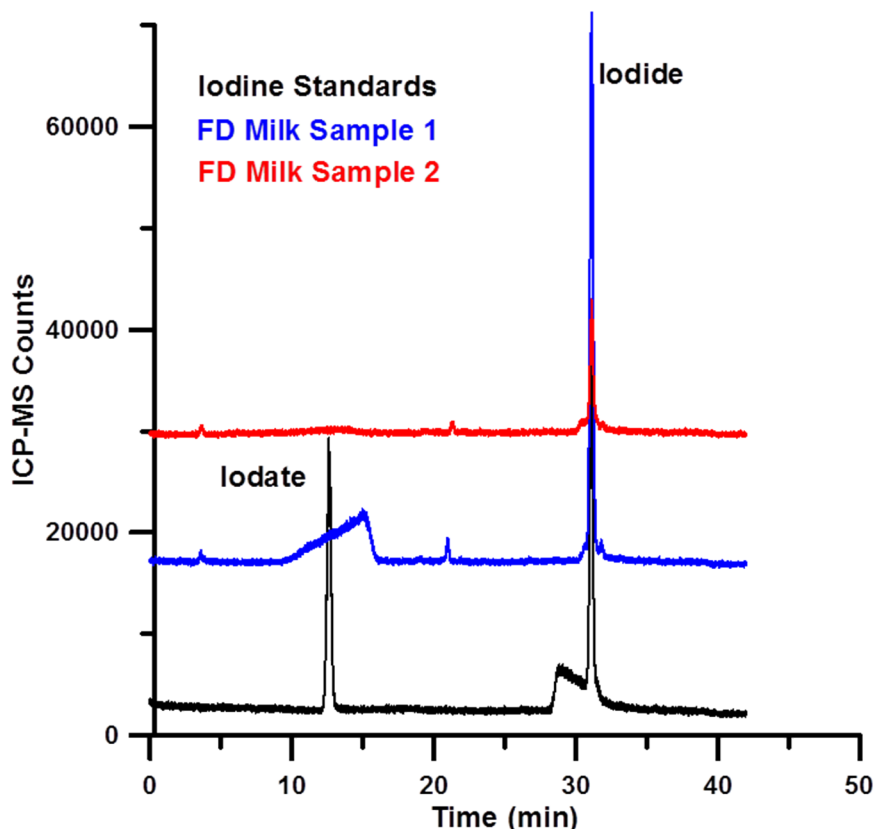
Figure B - 20. Ion Chromatographic determination of Iodine species in milk

following Fenton Digestion

Black trace: Iodide and Iodate standards 10 µg/L I each, dissolved in 0.2% NH4OH. Fenton digests of two milk samples showed only iodide. A third sample (not shown) showed the same result.

Ion chromatography was conducted on a Dionex IC system with a GP40 pump, EG40 eluent generator, LC30 oven (30 °C) an ASRS-Ultra 4-mm suppressor (SRS mode 100 mA) and a CD25 conductivity detector. Peaknet 6.0 chromatography software was used for system control. Separation was performed on a Dionex IonPac AG-16 (4 x 50 mm) guard column and IonPac AS-16 (4 x 250 mm) anion separation column. The injection loop volume was 20 µL. Gradient elution was performed as follows: 1-10 min 1.5 mM KOH, 10-20 min 1.5-10 mM KOH ramp, 20-35 min 10-55 mM KOH, 35-42 min 1.5 mM KOH.

Table B - 6. Difference in Results Between Pre-spiking and Post-

Sample	Pre digestion Spike		Post Digestion Spike		Percent Difference	SD diff
	Average	SD	Average	SD		
Whole Milk	638	12.2	493	21.2	22.8	4.2
Breast Milk (hindmilk)	94	15.8	76	10.8	19.6	20.2
Breast Milk (foremilk)	121	6.2	88	3.9	27.0	1.7
Formula	159	5.7	134	1.1	15.8	1.4
Soy Formula	131	4.3	116	12.8	11.6	12.0

Table B - 7. Examination of Loss on $Fe(OH)_3$

	Pre Digestion Spike		Post Digestion Spike		Percent Difference
	Average [I], µg/L	SD	Average [I], µg/L	SD	
2% NH$_4$OH addition	378.3	31.9	361.1	38.4	4.8
Water addition	374.9	4	313.5	4.2	19.6
2% HCl addition	384.1	4.1	332.6	0.6	15.5
Average	379.1		335.7		12.9
Standard Deviation	4.7		24.0		
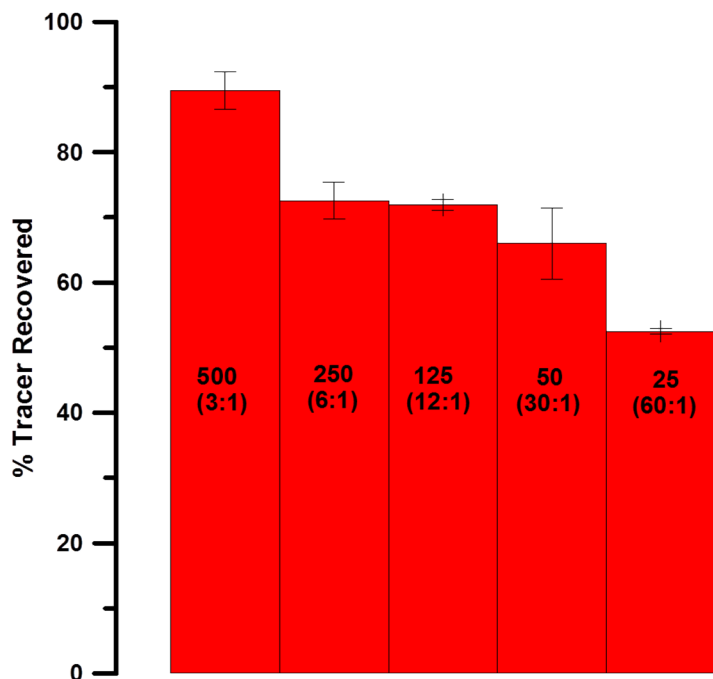
Figure B - 21. Percentage ^{129}I recovered as determined by ICP-MS using varying sample ratios and identical digest
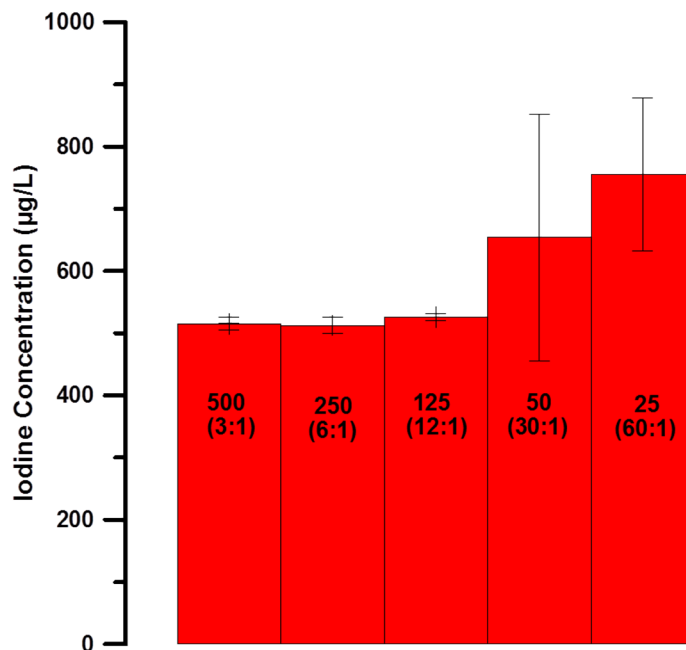
Figure B - 22. Dilution Corrected concentrations determined by ID-ICP-MS

In Figure B - 21, the top numeral is sample volume in microliters. The leftmost bar, with 500 μL sample and 1.5 mL H2O2 (30%) represents a 3:1 digestion reagent:sample volume ratio (inscribed as the second row text in each bar) and is the base case. There is a monotonic decrease in tracer recovery as the sample volume is decreased and this ratio is increased. Note that if any error were to occur due to ionization efficiency changes between samples, it would only exaggerate the difference as using smaller sample reduces salinity and therefore reduces any ionization suppression of the iodine signal. Figure B - 22 gives the calculated Iodine concentration following digestion using various digest:sample ratios
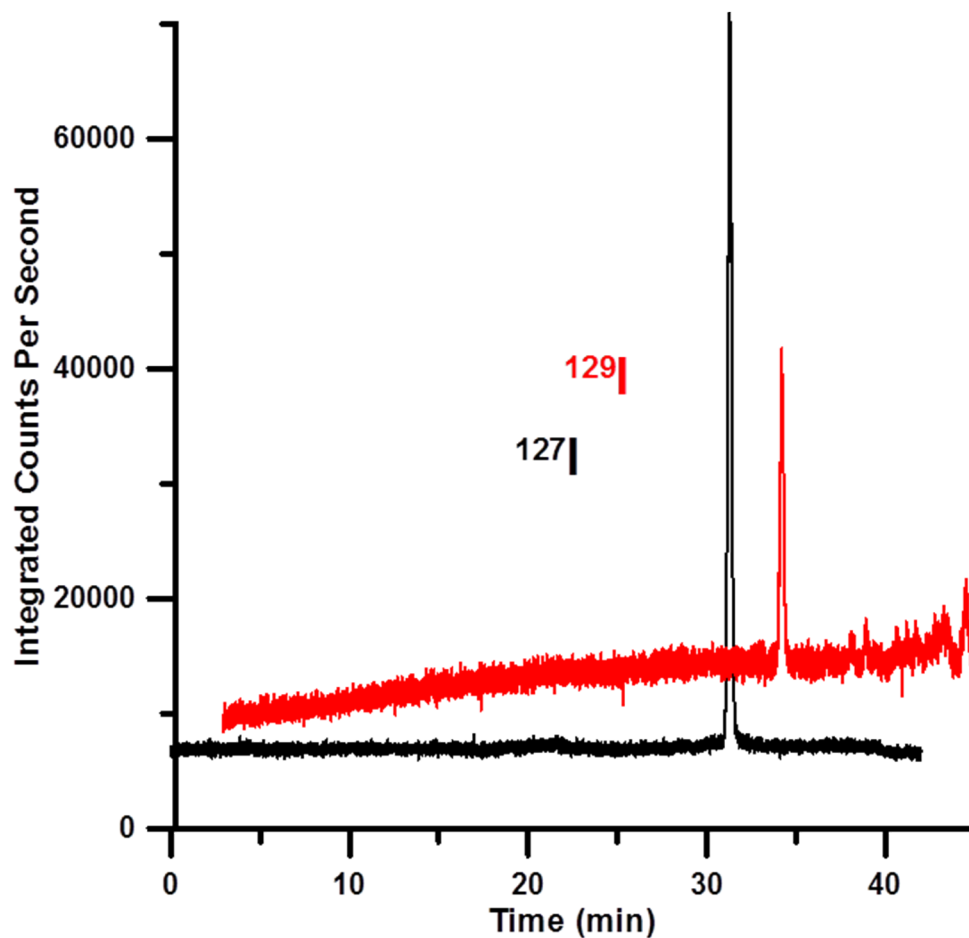
Figure B - 23. Iodine speciation following digestion at pH 0.64 of whole milk

Because the sample as such could not be introduced acidified (on column iron precipitation will occur with alkaline eluent), it was neutralized with ammonia first. If iodate is formed in the solution, it must have transient existence as iodate and iodide in acid solution must form iodine rapidly. As stated before, iodine or IO^- will rapidly from I^- with H_2O_2 in an ammoniacal solution. Accordingly, the IC-ICP-MS trace of the digest shows no presence of any species other than iodide is present. A dwell time of 150 ms was used for ^{127}I and 50 ms for ^{129}I.
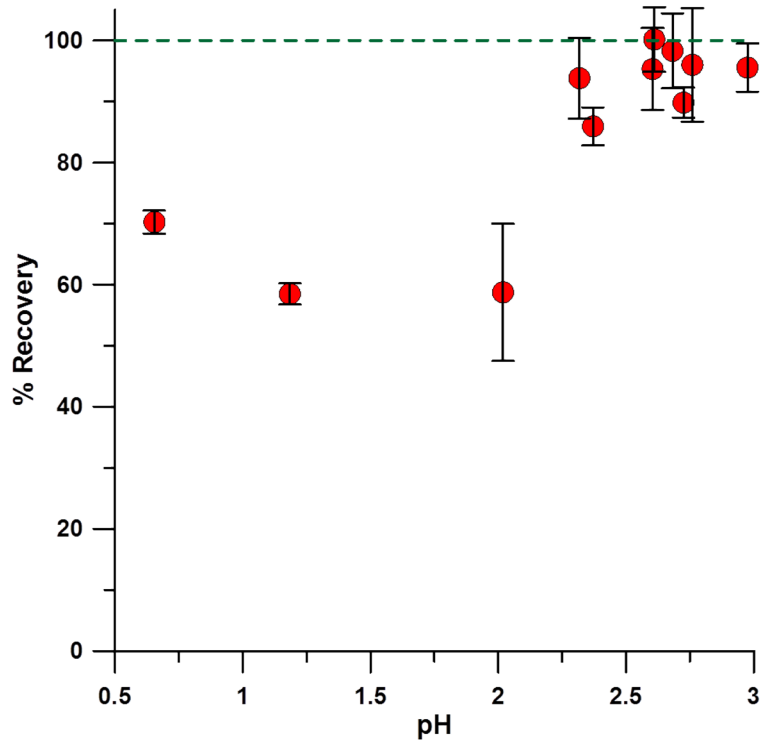
Figure B - 24. Loss Effect at varying digest pH's
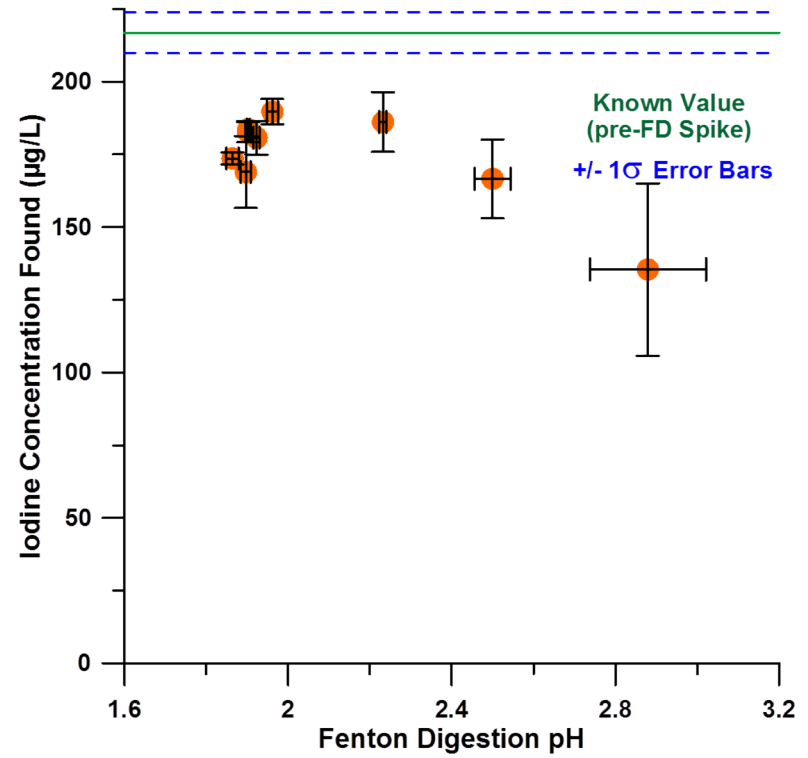
Figure B - 25. Breastmilk iodine content as a function of

post digestion pH

In Figure B - 24 it is shown that at a more acidic pH a clear increase in loss is observed. At very acidic pH ~0.64, less

loss is observed again suggesting the formation of Iodate. However, loss is still substantial. 129I tracer added post digestion as

iexcept to determine true value for which tracer was added prior to digestion as shown in Figure B - 25.

Table B - 8. Mass loss of digested samples

Sample ID	Mass Loss (mg)		Relative Loss (%)	
	Average	Stdev	Average	Stdev
Whole Milk	117.1	15.4	5.25	0.72
Breast Milk-1	138.4	19.5	6.41	1.19
Breast Milk-2	142.2	9.1	6.42	0.41
Formula Milk	116.3	10.4	5.18	0.49
Soy Formula	145.4	11.8	6.49	0.52
Blank	272.4	3.8	12.19	0.12
Average				
Sample	131	17.8	5.91	0.89

Because the blank loss was much higher than the real samples it was excluded from the total average.

Figure B - 26: 1 mL of sample, 1 mL of H_2O_2 were digested with varying amounts

of 0.1 M $Fe(NH_4)_2(SO_4)_2$ ranging from 0.05-1 mL of solution from left to right. Clear

digests are produced for all but the 50 µL sample. The yellow color is due to the

dissolved ferric iron.

Figure B - 26. Digests using varying amounts of catalyst

Figure B - 27: Digest of 1 mL Whole Milk samples with 100 µL ferrous ammonium sulfate and various amounts of H2O2 ranging from 4 mL(left) to 0.5 mL(right). Complete digestion occurs for all samples except 0.5 mL. At the high end, there is less observable ironaceous wall residues but oxygen continued to slowly evolve from these solutions after final dilution, increasing ICP-MS measurement noise. Either MnO2 or a greater ammonia concentration for final dilution are effective in removing the excess H2O2. However, for non ID-ICP-MS measurements, as iodine loss increases at high H2O2 content, the recommended practice is to use the lowest relative amount of H2O2. In this case, we chose to continue with a volume ratio of 1:1:0.1 for sample:30% H2O2: 0.1 M Fe(NH4)2(SO4)2.
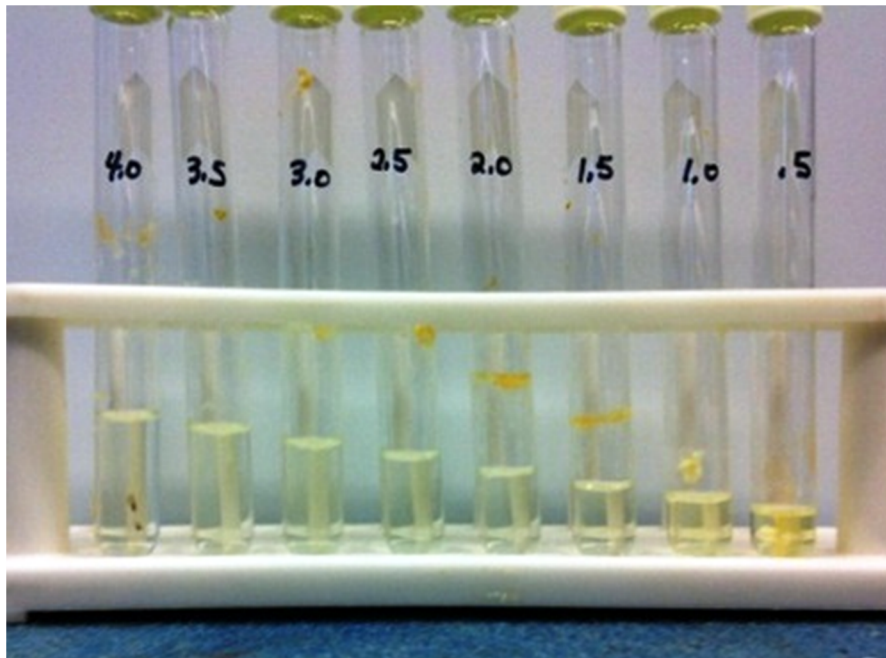
Figure B - 27. Milk digestion using various amounts of peroxide
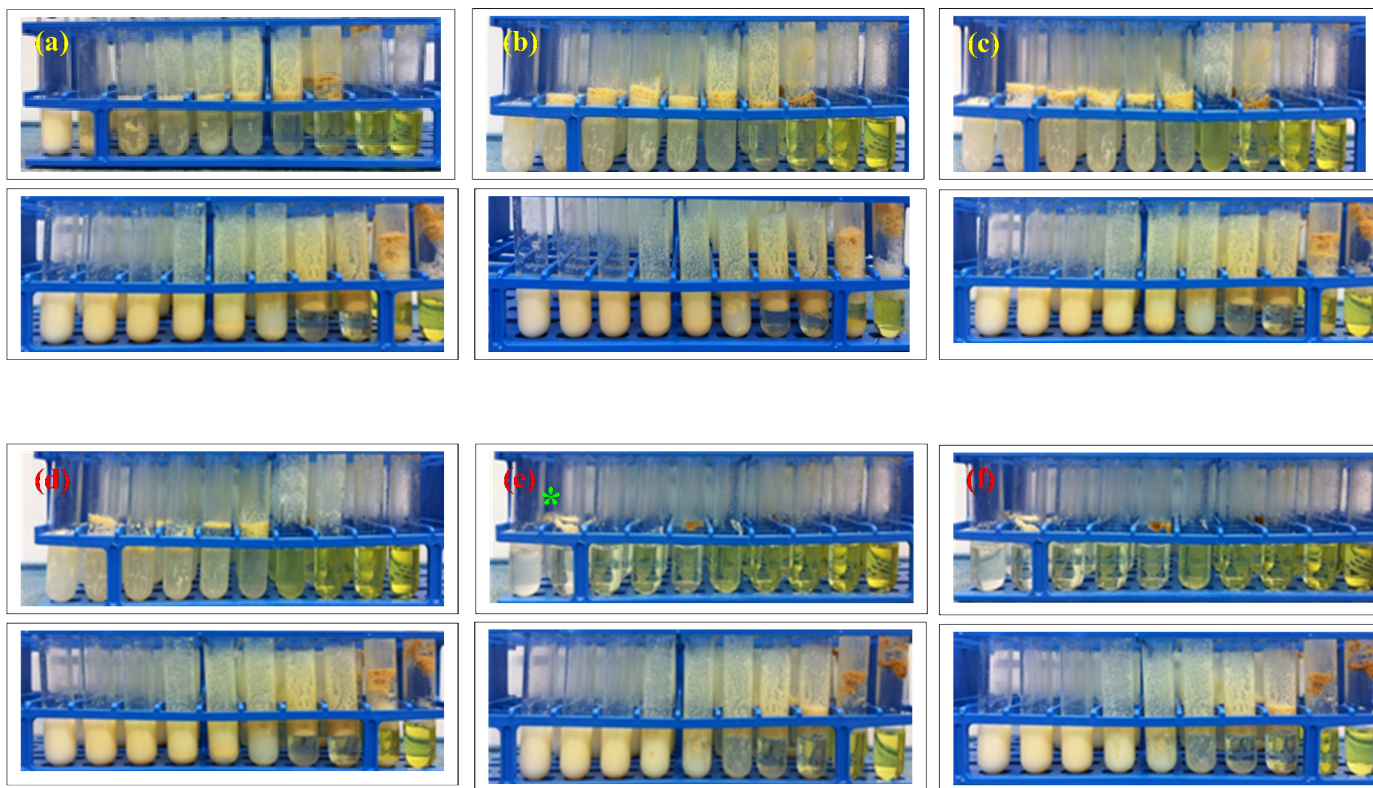
Figure B - 28: Reaction progression as a function of time and Temperature

Figure B - 28: In each case the top set is whole milk samples digested at 60°C while the bottom set is the same samples digested at room temperature. 1 mL of whole milk is digested with 1 mL of H_2O_2, various amounts of 0.1 M $Fe(NH_4)_2(SO_4)_2$. From left to right 50, 100, 150, 200, 250, 300, 400, 500, 750, and 1000 μL of catalyst was added. (a) 1 hour (b) 2 hours (c) 3 hours (d) 4 hours (e) overnight (12 hours) (f) 24 hours. The asterisked sample represents recommended conditions
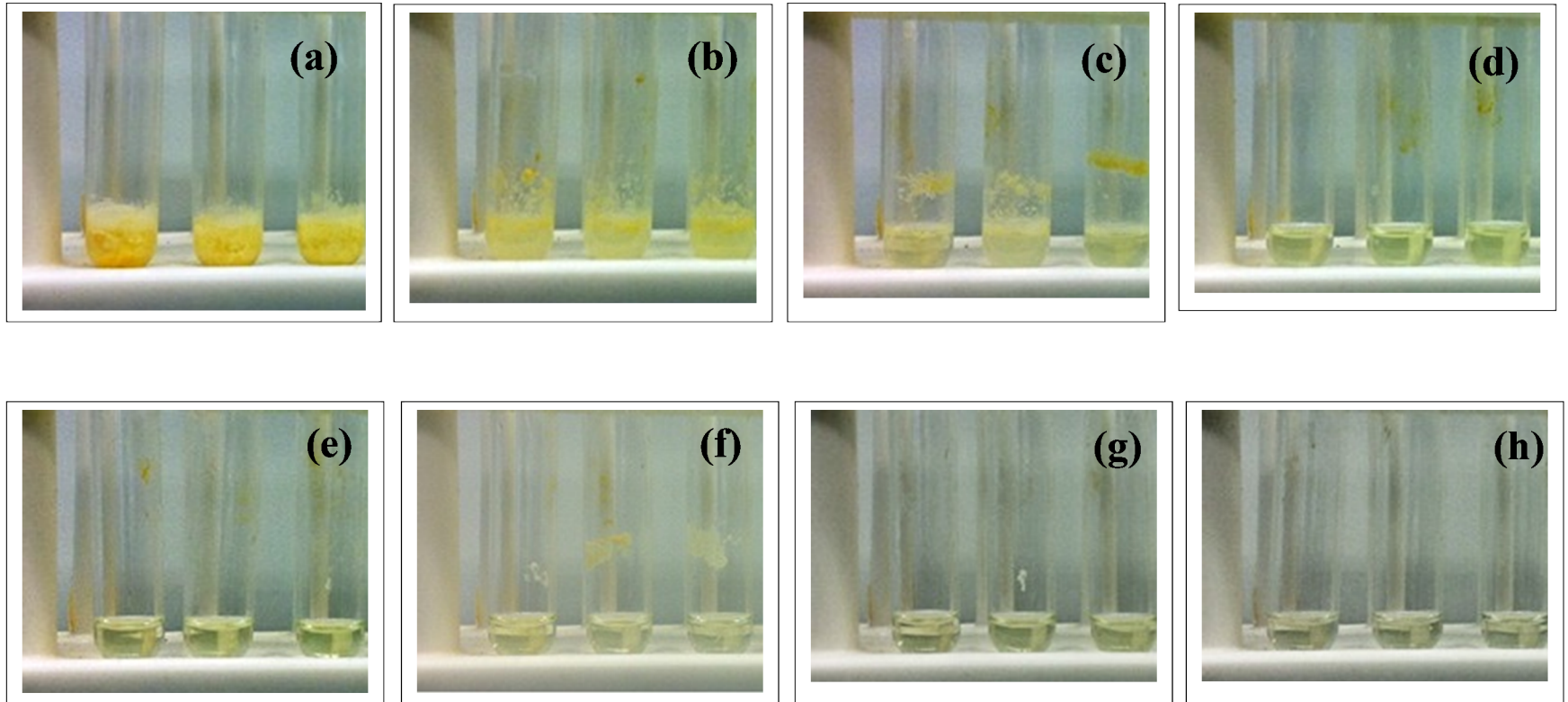
Figure B - 29: Reaction Progression at 90 °C

Figure B - 29: 0.5 mL whole milk digested with 50 µL Fe(NH4)2(SO4)2 and 0.5 mL H2O2. (a) 30 min (b) 60 min (c) 90 min (d) 120 min (e) 150 min (f) 180 min (g) 210 min (h) 240 min.
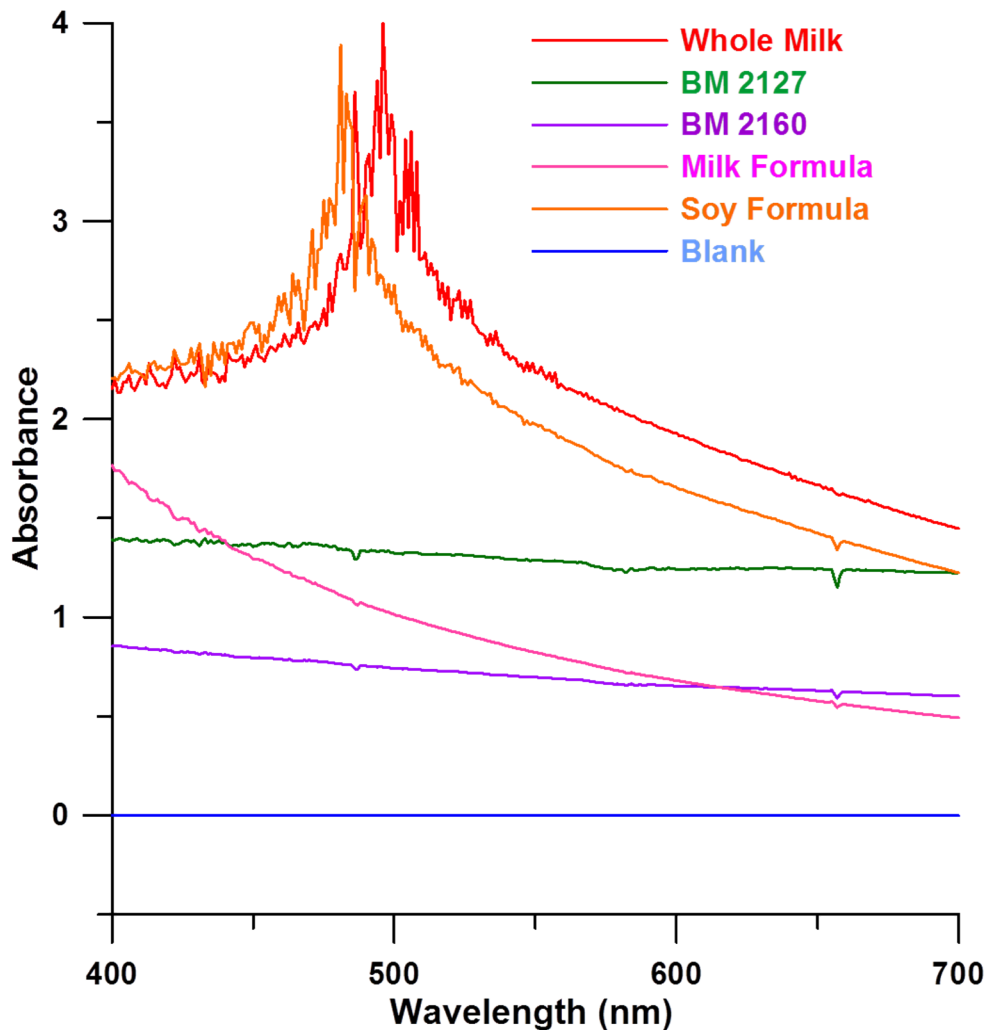
Figure B - 30. Absorption spectra of undigested Milk

Figure B - 30: Milk Samples including whole milk, two breast milk samples obtained from a local milk bank, soy formula, and milk based formula were diluted 1:100 and the absorbance measured on an Agilent 8453 Diode Array Spectrometer. We have observed that breastmilk samples thus diluted have a relatively near uniform absorbance across the visible range, this is not the case for the other samples. Even at 1:100 dilution the whole milk and soy milk is essentially opaque at 500 nm. Di water was used as the blank.
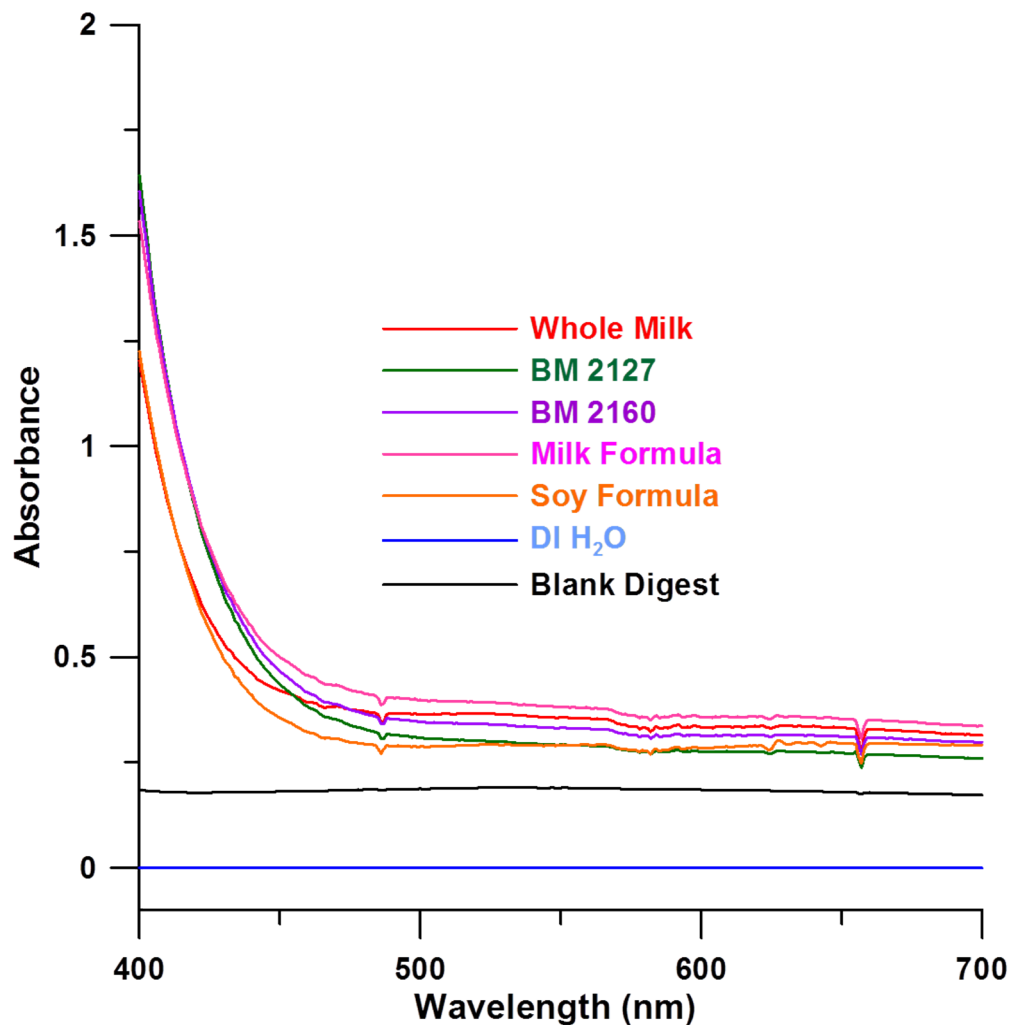
Figure B - 31. Absorption spectra of digested milk

Figure B - 31: Samples BM2127 and BM2160 are breast milk obtained from a local milk bank. Such similar absorbance spectra are indicative that regardless of the composition of milk or protein, the Fenton reaction works efficiently at decomposing the sample. Differences below 450 nm are likely caused by colloidal or chelated iron present. This digestion was performed overnight at 60 °C using 1 mL H_2O_2, 1 mL sample, and 100 µL 0.1 M $Fe(NH_4)_2(SO_4)_2.$

.

Appendix C

Supporting Information for Chapter 4

C.1 Alternative Discharge Cell Designs

Figure C - 1 shows the initial dielectric barrier discharge design as described by Puanngam et al[356]. Glass microscope slides were used as dielectric material, separating the electrodes from the plasma gas. PTFE spacers (75 mm x 10mm x 1mm) were used to separate the glass slides and provide a 5 mm wide path that is 1 mm deep. The device was then clamped together and sealed using silicone glue on all sides, except for the channel openings. Blocks made of glassed filled PTFE were constructed to hold the slide assembly at the entrance and exit The inlet block had a threaded port to accept standard ¼-28 chromatography fittings. The outlet was adapted to accept fiber optics terminated in SMA 905 connectors. A vent was included orthogonal to the slides and fiber optic to allow exit of the gas. Silicone RTV glue was used to seal the microscope slide assembly to the machined fittings. This design is advantageous in that it can be used with any desirable plasma gas. Eventually, fraying of the Teflon sheets resulted from proximity to the plasma and began to absorb iodine causing significant tailing. A concentric design was later developed to remove the need for Teflon in the discharging cell, Figure C - 2. A glass capillary used common in melt temp apparatus was
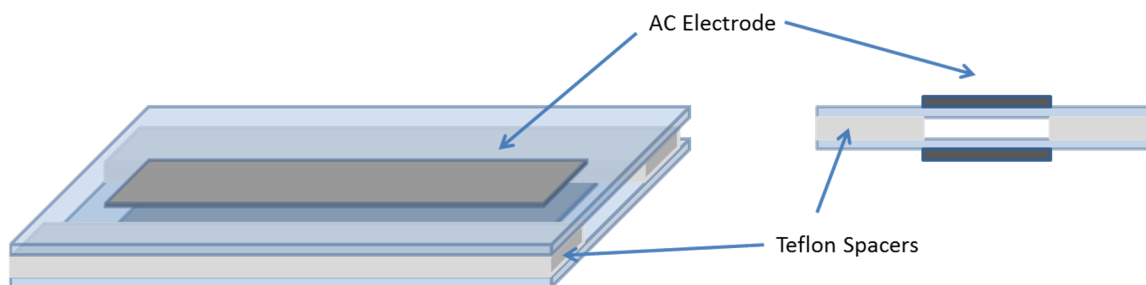
Figure C - 1. Planar electrode dielectric barrier discharge configuration

inserted through a PEEK tee. A steel wire was inserted into the capillary to serve as the high voltage electrode. A second glass tube (3.1 mm O.D. 2 mm I.D.) was mounted external to the capillary and wrapped in aluminum foil which served as the ground electrode. The glass tube was coupled to an outlet PEEK tee. A 1 mm fiber optic was connected to the tee to view the plasma. This device generates a stable plasma with only glass in contact with the plasma. The
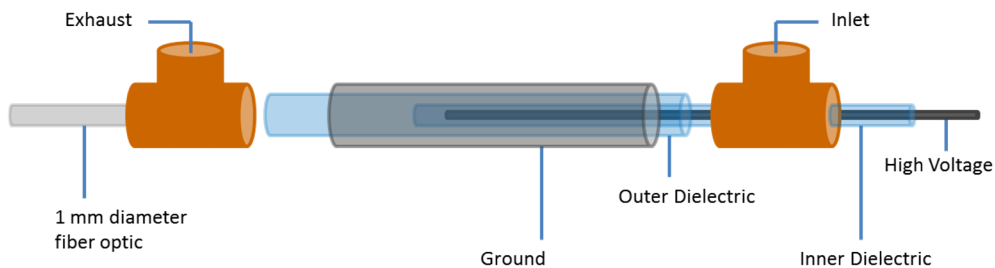
Figure C - 2. Concentric electrode dielectric barrier discharge design

high surface area and thin dielectric material used at the high voltage wire can easily generate

an intense plasma capable of melting the tubing used in the device. Any gas may be probed

using this configuration. However, because the plasma is generated between the glass

electrodes and the fiber optic optimally views the center of the channel, much of the light is

blocked by the central capillary and electrode.

C.2 Emission Spectra

Emission spectra of carrier gases and iodine were taken using the device shown in

Figure C - 1. Spectra using nitrogen as the carrier gas are shown in Figure C - 3 while that for

argon is Figure C - 4. The broad molecular fluorescence from ~425-525 nm is clearly

unobstructed in argon, while only minor interference occurs in nitrogen. The dominant emission

lines are not observable in nitrogen and the intense lines at 905 and 972 nm are obscured in

argon. In both gases the excimer emission at 341 nm is visible but difficult to measure due to

background emission lines.
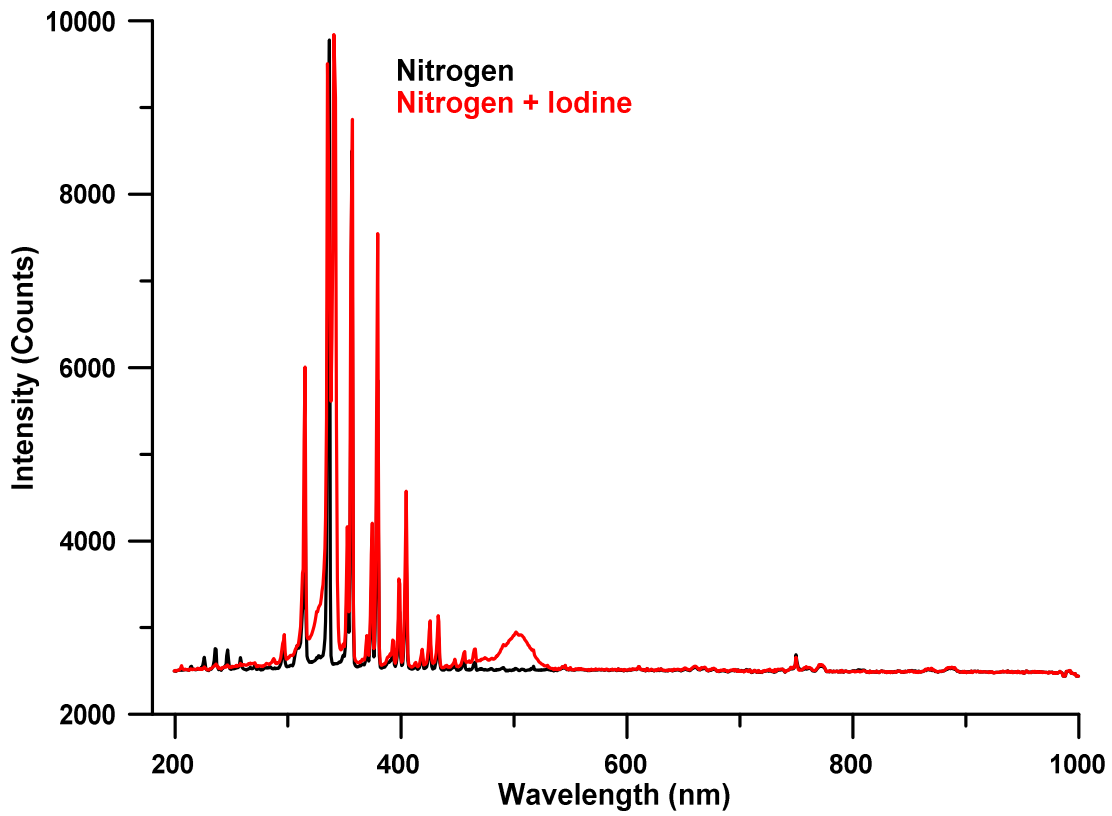
Figure C - 3. Emission spectra of nitrogen and iodine between 200-1100 nm
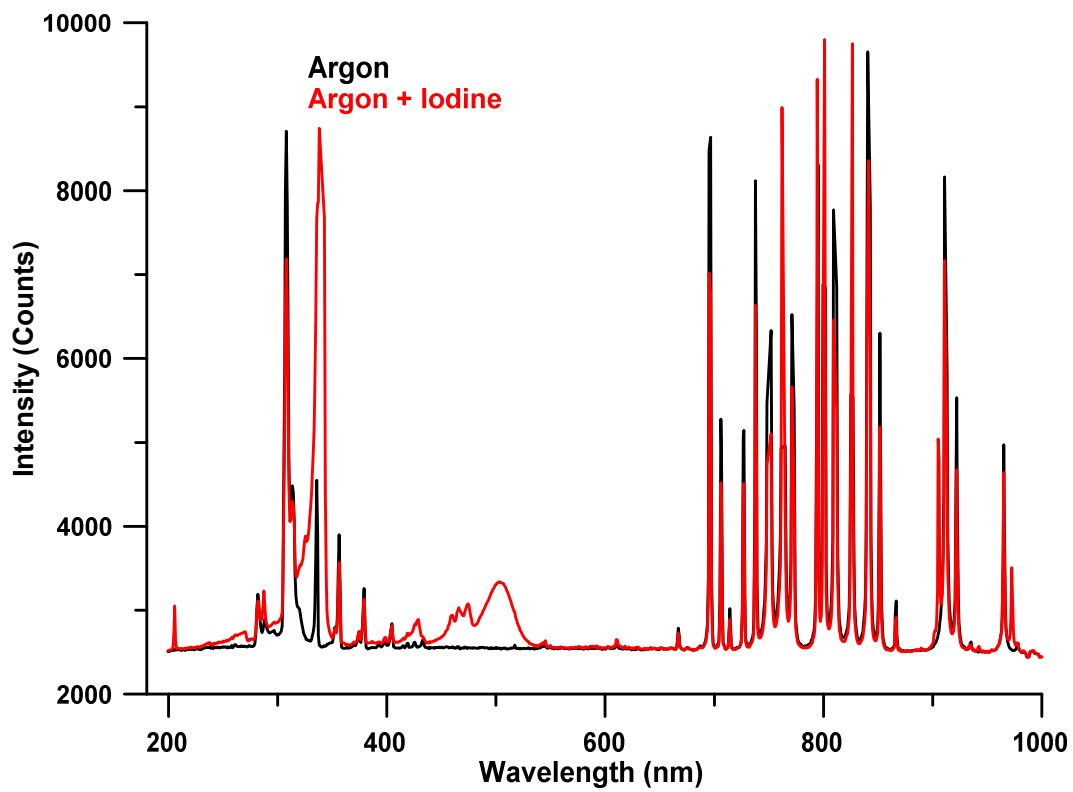
Figure C - 4. Emission spectra of argon and iodine between 200-1100 nm
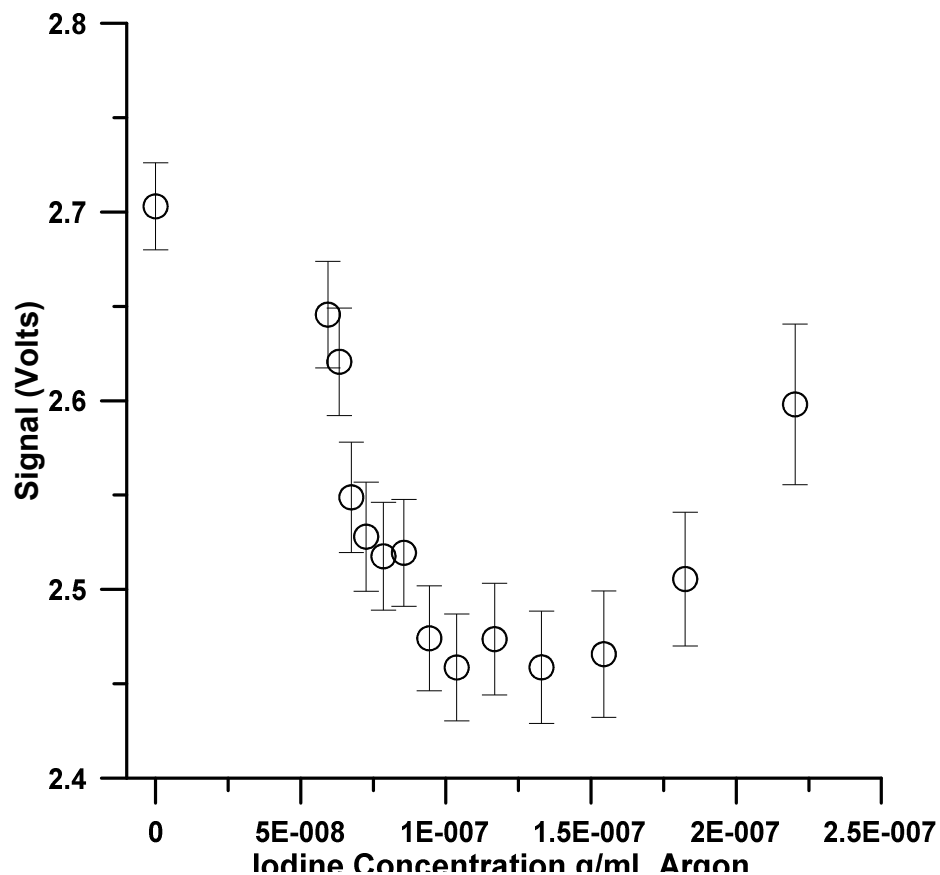
Figure C - 5. Iodine molecular fluorescence measurement in Argon plasma

Figure C - 5 shows the Iodine molecular fluorescence in an argon plasma. A Hamamatsu H5784-02 photomultiplier tube was equipped with a 500 nm interference filter with a 10 nm full width half maximum bandpass. An operational amplifier circuit was used to condition the signal providing up to 1100 times gain, and a 0.022 sec RC filter. A continuous gas phase concentration of iodine was made using the permeation tube setup.

C.3 Iodine preconcentration materials

Various materials were tested as suitable preconcentrators. Gold was first explored, having been used previously for detection with mercury[356] (Figure C - 6A). Initially promising results were seen, but were not reproducible. This may have been in part due to mercury sorbed to the gold from previous experiments. Mercury is known to be iodophilic and may have been the original sorbent observed. Silicone coatings were also tested. Silicone based glues were first dissolved in hexane. Then the filament was coated by adding drops of the dissolved silicone while gently heating the filament (using 3-4 volts DC) to evaporate the hexane. Low temperature silicone was not able to desorb iodine at a temperature that didn't result in degradation of the coating. High temperature silicone was able to desorb iodine, but this process is slow (Figure C - 6A) and the signal doesn't return to baseline so long as the heat remains on. It was also found that background counts were impacted by the concentration of iodine used. This likely results from a slow bleed from the material. Activated carbon was also tested. A ball mill was used to generate a very fine dust. A slurry was made in hexane and applied while heating the filament. Carbon however was very slow to desorb iodine, even when operated at 120 volts AC (the maximum rating for the bulbs). We attributed this to the porosity of the activated carbon. C60 fullurene was explored as an analog to carbon sorbent but without the porosity. It was first dissolved in toluene before being applied using the heated filament techniques. Figure C - 6B shows a nice response was produced. However, no subsequent signal was obtained after the initial measurement. Inspection of the preconcentrator revealed that the walls were coated in the preconcentrator material, indicating at the temperature necessary to liberate iodine, that the C60 too is also volatile or ejected from the filament.
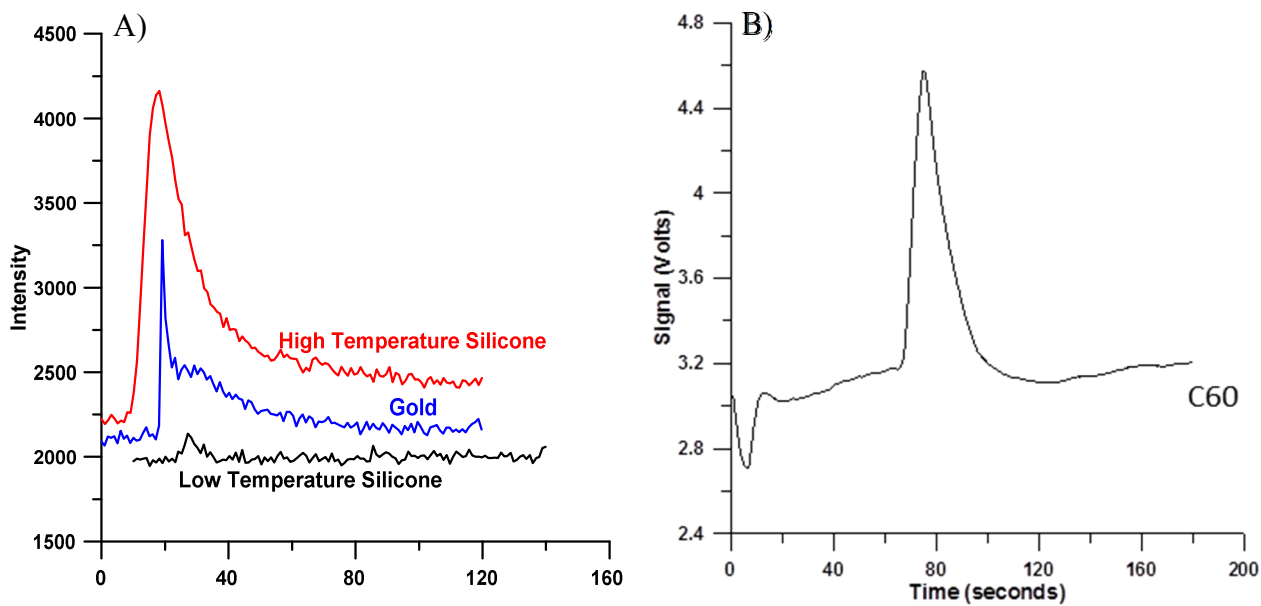
Figure C - 6. Measurement of Iodine desorbed from various preconcentrator materials: A) Silicone and gold coatingss, and B) C60 fullurene coating
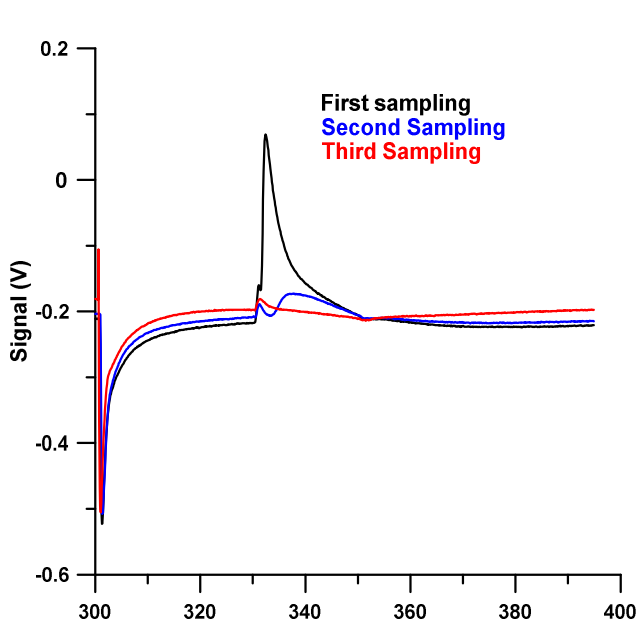
Figure C - 7. Peak measured using peroxide as oxidant with the synthetic urine matrix
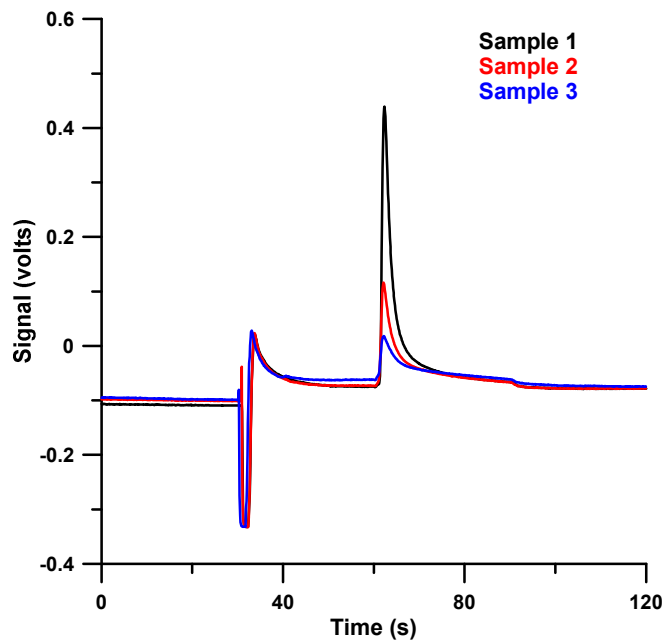
Figure C - 8. 3 subsequent samples of 100 µg/L I^- measured using NO_2^- as oxidant

184
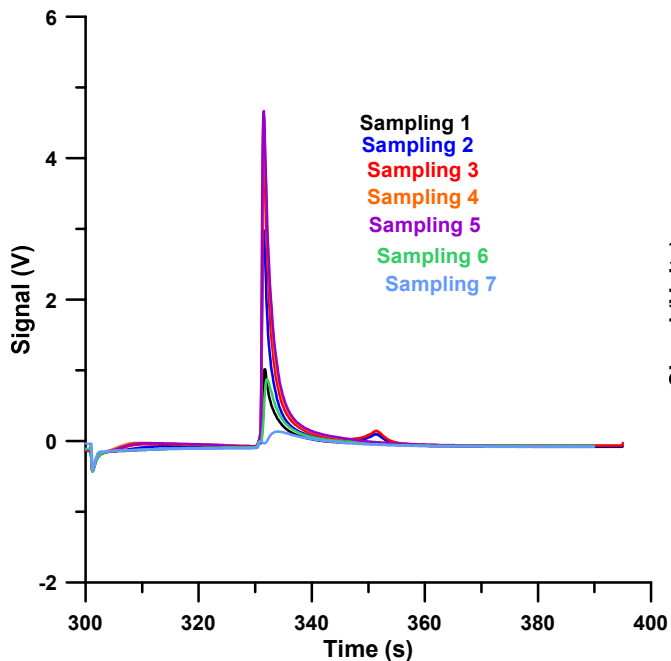
Figure C - 9. Subsequent measurement of a 10
mg/L I⁻ solution using Fe^{3+} as oxidant
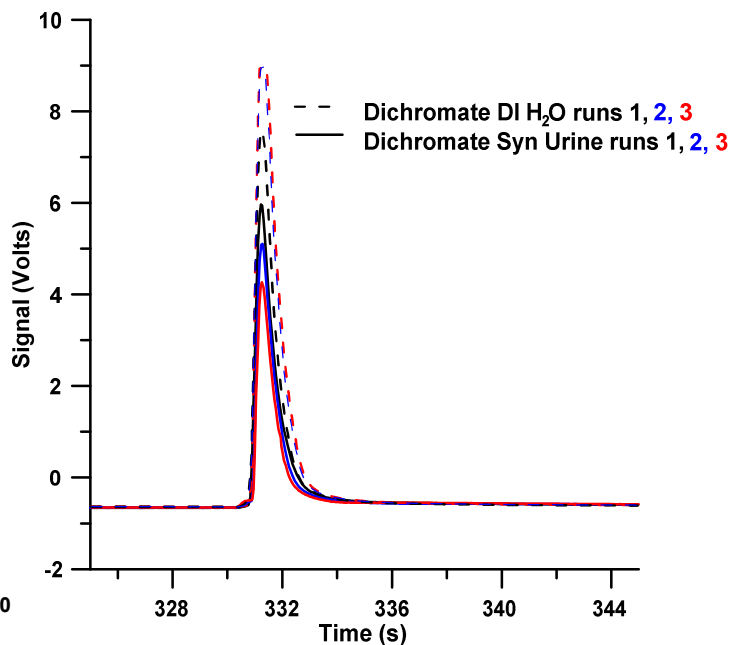
Figure C - 10. Comparison of the measurement of I⁻ using
dichromate as oxidant in DI water and synthetic urine matrix
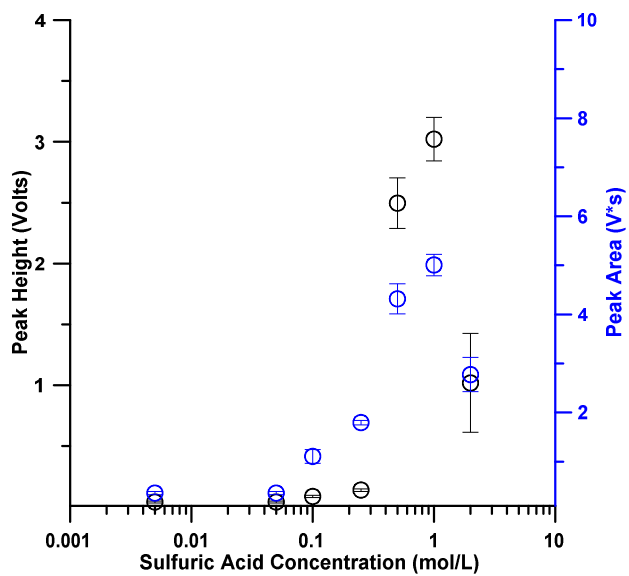
Figure C - 11. Peak height and areas of 500 µg/L I⁻
measured as a function of acid concentration in the
reaction mixture
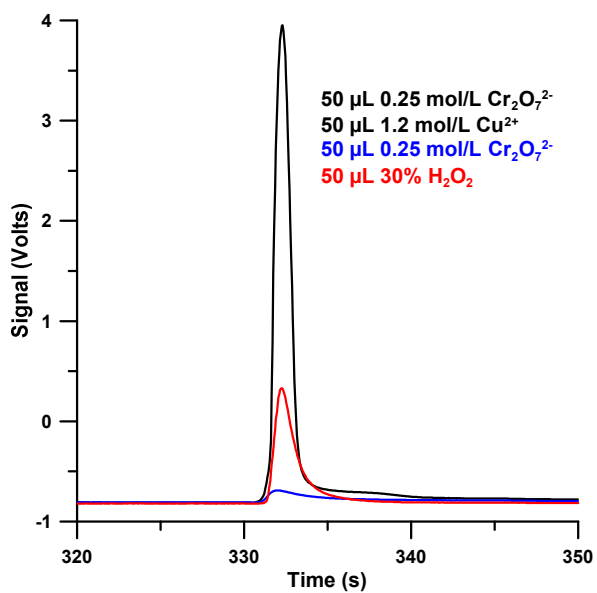
Figure C - 12. Iodine signal produced using
various oxidation schemes with 100 µL 1 mol/L
H_2SO_4 saturated in $(NH_4)_2SO_4$
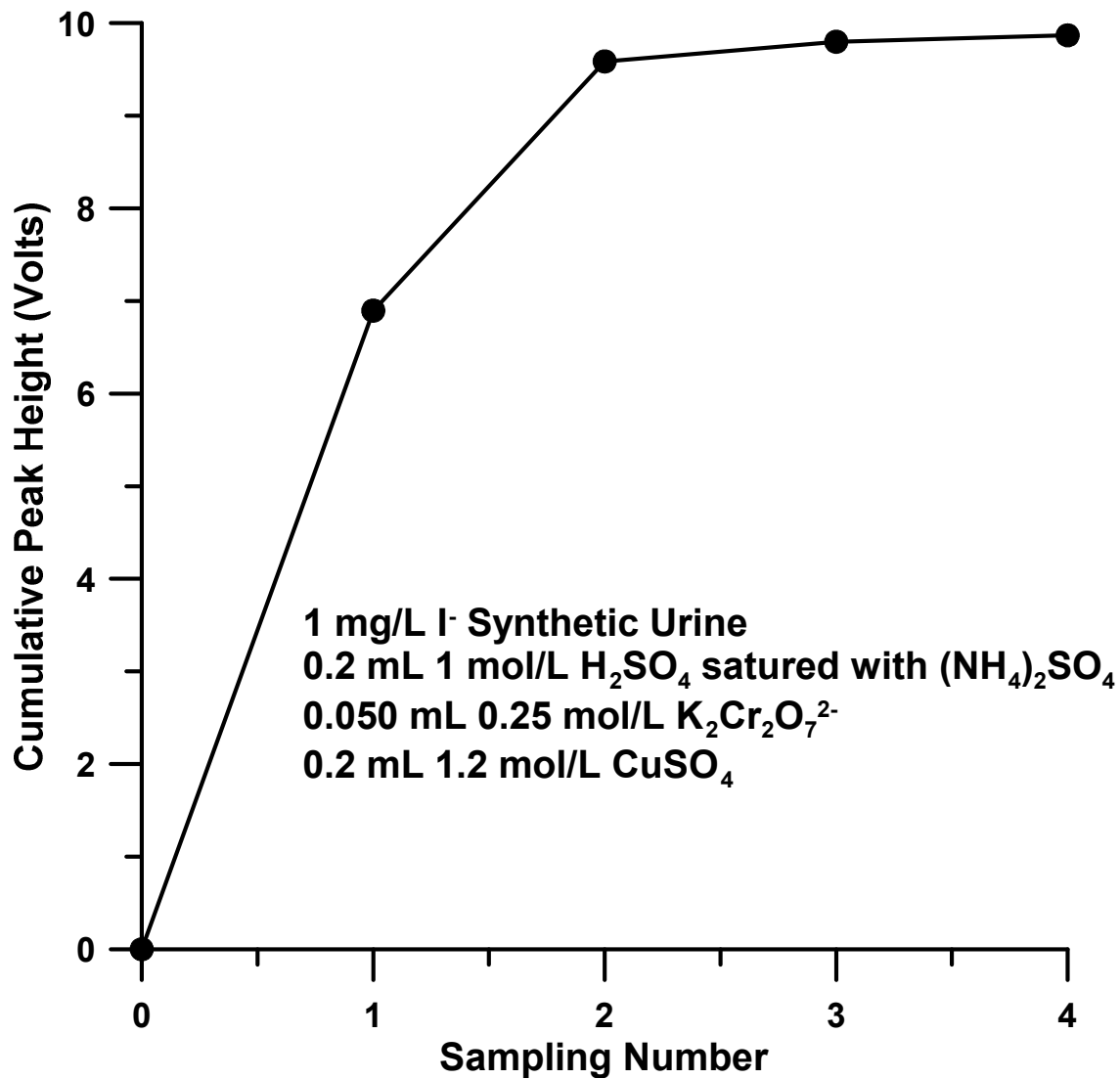
Figure C - 13. Serial sampling of a single standard and the cumulative peak height.

Sampling time is 5 minutes
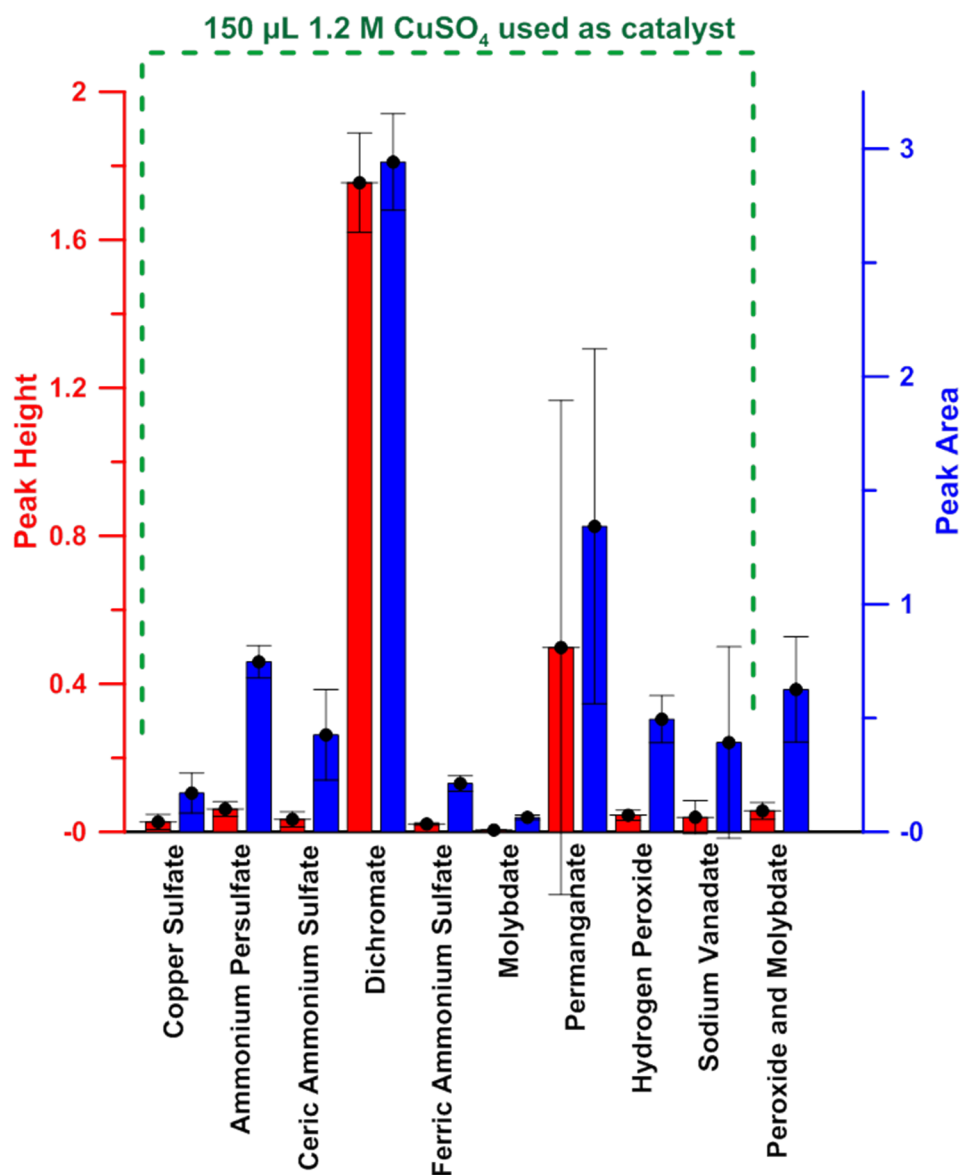
Figure C - 14. Test of various oxidants using Cu^{2+} as catalyst

1 mL of Synthetic urine matrix was used with 500 µg/L I^-. 0.2 mL of 1 mol/L H_2SO_4 saturated in $(NH_4)_2SO_4$, 0.15 mL 1.2 mol/L $CuSO_4$ and 50 µL 0.25 mol/L oxidant (or saturated if unable to be dissolved fully). Ceric ammonium sulfate was prepared by dissolving in 2 mol/L H_2SO_4 and sodium vanadate was prepared by boiling with NH_4OH present. Peroxide solution used was 30% (w/v).
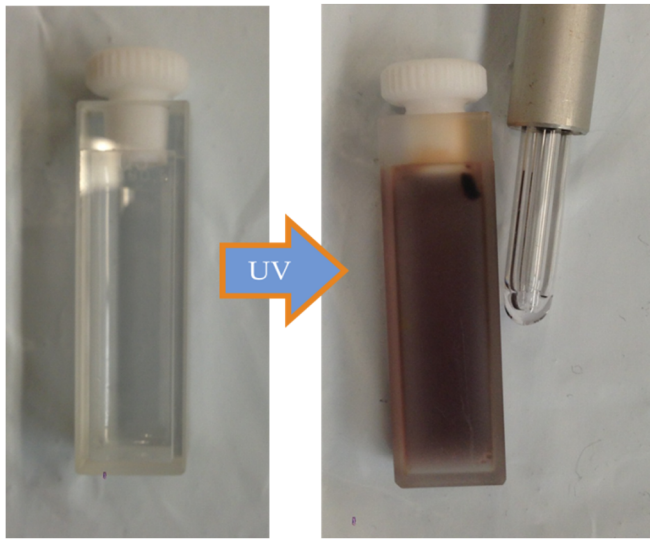
Figure C - 15. Treatment of CH$_3$I in a quartz Cuvette using a UV light
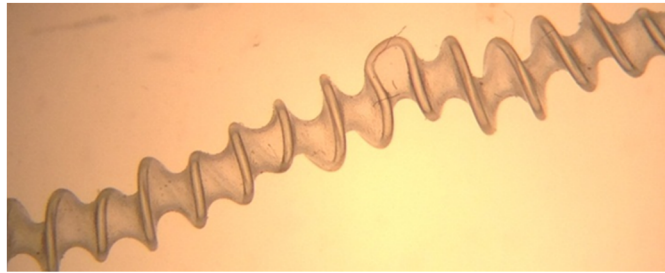
Figure C - 16. Image of the silicone tubing filled with self coiled 2 lb nylon fishing line
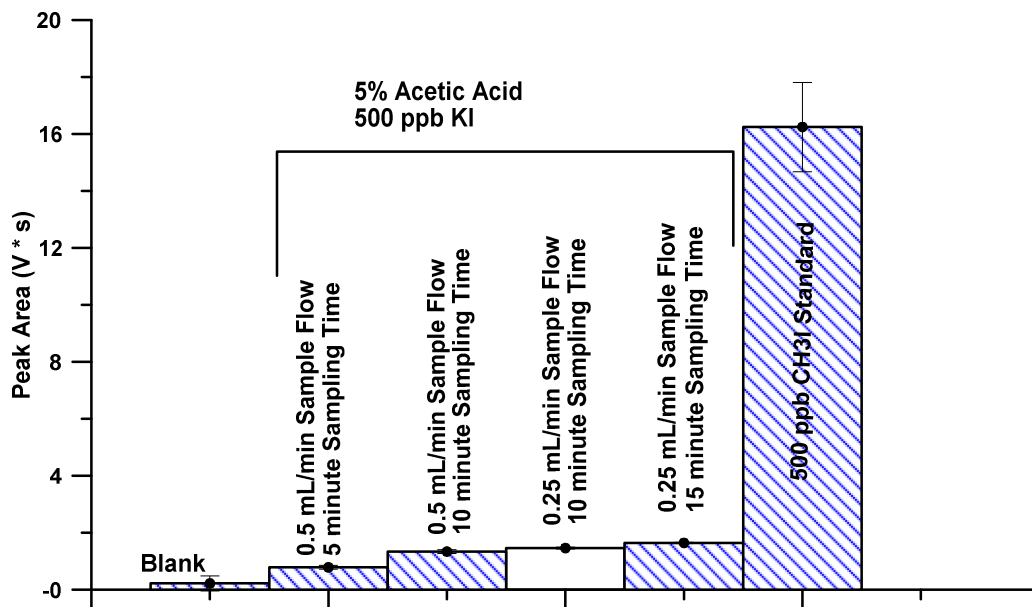
Figure C - 17. Peak areas using UV photochemical generation of CH$_3$I

188

Appendix D

Supporting Information for Chapter 5

In the presence of peroxide I_2 and I^- have the following relationship[435]:

$$\frac{[H^+]^2[I^-]^2}{[I_2]} = 6.05 \; x \; 10^{-14} + 1.47 \; x \; 10^{-9}[H^+]$$

The concentration of I_2 present as a fraction of the total iodine concentration is plotted in Figure D - 1 and Figure D - 2 under different conditions. Contributions of IO_3^- or IO_2^- are not included in the model above. Figure D - 2 should resemble that of the response factor plot in the main text. Similar shape is seen, but reduction in the fraction of I_2 present is observed ~2 orders of magnitude below that actually observed
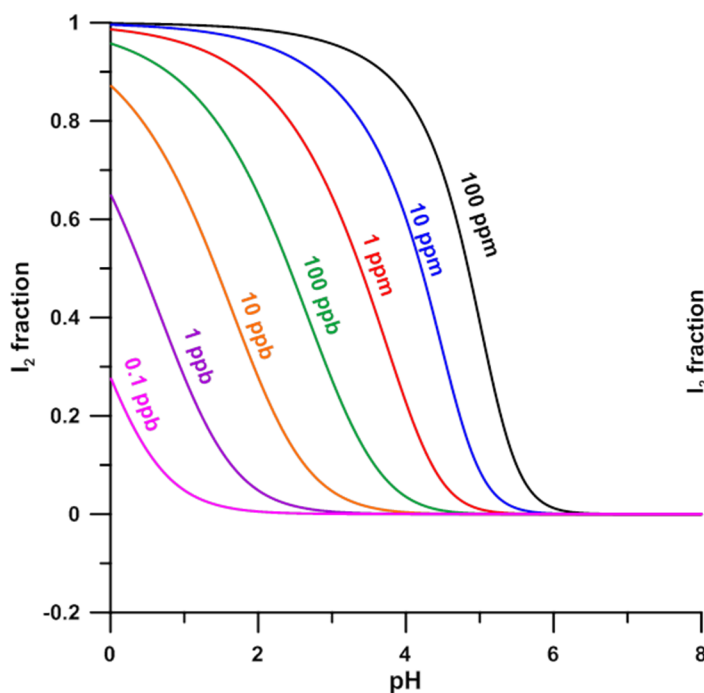
Figure D - 1. Plots of predicted fractions of I_2 at a given concentration as a function of pH
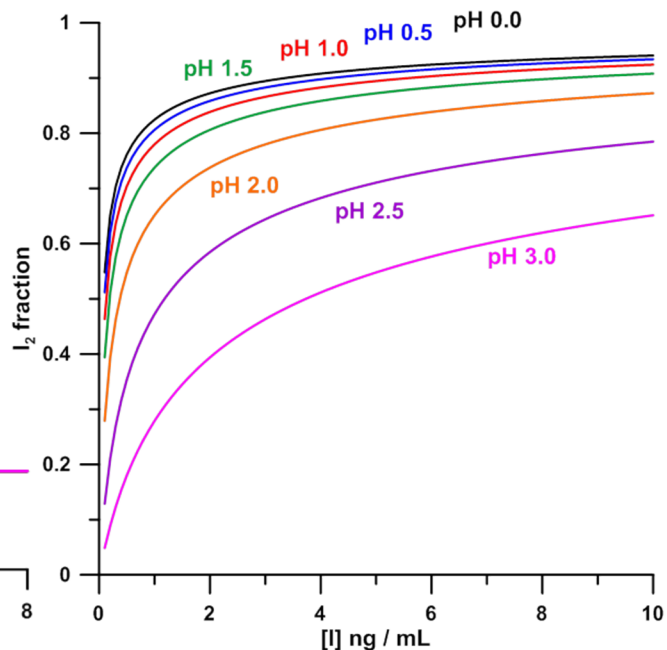
Figure D - 2. Plots of predicted fraction of I_2 in aqueous solution as a function of concentration at a given pH.

Figure D - 3 shows the fraction of I_2 present as predicted based on the disproportionation of I_2 in aqueous solution. The equilibrium reaction is expressed as[438]: K = [H+][I-][HIO]/[I2] = 3.13 x 10-13. The concentration of each species present can be calculated and the amount as I_2 can be plotted as the fraction of total iodine. The fraction of I^2 present should generally resemble the amount capable of being purged from solution.

Figure D - 4 shows the log-log plot of the SIA method. An improvement in R^2 is seen using such a plot. A slope higher than 1 indicates the signal is not linearly dependent upon concentration and is a higher order function..
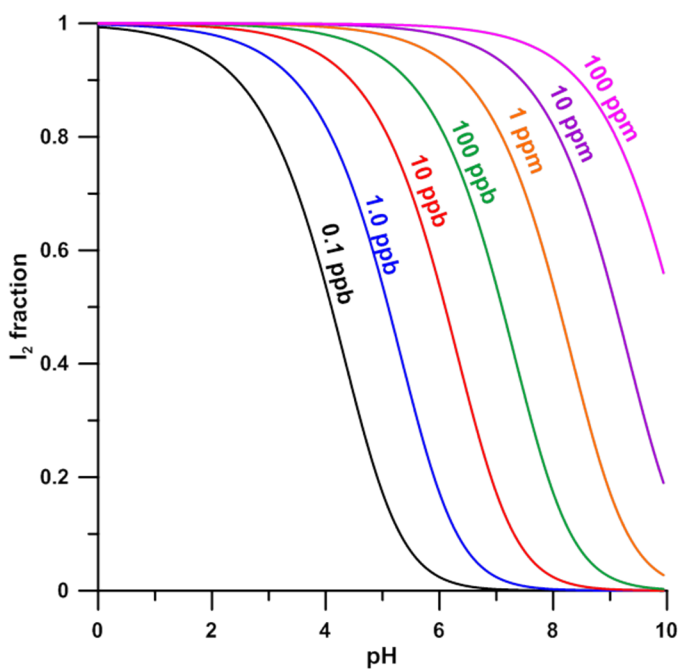
Figure D - 3. Plot of fraction of I_2 present based on disproportionation of I_2 into HOI and I^{-1}
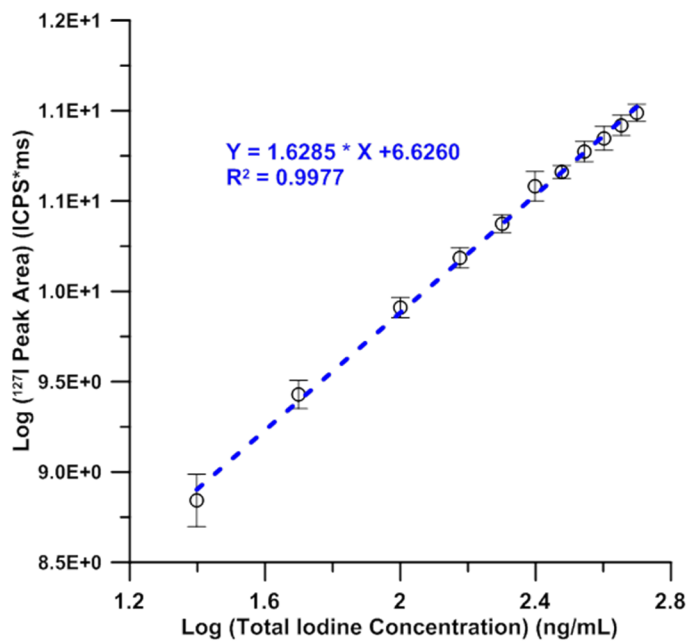
Figure D - 4. Log-Log plot of peak area vs. iodine concentration

Appendix E

What can In-situ Ion Chromatograpy Offer for Mars Exploration?

E.1 Introduction

There is a long line of evidence that points to a wet history at the surface of Mars including surface morphology,[451] elemental chemistry/mineralogy/diagenetic features,[452] and widespread detection of hydrated minerals.[453] The hydrated minerals include sulfates, e.g. gypsum and kieserite[454] that formed during the evaporation of high ionic strength acidic water,[455] and phyllosilicates, e.g., smectites[456,457] that formed under circum-neutral pH and lower ionic strength. Detailed investigations at Gale Crater by the *Curiosity* rover have revealed fine-grained sedimentary rocks inferred to represent an ancient lake environment suited for supporting life.[458] This is the first direct evidence of a past habitable environment on Mars, and given the widespread geologic evidence of liquid water activity on the planet, it suggests that significant portions of the planet's surface could have been habitable at some point in the past.

However, in order to further constrain present and past habitability it is critical to understand the soluble chemistry of Martian surface materials. Soluble ions determine the water activity (Aw) of aqueous solutions, an all-important parameter for life. The growth of terrestrial organisms is drastically inhibited at Aw<0.61.[459,460] Abundant and diverse microbial communities in anaerobic environments on Earth utilize soluble ions such as nitrate (NO_3^-), perchlorate (ClO_4^-), or sulfate (SO_4^{2-}) as electron acceptors, a key requirement for habitability. Nitrate, a compound that is central to life on Earth as a source of N and also in some metabolic processes,[461] remains undetected on Mars despite theoretical models predicting its existence near the surface.[462] Some soluble ions such as ClO_4^- are important anti-freeze agents, and stabilize liquid water solutions at temperatures well below freezing.[463,464] They also promote liquid condensation from water vapor by way of deliquescence,[465,466] this has been suggested as a possible source of liquid water for life even under present conditions.[467]

Yet, very few direct measurements have been made of the current pH, ionic strength, and soluble species in surface and subsurface materials. Only the Phoenix mission with the Wet Chemistry Labs (WCLs) has made these measurements.[468] The results were both novel and

striking, demonstrating a moderately alkaline soil (pH 7.7) in a carbonate buffered system,[469,470] that included soluble sulfates,[471] and large amounts of ClO_4^-.[470,468] The combined results from the Phoenix mission pointed to one of the most habitable environments on Mars under current conditions.[472]

Further detection of ClO_4^- in sediments at Gale Crater by the rover *Curiosity* suggests that this compound is widespread on the surface of the planet, which has important implications that go beyond habitability. For example, the presence of ClO_4^- at the Viking lander sites could explain the measurements made of chloro/dichloromethane after sample volatilization at 200 – 500°C because of the reaction between ClO_4^- and organics in the soil.[473] In addition, the creation of hypochlorite (ClO^-) and chlorine dioxide (ClO_2) gas from UV irradiation of perchlorate salts in the regolith could explain the otherwise inexplicable results observed from both the Viking Labeled Release experiment and Gas Exchange experiment.[474]

However, none of the instruments previously flown to Mars were capable of speciating different soluble ions, such as the series of oxychlorine anions. The serendipitous detection of ClO_4^- by the WCL was because of the high response of a NO_3^- selective electrode to ClO_4^-. Indeed, the high concentration of ClO_4^- in the regolith made it impossible to determine if any NO_3^- was present in the sample. Clearly, there is a need for alternative instruments for wet analysis, which can identify the oxychlorine and other soluble ionic species in Martian samples.

E.1.1 Ion chromatography for Space Exploration.

On Earth, the preeminent technique for soluble inorganic anion analysis is ion chromatography (IC).[475,476] The current practice of IC originated with Small et al.[477] (1975) who made two key inventions. First, they introduced surface agglomerated ion exchange packing that greatly improved column efficiency. Second, and more importantly, they provided the first practical method for sensitive electrical conductivity based detection. Solution electrical conductivity is the hallmark property of ions; indeed this is the property that distinguishes electrolytes (composed of ions) from nonelectrolytes (composed of uncharged molecules). But

ion exchange separations requires ionic eluents that are themselves highly conductive, the minor change in conductivity that occurs when an analyte ion elutes (with a concomitant and equivalent decrease in the background eluent ion concentration) is very difficult to discern leading to poor sensitivity. Small et al.[477] proposed the introduction of a second column, originally called the *stripper*, now universally called the *suppressor*, to remove the high conductivity background signal. A typical anion chromatography setup will use KOH as the eluent: The suppressor device continuously replaces all K^+ to H^+, resulting in a background of water. Any eluting ion, e.g., Cl^-, NO_3^-, SO_4^{2-}, or ClO_4^-, on the other hand, enters the detector as the corresponding acids HCl, HNO_3, H_2SO_4, $HClO_4$, etc., which are fully ionized and are sensitively detected against the low conductivity background of water. Moreover, an eluent gradient, where the KOH concentration is increased during the chromatographic run to increase the eluent strength, is invisible at the detector. This scheme allows for nanogram detection limits for strong acid anions.[478] Since its inception, IC has become the benchmark technique for aqueous anion analysis. Not surprisingly, IC has been the method of choice for investigating ClO_4^- in environmental and biological samples,[479-481] and to study the impact of perchlorate on human health.[482-484]

For planetary science applications, capillary IC, which uses small ($\leq$ 1 mm) diameter separation columns, is promising because it allows miniaturization of the instrument as well as reduction in the amount of sample needed (< 1 µL).[485] These reductions in size have allowed construction of field portable instruments that provide laboratory quality results.[486,487]

On Earth, analysis time is among the most critical performance parameters for IC, and this is especially true in the field where a shorter analysis time allows more samples to be processed on location. The desire for a high speed instrument leads to a tradeoff between two extremes: 1. An instrument with a heavy, power-intensive pump that allows operation at high pressures. 2. A low pressure open tubular column format that requires column diameters $\leq$ 20

μm for best separation and detection,[488] but is limited by the inability to build suppressors (critical to anion analysis) for columns <75 μm in internal diameter.[488,489]

Interestingly, for a Mars instrument as applied to soil extracts, the analysis time is far less critical (at least for the present), because it is not particularly meaningful to analyze soil repeatedly in the same vicinity. Power and terrain limitations for any extraterrestrial vehicle limit the speed (the top speed for *Curiosity*, powered by a ~120 W thermonuclear battery, is 4 cm/s in favorable terrain[490]). The volume of extractant water that can be carried on-board, the number of times extraction apparati can be (re)used, etc. also limit the number of samples that can be analyzed as in the WCL.[491] Analysis time is not a major limiting factor, unless there is significant power consumption related to analysis time. Most terrestrial liquid/ion chromatography systems are operated at flow rates much faster than the flow rate needed for best separation efficiency, often referred to as the Van Deemter minimum,[492] because it allows more rapid analysis (the critical factor on Earth) with acceptable separation of analytes. However, not only can the separation efficiency be maintained, it can often be *improved* by reducing the flow rate to be close to the Van Deemter minimum.[492] An order of magnitude reduction in the flow rate will increase a typical 20 minutes run time to just over 3 hours (this work), still quite acceptable for a planetary science application, with the notable advantage that there will be a concomitant and proportionate reduction in pressure. The latter would eliminate the need for a mechanical high pressure pump, allowing the use of pneumatic pumping. This, in turn, permits the use of almost entirely commercial off the shelf (COTS) components to construct a low pressure IC system that can provide the same state of the art anion analysis, albeit with a longer analysis time.

In this work we seek to demonstrate a low pressure COTS IC system that is capable of providing state of the art anion separations relevant to the soluble chemistry of the Martian regolith, and determine the limits of detection (LODs) for these anions. The ability to separate and detect non-perchlorate oxychlorine species and small organic ions are noted because of

196
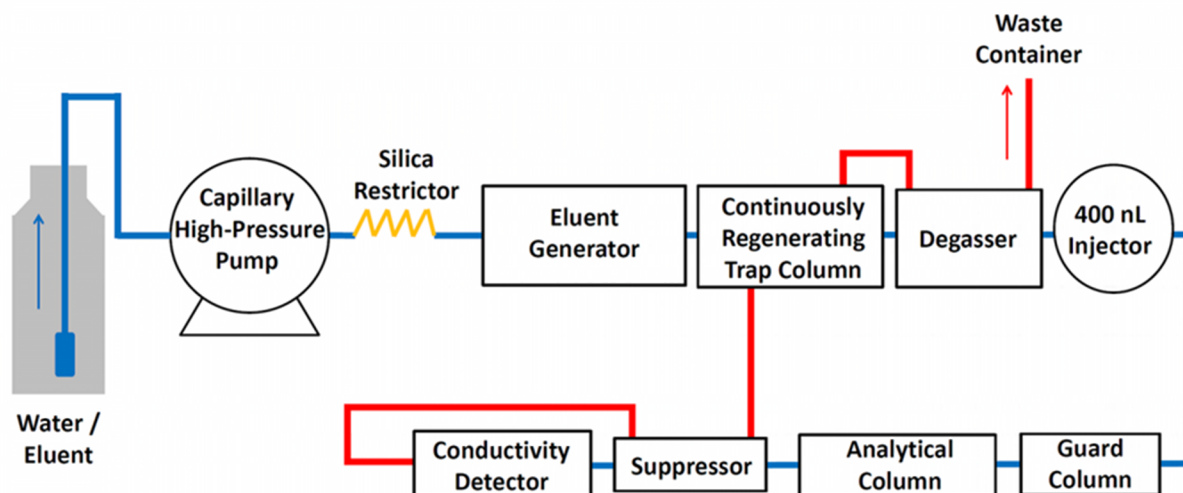
Figure E - 1. IC apparatus schematic. The flow path of the eluent is illustrated in blue prior to detection. The eluent is then used as the regenerant solution for the membrane based devices shown in red before going to waste. .

their suspected but unconfirmed presence on Mars.[468,474,493,494] In addition we demonstrate the systems performance in the presence of millimolar ClO_4^- (detected at these concentrations by direct and indirect measurements of the Phoenix lander and *Curiosity* respectively[470,495]) to verify that such large concentrations will not interfere with detecting the other ions of interest.

E.2 Experimental

E.2.1 Apparatus Description.

A modified Dionex ICS 5000 apparatus was used in this study (Figure E - 1). We used both the high pressure pump available in the system at the lowest flow rate of 1 µL/min, and a pneumatic pump (*vide infra*). When using the high pressure pump, a silica restrictor designed to produce a pressure drop of ~50 psi/µL/min was inserted directly after the pump as the pump has a safety shutdown mechanism if the pressure drops below 200 psi. Up to 80 mM LiOH eluent was prepared by pumping deionized water through an electrodialytic eluent generator at 1-10 μL/min. A custom eluent generator filled with LiOH at one quarter the normal strength concentration was used to reduce leakage of the LiOH into the eluent stream. Typically an

eluent generator is filled with the highest possible concentration of an alkali hydroxide (e.g., LiOH, NaOH, KOH, etc.) so that the reservoir lasts as long as possible. In principle, if no current is applied, there is no leakage of KOH into the acceptor water stream. In practice, however, there is leakage and such unwanted leakage is a greater problem at the lower acceptor flow rates being used here. Using LiOH instead of KOH, and using a lower concentration in the reservoir (leakage is typically proportional to the square of the reservoir concentration[496]) reduces the leakage. The eluent generator was followed by a continuously regenerated anion trap column (CR-ATC) that removed any non-hydroxide impurities, and then an eluent degasser. A four port 400 nL internal loop injection valve was used to introduce the sample on Thermofisher/Dionex IonPac AG20/AS20 guard and separator column pair. The suppressor following the column was a custom version of the self-regenerating capillary anion suppressor. The primary difference was the shorter length of the suppressor membrane. The standard suppressor is designed to operate at 10 μL/min, but a much smaller length of membrane is adequate to bring about complete suppression at lower flow rates. Moreover, using the standard suppressor brings about excessive peak dispersion at low flow rates, masking some of the performance improvement gained by operating at the flow rates closer to the Van Deemter minimum. Therefore, the modified suppressor was designed to provide optimum performance at flow rates of 1 – 3 µL/min and was operated at a correspondingly lower current of 3 mA. As in the standard configuration, the detector effluent was directed sequentially through the suppressor regenerant compartment, the CR-ATC regenerant compartment and the degasser jacket before heading to waste.
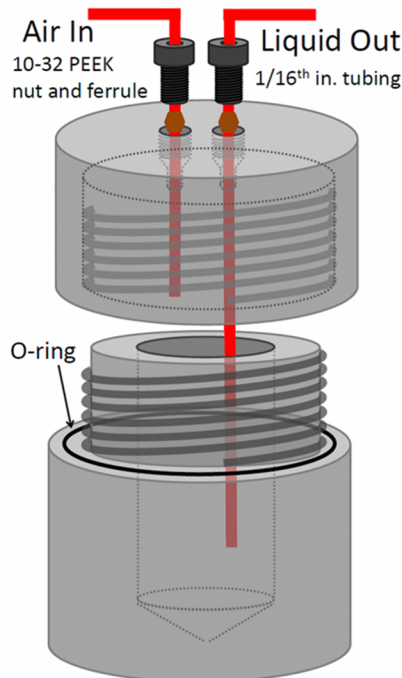
Figure E - 2. Aluminium pressure vessel used as a pneumatic pump.

Nitrogen is used to displace liquid in the reservoir

The pneumatic pump consisted of an aluminum vessel that could be pressurized using a regulated nitrogen source, and a 14 mL polypropylene culture tube cut to height was used to hold the water to be pumped and avoid direct contact with the aluminum wall (Figure E - 2). Because the breadboard setup with the pneumatic pump made partial use of the commercial instrument, the high pressure instrument pump (operating at low pressure) still had to be used to pump liquid through the restrictor and on to the waste to prevent a safety shutdown from occurring. However, these actions were not critical to the analytical results and could have been performed by the pneumatic pump alone in a stand-alone system.

E.2.3 Definition of Target Ions and Solution Preparation.

As discussed in the introduction, ClO_4^- detection is critical for its effect on both habitability and the measurement of organics in regolith samples. However, to understand the full chlorine (Cl) budget it is important to measure all of the oxychlorine species, including chloride (Cl^-). The global distribution of Cl on Mars is well established from soil sample measurements[497] (~20 – 80 wt% range), and by orbital measurements from the Gamma Ray

199

Spectrometer on the Mars Odyssey spacecraft.[498] Measurements from both the WCL and the

Sample Analysis at Mars instrument on the *Curiosity* rover showed that a large amount (but not

all) of the Cl is present as either Cl$^-$ or ClO$_4^-$,[499-501] and this indicates that other members of the

oxychlorine species, i.e., ClO$^-$, chlorite (ClO$_2^-$), and chlorate (ClO$_3^-$), are most likely present.

There are a number of other soluble inorganic anions beyond the oxychlorine species

whose quantification could provide further insight into the habitability of Mars, and should be

simultaneously detectable by an IC instrument. The other anions detected by WCL were sulfate

(SO$_4^{2-}$),[471] and an inferred detection of carbonate because of the pH buffering capability of the

solution.[469] The presence of sulfates and carbonates are clearly important as indicators of a

wetter climate;[453,469] but bromide (Br$^-$), not detected by WCL, can also provide evidence of

aqueous alteration. Bromine, thought to be present as Br$^-$, has been observed in-situ via

elemental analysis by the alpha particle X-ray spectrometer on the *Spirit* and *Curiosity*

rovers.[502,503,504] Bromate (BrO$_3^-$) is another interesting target as it may serve as an alternate

reservoir of the observed bromine analogous to the high ClO$_4^-$/Cl$^-$ ratios measured by WCL.[470]

The element chromium (Cr) is present on Mars.[502,503,504] The soluble anion chromate (CrO$_4^{2-}$) is

therefore worth focusing on, especially because of its terrestrial presence alongside ClO$_4^-$ in the

Atacama desert,[505,506] and the possibility that they both may have similar origins.[507] Nitrate (NO$_3^-$

), is another species of high interest to astrobiology that has never been detected on the Martian

surface. Lack of nitrate detection so far may be due to leaching during previously wet times,[462]

and/or the difficulty in detecting it remotely at its current surface concentrations.[508] Therefore, in-

situ measurements are needed to determine its presence or absence.

Small organic acids have also been plausibly hypothesized as a good reservoir of the

missing organics on Mars,[493] given what the influx rates of organics from meteorites should

be.[509] Formate (HCOO$^-$), the simplest of the carboxylic acid anions is present in large amounts

in most carbonaceous meteorites.[510,511] Acetate (CH$_3$COO$^-$) and benzoate (C$_6$H$_5$COO$^-$) have

been highlighted as two possible stable anion end products of oxidation of a variety initial input

organics including alkanes and polynuclear aromatic hydrocarbons (PAHs).[493] UV radiation at the Martian surface will lead to the degradation of these molecules,[494] but there is reason to expect that at moderate depths they would survive over geologic timescales.[512]

For this work, the master "Mars mix" of 11 anions included the inorganic ions Cl^-, ClO_3^-, ClO_4^-, Br^-, BrO_3^-, CrO_4^{2-}, NO_3^- and SO_4^{2-}, and the organic acid anions $HCOO^-$, CH_3COO^- and $C_6H_5COO^-$. Two mix solutions were made for evaluating the effect of flow rate on system performance (the key factor in determining whether a low pressure system will still provide the quality of separation required). The first one contained 100 µM of all 11 anions, the other contained 100 µM of five well-resolved ions (Cl^-, Br^-, SO_4^{2-}, CrO_4^{2-}, ClO_4^-). Both solutions were used to evaluate the system at flow rates from 1-3 µL/min in 0.5 µL/min increments, as well as compare the mechanical pump to the pneumatic pump.

Additional mix solutions were prepared to evaluate the effect of the large, Mars relevant, amounts of ClO_4^- on the system performance (the second key goal of this work in demonstrating the effectiveness of an IC system for Mars exploration). An initial stock of 5 mM ClO_4^- and 100 µM each of other analytes was prepared. This was then serially diluted up to 200 times, with injections made at seven different dilutions.

Lastly, ClO_2^- was added to the sample mix to determine whether it could be separated as well, allowing for separation and detection of all but one of the oxychlorine species. The only remaining member of the group, ClO^-, is known to bring about Hoffman degradation of quaternary ammonium groups, the anion exchanger functionality in these columns and was not measured to avoid loss of column capacity. Furthermore, HOCl (the conjugate acid) is too weak an acid to be sensitively detected by suppressed conductometry and so would not be well measured in this setup.

E.3.1 Separation of the Mars Mix.

Separation of all 11 species at concentrations of 100 µM in the Mars mix was possible using a gradient run at the flow rates of interest (Figure E - 3). While the data were originally acquired as a time-dependent signal, the data are depicted with eluent volume flowed through the column as the abscissa, by multiplying the elapsed time from sample injection with the eluent flow rate. This depiction makes comparison between the different flow rates easier, because though the flow rate changes, in principle the analytes still elute at the same eluent volumes. Under the elution conditions used, only benzoate and nitrate were not baseline resolved. Initially, persulfate ($S_2O_8^{2-}$), a potent oxidizer, was also included in the test mix but it appeared to be reacting with the column and was not investigated further (Figure E - 4). The persulfate peak height decreased with decreasing flow rate. The longer residence time at low flow rates allows more complete reaction of persulfate with the stationary phase.
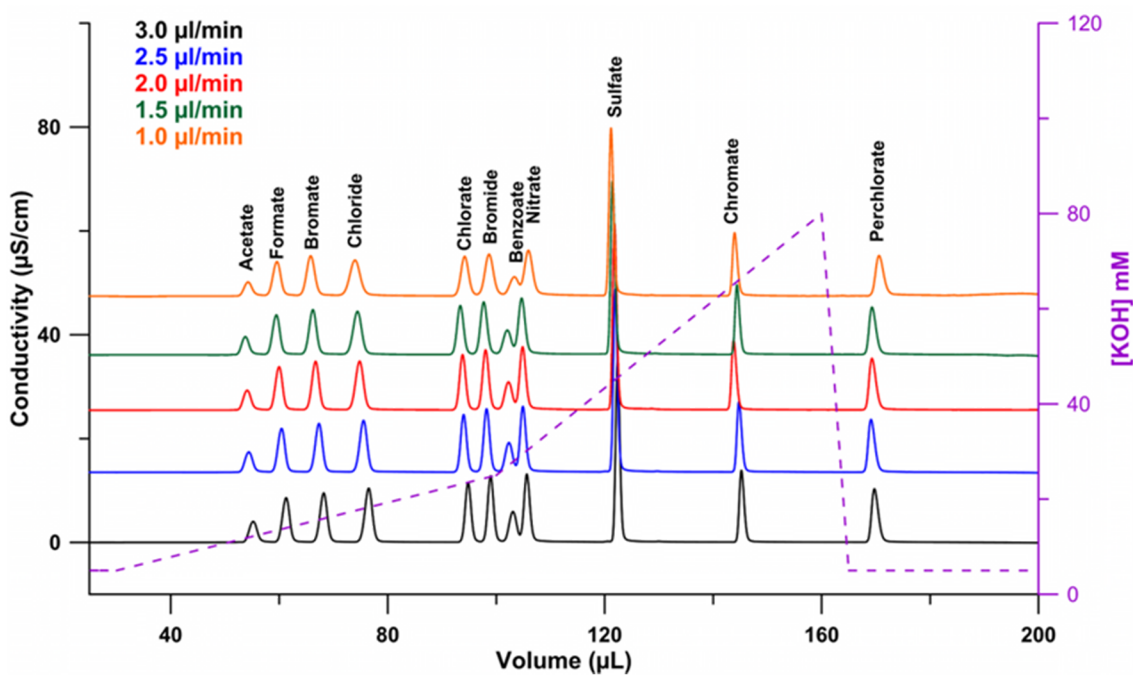
Figure E - 3. Separation of the 11 species Mars mix at different flow rates (100 µM each anion)
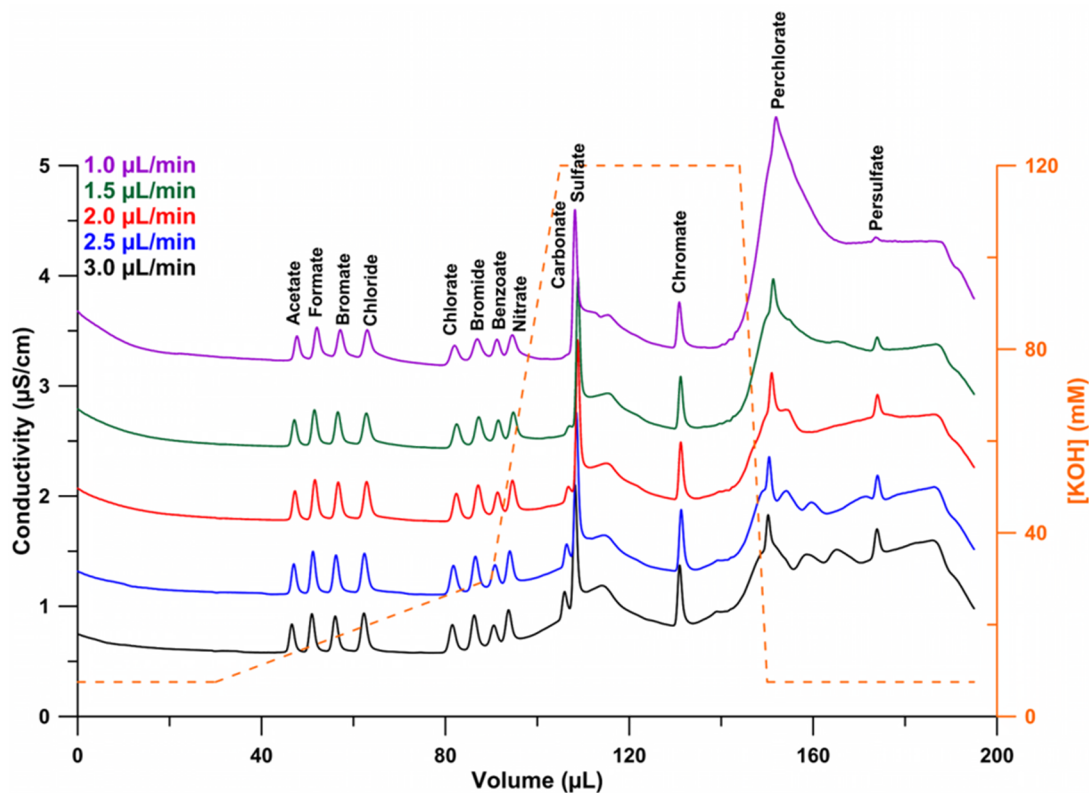
Figure E - 4. Anion separation using ICS-5000 Capillary Scale Chromatogaph. All ions are 10

µM in concentration.

The five anion mix was separated in triplicate (Figure E - 5), peak efficiencies were

calculated according to conventional methods (European Pharmacoepia Standards, vendor

software) for both the low flow system (Figure E - 7), and the high pressure 10 µL/min system

with the standard suppressor using otherwise identical gradient elution programs. Because

these data originate from gradient elution conditions, a comparison of the calculated efficiencies

for ions eluting at different times is not meaningful, rather the item of interest is how for a given

ion the efficiency changes as a function of flow rate. The data have also been normalized, with

the highest efficiency observed for any analyte set to unity. There was a clear loss of efficiency

at the lowest flow rates (< 2.6 uL/min), but there was relatively little change between 3 µL/min

and 10 µL/min (Data not shown). Further examination of the data also indicates that the loss in

efficiency at the lower flow rates was much greater for the early eluting ions. This suggests that

there was a source of extra column broadening of small but more or less constant magnitude,

which thus affected the lower volume eluting bands more than the larger volume ones. Lower

volume bands are more greatly affected because they elute first and experience less dispersion during the separation, and are therefore much more sensitive to small additional dispersions after the separation than the larger volume bands whose dominant dispersion takes place during separation. The most likely and obvious source for the additional dispersion is the suppressor, which was customized as described in section 2.1 from a suppressor designed to operate at 10 µL/min flow, but clearly could be shortened further to function ideally at 1 µL/min flow. Peak asymmetry either did not
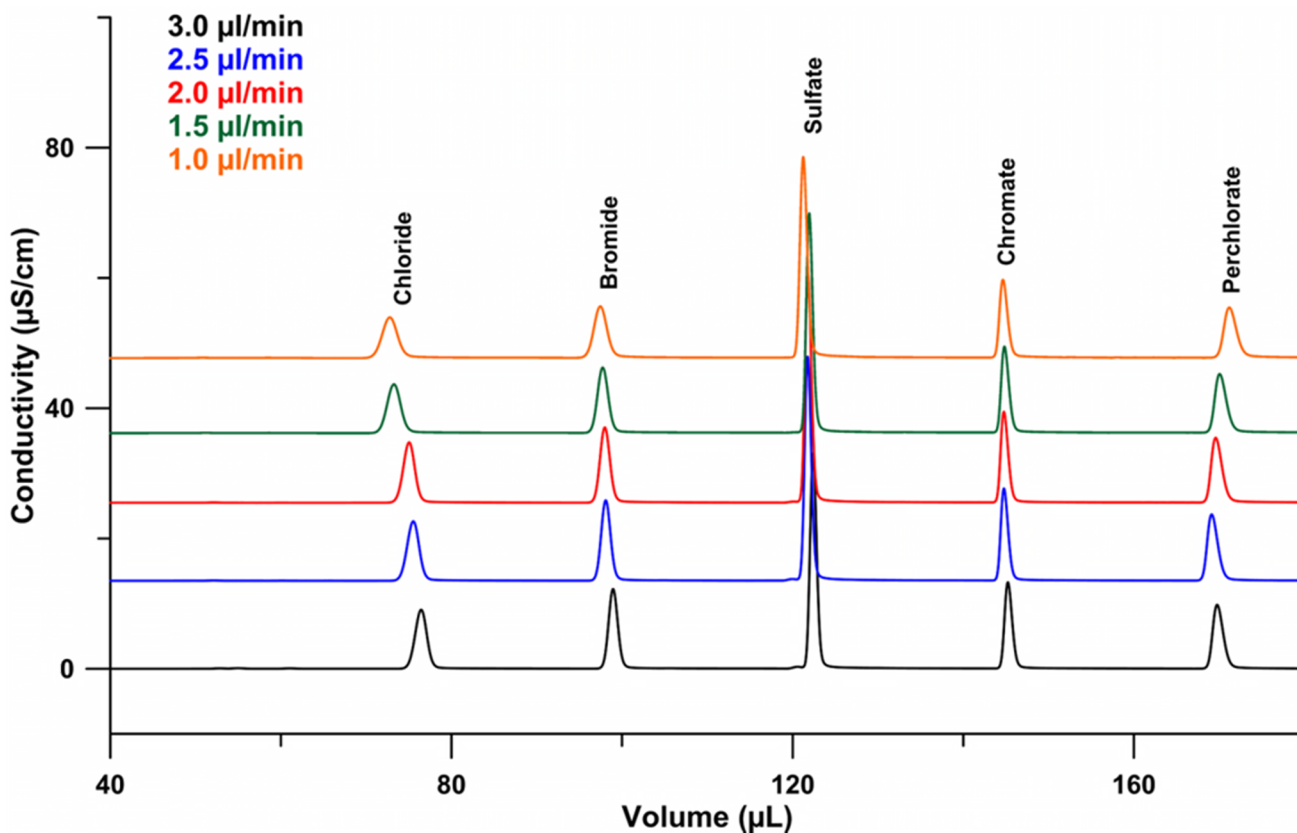
Figure E - 5. 5 Anion separation using ICS-5000 Capillary Scale Chromatograph. All ions are 100 µM in concentration, runs completed in triplicate
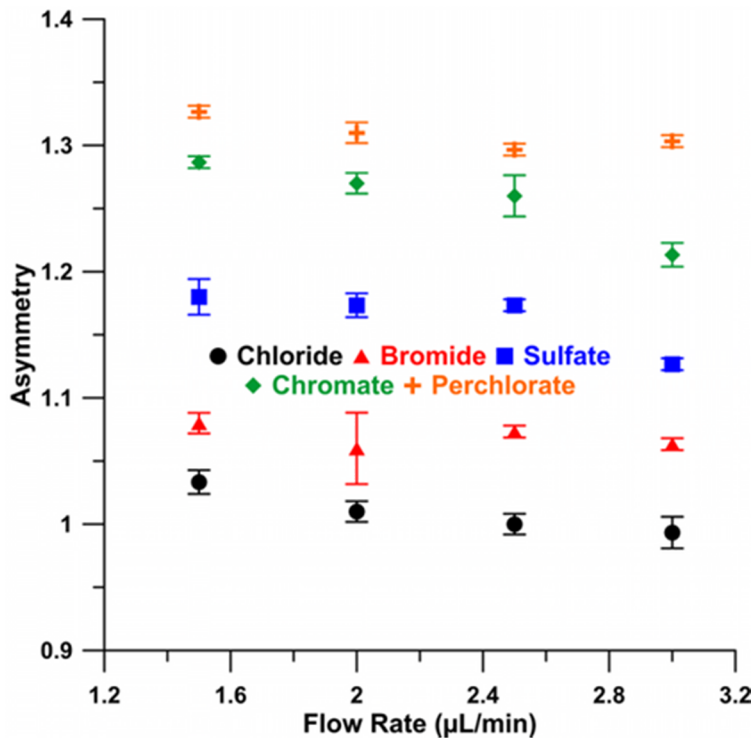
Figure E - 6. Peak asymmetries as a function of flow rate.

Lower flow do not significantly affect peak asymmetry
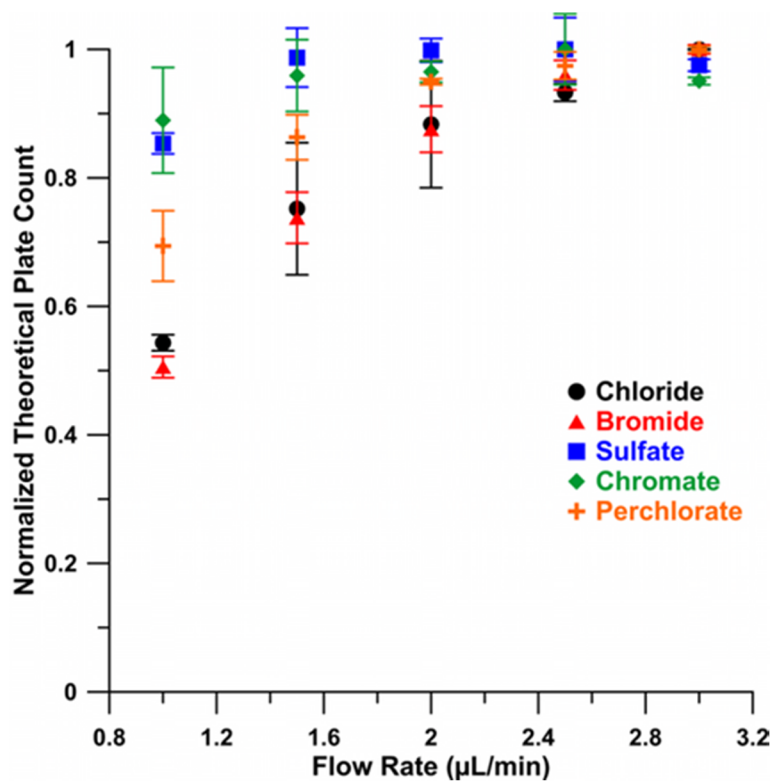
Figure E - 7. Peak efficiencies as a function of flow

rate, normalized to unity

change or saw a minor increase at decreased flow rates, also indicative of an extra column dispersion source (Figure E - 6).

E.3.2 Separations in the Presence of Large Perchlorate Concentrations.

If perchlorate is as prevalent globally on Mars as the results from Phoenix and *Curiosity* are beginning to indicate,[470,499] it is necessary to investigate whether effective separation and determination of other ions of interest can be conducted in the presence of large amounts of perchlorate. Overloading of the column with perchlorate is likely to affect plate counts, and a loss of resolution between one or more adjacent pairs of peaks is possible. Despite the possibility for interference, good separation of the Mars mix in the presence of 50x greater ClO_4^- concentrations was demonstrated (Figure E - 8). A stock solution of 5 mM ClO_4^- and 100 μM
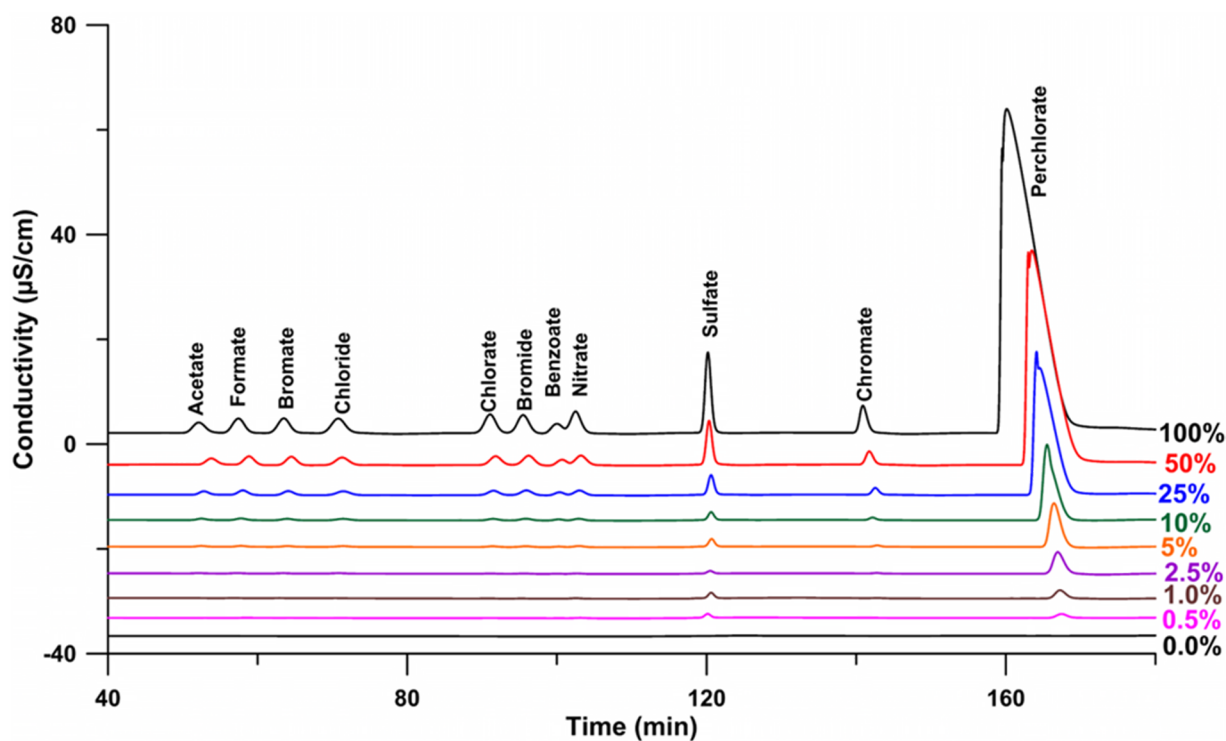
Figure E - 8. 100 μM test ions and 5 mM perchlorate, gradient IC separation at a flow rate of 1.0 μL/min. Traces show dilutions from 0.5-100% of the original solution and are offset for clarity. All species could be detected down to 0.5 μM

anions was used and then diluted up to 200x. While the tailing of the perchlorate peak became pronounced at higher injected concentrations, it did not result in perchlorate overlapping with any of the ions in the test mixture. It is also clear that even with an injected concentration of 5 mM perchlorate, adequate separation is maintained between all other remaining ions. Not surprisingly, the best efficiencies were obtained at the lowest concentration of ions. Even at the 1 μM level, peaks were clearly visible with estimated LODs of $\leq$500 nM (Figure E - 9), with the exception of sulfate and chromate which are obscured by the gradient disturbance at this level (Figure E - 10). The limit of quantitation for the other ions was $\leq$1.5 μM corresponding to injected amounts 0.6 pmol. In other words, if 1.5 g soil was extracted with 25 mL of water as was done in WCL experiment, and we assume a formula weight of 100 for the anion, 40 parts per trillion (4 x 10^{-11}) by weight of the extractable ion would be detectable. No other instrument deployed thus far for extraterrestrial explorations can match this capability. The low sample volume required for the IC (400 nL), combined with the low limits of detection also imply that much smaller amounts of both regolith and solvent could be used for determining the anions present.
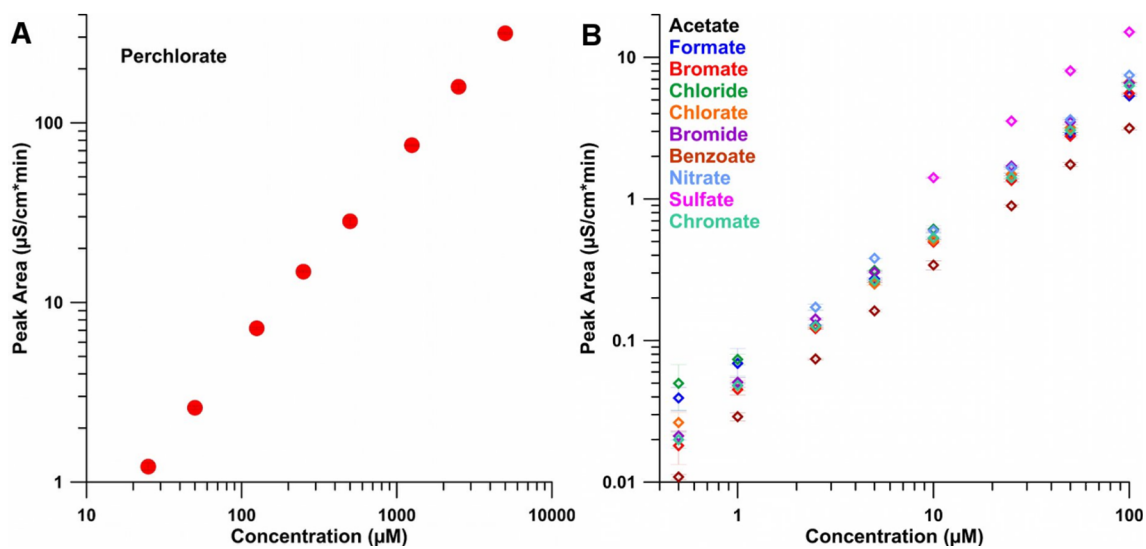
Figure E - 9. A) Perchlorate calibration curve B) Calibration curves of non-perchlorate anions.
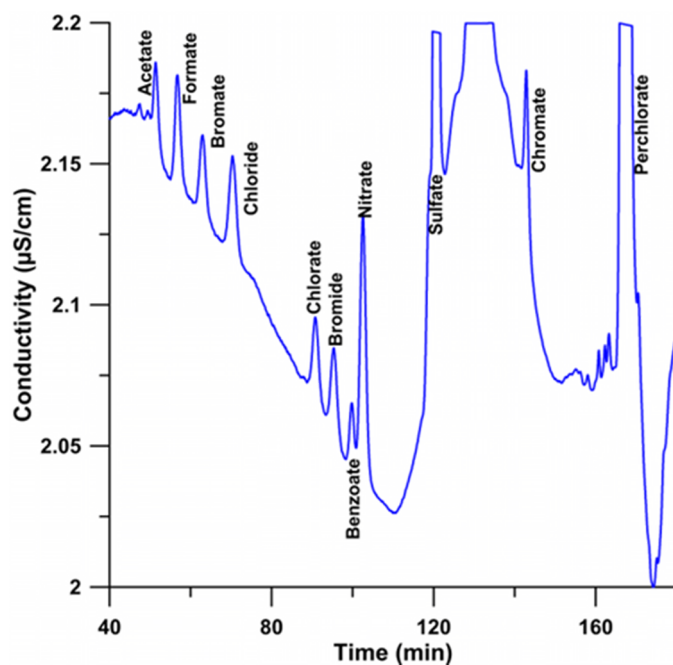
Figure E - 10. Magnification of the 1% dilution, i.e. 1 µM test anions and

50 µM perchlorate. The baseline shift is gradient induced.
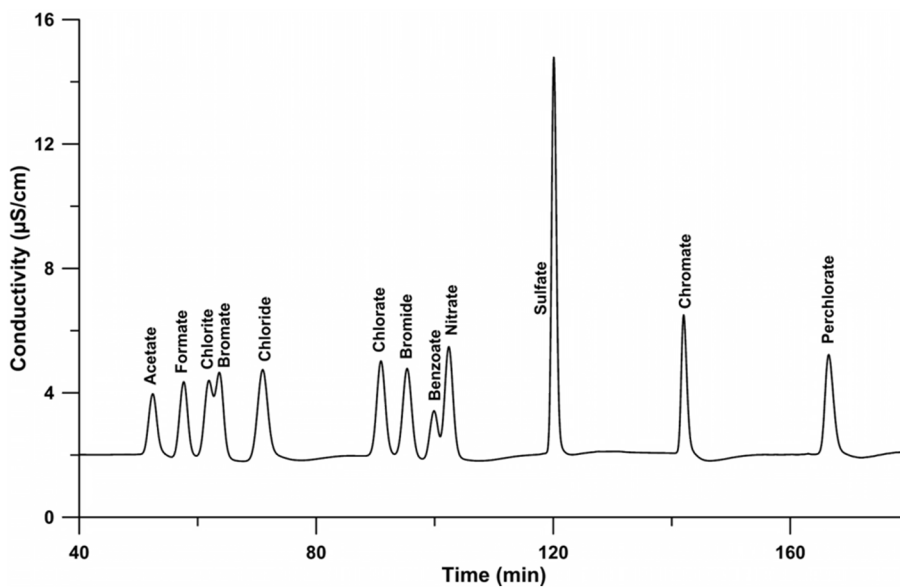
Figure E - 11. Demonstration of inclusion of chlorite (ClO_2^-) to the analyte mix.

Additionally, it was possible to include ClO_2^- in the mixture and separate four out of five

of the oxychlorine species (Figure E - 11). While baseline separation was not achievable

between ClO_2^- and BrO_3^- but two distinct peaks are measurable.

208

E.3.3 Use of Pneumatic Displacement Pumping.

The aluminum vessel was pressurized to a level similar to the pressure recorded by the sensor on the mechanical pump when operating at a flow rate of 1 μL/min. As there is some pressure drop between the sensor and the injector for the mechanical pump (but not the aluminum vessel), this resulted in a slightly higher (gravimetrically measured) flow rate of 1.07 μL/min. A near identical results (Figure E - 12). The increased flow rate led to a slightly lower eluent concentration, which resulted in comparison of the separation using the same current gradient program on the mechanical pump at 1 μL/min vs. the pneumatic pump at 1.07 μL/min shows somewhat later elution of all the analyte ions so that a slightly greater dispersion of the peaks was observed.
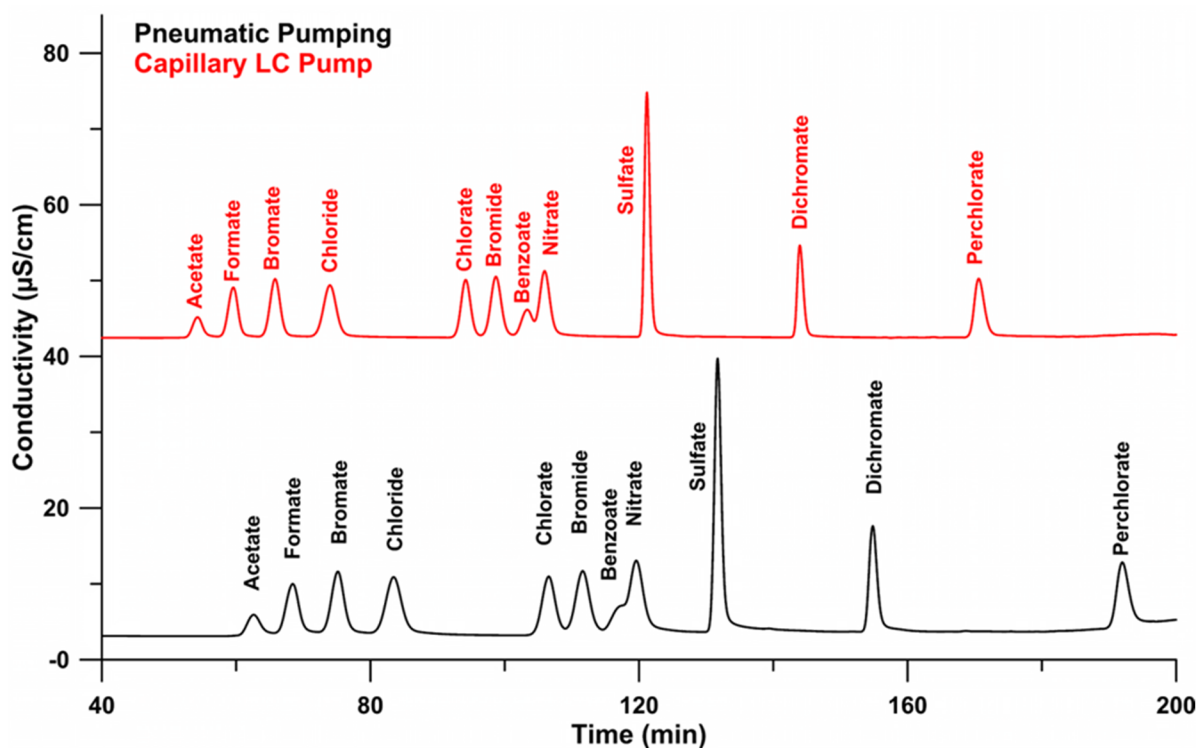
Figure E - 12. Comparison of the Mars mix separation using the capillary high pressure pump and the aluminum pressure cylinder. The capillary pump delivered 1 μL/min while the pressure vessel had a measured flow rate of 1.07 μL/min.

E.4 Discussion

This works demonstrates that a low pressure IC system is capable of delivering state of the art analytical separations, albeit on longer timescales (hours instead of minutes). While the present experiments were on a breadboard setup based on a commercial system, a system requiring larger more powerful pumps (the largest part of the system) has been previously packaged into a briefcase sized portable instrument[486], suggesting that the components of this current system could easily be packaged small enough for flight. Longer analysis time is a reasonable compromise for a flight instrument where mass/volume/power considerations are critical. This is all the more true given that sample acquisition and analysis on a rover/lander is not as yet a high throughput activity where analysis time becomes the rate limiting step.

The limits of detection demonstrated are also more than sufficient for measuring the inorganic ions at their measured/expected concentrations, and are a factor of ≥20x lower than WCLs.[491]. The ions, SO_4^{2-}, ClO_4^-, and Cl^- were measured at 4.8 mM, 2.5 mM, and 0.4 mM concentrations respectively in solution by the Phoenix lander,[468,470,471] making them all well above the threshold for detection by an IC system. The global mapping of atomic chlorine and sulfate minerals,[453,498] along with the suspected confirmation of widespread ClO_4^- by *Curiosity,*[499] indicates that these concentrations are useful guidelines for much of Mars and not just specific to the Phoenix landing site. No mention of a Br^- detection by WCL was published,[468] implying that if it was present it was below the 10 µM detection limit of the instrument.[491] Referring to the element, bromine in some form has been detected at the tens – hundreds of ppm level by both the Mars exploration rovers and *Curiosity,*[502,503,504] and Br^- has been measured in Martian meteorites at the ppb level[513] although in all cases the amount varied significantly from sample to sample. However, even 10 ppb of soluble bromide in the soil will be easily detectable using this system assuming a Phoenix like extract (i.e., 1.5 g soil/25 ml water). Currently NO_3^- has not been detected on Mars. Compact Reconnaissance Imaging Spectrometer for Mars (CRISM) suggest that at the surface NO_3^- must be <1 wt%,[462,508] but

subsurface NO_3^- could be significantly greater: surface nitrate may have decreased due to leaching during previous phases of aqueous activity.[462] By providing a sub-ppb level of sensitivity to NO_3^-, this IC system could help provide an answer to whether there are any appreciable amounts of NO_3^- in accessible samples.

Large concentrations of ClO_4^- are another concern when making sensitive measurements of NO_3^- (e.g., Phoenix[470]) or organics (e.g., *Viking/Curiosity*[473,501]), but were not observed to cause a problem with the IC system at concentrations 50x the other target ions (Figure E - 10). In IC, the strongly bound ClO_4^- elutes last and does not interfere with the other analytes or mask them in a tailing peak. The IC sample preparation does not require heating either, hence ClO_4^- is not activated at high temperatures and this prevents the cross-reactions observed during pyrolysis-MS, which decompose target organic molecules.[473]

In addition to ClO_4^-, large amounts of SO_4^- and Cl^- were present at the Phoenix landing site, and they too could potentially mask lower concentration species of interest. Fortunately, both these species are well separated by this system (Figure E - 8) and even at significantly higher concentrations are not likely to overshadow other species. In general, the range of possible concentrations of each species in a Martian sample will lead to more complex chromatograms than the idealized lab standards shown. However, the high degree of peak resolution and high sensitivity of the detection will allow for a broad range of anions at different concentrations to be detected simultaneously.

Another important capability of the system is the ability to separate all of the oxychlorine species save ClO^- (Figure E - 11). UV Irradiation of perchlorate soils experiments suggest that generation of the much more reactive (and much less hospitable to life) ClO_2^- and ClO^- species is likely.[474] Furthermore, experimental evidence also shows that electron irradiation of chlorine and carbon dioxide bearing ices relevant to Mars can lead to the generation of these oxychlorine species, and perhaps all the way to ClO_4^- itself answering the question of where all the ClO_4^- comes from.[514]

Overall an IC system will significantly improve a future mission's ability to determine the habitability of any given site by determining the soluble anions present. The ability to measure NO_3^- is an especially important feature to astrobiology given that it is the only source of bioavailable or "fixed" nitrogen.[515] While some organisms can fix their own nitrogen on Earth from atmospheric N_2, it requires significant metabolic energy, and finding bioavailable nitrogen would greatly enhance the estimated habitability of a given location on Mars.[472] *Curiosity* has made measurements suggesting an indigenous source of potentially bioavailable nitrogen at Yellowknife bay,[516] but a completely unambiguous assignment of the parent species was not possible. A future IC system would provide a useful complement to established instruments, e.g. a GC-MS, in helping to unravel the past and present habitability of Mars.

Lastly, IC methods are also well-suited for robotic exploration of other bodies and future manned missions to Mars. The large amount of ClO_4^- on Mars is relevant as a human health hazard (it is a potent iodide uptake inhibitor severely affecting thyroid function and production of thyroid hormones T3 and T4[482]), and also a potential resource in any manned mission.[517] However, the global distribution of ClO_4^- on Mars is still not properly understood, and instruments that can further map this will be critical in paving the way for eventual human exploration. Outside of Mars, icy planetary missions are an area where analysis of soluble ions will be of great interest. For example, on a Europa lander, an IC system would allow true speciation of the ions present to understand the redox couples potentially available for supporting life, a measurement that would not be possible by volatilization of a sample followed by mass spectrometry.[518] In general, IC is the state of the art for trace ion analysis in water here on Earth, so it would be the natural choice for the analysis of soluble species on Mars, or other icy worlds.

E.5 Acknowledgments

.

Appendix F

Continuous Total Organic Carbon Monitoring by Ultra-Violet Cavity Enhanced Absorption

Spectroscopy

F.1 Introduction

Total Organic Carbon (TOC) analysis is one of the most critical tests performed in high purity water systems used in the pharmaceutical and semiconductor industries. TOC is a measure of the total carbon present excluding all inorganic carbon in the form CO_2 or CO_3^{2-}. Stringent sub µg/L restrictions have been set for ultra-pure water (UPW) by the International Technology Roadmap for Semiconductors (ITRS)[519] and the Semiconductor Equipment and Materials International (SEMI)[520] due to the deleterious effect of even trace organics on production. Additionally, SEMI F63 stipulates that any TOC analyzer should have a limit of detection of 50 ng/L or less. Pharmaceutical TOC however is less critical requiring water for injection to be less than 500 µg/L carbon according the United States and European Pharmacopeias,[521,522] and any method used for TOC must not have a limit of detection above 50 µg/L carbon.

Because it is a nonselective technique, TOC has also become an effective means of cleaning validation in pharmaceuticals[523-528] using either the final rinse of the equipment or a swab of the surface. Typical acceptance criteria used in determining TOC limits after cleaning, are that the final rinse should contain 1/1000th of the lowest therapeutic dose administered or a maximum level of 10 mg/L.[528,529] Removal of any cleaning compounds or detergents should also be verified. Chromatographic methods are capable of measuring both the drug and any chemicals used in the cleaning process but these are time consuming and require a separate method for each drug produced.[526] TOC analyzers are not able to distinguish between the drug and detergents added, so a minimum TOC limit may be set based on the lowest of the above acceptance criteria. Transfer of samples from the source to the lab consistently results in higher or more variable TOC[523,530] and has led to the incorporation of TOC analyzers into the rinse water return line. Additionally, because this information is available instantaneously, the rinse

may be changed or terminated as necessary ultimately resulting in an increase in productivity and a reduction in the use of rinse water.[528]

Because TOC is a measure of all organic compounds present, it is expected that no single technique will be adequate to measure the compounds directly due to the range of chemistries present. For this reason, nearly all TOC analyzers are dependent upon the indirect measurement of carbon species following oxidation of the organics and measurement as CO_2. The two primary methods of determination of the produced CO_2 are non-dispersive infrared absorption spectroscopy (NDIR)[524,526,527,531,536] and conductivity.[537-542] For low level TOC measurements, removal of inorganic carbon must be considered a priori. Water when exposed to the atmosphere rapidly absorbs CO_2. If conductivity is to be used, a two detector setup may be used in which conductivity is measured before and after oxidation,[542] or a single detector inside the oxidation chamber may be used to measure the change in conductivity over time.[541] Alternatively, acidification and purging off of CO_2 may be used prior to oxidation, but in many cases this may lead to loss of volatile organic compounds and an underestimation of the TOC present.[543] Oxidation is most often carried using a low pressure Hg lamp making use of the 254 and more importantly 185 nm emission lines.[542]   A catalyst such as TiO_2[544] or platinum on TiO_2[545] may be incorporated.[546] Not surprisingly, photo- oxidation requires dissolved oxygen to occur. In systems with low oxygen content or those in which H_2 is added to remove oxygen (thus creating a reducing environment), oxidation is incomplete and will result in severely underestimated TOC[547] (In semiconductor UPW the dissolved oxygen content recommended by SEMI F63 and ITRS is less than 10 ppb[519,520]). In such cases UV mediated persulfate oxidation is used.[548] UV-persulfate oxidation has also been shown to be more effective than UV digestion alone for difficult to oxidize compounds such as urea, tetramethyl ammonium hydroxide, and trimethyl amine.[547]

Urea is of particular importance because it is nonionic, has a low molecular weight, and is difficult to oxidize making its removal problematic. Upon photo-oxidation urea produces CO_2 and NH_3. In solution NH_3 becomes NH_4^+ replacing the far more conductive H^+ present from the auto-ionization of water.[549,550] When measured directly this, results in a decrease in the conductivity signal when low concentrations of urea are present rather than an increase.

Conductivity is used most frequently as the detector following digestion because it can measure with great sensitivity low concentrations of CO_2 from the H^+ and HCO_3^- ions produced[542] and is relatively simplistic and inexpensive. The dissociation of carbonate however is nonlinear, and at concentrations around 50 μg/L carbon NDIR becomes a more competitive method. The nonlinearity of carbonate has further contributions that are dependent upon temperature, other chemical constituents, and its own concentration requiring complicated compensation algorithms.[542,551] This limits the accuracy of techniques that depend upon measurement of CO_2 directly following UV-digestion. Additionally, because conductivity is not a selective technique any other ions produced during the oxidation process will contribute to the total signal. Likely leachates from deionizing resins are trimethylamine and benzenesulfonic acid [552,553] and produce the resulting inorganic ions nitrate (though as is seen with urea ammonium may be more likely) and sulfate upon oxidation, contributing a greater response to the conductivity and producing a positive bias to the measured TOC. The same holds true for halogenated compounds such as chloroform which may be also difficult to remove and will produce HCl upon oxidation.[543] The more precise analyzers then use gas permeable membranes to separate the digested solution from a clean source of water containing the conductivity detector. CO_2 produced is selectively transferred to the clean water source where it is measured free of other inorganic constituents.[537,538] This is particularly useful when UV-

217

persulfate is used for oxidation to isolate the CO_2 from the resulting sulfate ions. NDIR determination of TOC is based on the absorbance of light in the infrared by CO_2.[554] While this technique is more selective than conductivity it is not as sensitive. Due to a slight absorption overlap, CO_2 must be measured in the gas phase after substantial removal of water.[543,554]

Because complete oxidation must be carried out prior to analysis, most methods based on CO_2 production are necessarily batch analyzers. Real-time continuous analyzers have been produced with flow through UV digestors,[542] but these have been shown to respond poorly to compounds that are more difficult to oxidize due to the low residence time in the digestion cell.[547] This incomplete oxidation is especially problematic because it is compound dependent and may lead to positive or negative biases.[543] Most obviously, when small fractions of the organics present are oxidized, a lower than expected TOC value will be observed. When oxidation, however, results in the production of organic acids that ionize to a greater degree than H_2CO_3, this leads to a positive bias. Real time analysis is beneficial because it allows for the sudden determination of real system upsets. Use of real time systems can also lead to a reduction holding tank size for reclaim/recycle systems reducing the water intake and discharge.[542,543] Accuracy of any real time TOC measurement based on CO_2 production will always be limited by the completeness of the digestion, and for systems that depend upon CO_2 diffusion across a membrane, real time analysis may never be achieved.

Absorption spectroscopy offers an alternative, not requiring digestion prior to analysis. In the deep UV, all compounds absorb to some degree. Absorption methods have been used previously to measure TOC in a variety of matrices such as waste waters,[555-557] natural fresh[556,558-561] and sea waters,[562,563] and purified water streams.[564,565] One of the key features observed in optical TOC measurements is the featureless

absorption spectrum that shows a continuous exponential rise towards shorter wavelengths. The steepness of the curvature using multi wavelength measurements has been correlated to the average molecular weight of the components present wherein broader absorption spectra are observed in waters containing larger molecular weight fractions.[558,560] When used in conjunction with other TOC analyzers UV absorbance may also determine the percent aromaticity.[566] In pure water systems the contribution due to larger molecular weights is likely negligible as these are easily removed, necessitating the need for deeper UV measurement. Extracts from ion exchange resins used in semiconductor and nuclear water purification systems have been shown to be readily measured at sub 220 nm wavelengths even at sub ppm levels.[552,553] Comparison studies with commercial analyzers have shown good agreement with optical methods[555,556,565,567] however interferences from NO_3 and Br^- can cause over estimations of TOC[561]. Currently these devices have only been operated in the low to high mg/L range. Current commercially available equipment has a lower operating limit of 0.1 mg/L, which does not even meet the mandated LOD for pharmaceutical waters, much less the semiconductor industry.[567]

In Dobb's work comparing the 254 nm absorbance to TOC at multiple waste treatment plants, He obtained an approximate absorption value of 20 Au /cm/ (g L⁻ C).[555] The user has no control to exert over the extinction coefficient, leaving path length the only option available to increase sensitivity. If Dobb's relation were to hold true for high purity water systems, to measure 1 µg/L at a level reasonably above the LOD (assumed to be 10 mAu), a path length of 5 m would be required. Clearly a cell of such proportions would not be practical, and even if it were the amount of light lost before reaching the detector would be considerable due to beam divergence. Evaluation of estuary waters shows absorption maxima in the region of 210-220 nm[560] at up to 10 times that seen at

254 nm. The difference in absorbance is greater for waters containing a greater fraction of small molecules. A 10 fold improvement factor by moving to the deeper UV would still require the use of a 0.5 m long path. While this represents a far more practical path length, many of the more intensely absorbing chromophores have likely been filtered out in the pure water systems of interest here. Cavity enhanced techniques may be used to increase the effective path length thereby lowering the limit of detection without requiring larger physical paths.

In cavity enhanced absorption spectroscopy (CEAS), the absorbance cell has reflective surfaces so that light must bounce back and forth across the same path multiple times before detection. In the gas phase, White[568] and Herriott[569] cells have seen considerable use. Concave mirrors are aligned so that coherent light must travel a single path while passing multiple times through the sample cell. In liquid phase, light immediately diverges and such a design is not feasible. In 1984 Dasgupta introduced a silvered helical cell wherein the light upon entering the coil must reflect back and forth before reaching the exit.[570] Later a simplified device was introduced by Dasgupta and Rhee using partially transmissive mirrors on each side of a cuvette.[571] In both instances it was observed that the effective path length, from henceforth denoted $\bar{b}$, was greater than the physical path length of the cell. One year later O'Keefe and Deacon published their now celebrated work on cavity ring down spectroscopy (CRDS) which in concept resembles the silvered cuvette above, but much higher reflectivity mirrors were used with a pulsed laser source and high speed detector.[572] The first order decay of the signal is monitored and is directly proportional to the absorbance in solution. It was not until a decade later that continuous sources were used obviating the need for the high speed detector[573,574] and becoming identical in approach to that of Dasgupta and Rhee. To

date only a few examples of CEAS have been shown in the liquid phase[575-578] and to the best of our knowledge the technique has yet to be utilized in the UV.

Polytetrafluoroethylene (PTFE) is a well-known diffuse reflector maintaining high reflectivities even into the deep UV[579-584] leading to its use in integrating spheres.[585] We utilize the UV reflectivity of PTFE to develop a CEAS cell for the real-time, digestion-free determination of TOC in high purity water.

<div align="center">F.2 Experimental</div>

The experimental configuration is shown in Figure F - 1. Sample solution is continually aspirated through the absorbance cell by a Rainin Dynamax peristaltic pump at a flow rate of 6.7 mL/min. A PEEK tee (www.upchurch.com) prior to the entrance to the cell allows the deionized water stream, Milli-Q (www.millipore.com) $\geq$18.2 MΩ/cm resistivity and <1 ppb TOC, to be mixed with an organic carbon standard injected using a
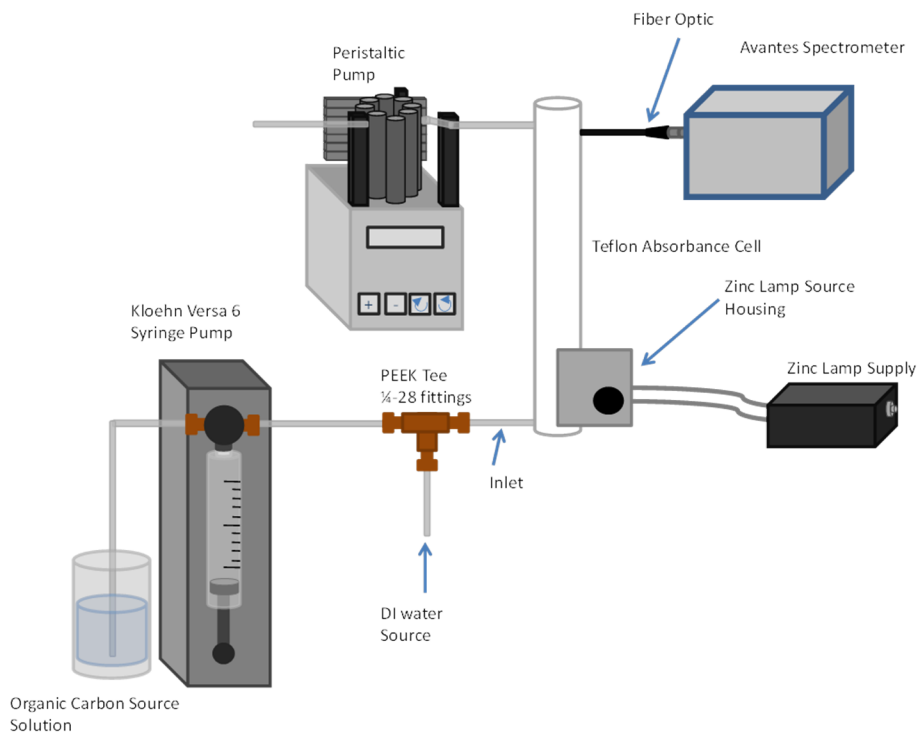
Figure F - 1, Analytical Setup for injecting carbon into a pure water stream

Kloehn Versa 6 syringe pump. A zinc pen-ray lamp (www.uvp.com) mounted directly to the absorbance cell is used as the light source (powered using a Isodyne ISO-28V 2-8 watt ballast adjustable power supply) and an Avantes 1024x58 array TEC cooled CCD Spectrometer equipped with a 1000 lines/mm grating blazed at 250 nm and a 50 μm slit (Wavelength range 200-660), is used as the detector (www.Avantes.com) equipped with a 1 mm High -OH silica optical fiber (www.polymicro.biz). The integration time was set to 2.0 seconds. The 214 nm zinc emission line is monitored for absorbance and the 468.2 nm line is used as a reference line to correct for any lamp drift. The emission spectrum as measured by the Avantes spectrometer through the absorbance cell is shown in Figure F - 2.

The cavity enhanced absorbance cell (Figure F - 3) was made from a R-11 resin extruded PTFE pipe (Length 12 in., I.D. 5/8 in., O.D. 1-1/2 in.) with two PTFE end caps (1.5 in. diameter, 0.5 in. thick). The PTFE pipe and caps underwent a 30 minute plasma surface treatment by PVA TePla America to make the surface more hydrophilic.
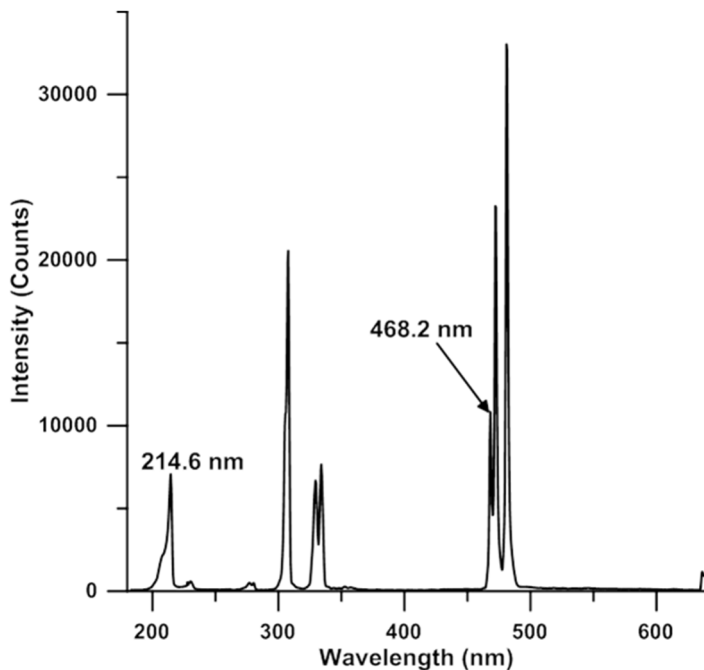
Figure F - 2. The zinc emission spectrum measured through the PTFE cell
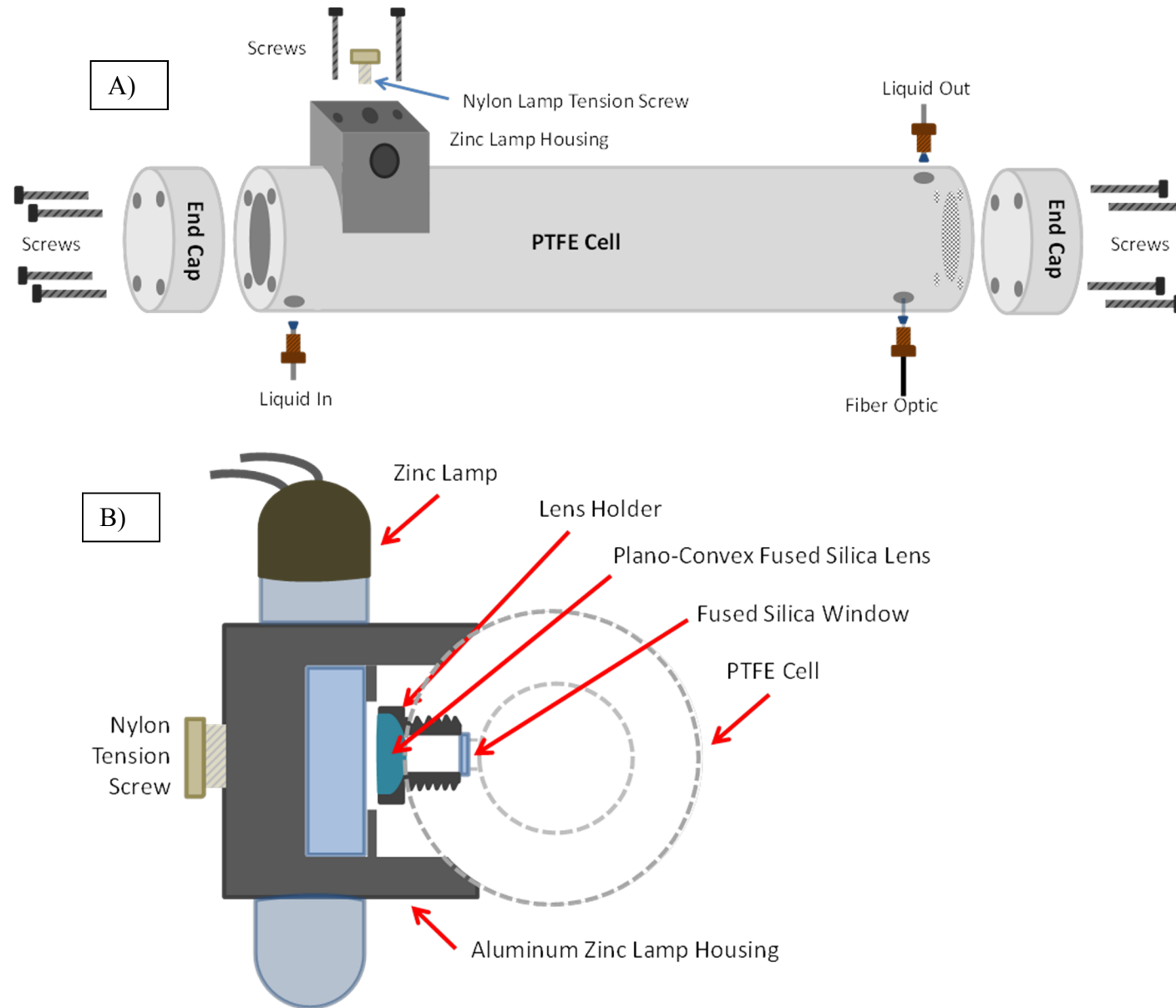
Figure F - 3. A) Cavity Enhanced Absorption Cell. B) Cross Section of Zinc Lamp Housing

The contact angle measured on the treated disc was 15° compared to >120° for the untreated PTFE. A lamp housing was constructed for the zinc lamp out of aluminum (Cross section Figure F - 3B). A large Teflon nut was made to contain a pocket for a plano-convex fused silica lens (20 mm Diameter, 30 mm focal length, www.edmundoptics.com). The lamp house block, when attached to the PTFE pipe, presses against the plano-convex lens holding it in place. The nut inner diameter is 8.6 mm. Into the pipe wall the corresponding thread was made and terminated approximately 2 mm from the central channel. A 9 mm hole was drilled through to the central channel. The nut was used to hold in place a fused silica window (10 mm diameter, www.edmundoptics.com) which formed a seal against the PTFE. The aluminum block was machined to fit snugly against the Teflon pipe. A hole was made through the entire length of the block to fit the zinc lamp. A PTFE sheet was used behind the lamp to reflect additional UV light into the cell. The lamp is held in place using a nylon screw to provide tension. A window was cut into the aluminum between the fused silica lens and the zinc lamp. The window is 10 mm wide and 25 mm long. The long edge runs parallel to the length of the lamp. The narrower width allows the aluminum block to press against the lens and retain it in place. Inlet and outlet ports were drilled into the wall of the pipe approximately 1 cm from the end caps to allow the use of standard ¼-28 polyether ether ketone (PEEK) fittings. Opposite the outlet port, and 5 mm nearer the lamp, a 1.3 mm hole was drilled to fit the 1 mm core silica optical fiber so that the fiber can be in contact with the liquid and flush with the wall. The fiber was held in place using a ¼-28 nut and ferrule. The measured volume of the cell is 54.4 mL.
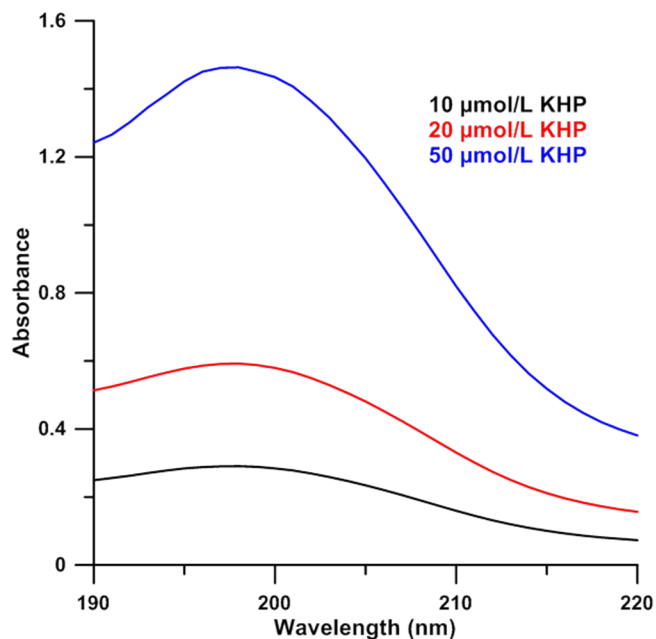
Figure F - 4, KHP absorption spectrum
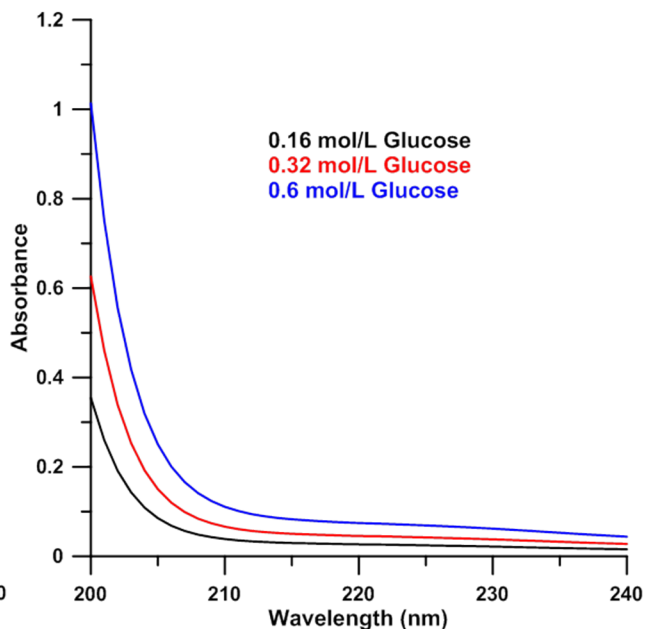
Figure F - 5, Glucose absorption spectrum

Potassium Acid Phthalate (KHP, >999.95% purity, Mallinckrodt) and glucose (analytical reagent, Mallinckrodt) were used as total organic carbon standards for assessing the device. Solutions of KHP and glucose were prepared in Milli-Q water and the absorption spectra was taken using a Hewlett Packard 8453 spectrophotometer to obtain molar absorptivities at 214 nm, Figure F - 4 and Figure F - 5. The standards were then loaded into the syringe pump to be injected into the cavity enhanced absorption cell. Aliquots of standard were injected at 18 mL/min into the flowing DI water stream, ranging in volume from 0.25 mL-10 mL for 5 and 50 µM solutions of KHP and 50 mM solution of glucose. The tubing was of sufficient volume leading back to the DI water source that no cross-contamination occurred even though the syringe injection rate is faster than the aspiration rate of the peristaltic pump. Raw data for injections of KHP and glucose injections are shown in Figure F - 6 and Figure F - 7 respectively. The concentration measured is calculated based on dilution of the initial injected aliquot into the 54.4 mL cell. Measured values ranged from 2.3-644 nM KHP (0.22-62 µg/L carbon) and 0.23-9.2 mM glucose (16-662 mg/L carbon). The cell was also filled with prepared standards of KHP and the absorbance was measured under static and flowing conditions.

225
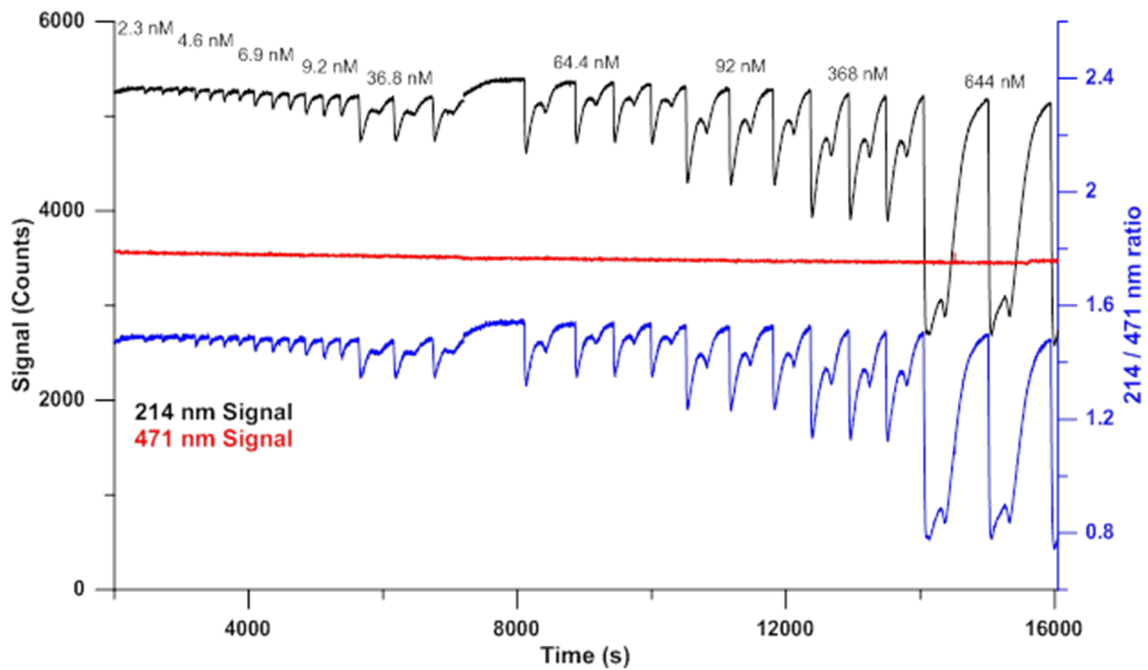
Figure F - 6. The 214 and 471 nm signals produces as KHP is injected. The 214 nm signal referenced to the 471 nm signal is provided in blue
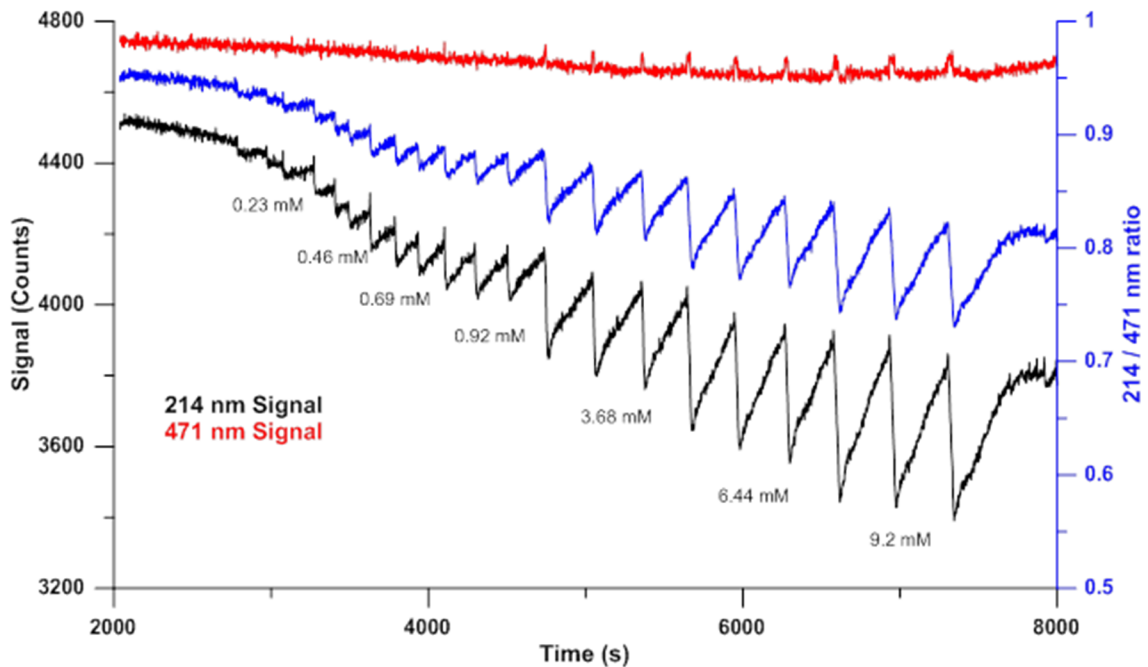
Figure F - 7, The 214 and 471 nm signals produces as Glucose is injected. The referenced signal is provided in blue

F.3 Results and Discussion

Absorption spectroscopy is unequivocably the most used quantitative technique used for analysis. Absorbance, A, is governed by Beer's law, $A=\varepsilon_\lambda bc$, where b is the path length, c is the concentration of the analyte, and ε_λ is the absorptivity of the analyte at a given wavelength. Without chemical modification or preconcentration, the only parameters the analytical chemist has control over are the wavelength measured at, and the path length of the cell. For the best sensitivity, the wavelength of maximum absorption is most often chosen. The luxury of the optimum wavelength is not always available when line or laser sources are used as is the case here. The only remaining option then is to increase the path length. In the gas phase, differential optical absorption spectroscopy[586] (DOAS) has relied on single long atmospheric paths, and single path multi-reflection cells such as the White cell[568] or Herriott[569] cell have been around since 1942. These methods rely on a relatively coherent beam of light and in the liquid phase where beam divergence is much greater, these methods are not generally applicable. Long glass tubes were used by Wei et al.[587] and relied on the reflection of the glass-air interface and later the same group pioneered the use of liquid-core waveguides using high refractive index organic solvents in glass or silica capillaries.[588,589] True aqueous based LCW's only became possible after the invention of Teflon AF which has a refractive index less than that of water. The previous techniques all behave as single path cells, meaning the light follows a single well defined path. It is important to note that in these cases, the spectrometer used will always have the same absorbance span. Any improvement to the limit of detection created by increasing the path length will necessarily sacrifice measurement at the high end.

Multipath cells however behave differently, leading to enhanced dynamic range. This is most easily illustrated using a problem from an introductory textbook by Hieftje.[590] A student is asked to consider an L-shaped cell wherein the path length of the top part of the cell (b) is half that of the bottom (2b). Equal incident light occurs on each section of the cell and the sum of the transmitted light is measured. The student is asked to derive an expression for the effective path length ($\overline{b}$) and its value at low and high absorbance limits.   At the low absorbance limit, A=0, the light transmitted through both halves will be equal, so that $\overline{b}$ is an average of the two paths or 1.5 b. Put another way $\lim_{A=0} \overline{b}$ =1.5 b. Conversely at the high absorbance limit, A=∞, the longer half contributes little to the transmitted light so that $\overline{b}$ becomes b or $\lim_{A=\infty} \overline{b}$ = b. It is apparent then that in multipath cells, $\overline{b}$ is a function of absorbance. For a multiplicity of path lengths, b_i, each with a fraction of the total light f_i ($\sum f_i$ = 1), it was shown by Dasgupta in 1984[570] that at the low absorbing limit that $\overline{b}$ is simply the sum of the path lengths weighted by the fraction of light through that path:

$$\overline{b} = \sum f_i b_i$$

It is not feasible to physically construct numerous paths, and so an internally mirrored helical coil was created. Light must proceed through the coil in a series of reflections and due to the curvature of the tubing, the beam diverges creating essentially an infinite number of paths.

Three years later Dasgupta and Rhee published a simpler design for a nonlinear absorbance amplifier consisting of a conventional cell with partially mirrored surfaces.[571] Light introduced into the cell would reflect back and forth between the two partially transmissive windows with some light being loss to absorbance in the medium or transmitted through the windows. An identical arrangement was conceived by O'Keefe and Deacon in their now celebrated paper on CRDS although which much higher

reflectivity mirrors and a pulsed laser source.[572] Measurement is made in the time domain and the first order decay constant has a linear relationship with the absorbance in the medium requiring the use of a high speed detector. The high mirror reflectivity equates a low transmissitivity and necessitates the need for both a powerful laser source and highly sensitive detector. These instrument requirements have undoubtedly limited the use of CRDS as a routine technique despite the low detection limits achievable. A decade later, O'Keefe proposed performing the same experiment using continuous sources, thereby obviating the need for a high speed detector.[573,574] In this fashion the method is identical to that proposed by Dasgupta and Rhee. The authors differed in their theoretical expressions for the systems. Dasgupta and Rhee treated the cell as etalon and used interferometric principles, while O'keefe treated each pass of light through the cell as having infinitesimal absorbance. Neither theory is entirely correct. Interferometric principles are clearly inapplicable since the observed path length gain occurs regardless of the wavelength, and O'keefe's method does not adequately predict values when faced with finite absorbances through the cell. We have recently addressed these issues and proposed a more generally applicable formula not limited to high reflectivity mirrors or infinitesimal absorbances.[591]

In the previous two cases it is assumed that light repeatedly traverses the same path between the two mirrors. No consideration has been given to beam divergence. Additionally, the high reflectivity dielectric mirrors used in CRDS have an incidence-angle dependence with reflectivity reaching a maximum at the normal. Upon entering the condensed medium even coherent sources will undergo divergence, and the mirror reflectivity will decrease resulting in a greater fraction of the light being transmitted. To reduce the contribution from divergent beams, the detector area may be reduced. In many circumstances this may lead to further reduced sensitivity or is just impractical,

such as when silvered cuvettes are used in a commercial spectrophotometer.[571,591] Because beam divergence is unavoidable, we have also considered the case wherein a silvered cuvette has two holes placed in the silver coating on opposite faces at different vertical levels.[591] Because the detector and light source no longer lie on the same horizontal axis, a minimum number of reflections must occur before detection. This configuration has the added benefit that the emitter and detector no longer have reflective coatings; the greater light throughput simultaneously reduces the need for a sensitive detector and powerful source. It was also observed that though a laser provided the highest limiting $\overline{b}$ ($\lim_{A->0}$). When a spectrophotometer was used, no limiting $\overline{b}$ was discovered and in fact an exponential increase was observed for decreasing absorbance within the measurable range. This phenomenon was found to be dependent on slit width, increasing monotonically with the slit size. We speculate that beam divergence is key to this behavior. When a wide angle LED emitter is used to replace a narrow beam LED, a similar deviation from predicted behavior is observed. Plots of Log A vs. Log c show that under low absorbances this relationship is linear before reaching a minimum $\overline{b}$ value representative of the shortest physical path light must travel. The $\overline{b}$ for the divergent source was generally lower, approximately 20-50% of that of the laser source for 0.2 nm to 5 nm slit width respectively.

In the deep UV, even the best aluminum and magnesium fluoride broad spectrum specular reflectors have only up to 90% reflectance at 200 nm[592] and are cost prohibitive. Alternating layers of HfO_2 and SiO_2 has shown some promise in achieving ~98.8% reflectivity at 250 nm.[593] It is ideal to measure deeper in the UV as the extinction coefficient increases with decreasing wavelength.[560] If adequate analytical results are achieved using divergent sources mentioned above, then the requirement for specular reflectors to maintain a coherent beam need no longer be met, and thus diffuse reflectors

may be used so long as the total reflectivity is high.   When PTFE powder is pressed[579] or sintered,[582,585] it produces a near perfect diffuser over the 200-2500 nm range. For a 1 cm block of pressed PTFE, a maximum reflectance of 99.4% was achieved from 500-1150 nm and only decreases to 96.2% at 200 nm.[579] As a point of reference, in conventional CRDS, mirror reflectivities of 90% and 96.2% would give limiting path lengths of ~9.5 b and 25.8 b respectively (where b is the actual physical path length). Expanded PTFE, has also proven to be an excellent diffuse reflector with reflectance increasing up to even 250 nm.[580,581,584] Reflectivities between 200-250 nm for this material could not be found but measurements at 175 nm have shown expanded PTFE to have the lowest reflectivity compared to other PTFE production methods including extrusion.[583] This was attributed to oxygen retained in the pores, but given the porous structure of expanded PTFE and its known gas permeability, oxygen retention should not be an issue in the vacuum UV if the expanded PTFE was given enough time to outgas. Commercial expanded PTFE may often incorporate additional layers or fillers such as polyvinylidine fluoride (PVDF) to further enhance the reflectivity in the visible which can lead to further absorbance in the deep and vacuum UV regions.[580]   At 175 nm even extruded PTFE showed 64-73% reflectivity for a 5 mm thick section.[583]

No other data on extruded PTFE reflectivity could be located, but it is likely that at the longer wavelength operated here and combined with the thicker wall, higher reflectivities than those seen for a 5 mm piece in the VUV will be achieved. In addition, the virgin PTFE used here should be absent of any absorbing compounds such as PVDF and with no available pores, absorbance due to oxygen within the PTFE should be negligible. Early experiments using small PTFE cells in the visible region showed that absorbance measurements made in aqueous solutions were less reproducible than those made in organic solvents. The hydrophobic surface of the PTFE is difficult to wet, and

bubbles readily form at the PTFE-water surface. To improve the wettability of the PTFE, it underwent oxygen plasma treatment. The measured contact angle was reduced from 120° to 15°.and the reproducibility improved. Because the treatment depth is only in the 10's of nanometers, the reflective properties are largely unchanged in the visual region. Presumably though, the plasma treatment results in hydroxyl and carboxyl functionalities on the PTFE surface. In the deep UV these likely contribute to absorbance, reducing the effective path length. In systems where dissolved gases are low, cavitation will no longer occur and plasma treatment may be unnecessary.

The present cell was evaluated using KHP and glucose, two compounds commonly used in evaluation of TOC systems and with vastly different absorption properties. Measured molar absorptivities at 214 nm for KHP and glucose are 11282 and 0.1243 L mol^{-1} cm^{-1} respectively. Aliquots of the standard solutions were injected using the syringe pump into the flowing stream of purified water (Figure F - 6 and Figure F - 7, the data has also been presented in absorbance units in Figure F - 8 and Figure F - 9). The absorbance was calculated using the peak height from the nearest preceding valley. Plots of log concentration vs. log absorbance are shown in Figure F - 10. In conventional absorbance spectroscopy in which Beer's law is followed, plots of log concentration vs. log absorbance will yield a slope of 1 since it is a linear relationship. Here, slopes of 0.6566 ± 0.0207 and 0.6079 ± 0.0155 were obtained for KHP and glucose respectively. This is in agreement with the multipath theory presented.

The center of the zinc lamp entrance aperture and fiber optic are separated by a length 25 cm and a width of 1.5 cm. The total physical path length is 25.045 cm and represents a minimum distance light must traverse before reaching the detector. The contribution from the width of the cell is only 0.045 cm which is less than the diameters of the entrance and exit apertures. Because the contribution due to the width is below the
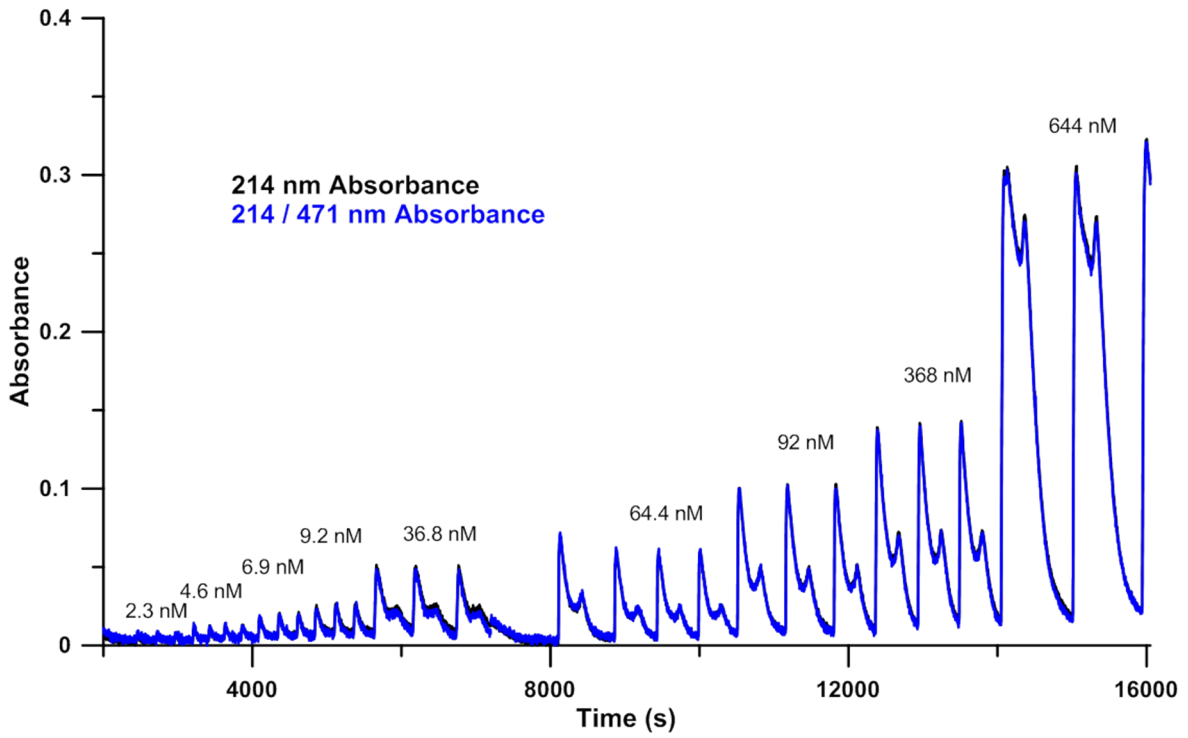
Figure F - 8. Absorbance signal produced as KHP is injected
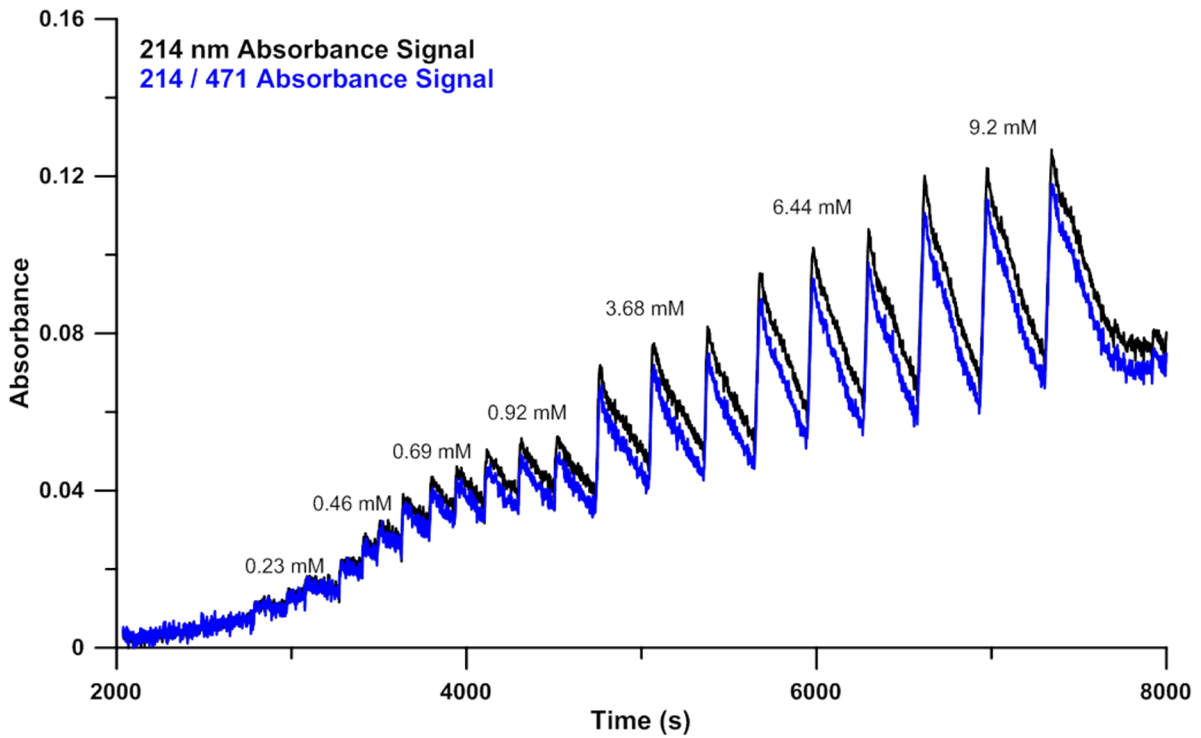
Figure F - 9. Absorbance signal produced as Glucose is injected
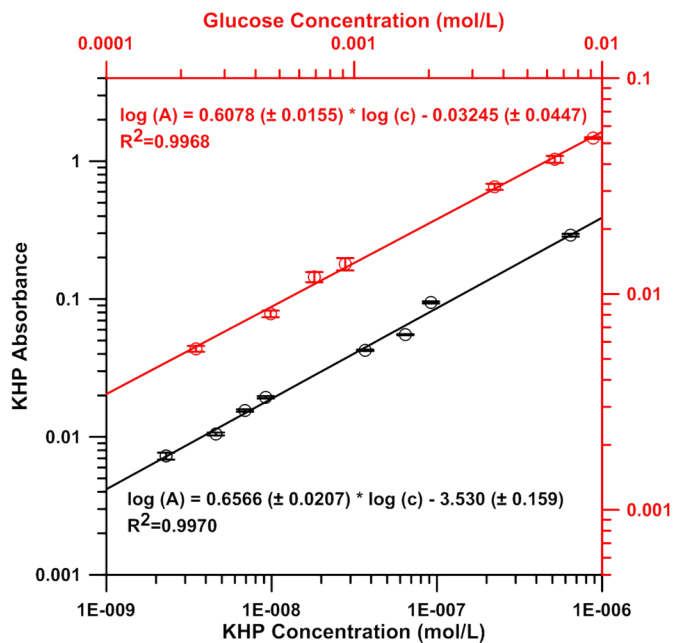
Figure F - 10. Peak absorbance of KHP and
glucose vs. concentration
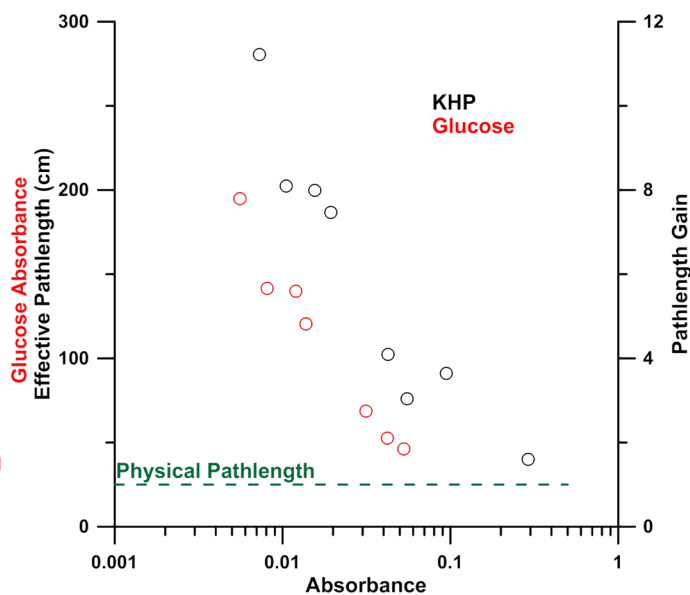
Figure F - 11. Effective path length of the
CEAS as a function of absorbance

error associated in measuring the true physical path length it has been ignored and a

physical path of 25 cm has been used as a reference. Figure F - 11 shows the effective path

length as a function of absorbance. The effective path length was calculated using the known

absorbance value, the concentration injected, and the molar absorptivity of the compound. The

gain over the physical path of 25 cm is also shown. The largest effective path length observed

was 280 cm representing more than 11 fold increase over the true path length. Regardless of

the compound, the path length dependence on absorbance should remain the same. However,

glucose produced consistently lower results. We attribute this to the difficulty in ascertaining the

glucose molar absorptivity at 214 nm. Glucose is very weakly absorbing, almost 5 orders of

magnitude less than KHP. Larges amounts were necessary to even obtain an absorbance

reading at 214 nm. Changes in refractive index become considerable at the levels used. The

longer path used here may help reduce the relative contribution of refractive index effects.

Evidence of refractive index effects may be seen in the absorption spectrum (Figure F - 12):

positive absorbance is seen up to almost 400 nm above which negative absorbance becomes

apparent. Because of the wavelength dependence upon refractive index, a correction using

another wavelength is difficult. It is intuitive however that because everything below 400 nm is

234
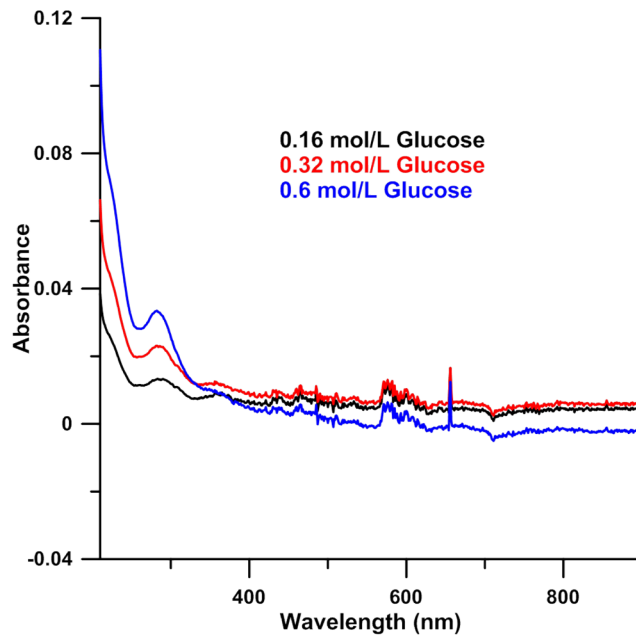
Figure F - 12. Glucose absorption spectrum 200-900 nm

positive that refractive index contributions at 214 nm are also positive. This leads to the

conclusion that the measured molar absorptivity at 214 nm is likely an overestimation of the true

molar absorptivity resulting in lower calculated effective path lengths. Inspection of the raw data

for glucose injections shows that disturbances in the reference baseline are seen at the point of

injection. The concentrated sample upon entering the cell passes the lamp increasing

transmittance briefly into the cell. No corresponding increase or decrease is seen at the other

end after the sample has been thoroughly mixed. It is also interesting to note that this blip does

not correspond with a maximum in absorption either but precedes it.

The cell acts as an integrator; complete mixing is not required for accurate absorbance

measurements, nor does the cell need to be filled with homogenous solution. The total amount

of absorbing species in the cell will have the same absorbance regardless of its location. Such

a setup can help reduce turbidity interferences which have a deleterious effect when using

optical methods to measure TOC[594] We have assumed that because the sample cell is

significantly larger than the amount injected, all of the standard will reside within the cell at the

peak height before being washed out. We confirmed this by filling the cell with prepared KHP

solutions and measuring the absorbance. This was done under both flowing and static
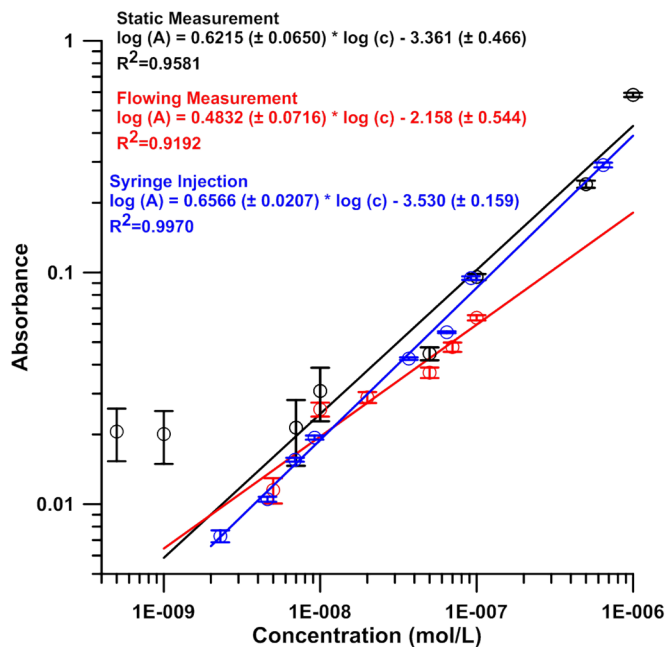
Figure F - 13. Comparison of KHP measurement using flow injection and continuous measurement
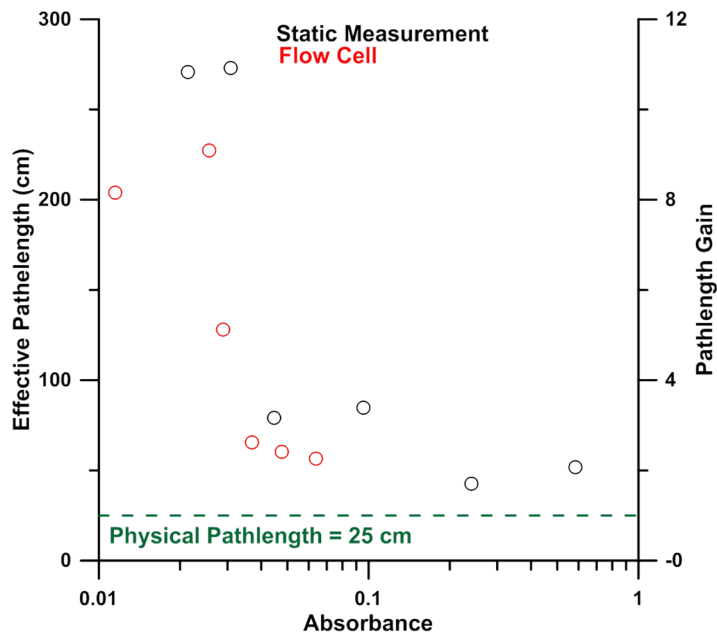
Figure F - 14. Effective path lengths obtained using KHP under static and flowing conditions

conditions in two separate experiments (Figure F - 13). Results are comparable with the injected mode, but both the flowing and static modes were less reproducible and gave poorer correlation coefficients (R^2 = 0.9581, 0.9192, and 0.9970 for static, flowing, and injected measurements). In addition, for the static measurements, the limit of detection was worse. Anything below 10 nM was statistically indistinguishable, although still produced a noticeable absorbance compared to the blank. This is likely due to the ease of contamination at such low levels.[523,530] Similar path length gains (Figure F - 14) were seen with the static measurements achieving an effective path length of up to 270 cm compared to 280 cm achieved using syringe injection.

Injection of blank solutions showed no change in the baseline, so the LODs were calculated based on 3 times the standard deviation of the baseline signal for both KHP and glucose. The LODs for KHP and glucose are 0.484 nM and 64 µM. This corresponds to a carbon concentration of 46.5 ng/L and 4.6 mg/L respectively. These may be considered likely

upper and lower limits of sensitivity. Real TOC measurements will likely reside somewhere in between.

F.4 Conclusion

We have presented a CEAS method for the measurement of carbon species in pure waters. With regards to TOC, such a device will easily fit the needs of clean in place systems for the pharmaceutical industry where the absorbance of the pharmaceuticals or cleaning solutions is known ahead of the rinsing and limits may be readily set. Incorporation into pure water systems will likely be system dependent requiring site specific calibration or a secondary TOC monitor. When used in conjunction with a secondary analyzer such a device may also be useful in identifying potential sources of elevated TOC species. The current method has the advantage of being truly real time, a property sought after for recycle/reclaim systems. We remain optimistic that improvements in LOD for the cell will likely come about by using more reflective material such as sintered, pressed, or expanded PTFE. Currently the device noise limitation arises from the CCD spectrometer. Future work will focus on the use of a zinc emission filter and a photo blind PMT to increase the light throughput and reduce the noise.

F.5 Acknowledgements

.

Appendix G

Title of Appendix Here

G.1 Introduction

Açaí palms (*Euterpe oleraceae mart.*) are native to Central and South America and grow from Belize to Peru and Brazil.[595] Most of the genuine commercial açaí come from the Brazilian Amazon rainforest; commercial cultivation has also begun in Florida. The berries range from green to dark purple in color and ~90% of the mass of the berry is the pit. The health and wellness benefit claims surrounding açaí straddle the border of fact and fantasy; cure-all claims are all too common. There is, however, credible evidence that it has very high antioxidant content,[596,597] can remove reactive oxygen species,[598] inhibit nitric oxide (NO) synthase[599] and cyclooxygenase (COX) -1 and -2,[600] protect human vascular endothelial cells against oxidative stress and inflammation[601] and induce apoptosis in HL-60 leukemia cells in-vitro.[602] Indeed, the name açaí sells many products.

Despite many "açaí juice" products being on the market, strictly speaking, no "juice" can really be produced from the berry, if juice is defined as the aqueous product of squeezing the berry. Açaí is similar to olives in being oleaginous, oil, not juice, is produced on pressing. Instead, the outer portion of the fruit is scraped off the relatively large seed; water is then added to the berries to produce a purée that is often sold frozen. Depending on the amount of water added, açaí grosso (thick), médio (middle) or fino (fine) grades are produced, with the following respective amounts of total solids: >14%, 10-14% and <10%.[603] Authentic açaí products or supplements are expensive. They are also often sold in the freeze-dried form. Given the cost of the genuine product, the incentive for adulteration is high and given the perceived benefits, the market is significant. For other high-value products with perceived health benefits, such as pomegranate juice, international authenticity specifications have been set up.[604] There are many cautionary notes on the web[605] and elsewhere regarding the authenticity of

açaí products, and açaí berry scams have been the subjects of lawsuits by several state attorney generals in the US as well as the US Federal Trade Commission.[606]

At this time little data are available for the characteristic composition of açaí. Relative to other analysis techniques, suppressed conductometric anion chromatography (hereinafter called SCAC) provides rapid and sensitive analysis. Whereas reversed phase (RP) or ion-pair (IP) liquid chromatography may determine both ionic and nonionic species, this will make for a more complex chromatogram. On the other hand, with SCAC, the number of anionic analytes (the corresponding acids must have a pKa~<6 to be detected) is obviously more limited. Also, the RP or IP chromatography will obligatorily require an expensive mass spectrometer as a detector; as many of the analytes of interest (e.g., organic acids without unsaturated linkages) absorb poorly in the UV to be sensitively detected by optical absorption. In contrast, virtually all carboxylic acids ionize sufficiently in SCAC to be detected. In SCAC, the retention behavior of most of the anions is known for a number of different commercially available ion exchange columns, at least under some particular elution conditions, and can be predicted under most others.[607] If there are ions not identifiable on the basis of known retention behavior, they can be identified by tandem mass spectrometry (MS/MS). Once they are identified, further use of a mass spectrometer is not essential.

The ionic composition of açaí in general and its organic acid profile in particular have never previously been described. General approaches to the characterization of organic acid content of fruit (primarily grape) juices were reviewed some time ago.[608] This review tabulated conditions of liquid chromatographic (HPLC) and electrophoretic methods. Several gas chromatography (GC) methods were described early.[609,610] Attractive techniques were developed to trap the analytes on anion exchange resins, methylate them in-situ and perform supercritical fluid extraction prior to GC analysis.[611]

The general availability of GC-MS in many laboratories makes this particularly attractive; direct analysis without derivatization is possible in many cases.[612] Infrared spectroscopy, both in mid-IR[613,614] and near-IR,[613] have proven useful in determining major organic acids (and often other constituents) in a production setting.

These approaches are not without problems, many acids are thermally labile at GC temperatures and IR spectrometry is too insensitive to determine the acids present in lower levels. Liquid phase separations, especially HPLC, have therefore been primarily used for fingerprinting.[615] Capillary electrophoresis (CE) has been used for this analysis with[616] or without[617,618] prior derivatization but the use of HPLC has dominated this application.[619-625] Although some approaches use pre-derivatization prior to a reverse phase (RP) separation,[626] most do not.

Most reported approaches use reverse phase columns with a low pH eluent to keep the analyte acids significantly in the unionized form; the basic separation mechanism is ion exclusion[627,628] with stronger acids eluting first. Some approaches directly use strong acid form cation exchangers and a mineral acid eluent to accomplish the same ends.[629-631] Ion pairing agents such as tetrabutylammonium are applicable,[620] but have not been commonly used. UV absorbance measurement singly[632] or simultaneously/sequentially at multiple wavelengths has been used[627,633-639] but suppressed conductivity and mass spectrometry provide much better limits of detection (LODs).

We aim in this work to characterize the anion profile of both Brazilian and Floridian açaí and thence to determine if this can be used for authentication.

G.2 Materials and Methods

Brazilian açaí berries were bought directly in a market in Belém, Pará, Brazil. They were washed and disinfected with chlorinated water, then transferred to pulping

apparatus to obtain the edible portion (pulp + peel). Water was added to obtain "açaí médio", followed by freezing. The frozen pulp (including added water) was lyophilized in the author's laboratory in Rio de Janeiro to obtain a powder. Lyophilized açaí powder was also obtained from an açaí cultivation farm in Florida. Both samples were sent to the Kansas City district laboratories of the US Food and Drug Administration (FDA). Various other characterizations of these samples (e.g., lipid composition), not discussed here, were carried out at the FDA. Ion chromatographic analysis was conducted at the University of Texas at Arlington. In addition, a sample of white grape juice (brand W), a beverage sample labeled açaí (brand S, did not claim to be a juice and contained undissolved settled solids, only the decantate was used for analysis) and another labeled açaí-pomegranate juice (brand O) were bought from local grocery stores in Arlington, TX. Both the açaí-and the açaí-pomegranate juice were dark purple in color.

Accurately weighed samples (~28 mg) of the lyophilized açaí powders were transferred to a 25 mL volumetric flask, Milli-Q deionized water added to the mark, and the contents sonicated for 20 min. The liquid was divided into two equal portions and was then centrifuged at 7650 rpm for 20 min, followed by filtration through a 0.2 μm nylon syringe filter (13 mm). The filtered sample was diluted four-fold before IC analysis.

The store-bought "juice" samples were filtered through a Hi-Load C-18 Sep-Pak column (www.water.com) and then a 0.2 μm syringe filter. The açaí-pomegranate juice and grape juice were diluted 200-fold while the açaí extract was diluted 100-fold prior to IC analysis.

Chromatography was conducted on an ICS2000 ion chromatograph, equipped with an ASRS Ultra II 2 mm anion self-regenerating SRS Suppressor and a CD 25 conductivity detector with a DS3-1 detector cell. Three different sets of guard and separator columns were examined for the desired separation: AG11+AS11, AG24+AS24,

and AG15+AS15, all 2 mm in diameter. All of the above were from www.dionex.com.

The sample injection volume was 20 µL. Gradients used on each column were optimized

for the best separation; the KOH gradient elution programs used with each column set is

presented in Table G - 1. The background conductivity was usually 0.8 to <3 µS/cm for

gradients of 2.5-80 mM KOH.

Table G - 1. KOH Gradient Programs with IonPac AS11, 15 and 24

Time (min)	KOH (mM) on AS24	KOH (mM) on AS15	KOH (mM) on AS11	Suppressor Current (mA)
0	2.5	2.5	2.5	50
10	2.5	2.5	2.5	50
24	18.0	18.0	18.0	50
40	64.0	64.0	64.0	50
44	70.0	-	-	50
46	2.5	72.0	72.0	50
48	-	2.5	2.5	50
50	-	-	-	50
52	2.5	2.5	2.5	50

IC-MS/MS was performed using the AG24-AS24 column sets and a TSQ

Quantum Discovery Max triple quadrupole mass spectrometer equipped with enhanced

mass resolution and heated electrospray ionization probes. A model AS autosampler (all

MS equipment from www.thermo.com) was used for convenience. The injection volume

was 2 µL for selected ion monitoring (SIM) mode, while 25 µL was used to obtain high

resolution and fragmentation spectra. Instrument parameters were: Electrospray voltage

of 3 kV, vaporizer temperature: 350 °C, capillary temperature: 250 °C, skimmer offset: 0

V, collision gas pressure (fragmentation only): 1.5 mTorr, collision energy: 10 V and

chromatographic filter: 45 seconds. Thomson (Th) units are used for m/z hereinafter. For

fragmentation of hexanoic acid in the scan-centroid mode, the parent ion was at 115 Th,

the scan range was 30-114 Th over 0.200 s. For fragmentation of phytic acid in the scan-

centroid mode, the parent ion was at 218.96 Th, the scan range for segment 1 was 30-

218 Th over 0.200 s and that for segment 2 was 221-660 Th over 0.300 s. In both above cases Q1 and Q3 resolutions were 0.7 and 0.3 Th, respectively in full width half maximum (FWHM). The SIM/Profiling mode utilized Q1 and Q3 resolutions of 0.5 and 0.4 Th FWHM, respectively. The high resolution scan for the phytic acid in profile mode used Q1 resolution set at "pass" and the Q3 resolution at 0.04 FWHM. The scan range was 218.5-220 Th over 0.100 s.

G.3 Results and Discussion

G.3.1 Chromatographic Separation.

Standards containing quinate, lactate, acetate, formate, hexanoate, galacturonate, chloride, sulfate, malate, phytate (*myo*-inositol hexakisphosphate), oxalate, tartrate, phosphate, citrate and isocitrate (hereinafter called the standard mixture), as well as samples of interest were analyzed on all three column sets. The standard mixture is: 20 μM quinate, 10 μM lactate, 10 μM acetate, 10 μM formate, 27 μM hexanoic acid, 10 μM galacturonate, 10 μM chloride, 10 μM sulfate, 10 μM malate, 10 μM tartrate, 10 μM oxalate, 10 μM phosphate, 10 μM citrate, 10 μM isocitrate, 2 μM phytate. The resulting chromatogram on the AS24 column is shown in Figure G - 1 and the 28-40 min region of this chromatogram is shown in magnified view in Figure G - 2. Phytate is the last peak to elute at ~40 min.
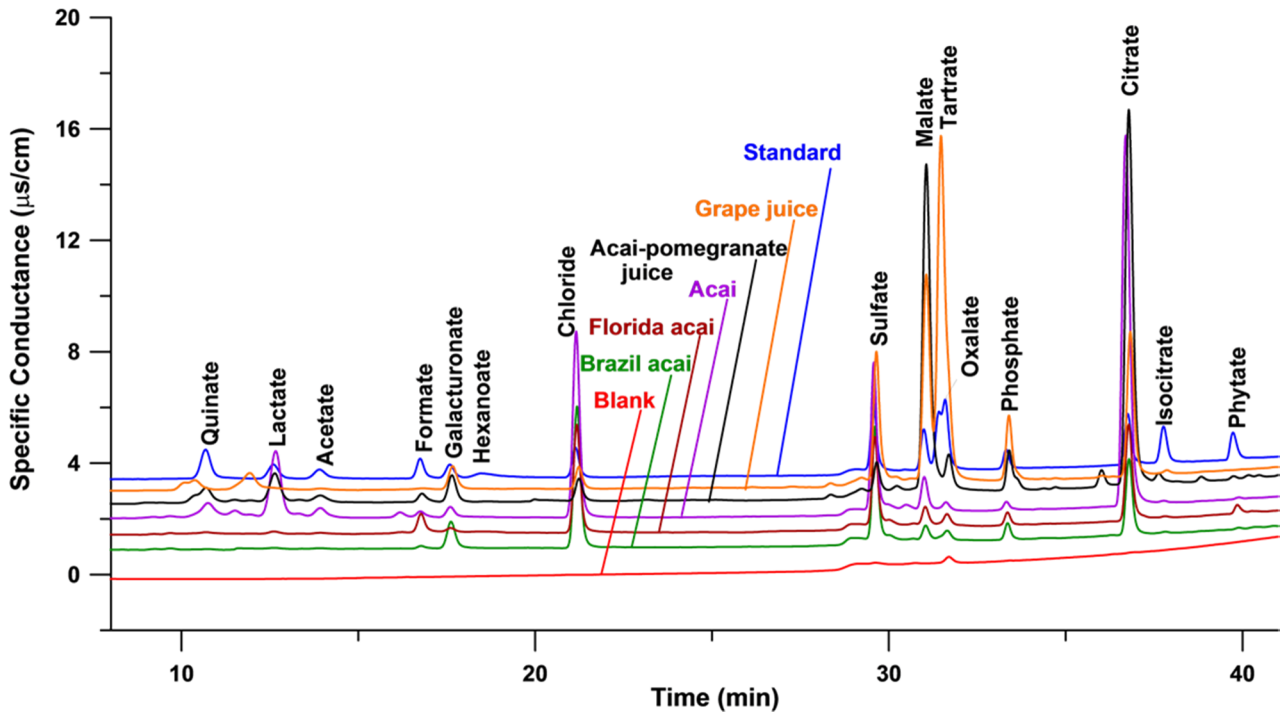
Figure G - 1. Chromatograms of blank, samples and standards on AG24-AS24 column set
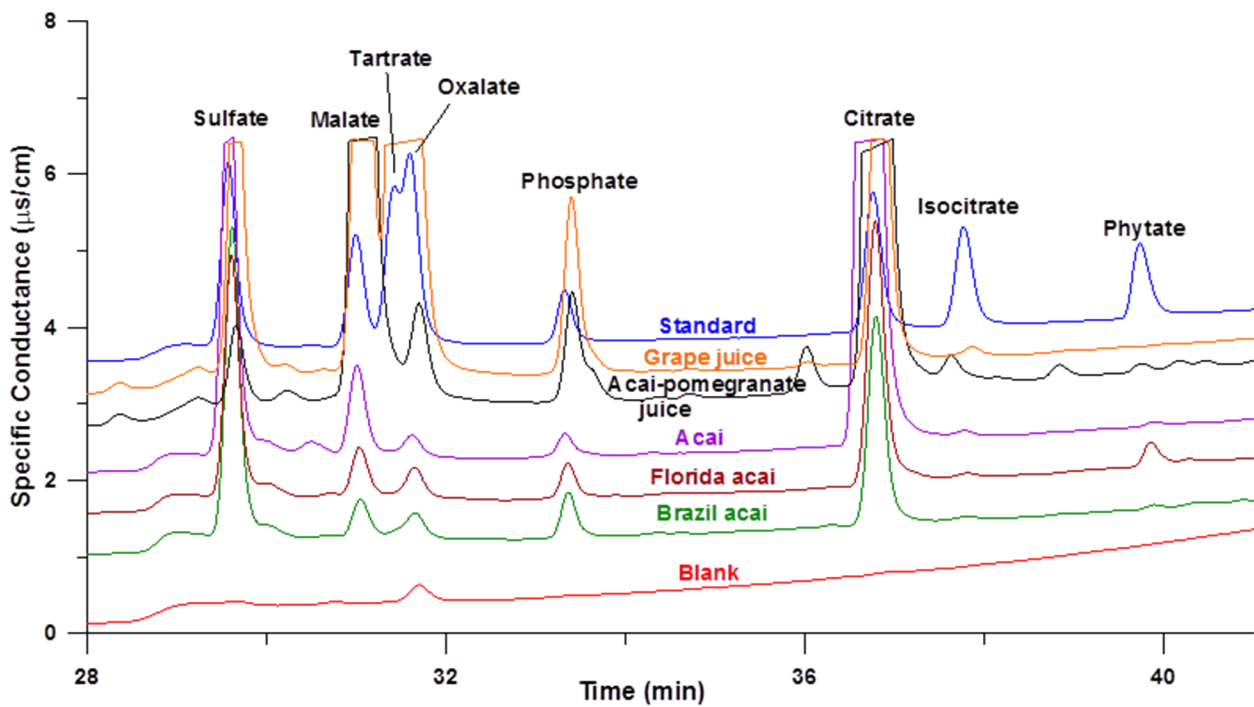
Figure G - 2. Detailed view in 28-41 min region Figure G - 1

245
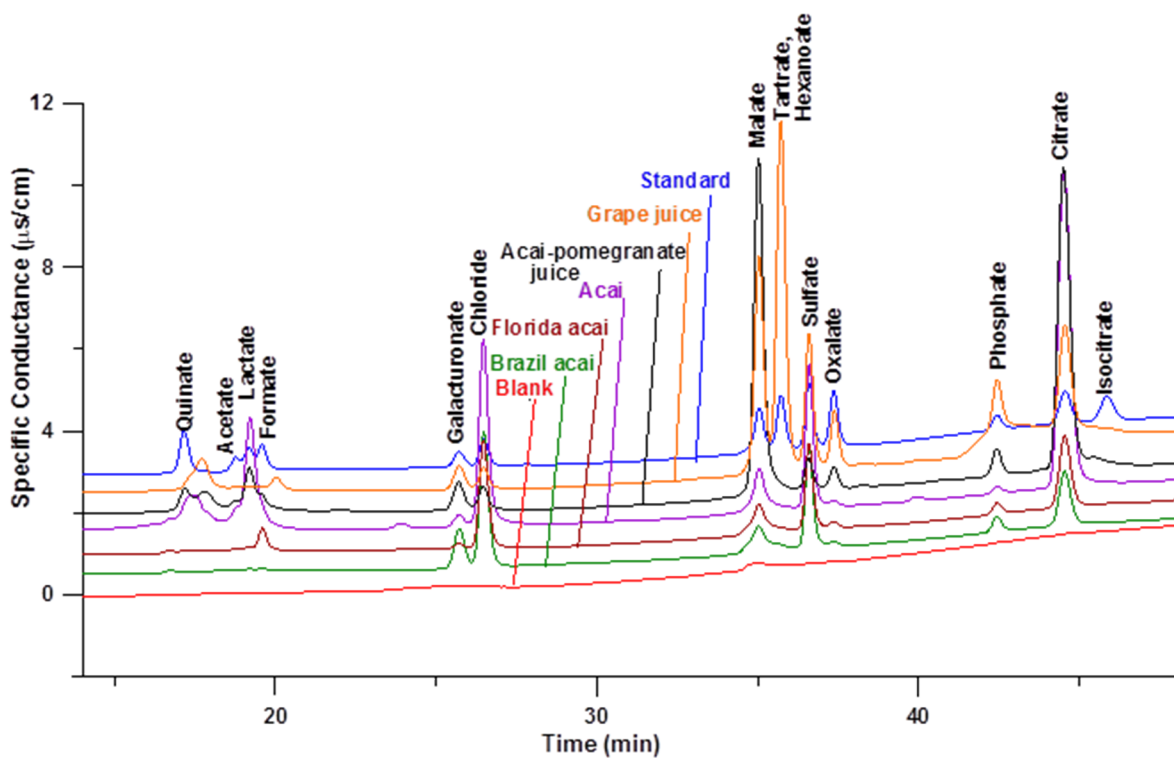
Figure G - 3. Chromatograms of blank, samples and standards on the AS15 column set
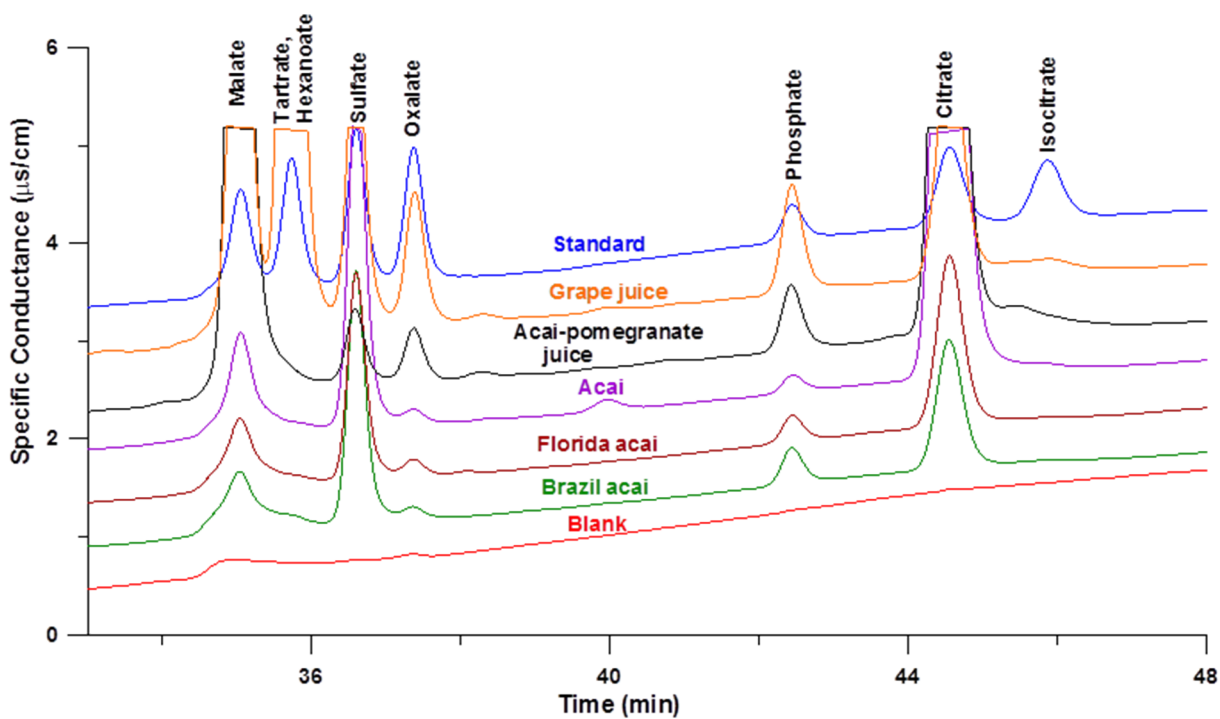
Figure G - 4. Detailed view of the 33-48 min region of Figure G - 3.

Figure G - 3 and Figure G - 4 shows the corresponding chromatograms for the AS15 column set (identical concentrations). In this case, phytate does not elute within an hour. Dissolved CO_2 appears as the carbonate peak in all samples; it is a broad peak and can obscure the elution of some peaks of interest. This can be seen in Figure G - 5 for the malate peak on the AS15 column. Blank, standard mix and sample chromatograms on the AS11 column is shown in Figure G - 6. Carbonate and tartrate coelute under these conditions (we also could not separate them on this column under all other conditions we tested) and this peak in turn elutes very close to malate. The separation from malate shown here was the best separation observed.
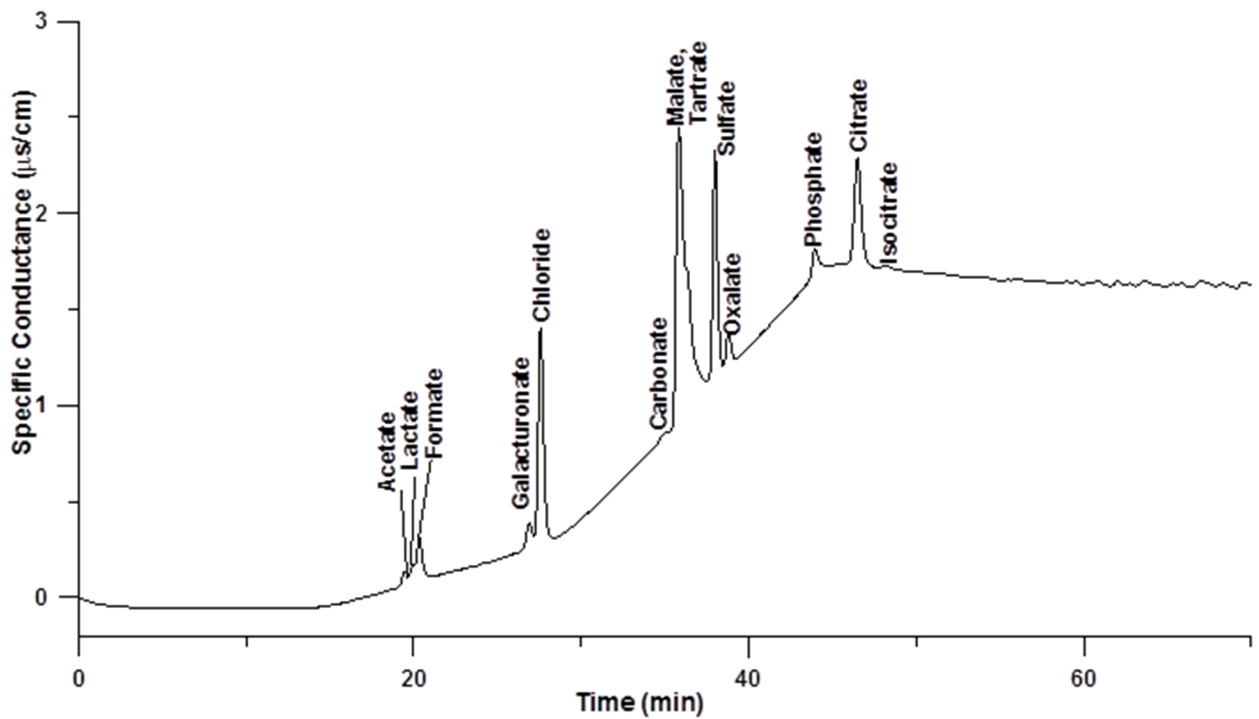
Figure G - 5. Chromatograms of the standard mixture on the AS15 column
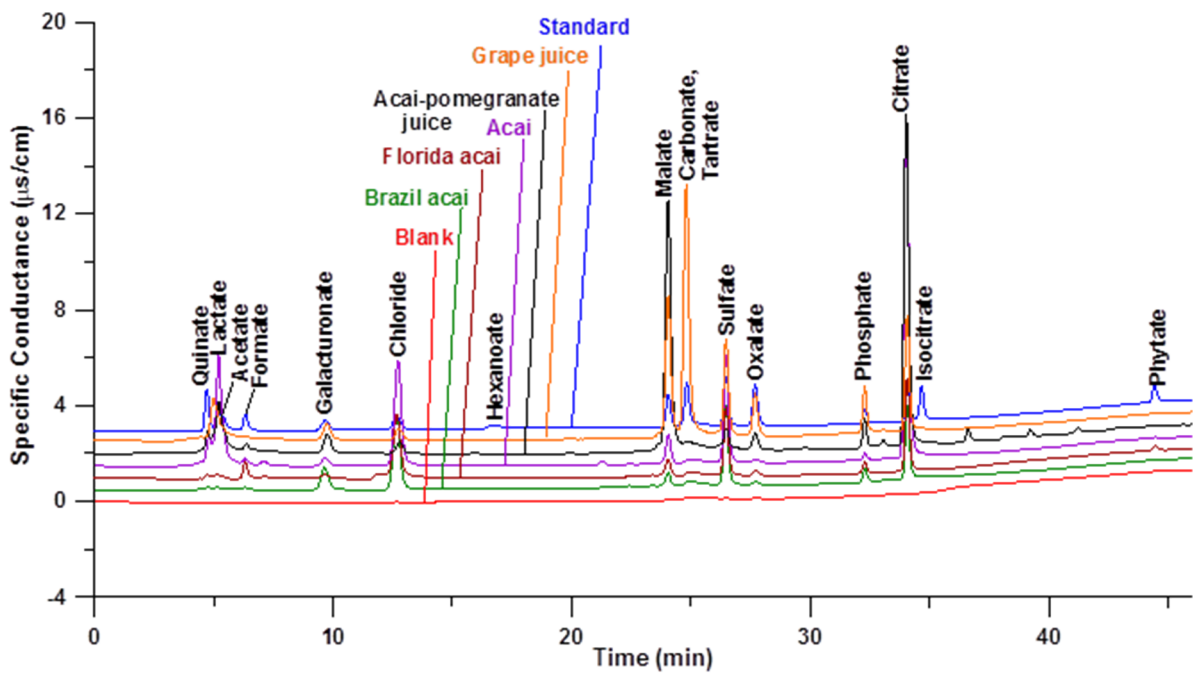
Figure G - 6. Chromatograms of blank, samples and standards on the AS11 column
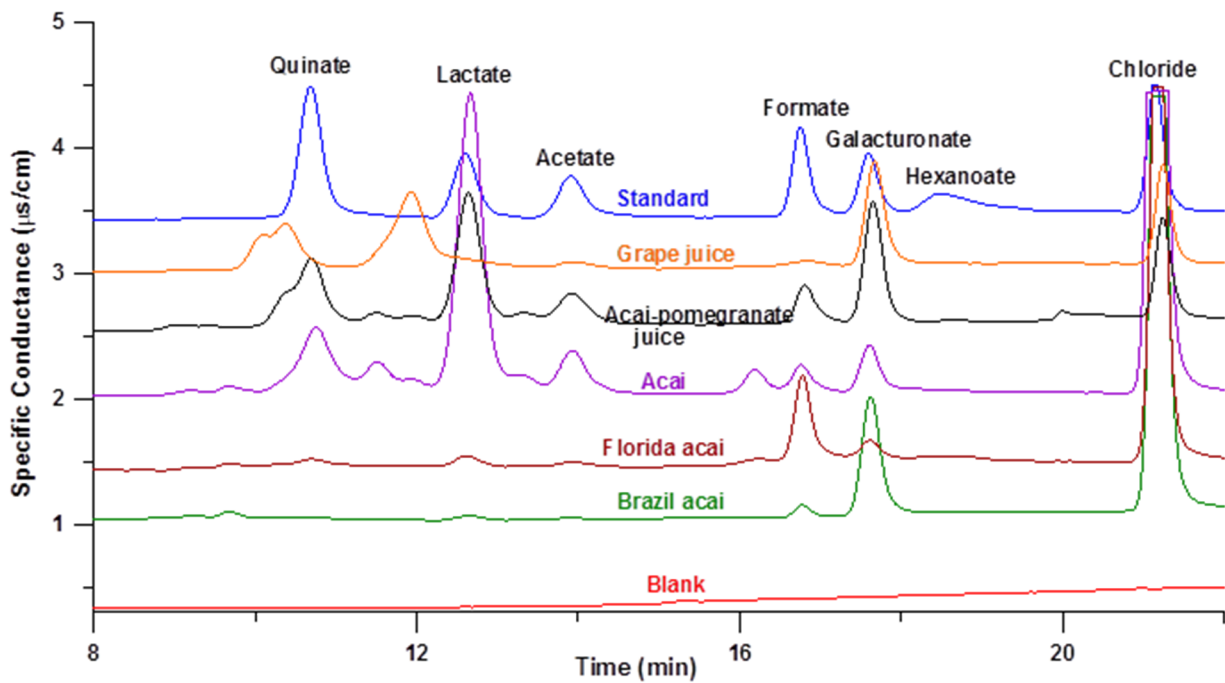
Figure G - 7 Chromatograms of blank, samples and standards from 8-22 min in Figure G - 1

248

Although a relatively low eluent concentration (2.5 mM KOH) was used for all three columns for the first 10 min, the early eluting ions lactate, acetate and formate were well separated only on the AS24 column (Figure G - 7). But tartrate and oxalate elute too close to each other on this column under this condition; accurate quantitation will be impossible if both are present. One critical question (see below), if tartrate is present at all, can likely be answered nevertheless, especially if a standard containing both is run at the same time (compare the traces for the standard mix and the açaí sample traces in Figure G - 2). However, Tartrate was well separated from all other anions (except for hexanoate) only on the AS15 column. Hexanoate was observed in only the Floridian açaí and that in trace amounts. Accurate determination of tartrate should thus be possible by the stated method on the AS 15 column. Tartrate was not detected in any of the açaí samples, but it was one of the dominant components in grape juice (Figure G - 1, G - 2, G - 4), at a concentration of 1.92 mg/g.

Concentrations of all the anions, determined using the AS24 column, are listed in . The calibration plots for these analyte ions are given in the Figure G - 8 through Figure G - 11. The calibration range ranged from 0.2 μM at the low end to 100 μM at the high end, depending on the analyte. The calibration equations are listed in Table G - 3. Calibration equation, range, and LOD
 for the stated ranges; even for the weak acids, at the low concentrations examined, the peak area response was acceptably linear. The linear determination coefficient (r^2) ranged from 0.9914 for hexanoate to 0.9996 for phytate; these are listed in the Table. Also given therein are the limits of detection (LOD) for each ion under these chromatographic conditions based on the S/N=3 criterion; these ranged from 3 nM for the hexaprotic acid anion phytate to 200 nM for monoprotic weak acid anion hexanoate.

Table G - 2. Concentrations of Anions in Açaí, mg/g

Sample/ Analyte ion	Floridian açaí	Brazilian açaí	Açaí	Açaí-pomegranate juice	Grape juice
Quinate	0.555±0.012[a]	0.192±0.034	0.185±0.006	0.366±0.013	<0.003
Lactate	0.413±0.022	0.202±0.015	0.308±0.006	0.251±0.005	<0.001
Acetate	0.260±0.012	0.136±0.003	0.046±0.002	0.067±0.005	0.014±0.002
Formate	1.58±0.01	0.228±0.014	0.012±0.001	0.038±0.003	0.007±0.001
Galacturonate	1.83±0.14	12.3±0.2	0.126±0.001	0.661±0.026	0.565±0.014
Hexanoate	1.55±0.12	<0.108	<0.003	<0.006	<0.006
Chloride	4.09±0.01	5.52±0.04	0.200±0.000	0.048±0.002	0.047±0.001
Sulfate	4.18±0.07	5.44±0.12	0.190±0.001	0.067±0.001	0.322±0.002
Malate	2.01±0.08	1.81±0.13	0.103±0.004	2.52±0.03	1.44±0.02
Tartrate	<0.016	<0.016	<0.001	<0.001	1.92±0.05
Oxalate	0.38±0.02	0.214±0.020	0.013±0.001	0.072±0.002	0.184±0.006
Phosphate	1.92±0.05	2.75±0.72	0.042±0.001	0.406±0.007	0.576±0.007
Citrate	15.7±0.1	13.1±0.8	1.90±0.03	3.67±0.02	1.31±0.02
Isocitrate	0.255±0.016	0.278±0.008	0.009±0.0001	<0.002	0.036±0.002
Phytate	1.34±0.01	0.229±0.010	0.007±0.0003	0.025±0.001	<0.003

[a] All results listed as average ± standard deviation (n=3). The ions are listed in order of elution.
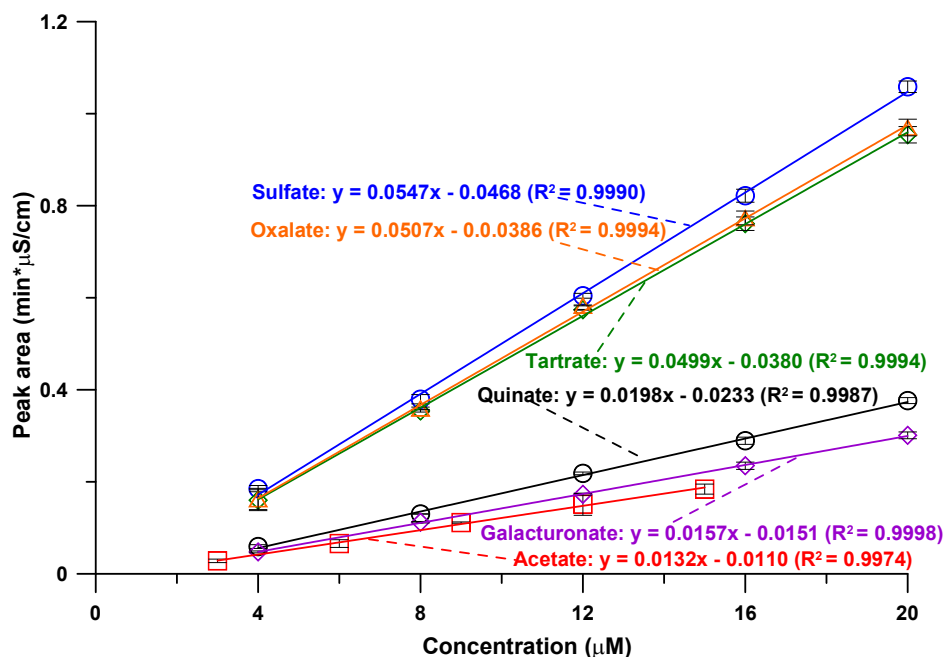
Figure G - 8. Calibration curves for Quniate, acetate, galacturonate, and sulfate using

AS24 column set and tartate and oxalate using AS15 column set
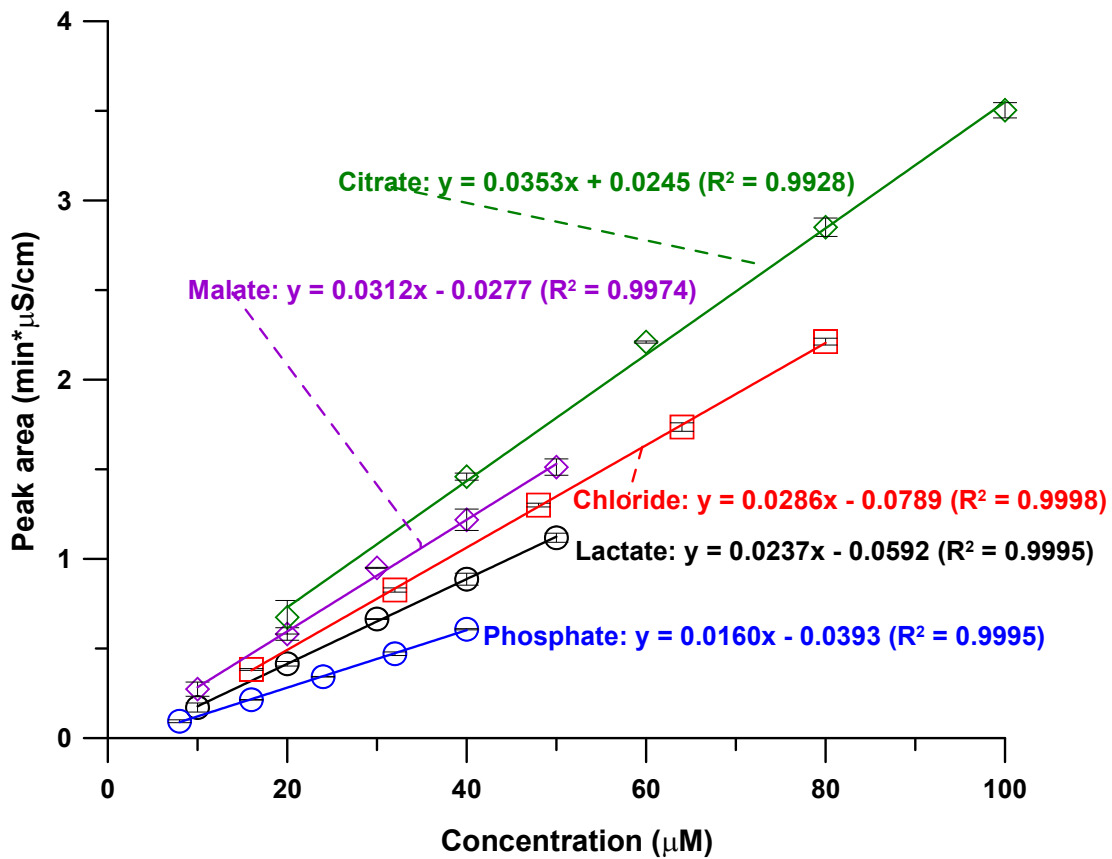
Figure G - 9. Calibrations curves for lactate, chloride, malate, phosphate, and citrate

using AS24 column set
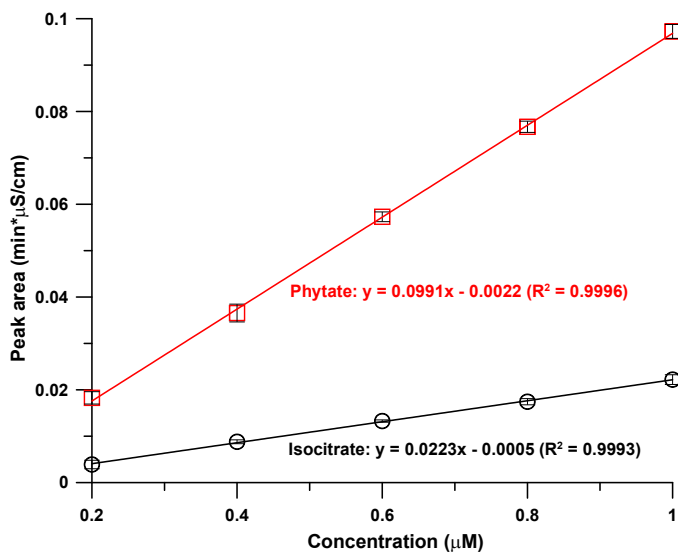
Figure G - 10. Calibration curves for isocitrate and

phytate, using AS24 column set
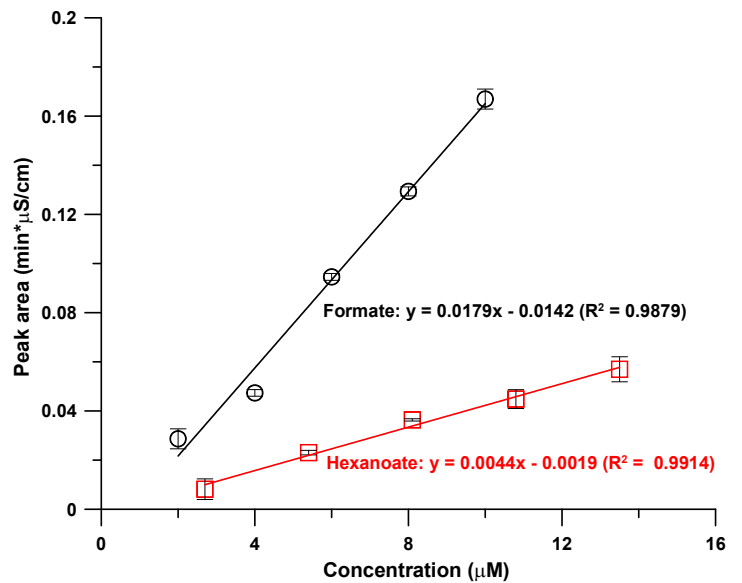
Figure G - 11. Calibration curves for formate and

hexanoate, using AS24 column set

Table G - 3. Calibration equation, range, and LOD

Ion	Column	Calibration Equation (Y: Peak area, min*μS/cm)	Linear r^2	Calibration Range, μM	Limit of Detection, nM
Quinate	AS24	Y = 0.0198 *(C, μM) - 0.0233	0.9987	4 - 20	32
Lactate	AS24	Y = 0.0237 *(C, μM) - 0.0592	0.9995	10 -50	29
Acetate	AS24	Y = 0.0132 *(C, μM) - 0.0110	0.9974	3 - 15	54
Formate	AS24	Y = 0.0179 *(C, μM) - 0.0142	0.9879	2 -10	25
Galacturonate	AS24	Y = 0.0157 *(C, μM) - 0.0151	0.9998	4 - 20	32
Hexanoate	AS24	Y = 0.0044 *(C, μM) - 0.0019	0.9914	2.7 - 13.5	200
Chloride	AS24	Y = 0.0286 *(C, μM) - 0.0789	0.9998	16 - 80	14
Sulfate	AS24	Y = 0.0547 *(C, μM) - 0.0468	0.999	4 - 20	7
Malate	AS24	Y = 0.0312 *(C, μM) - 0.0277	0.9974	10 - 50	15
Tartrate[a]	AS15	Y = 0.0499 *(C, μM) - 0.0380	0.9994	4 - 20	4
Oxalate[a]	AS15	Y = 0.0507 *(C, μM) - 0.0386	0.9994	4 - 20	6
Phosphate	AS24	Y = 0.0160 *(C, μM) - 0.0393	0.9995	8 - 40	24
Citrate	AS24	Y = 0.0353 *(C, μM) + 0.0245	0.9928	20 - 100	9
Isocitrate	AS24	Y = 0.0223 *(C, μM) - 0.0005	0.9993	0.2 - 1	14
Phytate	AS24	Y = 0.0991 *(C, μM) - 0.0022	0.9996	0.2 - 1	3

There is no particular column that is uniquely better than all others to perform juice/extract analysis either for authentication, or differentiate between different strains of açaí. While AS24 can separate most anions, it cannot separate tartrate and oxalate. The latter separation is facile on AS15 but it cannot separate early eluting ions, e.g., acetate, formate and lactate or elute phytate in an hour. Thus, quantitation of all but oxalate and tartrate was done on the AS24 column while oxalate and tartrate were separated and quantitated on the AS15 (see Figure G - 8).

G.3.2 Mass Spectrometric Identification of Galacturonate, Hexanoate and Phytate.

Some peaks were not initially identifiable based on known chromatographic retention behavior. The gradient described for the AS24 column was stretched out some over time in order to better elucidate the nature of these peaks. The chromatogram of the Floridian açaí extract under these conditions is shown in Figure G - 12. The black trace uses the right ordinant while the blue, orange, and green traces are the single ion monitoring counts for

252

hexanoate, galactouranate, and phytate respectively and use the left ordinant. The virtually co-eluting peaks at 21 min revealed, on negative ion mode mass spectrometric selected ion monitoring study, ions at 115 and 193 Th. The 193 Th signal was ascribed to galacturonate. The retention time and the fragmentation pattern matched exactly with a standard.

The 115 Th response was ascribed to hexanoate. A hexanoate standard was used for confirmation; the retention time was within 0.02 min of that in the sample, this is well within the
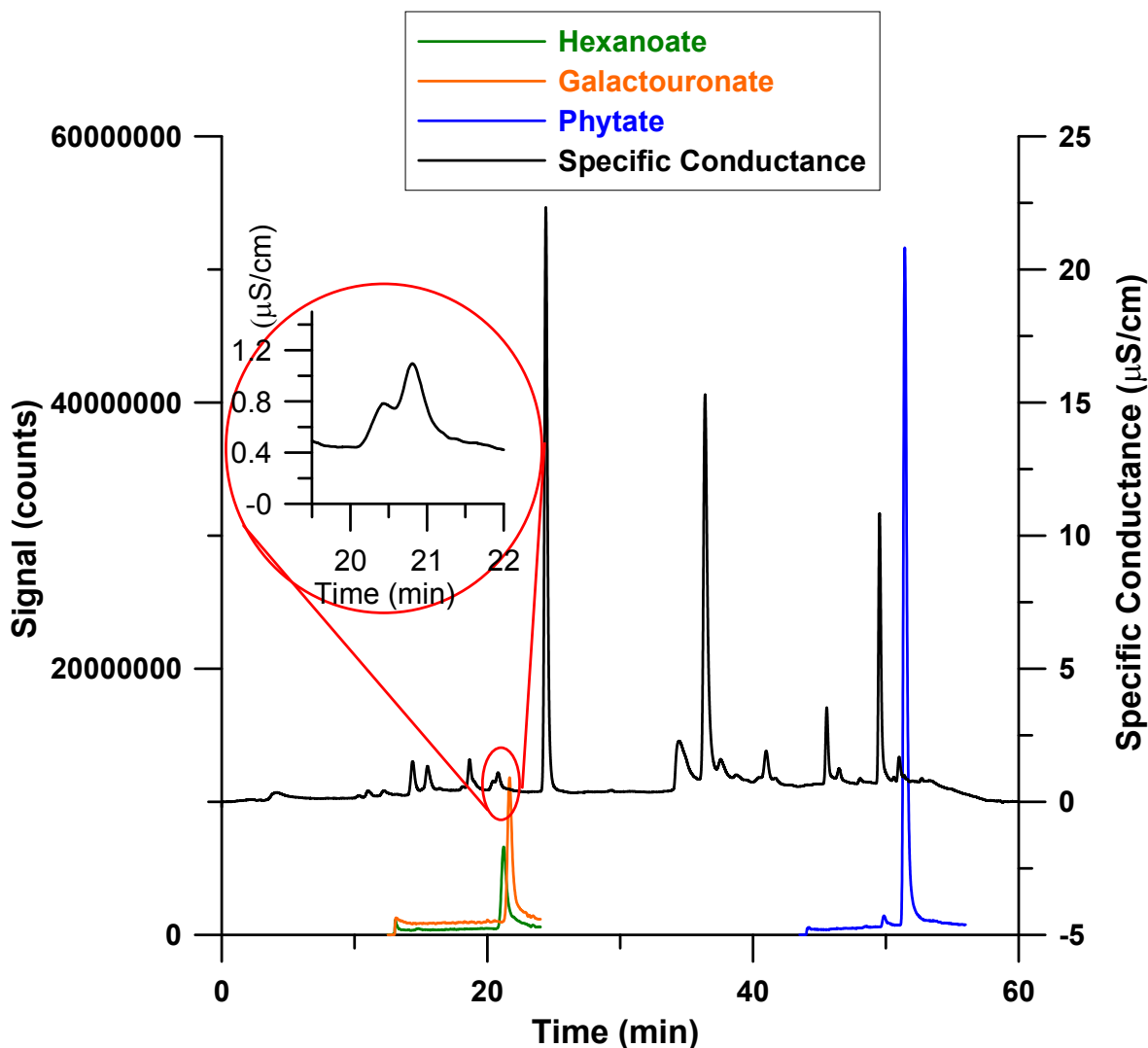
Figure G - 12. Chromatogram of Floridian Açaí with mass spectrometry detection on AS24 column set.
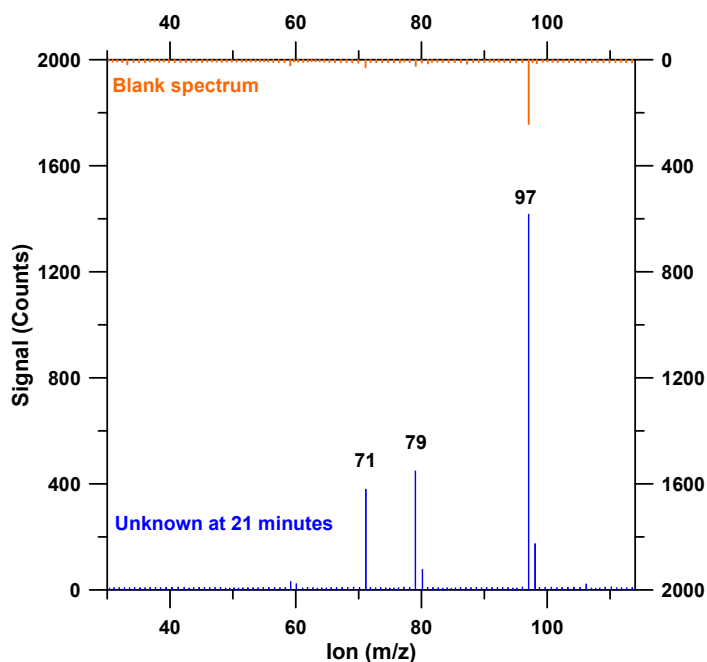
Figure G - 13. Fragmentation pattern of

the 115 Th peak eluting at 21 min
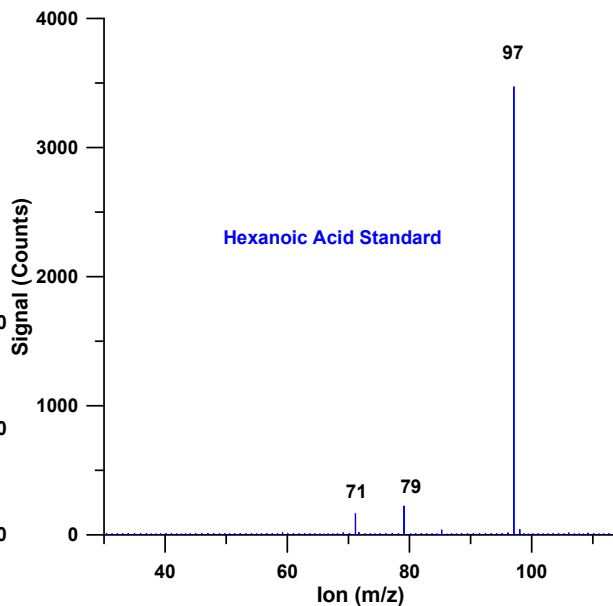
Figure G - 14. Fragmentation pattern of 135 µM

hexanoic acid standard

reproducibility of retention times under these conditions. The hexanoate concentration in the

sample was too low to quantitatively compare the relative peak intensities in the fragmentation

pattern in the sample and the standard. However, the Th values of all the fragment peaks were

identical in the sample and the standard, within the mass resolution of the instrument. The

relevant data are shown in Figure G - 13 and Figure G - 14.

The peak that eluted after citrate at ~52 min was also initially not identified. This peak

produced an intense signal at 219 Th. The peak was asymmetric and tailed into the higher Th

range, often a characteristic of multiply charged ions that fragment into a less charged ion at a

higher Th. Reinvestigation of the full spectrum scan showed the presence of a weaker signal at

329 Th. Both the signals at 219 and 329 Th would be consistent with being derived from a

neutral species of 660 mass units: the above two signals resulting respectively from loss of

three and two protons. As the singly charged species was not observed, we suspected the

parent compound to be a multiprotic strong acid.

Higher resolution spectra were used for confirmation and are shown in the Figure G -

16. Note that a clear isotope distribution, separated by ~0.33 Th, is observed for the 219 Th

peak, indicating a triply charged ion. Fragmentation was performed from 30-218 and 220-659 Th; the results are shown in Figure G - 16. The parent mass and isotope distribution suggested a possible chemical formula of $C_6P_6O_{24}H_{18}$. Nominal Th values of all of the major ions seen are consistent with fragments that will logically be generated from the triply charged phytate ion (Table G - 4). Additionally, given that the chromatographic retention time matched exactly with an authentic standard of phytate (*myo*-inositol hexakisphosphate), we positively identified this chromatographic peak as phytate. Table G - 5 contains a list of all major fragments ions listed in the order of their intensity along with their origin.
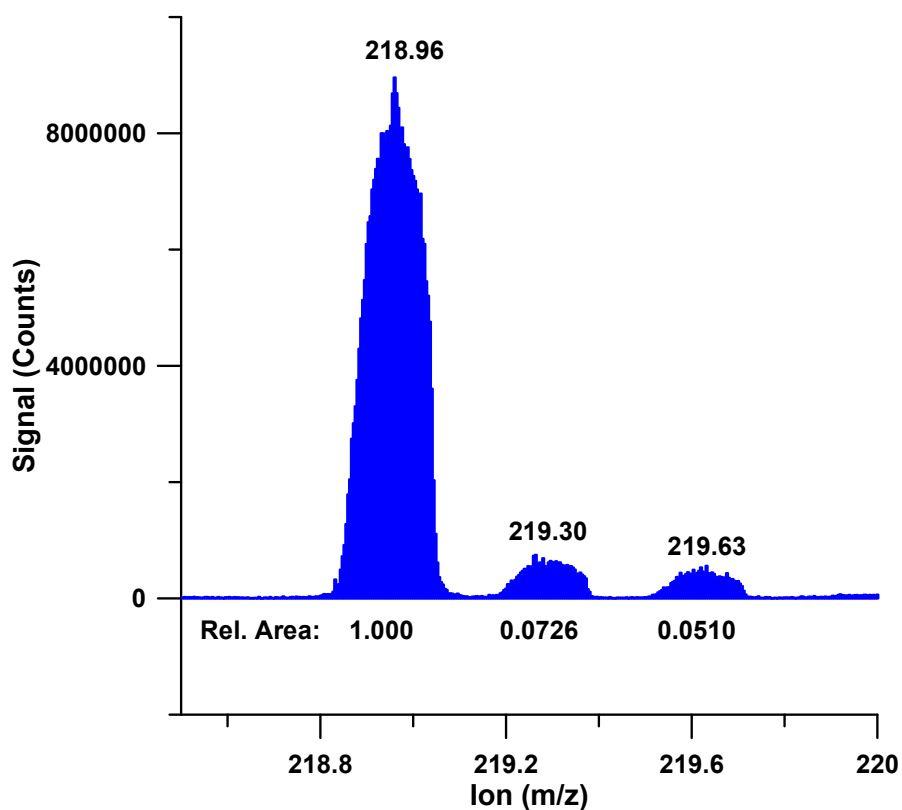
Figure G - 15. Mass spectrum of the peak eluting at 52 min in Figure G - 12
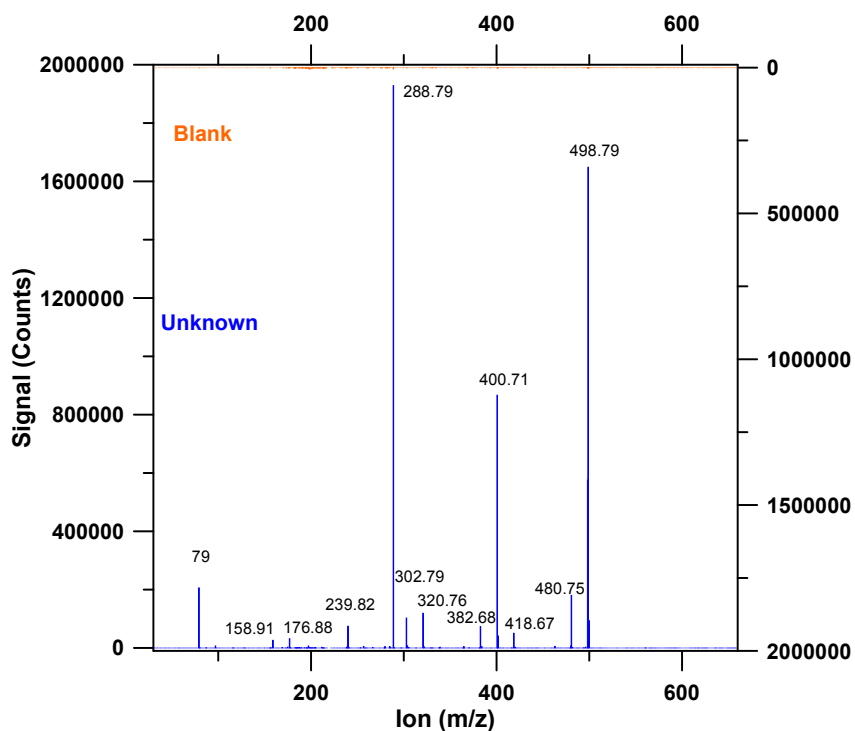
Figure G - 16. Fragmentation spectrum produced upon fragmenting the 219 Th peak

Table G - 4. Proposed Fragmentation Scheme of Phytate^{3-} (nominal masses)

m/z	Ion	Loss
219	*$C_6P_6O_{24}H_{15}^{3-}$*	*Parent ion*
289	$C_6P_5O_{21}H_{15}^{2-}$	PO_3^-
499	$C_6P_4O_{18}H_{15}^-$	$2*PO_3^-$
401	$C_6P_3O_{14}H_{12}^-$	$2*PO_3^-+HPO_3^-+H_2O$
79	PO_3^-	Ejected ion
481	$C_6P_4O_{17}H_{13}^-$	$2*PO_3^-+H_2O$
321	$C_6P_2O_{11}H_{11}^-$	$2*PO_3^-+2HPO_3^-+H_2O$
303	$C_6P_2O_{10}H_9^-$	$2*PO_3^-+2HPO_3^-+2H_2O$
240	$C_6P_4O_{17}H_{12}^{2-}$	$PO_3^-+HPO_3^-+H_2O$
383	$C_6P_3O_{13}H_{10}^-$	$2*PO_3^-+HPO_3^-+2H_2O$
419	$C_6P_3O_{15}H_{14}^-$	$2*PO_3^-+HPO_3^-$
177	$H_3P_2O_7^-$	Possible gas phase recombination
159	$HP_2O_6^-$	Possible gas phase recombination

256

Table G - 5. Putative Ion Identification of Parent and Daughter Ions of Phytate^{3-}

m/z (Th)	Ion	Loss
219	$C_6P_6O_{24}H_{15}^{3-}$	*Parent ion*
289	$C_6P_5O_{21}H_{15}^{2-}$	PO_3^-
499	$C_6P_4O_{18}H_{15}^-$	$2*PO_3^-$
401	$C_6P_3O_{14}H_{12}^-$	$2*PO_3^-+HPO_3^-+H_2O$
79	PO_3^-	Ejected ion
481	$C_6P_4O_{17}H_{13}^-$	$2*PO_3^-+H_2O$
321	$C_6P_2O_{11}H_{11}^-$	$2*PO_3^-+2HPO_3^-+H_2O$
303	$C_6P_2O_{10}H_9^-$	$2*PO_3^-+2HPO_3^-+2H_2O$
240	$C_6P_4O_{17}H_{12}^{2-}$	$PO_3^-+HPO_3^-+H_2O$
383	$C_6P_3O_{13}H_{10}^-$	$2*PO_3^-+HPO_3^-+2H_2O$
419	$C_6P_3O_{15}H_{14}^-$	$2*PO_3^-+HPO_3^-$
177	$H_3P_2O_7^-$	Possible gas phase recombination
159	$HP_2O_6^-$	Possible gas phase recombination

G.3.3 Significance of Phytic Acid.

The structure of phytic acid is shown in Supporting information (Figure G - 17). It is found in soil, cereals, legumes, nuts, oil seeds, pollen and spores.[640] Reported health effects of phytic acid are somewhat contradictory. While it has been called an anti-nutrient for several decades (it removes metals like calcium as water-insoluble complexes preventing absorption in the gut) but it is now known that it also act as an antioxidant and anti-cancer agent.[641] Phytate may also help prevent Alzheimer's disease and other neurodegenerative diseases by chelating iron (it has greater affinity for iron than calcium) and keeping it from initiating oxidative damage.[642] The main sources of phytate in the daily diet are cereals and legumes, especially
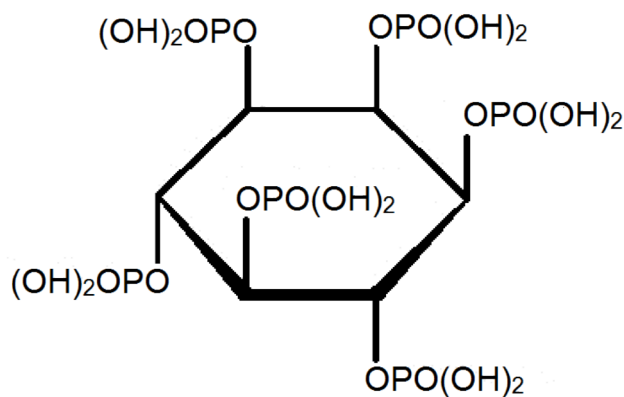
Figure G - 17. Structure of phytic acid (*myo*-inositol hexakisphosphate)

oily seeds and nuts with estimated daily intake in the West ranging between 0.3-2.6 g.[641] The recommended daily dosage for açaí powder formulated as capsules and taken as supplement is 2 g/day. The Floridian açaí contained a much greater amount of phytate (~7x) than the Brazilian açaí. However, on an absolute scale, the amount of phytate in the Floridian sample was only 1.34 mg/g; it will not be a significant source for phytate. On the other hand, it is possible that Floridian and Brazilian açaí can be distinguished by their phytate content.

G.3.4 Implications on Phytate Analysis.

The analysis of phytate is important, the present method provides a superior alternative to extant methods. AOAC method 986.11[643] uses anion exchange separation, then complete hydrolysis and colorimetric phosphate determination. If other inositol phosphates are not completely separated, a positive error results.

In SCAC (obligatorily with an alkaline eluent), phytate will have a charge of -12. The normal expectation will be that it will not elute in a reasonable period, as was presently observed with the AS15 column. Indeed, in previous studies[644] even to elute the triphosphate from an AS4A column required high concentrations of 4-cyanophenolate, an extremely strong eluent. Only the mono and diphosphate could be eluted with a high concentration gradient of NaOH and NaOAc from a PA-10 column.[645] Strong acid eluents with anion exchange columns and post column reactions with Fe^{3+} can separate and detect (by UV absorption) all inositol phosphates.[646-648] However, unlike the present method, it will not sensitively detect other ions, e.g.; organic acids, or be compatible with mass spectrometry.

The present method can elute phosphate in a reasonable period with a hydroxide eluent. If phytate is the only inositol phosphate analyte of interest, we have found that it can be eluted much sooner using a stronger eluent gradient but without causing coelution with the peaks eluting earlier.

G.3.5 Implications on the Authentication of Açaí.

There is considerable interest in authentication of expensive food and beverages that can be easily adulterated. For example, for pomegranate juice, an international multidimensional authenticity specification algorithm has recently been established.[604] The present work suggests on a preliminary basis that the absence of tartrate may provide a useful tool to determine the authenticity of pure açaí and/or pomegranate products, especially as the common adulterant juices are all known to contain large to easily detectable levels of tartrate. Of course, many more samples would have to be analyzed to establish the validity of this observation. It is important that any such analysis be done on genuine açaí. For example, it was recently reported that a product labeled "açaí juice" contained 0.6 mg/L nitrate.[603] Nitrate is unlikely to be present inside the fruit and no nitrate was found in any of the açaí samples in the present study. The ability to differentiate between Floridian and Brazilian açaí on the basis of phytate content will also need to be validated by analysis of a much larger number of samples.

The measurement of principal organic acids in fruit juice, especially grape juice (for general characterization and for determination of maturity for harvesting) by SCAC has been previously advocated.[649-651] The SCAC technique has grown considerably in power since; presently it is possible to generate an essentially complete anion profile, including that of the organic acids, even those present at low levels. The different selectivities of the multitude of columns presently available permits complete separation, and also aids identification through multidimensional retention mapping as shown in Figure G - 18. For example, lactate elutes before acetate on a AS24 column while the reverse elution order is observed on a AS15. Similarly the elution orders of sulfate and malate are reversed between AS24 and AS11, among many such instances. In most cases, the use of mass spectrometry is not essential. With the açaí products as the focus, we hope to have clearly established the power of this technique.
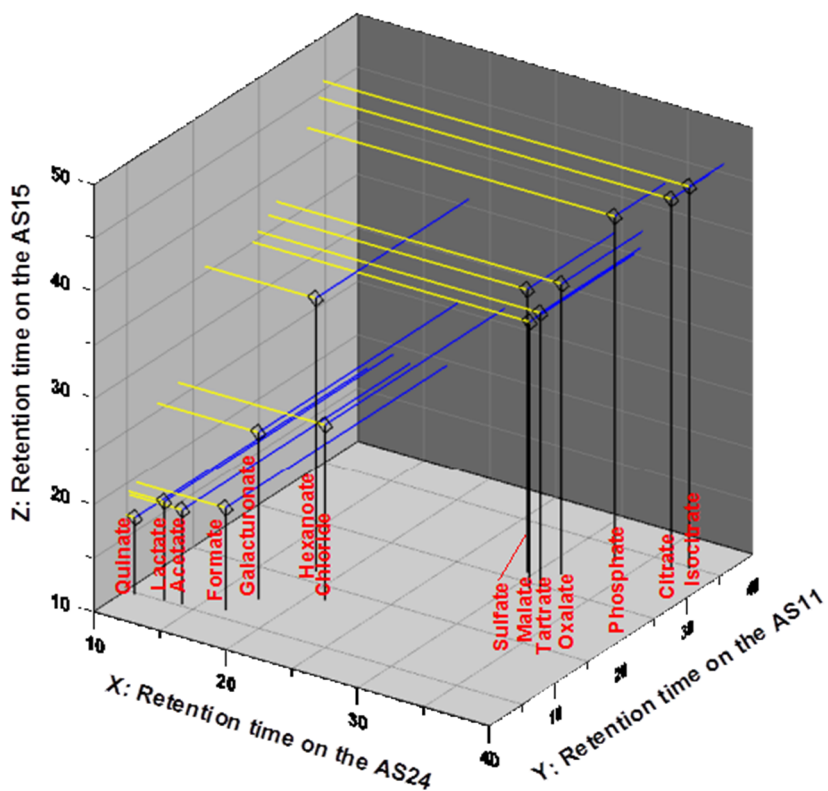
Figure G - 18. 3D retention map of different anions on the

AS24, AS15, and AS11 columns

G.4 Acknowledgement

.

References

[1] M.B. Zimmermann, Endocr. Rev., 30 (2009) 376.

[2] D. Marine, O.P. Kimball, J. Lab. Clin. Med., 3 (1917) 40.

[3] UNICEF Regional Office CEE/CIS. March 2006. The use of iodized salt in food

processing industry in Switzerland. 22 pp.

http://www.iodinenetwork.net/documents/2006_IS_Study_Tour_.pdf

Accessed November 27, 2010.

[4] H. Markel, Am. J. Public Health, 77 (1987) 219.

[5] Q. T. Ngyuen. Iodized Salt and U.S. Development. http://econweb.umd.edu/~nguyen-

q/job%20market/Quynh%20Nguyen%20-%20Job%20market%20paper%20-

%2030%20oct%202009.pdf Accessed November 27, 2010

[6] Food and Nutrition Board, Institute of Medicine. *Dietary reference intakes*; National

Academy Press: Washington DC, 2001; p 258.

http://www.nap.edu/openbook.php?record_id=10026 Accessed January 11,

2011.

[7] R.D. Utiger, N. Engl. J. Med., 354 (2006) 2819.

[8] World Health Organization. Assessment of iodine deficiency disorders and monitoring

their elimination. A guide for programme managers, 3rd ed. 2008.

http://www.who.int/nutrition/publications/micronutrients/iodine_deficiency/978924

1595827/en/index.html Accessed January 12, 2011.

[9] H. Backer, J. Hollowell, Environ. Health Perspect., 108 (2000) 679.

[10] R.T. Zoeller, J. Rovet, J. Neuroendocrinol., 16 (2004) 809.

[11] F. Delange, Postgraduate Medical Journal, 77 (2001) 217.

[12] P. Santiago-Fernandez, R. Torres-Barahona, J.A. Muela-Martinez, G. Rojo-Martinez, E. Garcia-Fuentes, M.J. Garriga, A.G. Leon, F. Soriguer, J. Clin. Endocrinol. Metab. 89 (2004) 3851.

[13] J.G. Hollowell, N.W. Staehling, W.H. Hannon, D.W. Flanders, E.W. Gunter, G.F. Maberly, L.E. Braverman, S. Pino, D.T. Miller, P.L. Garbe, D.M. DeLozier, R.J. Jackson, J. Clin. Endocrinol. Metab., 83 (1998) 3401.

[14] J.A.T. Pennington, S.A. Schoen, Int. J. Vitam. Nutr. Res., 66 (1996) 342.

[15] E.N. Pearce, S. Pino, X. He, H. R. Bazrafshan, S. L. Lee, L. E. Braverman J. Clin. Endocrinol. Metabol. 89 *(*2004) 3421

[16] P.K. Dasgupta, Y. Liu, J.V. Dyke, Environ. Sci. Technol., 42 (2008) 1315.

[17] S. Havas, Cereal Foods World, 53 (2008) 17.

[18] K.B. Harris, K.A. Pass, Mol. Genet. Metab., 91 (2007) 268.

[19] J. Rovet, D. Daneman, Paediatr. Drugs, 5 (2003) 141.

[20] Centers for Disease Control and Prevention (CDC). National Center for Health Statistics (NCHS). National Health and Nutrition Examination Survey Data. Hyattsville, MD: U.S. Department of Health and Human Services, Centers for Disease Control and Prevention, [2007-2008] http://www.cdc.gov/nchs/nhanes/nhanes2007-2008/nhanes07_08.htm

[21] J.A.M. Martinez, A.G. Leon, R.T. Barahona, P.S. Fernandez, F.S. Escofet, Psicothema, 20 (2008) 279.

[22] F. Vermiglio, V.P. Lo Presti, M. Moleti, M. Sidoti, G. Tortorella, G. Scaffidi, M.G. Castagna, F. Mattina, M.A. Violi, A. Crisa, A. Artemisia, F. Trimarchi, J. Clin. Endocrinol. Metab., 89 (2004) 6054.

[23] P.K. Dasgupta, Anal. Chim. Acta, 567 (2006) 1.

[24] P.K. Dasgupta, Environ. Chem., 6 (2009) 7.

[25] R. Renner, Environ. Health Perspect., 118 (2010) A439.

[26] E.B. Sandell, I.M. Kolthoff, Mikrochim. Acta, 1 (1937) 9.

[27] H. Shintani, P.K. Dasgupta, Anal. Chem., 59 (1987) 1963.

[28] W. May, D. Wu, C. Eastman, P. Bourdoux, G. Maberly, Clin. Chem., 36 (1990) 865.

[29] J.V. Dyke, P.K. Dasgupta, A.B. Kirk, Talanta, 79 (2009) 235.

[30] P.J. Ke, R.J. Thibert, R.J. Walton, D.K. Soules, Mikrochim. Acta (1973) 569.

[31] M.C. Sanz, T. Brechbuhler, I.J. Green, Clin. Chim. Acta, 1 (1956) 570.

[32] P.K. Dasgupta, A.B. Kirk, J.V. Dyke, S.I. Ohira, Environ. Sci. Technol., 42 (2008) 8115.

[33] S.I. Ohira, A.B. Kirk, J.V. Dyke, P.K. Dasgupta, Environ. Sci. Technol., 42 (2008) 9419.

[34] J.G. Dorea, J. Am. Coll. Nutr., 23 (2004) 97.

[35] S.B. Barker, M.J. Humphrey, M.H. Soley, J. Clin. Invest., 30 (1951) 55.

[36] J.R. Bellanger, J.C. Tressol, H.P. Piel, Ann. Rech. Vet., 10 (1979) 113.

[37] O.P. Foss, L. Hankes, D.D. Van Slyke, Clin Chim Acta, 5 (1960) 301.

[38] P.W.F. Fischer, M.R. Labbe, J. Assoc. Off. Anal. Chem., 64 (1981) 71.

[39] N. Patzeltova, Chem. Pap.-Chem. Zvesti., 47 (1993) 237.

[40] P.W.F. Fischer, M.R. Labbe, A. Giroux, J. Assoc. Off. Anal. Chem., 69 (1986) 687.

[41] US Food And Drug Administrtion. Kansas City Laboratory. Determination of Iodine in Foods. KAN-LAB-MET.95 Ver. 3.2. Updated August 2007. Tammy Smith, USFDA. Personal communication, November, 2010.

[42] B. Zak, H.H. Willard, G.B. Myers, A.J. Boyle. Anal Chem. 24 (1952) 1345.

[43] J. Benotti, N. Benotti, S. Pino, H. Gardyna, Clin. Chem., 11 (1965) 932.

[44] H. Hoch, C.G. Lewallen, Clin. Chem., 15 (1969) 204.

[45] B. Tiran, O. Wawschinek, O. Eber, A. Beham, S. Lax, M. Dermelj, Exp. Clin. Endocrinol., 98 (1991) 32.

[46] S. Pino, S.L. Fang, L.E. Braverman, Exp. Clin. Endocrinol. Diabetes, 106 (1998) S22.

[47] D. Bier, J. Rendl, M. Ziemann, D. Freystadt, C. Reiners, Exp. Clin. Endocrinol. Diabetes, 106 (1998) S27.

[48] D. Gnat, A.D. Dunn, S. Chaker, F. Delange, F. Vertongen, J.T. Dunn, Clin. Chem., 49 (2003) 186.

[49] K.L. Caldwell, C.B. Maxwell, A. Makhmudov, S. Pino, L.E. Braverman, R.L. Jones, J.G. Hollowell, Clin. Chem., 49 (2003) 1019.

[50] Y.P. Zhang, D.X. Yuan, J.X. Chen, T.S. Lan, H.Q. Chen, Clin. Chem., 42 (1996) 2021.

[51] B. Rollmann, C. Regaert, J.P. Herveg, Arch. Int. Physiol. Bio., 93 (1985) B51.

[52] R.A. Zaroda, Clin. Chem., 15 (1969) 555.

[53] J.E. Rae, S.A. Malik, Chemosphere, 33 (1996) 2121.

[54] D.S. Wu, H.W. Deng, W.Y. Wang, H.Y. Xiao, Anal. Chim. Acta, 601 (2007) 183.

[55] A. Grossmann, G.F. Grossmann, Clin. Chem., 4 (1958) 296.

[56] S. Passen, R. von Saelski, Am. J. Clin. Pathol., 51 (1969) 166.

[57] G. Kessler, V.J. Pileggi, Clin. Chem., 16 (1970) 382.

[58] G. Palumbo, M.F. Tecce, G. Ambrosio, Anal. Biochem., 123 (1982) 183.

[59] V.J. Pileggi, G. Kessler, Clin. Chem., 14 (1968) 339.

[60] N. Baudry, B. Mallet, P.J. Lejeune, L. Vinet, J.L. Franc, J. Endocrinol., 153 (1997) 99.

[61] P.J. Garry, D.W. Lashley, G.M. Owen, Clin. Chem., 19 (1973) 950.

[62] D. Jungst, L. Strauch, Z. Klin. Chem. Klin. Bio., 7 (1969) 636.

[63] M. Mantel, Clin. Chim. Acta, 33 (1971) 39.

[64] W.F. Rayburn, A. Robinson, L.E. Braverman, X.M. He, S. Pino, M.L. Gargas, J.H. Kinzell, Reprod. Toxicol., 25 (2008) 129.

[65] C. Wuethrich, S.E. Jaeggi-Groisman, H. Gerber, Clin. Chem. Lab. Med., 38 (2000) 1027.

[66] P. Houze, M. Corvisier, M.E. Toubert, B. Gourmel, B. Bousquet, Ann. Biol. Clin.-Paris, 62 (2004) 222.

[67] H. Hussain, W. Nazaimoon, W. Mohamud, Trop. Biomed., 23 (2006) 109.

[68] T. Ohashi, M. Yamaki, C.S. Pandav, M.G. Karmarkar, M. Irie, Clin. Chem., 46 (2000) 529.

[69] S. Kaufman, J. Pediatr., 68 (1966) 990.

[70] J. Benotti, N. Benotti, Clin Chem, 12 (1963) 408.

[71] R. Okennedy, P. Keating, J. Immunol. Methods, 163 (1993) 225.

[72] R. Thomas. Practical Guide to ICP-MS. Marcel-Dekker, New York, 2004.

[73] M. Haldimann, B. Zimmerli, C. Als, H. Gerber, Clin. Chem., 44 (1998) 817.

[74] V. Poluzzi, B. Cavalchi, A. Mazzoli, G. Alberini, A. Lutman, P. Coan, I. Ciani, P. Trentini, M. Ascanelli, V. Davoli, J. Anal. At. Spectrom., 11 (1996) 731.

[75] R. Santamaria-Fernandez, P. Evans, C.S.J. Wolff-Briche, R. Hearn, J. Anal. At. Spectrom., 21 (2006) 413.

[76] W. Buchberger, B. Czizsek, S. Hann, G. Stingeder, J. Anal. At. Spectrom., 18 (2003) 512.

[77] Centers for Disease Control and Prevention, Division of Laboratory Science. Iodine in Urine, DLS method code: 2001/04-OD. Revised August 22, 2001, CLIA methods. Atlanta, GA: Centers for Disease Control and Prevention, 2001:1-20.

[78] R.G. Wuilloud, N. Selar, S.S. Kannamkumarath, J.A. Caruso, J. Anal. At. Spectrom., 19 (2004) 1442.

[79] H.J. Stark, J. Mattusch, R. Wennrich, A. Mroczek, Fresenius J. Anal. Chem., 359 (1997) 371.

[80] M. Leiterer, D. Truckenbrodt, K. Franke, Eur. Food Res. Technol., 213 (2001) 150.

[81] L.F. Sanchez, J. Szpunar, J. Anal. At. Spectrom., 14 (1999) 1697.

[82] B. Michalke, P. Schramel, Electrophor., 20 (1999) 2547.

[83] B.P. Jensen, B. Gammelgaard, S.H. Hansen, J.V. Andersen, J. Anal. At. Spectrom., 18 (2003) 891.

[84] M. Takeuchi, P.K. Dasgupta, J.V. Dyke, K. Srinivasan, Anal. Chem., 79 (2007) 5690.

[85] M. Wind, A. Eisenmenger, W.D. Lehmann, J. Anal. At. Spectrom., 17 (2002) 21.

[86] P. Schramel, S. Hasse, Mikrochim. Acta, 116 (1994) 205.

[87] E.H. Larsen, M.B. Ludwigsen, J. Anal. At. Spectrom., 12 (1997) 435.

[88] M.F. Mesko, P.A. Mello, C.A. Bizzi, V.L. Dressler, G. Knapp, E.M.M. Flores, Anal. Bioanal. Chem., 398 (2010) 1125.

[89] X. Hou, B. T. Jones. Inductively coupled plasma optical emission spectrometry. *Encyclopedia of Analytical Chemistry*, Wiley On-line library. Wiley, New York. 2008.

[90] E.A. Vtorushina, A.I. Saprykin, G. Knapp, J. Anal. Chem., 63 (2008) 643.

[91] J. Kucera, in V. R. Preedy, G. N. Burrow, R. R. Watson, Eds. *Comprehensive Handbook of Iodine,* Academic Press, Massachusetts 2009 pp 15-27.

[92] I. Varga, Microchem. J., 85 (2007) 127.

[93] W.E. Braselton, K.J. Stuart, J.M. Kruger, Clin. Chem., 43 (1997) 1429.

[94] E. Niedobova, J. Machat, V. Kanicky, V. Otruba, Microchim. Acta, 150 (2005) 103.

[95] J. Naozuka, M. da Veiga, P.V. Oliveira, E. de Oliveira, J. Anal. At. Spectrom., 18 (2003) 917.

[96] T. Nakahara, T. Wasa, Appl. Spectrosc., 41 (1987) 1238.

[97] M.R. Cave, K.A. Green, J. Anal. At. Spectrom., 4 (1989) 223.

[98] E. Niedobova, J. Machat, V. Otruba, V. Kanicky, J. Anal. At. Spectrom., 20 (2005) 945.

[99] S.P. Dolan, S.A. Sinex, S.G. Capar, A. Montaser, R.H. Clifford, Anal. Chem., 63 (1991) 2539.

[100] G.B. Souza, E. Carrilho, C.V. Oliveira, A.R.A. Nogueira, J.A. Nobrega, Spectrochim. Acta Part B-At. Spectrosc., 57 (2002) 2195.

[101] M. Kahn, J. Kleinberg, Radiochemistry of Iodine, Nuclear Science Series, National Academy of Sicences-National Research Council, NAS-NS-3062

[102] J. Kucera, Z. Randa, L. Soukal, J. Radioanal. Nucl. Chem., 249 (2001) 61.

[103] Y. Serfor-Armah, B.J.B. Nyarko, J. Holzbecher, E.H.K. Akaho, E.K. Osae, A. Chatt, J. Radioanal. Nucl. Chem., 256 (2003) 259.

[104] B.J.B. Nyarko, Y. Serfor-Armah, S. Osae, E.H.K. Akaho, S. Anim-Sampong, B.T. Maakuu, J. Radioanal. Nucl. Chem., 251 (2002) 281.

[105] M.M. Mason, V.L. Spate, J.S. Morris, C.K. Baskett, T.P. Cheng, C.L. Reams, L. Lemarchand, B.E. Henderson, L.N. Kolonel, J. Radioanal. Nucl. Chem.–Artic., 195 (1995) 57.

[106] X.L. Hou, C.F. Chai, Q.F. Qian, C.S. Li, K. Wang, Fresenius Journal of Analytical Chemistry, 357 (1997) 1106.

[107] L.A. Currie, Analytical Chemistry, 40 (1968) 586.

[108] X.L. Hou, H. Dahlgaard, B. Rietz, U. Jacobsen, S.P. Nielsen, J. Radioanal. Nucl. Chem., 244 (2000) 87.

[109] S.J. Parry, J. Radioanal. Nucl. Chem., 248 (2001) 137.

[110] H.J. Bowen, Biochem. J., 73 (1959) 381.

[111] E.M. Smith, J.M. Mozley, H.N. Wagner, Jr., J. Nucl. Med., 5 (1964) 828.

[112] M.M. Heckman, J. Assoc. Off. Anal. Chem., 62 (1979) 1045.

[113] P. Bermejo-Barrera, M. Aboal-Somoza, A. Bermejo-Barrera, J. Anal. At. Spectrom., 14 (1999) 1009.

[114] M.C. Yebra, M.H. Bollain, Talanta, 82 (2010) 828.

[115] O. Haase, J.A.C. Broekaert, Spectrochim. Acta Part B-At. Spectrosc., 57 (2002) 157.

[116] P. Miles, J. Assoc. Off. Anal. Chem., 61 (1978) 1366.

[117] C.A. Gushurst, J.A. Mueller, J.A. Green, F. Sedor, Pediatrics, 73 (1984) 354.

[118] J. Melichercik, L. Szijarto, A.R. Hill, J. Dairy Sci., 89 (2006) 934.

[119] W.L. Hoover, J.R. Melton, P.A. Howard, J. Assoc. Off. Anal. Chem., 54 (1971) 760.

[120] A.A. Almeida, X. Jun, J. Lima, Mikrochim. Acta, 127 (1997) 55.

[121] W. Zhang, A. Mnatsakanov, R. Hower, H. Cantor, Y.Z. Wang, Front. Biosci., 10 (2005) 88.

[122] J. Rendl, S. Seybold, W. Borner, Clin. Chem., 40 (1994) 908.

[123] T.R.I. Cataldi, A. Rubino, M.C. Laviola, R. Ciriello, J. Chromatogr. B-Anal. Technol. Biomed. Life Sci., 827 (2005) 224.

[124] C. Bruggink, W.J.M. van Rossum, E. Spijkerman, E.S.E. van Beelen, J. Chromatogr. A, 1144 (2007) 170.

[125] Dionex Corporation. Disposable electrodes for electrochemical detection. http://www.dionex.com/en-us/webdocs/42552-Disposable%20Electrodes_DataSheet_V30_released102706.pdf Accessed December 4, 2010

[126] T.R.I. Cataldi, A. Rubino, R. Ciriello, Anal. Bioanal. Chem., 382 (2005) 134.

[127] O. Chailapakul, M. Amatatongchai, P. Wilairat, K. Grudpan, D. Nacapricha, Talanta, 64 (2004) 1253.

[128] T.K. Malongo, S. Patris, P. Macours, F. Cotton, J. Nsangu, B.M. Kauffmann, Talanta, 76 (2008) 540.

[129] F.C. Pereira, L.M. Moretto, M. De Leo, M.V.B. Zanoni, P. Ugo, Anal. Chim. Acta, 575 (2006) 16.

[130] K.K. Hu, W.X. Huang, Y.H. Su, R.Z. Hu, Chin. Chem. Lett., 20 (2009) 1483.

[131] V.V. Kuznetsov, Y.V. Ermolenko, L. Seffar, J. Anal. Chem., 62 (2007) 479.

[132] V.V. Kuznetsov, Y.V. Ermolenko, L. Seffar, J. Anal. Chem., 59 (2004) 688.

[133] Z.O. Tesfaldet, J.F. van Staden, R.I. Stefan, Talanta, 64 (2004) 1213.

[134] A. Waseem, M. Yaqoob, A. Nabi, Luminescence, 23 (2008) 316.

[135] M. Yaqoob, R. Atiq ur, A. Waseem, A. Nabi, Luminescence, 21 (2006) 221.

[136] J.L. Burguera, M.R. Brunetto, Y. Contreras, M. Burguera, M. Gallignani, P. Carrero, Talanta, 43 (1996) 839.

[137] N. Ratanawimarnwong, N. Amomthammarong, N. Choengchan, P. Chaisuwan, M. Amatatongchai, P. Wilairat, I.D. McKelvie, D. Nacapricha, Talanta, 65 (2005) 756.

[138] D. Nacapricha, P. Sangkarn, C. Karuwan, T. Mantim, W. Waiyawat, P. Wilairat, I. Cardwell, I.D. McKelvie, N. Ratanawimarnwong, Talanta, 72 (2007) 626.

[139] S.D. Nikolic, J.J. Mutic, A.D. Lolic, D.D. Manojlovic, Anal. Sci., 21 (2005)

[140] T. Mitsuhashi, Y. Kaneda, J. Assoc. Off. Anal. Chem., 73 (1990) 790.

[141] D.J. Doedens, J. Anal. Toxicol., 9 (1985) 109.

[142] S. Grys, J. Chromatogr., 100 (1974) 43.

[143] H.B. Li, F. Chen, X.R. Xu, J. Chromatogr. A, 918 (2001) 335.

[144] P. Pantuckova, L. Krivankova, Electrophoresis, 25 (2004) 1102.

[145] V. Maheswari, N. Balasubramanian, Analusis, 25 (1997) 2.

[146] N. Ahmad, Aust. J. Dairy Technol., 32 (1977) 103.

[147] R. Kesari, R. Rastogi, V.K. Gupta, Chem. Anal. (Warsaw), 43 (1998) 201.

[148] U. Divrikli, M. Soylak, M. Dogan, Chem. Anal. (Warsaw), 45 (2000) 257.

[149] P.L. Jooste, E. Strydom, Best Pract. Res. Clin. Endocrinol. Metab., 24 (2010) 77.

[150] T. Dearth-Wesley, A. Makhmudov, C.M. Pfeiffer, K. Caldwell, Food Nutr. Bull., 25 (2004) 130.

[151] M.D. Huang, H. Becker-Ross, S. Florek, M. Okruss, B. Welz, S. Mores, Spectrochim. Acta Part B-At. Spectrosc., 64 (2009) 697.

[152] V.S. Burakov, A.V. Isaevich, P.Y. Misakov, P.A. Naumenkov, S.N. Raikov, J. Anal. At. Spectrom., 9 (1994) 307.

[153] M. Butler, R. Okennedy, Anal. Lett., 27 (1994) 681.

[154] T. Tomiyasu, M. Nonaka, M. Uchikado, K. Anazawa, H. Sakamoto, Anal. Sci., 20 (2004) 391.

[155] J. Rendl, D. Bier, T. Groh, C. Reiners, Exp. Clin. Endocrinol. Diabetes, 106 (1998) S12.

[156] N. Yamaguchi, M. Nakano, R. Takamatsu, H. Tanida, J. Environ. Radioact., 101 (2010) 451.

[157] P. Unak, S. Darcan, F. Yurt, Z. Biber, M. Coker, Biol. Trace Element Res., 71-2 (1999) 463.

[158] S.Z. Yao, P. Chen, W.Z. Wei, Food Chem., 67 (1999) 311.

[159] The World Health Organization. Mental retardation.

http://www.afro.who.int/mentalhealth/related_diseases/mental_retardation.html

[160] van den Hove, M. F.; Beckers, C.; Devlieger, H.; de Zegher, F.; De Nayer, P.

Hormone synthesis and storage in the thyroid of human preterm and term

newborns: effect of thyroxine treatment. *Biochimie* **1999**, *81*, 563–570.

[161] Savin, S.; Cvejic, D.; Nedic, O.; Radosavljevic, R.; Thyroid hormone synthesis and

storage in the thyroid gland of human neonates. *J. Pediatr. Endocrinol. Metab.*

2003, *16*, 521–528.

[162] Dasgupta, P. K. *Environ. Chem.* **2009,** *6*, 7–9.

[163]Renner, R. *Environ. Hlth. Persp.* **2010,** *118*, A438-A442.

[164] Kirk, A. B.; Martinelango, P. K.; Tian, K.; Dutta, A.; Smith, E. E.; Dasgupta, P. K.

Environ. Sci. Technol. **2005,** *39*, 2011-2017.

[165] Kirk, A. B.; Dyke, J. V.; Martin, C. F.; Dasgupta, P. K. *Environ. Hlth. Persp.* **2007,** *115,*

182- 186.

[166] Dasgupta, P. K; Kirk, A. B.: Dyke, J. V.; Ohira, S.-I. *Environ. Sci. Technol.* **2008,** *42,*

8115-8121.

[167] Anderson, S.; Karmisholt, J.; Pedersen, K. M.; Laurberg, P. *Brit. J. Nutr.* **2008,** *99,*

813-8.

[168] Ohira, S-I.; Kirk, A. B.; Dyke, J. V.; Dasgupta, P. K. *Environ. Sci. Technol.* **2008,** *42,*

9419–23.

[169] AllegEAZE. NA44. Iodopropynyl butylcarbamate. What are some products that may

contain iodopropynyl butylcarbamate?

http://www.allergeaze.com/PDFs/NA/NA44.PDF

[170] Dyke, J. V.; Dasgupta, P. K.; Kirk, A. B. *Talanta,* **2009,** *79*, 235-42.

[171] Lanigan, R. S. *Int. J. Toxicol.* **1998**, *17(5),* suppl 1-37.

[172] Shelor, C. P.; Dasgupta, P. K. *Anal. Chim. Acta* **2011,** *702,* 16-36.

[173] Sandell, E. B.; Kolthoff, I. M. *Mikrochim. Acta* **1937,** *1,* 9-25.

[174] May, W.; Wu, D.; Eastman, C.; Bourdoux, P.; Maberly, G. *Clin. Chem.* **1990,** *36,* 865-69.

[175] Barker, S. B.; Humphrey, M. J.; Soley, M. H. *J. Clin. Invest.* **1951,** *30,* 55-62.

[176] Bellanger, J. R.; Tressol, J. C.; Piel, H. P. *Ann. Rech. Vet.* **1979,** *10*, 113-118.

[177] Foss, O. P.; Hankes, L.; Van Slyke, D. D. *Clin Chim Acta,* **1960,** *5,* 301-326.

[178] Moreda-Piñeiro, A.; Bermejo-Barrera, A.; Bermejo-Barrera, P. *Botanica Marina* **2007,** *50,* 65-71.

[179] Fischer, P. W. F.; L'Abbe, M.R.; *J. Assoc. Off. Anal. Chem.* **1981,** *64,* 71-74.

[180] Patzeltova, N. *Chem. Pap.-Chem. Zvesti.* **1993,** *47*, 237-239.

[181] Fischer, P. W. F.; Labbe, M. R.; Giroux, A. *J. Assoc. Off. Anal. Chem.* **1986,** *69,* 687-689.

[182] US Food And Drug Administration. Kansas City Laboratory. Determination of Iodine in Foods. KAN-LAB-MET.95 Ver. 3.2. Updated August 2007.

[183] Zak, B.; Willard, H. H.; Myers, G. B.; Boyle, A. J. *Anal Chem.* **1952,** 24, 1345-1348.

[184] Benotti, J.; Benotti, N.; Pino, S.; Gardyna, H. *Clin. Chem.* **1965,** *11,* 932-936.

[185] Hoch, H.; Lewallen, C. G. *Clin. Chem.* **1969**, *15*, 204-215.

[186] Tiran, B.; Wawschinek, O.; Eber, O.; Beham, A.; Lax, S.; Dermelj, M. *Exp. Clin. Endocrinol.*, **1991,** *98*, 32-36.

[187] Pino, S.; Fang, S. L.; Braverman, L. E. *Exp. Clin. Endocrinol. Diabetes,* **1998,** *106*, S22-S27.

[188]Bier, D.; Rendl, J.; Ziemann, M.; Freystadt, D.: Reiners, C. *Exp. Clin. Endocrinol. Diabetes,* **1998**, *106,* S27-S31.

[189] Gnat, D.; Dunn, A. D.; Chaker, S.; Delange, F.; Vertongen, F.; Dunn, J. T. *Clin. Chem.* **2003,** *49*, 186-188.

[190] Caldwell, K. L.; Maxwell, C. B.; Makhmudov, A.; Pino, S.; Braverman, L. E.; Jones, R. L.; Hollowell, J. G.; *Clin. Chem.* **2003,** *49*, 1019-1021.

[191] Zhang, Y. P.; Yuan, D. X.; Chen, J. X.; Lan, T. S.; Chen, H. Q. *Clin. Chem.* **1996,** *42*, 2021-27.

[192] Rollmann, B.; Regaert, C.; Herveg, J. P. *Arch. Int. Physiol. Bio.* **1985,** *93*, B51-B52.

[193] Zaroda, R. A. *Clin. Chem.* **1969,** *15*, 555-65.

[194] Grossmann, A.; Grossmann, G. F. *Clin. Chem.* **1958,** *4*, 296-99.

[195] Dyke, J. V.; Kirk, A. B.; Martinelango, P. K.; Dasgupta, P. K. *Anal. Chim. Acta*, **2006,** *567,* 73-78.

[196] Passen, S.; von Saelski, R. *Am. J. Clin. Pathol.* **1969,** *51,* 166-176.

[197] Kessler, G.; Pileggi, V. J. *Clin. Chem.* **1970,** *16,* 382-389.

[198] Palumbo, G.; Tecce, M. F.; Ambrosio, G.; *Anal. Biochem.* **1982,** *123*, 183-189.

[199] Pileggi, V. J.; Kessler, G. *Clin. Chem.* **1968,** *14*, 339-347.

[200] Garry, P. J.; Lashley, D. W.; Owen, G. M. *Clin. Chem.* **1973,** *19*, 950-953.

[201] Miles, P. *J. Assoc. Off. Anal. Chem.* **1978,** *61*, 1366-69.

[202] Gushurst, C. A.; Mueller, J. A.; Green, J. A.; Sedor, F. *Pediatrics* **1984,** *73*, 354-57.

[203] Melichercik, J.; Szijarto, L,; Hill, A. R. *J. Dairy Sci.* **2006,** 89, 934-37.

[204] Fenton, H. J. H. *J. Chem. Soc. Trans.* **1894,** *65,* 899-910.

[205] Neyens, E.; Baeyens, J. *J. Hazard Mater.* **2003,** *98,* 33-50.

[206] Uyan, Z. S.; Özek, E.; Bilgen, H.; Cebeci, D.; Akman, I. *Pediatr. Int.* **2005,** *47,* 252-57.

[207] Montgomery, R. R. NIST SRM 1849 Infant/Adult Nutritional Formula. *SRM Spotlight*, Ocober 2009, p1. http://www.nist.gov/srm/upload/October-2009-Spotlight-4-1.pdf

[208] Huang, C. P.; Dong, C.; Tang, Z. *Waste Mgmt.* **1993,** *13,* 361–377.

[209] Winterbourn, C. C. *Toxicol. Lett.* **1995**, *82/83*, 969-74.

[210] Lopez-Cueto, G.; Ostra, M.; Ubide, C.; Zuriarrain, J. *Anal. Chim. Acta* **2004,** *515,* 109-116.

[211] Hayashi, J.; Yamada, M.; Hobo, T. *Anal. Chim. Acta* **1991,** *247,* 27-35.

[212] Kaczmarek, M.; Lis, S.Source: *Anal. Chim. Acta* **2009,** *639,* 96-100.

[213] Kleindienst, T. E.; Shepson, P. B.; Hodges, D. N.; Nero, C. M.; Arnts, R. R.; Dasgupta, P. K. Hwang, H.; Kok, G. L.; Lind, J. A.; Lazrus, A. L.; MacKay, G. I.; Mayne, L. K.; Schiff, H. I. *Environ. Sci. Technol.* **1988,** 22, 53-61.

[214] Olasehinde, E. F.; Makino, S.; Kondo, H.; Takeda, K.; Sakugawa, H. *Anal. Chim. Acta* **2008,** *627,* 270-76.

[215] Sang, Y.; Zhang, L.; Li, Y. F.; Chen, L. Q.; Xu, J. L.; Huang, C. Z. *Anal. Chim. Acta* **2010,** *659,* 224-28.

[216] Altinbas, M. Aydin, A .F.; Sevimli, M. F.; Ozturk, I. J. Environ. Sci. Hlth **2003,** *A38,* 2229–40.

[217] Nieto, L. M.; Hodaifa, G.; Vives, S. R.; Casares, J. A. G.; Driss, S. B.; Grueso, R. *Water Sci. Technol.* **2009,** *59*, 2017-27.

[218] Dewil R.; Appels, L.; Baeyens, J.; Degr`eve, J. *J. Hazard. Mater.* **2007,** *146,* 577–81.

[219] Dębowski, M.; Krzemieniewski, M.; Zieliński. M. *Polish J. Environ. Stud.* **2007,** *16,* 43-50.

[220] Ping, L.; Dasgupta, P. K. *Anal. Chem.* **1989,** *61*, 1230-1235.

[221] Wu, S. G.; Wang, L. *Chin. J. Anal. Chem.* **2005,** *33*, 896-896.

[222] Dong, S.; Dasgupta, P. K. *Talanta* **1991,** *38,* 133-137.

[223] Petrucci, E.; Di Palma, L.; Merli, C. *Ann. Chim (Rome)* **2003,** *93*, 935-45.

[224] Luong, H. V.; Lin, H. K. *Anal. Lett.* **2000,** *33*, 3051-3065.

[225] Pearce, E. N.; Leung, A. M.; Blount, B. C.; Bazrafshan, H. R.; He, X.; Pino, S.;
Valentin-Blasini L.; Braverman, L. E. *J Clin Endocrinol Metab.* **2007,** *92*, 1673-77.

[226] Blount, B. C.; Valentin-Blasini, L.; Osterloh, J. D.; Mauldin, J. P.; Pirkle, J. L. *J. Expo.
Sci. Environ. Epidemiol.* **2007,** *17,* 400–407.

[227] Bitman, J.; Tao, H.; Akers, R. M. *J. Dairy Sci.* **1984,** *67,* 2614-19.

[228] Brüchert, W.; Helfrich, A.; Zinn, N.; Klimach, T.; Breckheimer, M.; Chen, H.; Lai, S.;
Hoffmann, T.; Bettmer, J. *Anal. Chem.*, **2007**, *79*, 1714-19.

[229] Bray, W. C.; Liebhafsky, H. A.; J. Am. Chem. Soc. 1931, 53, 38-44

[230] Hansen, J. C. *J. Chem. Ed.* **1996,** *73,* 728-732.

[231] Kazantseva, N. N.; Ernepesova, A.; Khodjamamedov, A.; Gledyev, O.A.; Krumgalz,
B.S. *Anal. Chim. Acta,* **2002**, *465,* 105-119.

[232] Murray, C.W.; Egan, S. K.; Kim, H.; Beru, N.; Bolger, P. M. US Food and Drug
Administration's Total Diet Study: Dietary intake of perchlorate and iodine. *J.
Expo. Sci. Env. Epid.* **2008,** *18,* 571-580.

[233] Ginsberg, G.; Rice, D. The NAS perchlorate review: questions remain about the
perchlorate RfD. *Environ. Health Persp.* **2005,** *1131,* 1117-1120.

[234] Zoeller R.T.; Rice, D. C. Critical effect of perchlorate on neonates is iodide uptake
inhibition. *Regul. Toxicol. Pharmacol.* **2004,** *40,* 376-377.

[235] Strawson, J.; Zho, Q.; Dourson, M. Reference dose for perchlorate based on thyroid
hormone change in pregnant women as the critical effect. *Regul. Toxicol.
Pharmacol*. **2004,** *39,* 44-65.

[236] Ting, D.; Howd, R. A.; Fan, A. M.; Alexeeff, G. V. Development of a health-protective drinking water level for perchlorate. *Environ. Health Persp.* **2008,** *114*, 881-886.

[237] Kirk, A. B. Perchlorate: why it matters. *Anal Chim Acta*. **2006,** *567,* 4-12.

[238] Dohán, O.; Portulano, C.; Basquin, C.; Reyna-Neyra, A.; Amzel, L. M.; Carrasco, N. The Na+/I− symporter (NIS) mediates electroneutral active transport of the environmental pollutant perchlorate. *Proc. Nat. Acad. Sci.***2007,** *104,* 20,250-20,255.

[239] Kirk, A. B.; Smith, E. E.; Tian, K.; Anderson, T. A.; Dasgupta, P. K. Perchlorate in milk. *Environ. Sci. Technol.* **2003**, *37,* 4979-81.

[240] Kirk, A. B.; Martinelango, P. K.; Tian, K.; Dutta, A.; Smith, E. E.; Dasgupta, P. K. Perchlorate and iodide in dairy and breast milk. *Environ. Sci. Technol.* **2005,** *39*, 2011-2017.

[241] Tian, K.; Dasgupta, P. K.; Anderson, T. A. Determination of trace perchlorate in high salinity water samples by ion chromatography with online preconcentration and pre-elution. *Anal. Chem.* **2003,** *75*, 701-706.

[242] Tian, K.; Cañas, J. E.; Dasgupta, P. K.; Anderson, T. A. Preconcentration/pre-elution ion chromatography for the determination of perchlorate in complex samples. *Talanta* **2005,** *65,* 750-755.

[243] Martinelango, P. K.; Anderson, J. L.; Dasgupta, P. K.; Armstrong, D. W.; Al-Horr, R. S.; Slingsby, R. W. Gas phase ion association provides increased selectivity and sensitivity for measuring perchlorate by mass spectrometry. *Anal. Chem.* **2005,** 77, 4829 - 4835.

[244] Dyke, J. V.; Kirk, A. B.; Martinelango, P. K.; Dasgupta, P. K. Sample processing method for the determination of perchlorate in milk. *Anal. Chim. Acta*, **2006,** *567,* 73-78.

[245] Martinelango, P. K.; Gümüs, G.; Dasgupta, P. K. Matrix interference free determination of perchlorate in urine by ion association–ion chromatography–mass spectrometry. *Anal. Chim. Acta,* **2006,** *567,* 79-86.

[246] Martinelango, P. K.; Dasgupta, P. K. Dicationic ion-pairing agents for mass spectrometric determination of perchlorate. *Anal. Chem.* **2007***, 79,* 7198-7201.

[247] Dasgupta, P. K.; Martinelango , K.; Jackson, W. A.; Anderson, T. A.; Tian K.; Tock, R. W.; Rajagopalan, S. The Origin of Naturally Occurring Perchlorate: The role of atmospheric processes. *Environ. Sci. Technol.* **2005***, 39,* 1569-1575.

[248] Kang, N.; Jackson, W. A.; Dasgupta, P. K.; Anderson, T. A. Perchlorate production by ozone oxidation of chloride in aqueous and dry systems. *Sci. Tot. Environ.* **2008,** 405, 301-309.

[249] Kirk, A. B.; Dyke, J. V.; Martin, C. F.; Dasgupta, P. K. Temporal patterns in perchlorate, thiocyanate and iodide excretion in human milk. *Environ. Hlth. Persp.* **2007,** *115,* 182- 186.

[250] Dasgupta, P. K; Kirk, A. B.: Dyke, J. V.; Ohira, S.-I. Intake of iodine and perchlorate and excretion in human milk. *Environ. Sci. Technol.* **2008,** *42,* 8115-8121.

[251] Renner, R. More iodine or less perchlorate? *Environ. Hlth. Persp.* **2010,** *118,* A289.

[252] Dasgupta, P.K. Perchlorate: a cause for iodine deficiency? *Environ Chem*. **2009,** *6,* 7-9.

[253] Wilson, M. Science Review. Office of Inspector General Scientific Analysis of Perchlorate. Report No. 10-P-0101. Washington, DC: U.S. Environmental Protection Agency/Office of Inspector General, 2010.

[254] Clewell, R. A.; Merrill, E. A.; Robinson, P. J. The use of physiologically based models to integrate diverse datasets and reduce uncertainty in the prediction of perchlorate and iodide kinetics across life stages and species. *Toxicol. Ind. Hlth*. **2001,** *17,* 210-222.

[255] Walser, M.; Rahill, W. J. Nitrate, thiocyanate, and perchlorate clearance in relation to chloride clearance. *Am. J. Physiol.* **1965,** *208,* 1158-1164.

[256] Merrill, E. A.; Clewell, R. A.; Gearhart, J. M.; Robinson, P. J.; Sterner, T. R.; Yu, K. O.; Fisher, J. W. PBPK predictions of perchlorate distribution and its effect on thyroid uptake of radioiodide in the male rat. *Toxicol. Sci.* **2003,** *73*, 256–269.

[257] Merrill, E. A.; Clewell, R. A.; Robinson, P. J.; Jarabek, A. M.; Gearhart, J. M.; Sterner, T. R.; Fisher, J. W. PBPK model for radioactive iodide and perchlorate kinetics and perchlorate-induced inhibition of iodide uptake in humans. *Toxicol. Sci.* **2005,** *83*, 25-43.

[258] Capuco, A. V.; Rice, C. P.; Baldwin VI, R. L.; Bannerman, D. D.; Paape, M. J.; Hare, W. R.; Kauf, A. C. W.; McCarty, G. W.; Hapeman, C. J.; Sadeghi, A. M.; Starr, J. L.; McConnell, L. L.; Van Tassell, C. P. Fate of dietary perchlorate in lactating dairy cows: Relevance to animal health and levels in the milk supply. *Proc. Nat. Acad. Sci.* **2005,** *102,* 16152-16157.

[259] Seyfferth, A. L.; Struchio, N. C. Parker, D. R. Is perchlorate metabolized or re-translocated within lettuce leaves? A stable-isotope approach. *Environ. Sci. Technol.* **2008,** *42,* 9437-9442.

[260] Van Aken, B.; Schnoor, J. L. Evidence of perchlorate (ClO_4^-) reduction in plant tissues (poplar tree) using radio-labeled (ClO_4^-)-C-36. *Environ. Sci. Technol.* **2002,** *36,* 2783-2788.

[261] Yifru, D. D.; Nzengung, V. A. Organic carbon biostimulates rapid rhizodegradation of perchlorate. *Environ. Toxicol. Chem.* **2008,** *27,* 2419-2426.

[262] Nzengung, V. A.; Penning, H.; O'Niell, W. Mechanistic changes during phytoremediation of perchlorate under different root-zone conditions. *Int. J. Phytoremed*. **2004,** *6,* 63-83.

[263] Nzengung, V. A.; Wang, C. H.; Harvey, G. Plant-mediated transformation of perchlorate into chloride. *Environ. Sci. Technol.* **1999,** *33,* 1470-1478.

[264] Nzengung, V.A.; Yifru, D. D. Biostimulation and enhancement of rhizodegradation of perchlorate during phytoremediation. http://info.ngwa.org/gwol/pdf/062381339.pdf National Ground Water Association, 2007. Accessed November 10, 2011.

[265] Coates, J. D.; Michaelidou, U.; Bruce, R. A.; O'Connor, S. M.; Crespi, J. N.; Achenbach, L. A. Ubiquity and diversity of dissimilatory (per)chlorate-reducing bacteria. *Appl. Environ. Microbiol.* **1999,** *66,* 5234-5241.

[266] Wolin, M. J. Fermentation in the Rumen and Human Large Intestine. *Science*, **1981,** *213*, 1463-1468.

[267] Plummer, L. N.; Böhlke, J. K.; Doughten,M. W. Perchlorate in Pleistocene and Holocene Groundwater in North-Central New Mexico. *Environ. Sci. Technol.* **2006,** *40,* 1757-1763.

[268] Tellez, R. T.; Chacon, P. M.; Abarca, C. R.; Blount, B. C.; Van Landingham, C. B.; Crump, K. S.; Gibbs, J. P. Long-term environmental exposure to perchlorate through drinking water and thyroid function during pregnancy and the neonatal period. *Thyroid*, **2005,** *15,* 963-975.

[269] Crump, C.; Michaud, P.; Tellez, R.; Reyes, C.; Gonzalez, G.; Montgomery, E. L.; Crump, K. S.; Lobo, G.; Becerra, C.; Gibbs, J. P. Does perchlorate in drinking water affect thyroid function in newborns or school-age children? *J. Occup. Environ. Med.* **2000,** *42,* 603-612.

[270] Procter and Gamble. Align Probiotic Supplement. http://www.aligngi.com/information-on-Align-probiotic-supplement

[271] Yoshioka, H.; Iseki, K.; Fujita, K. Development and differences in intestinal flora in the neonatal period in breast-fed and bottlefed infants. *Pediatr.* **1983,** *72,* 317-321.

[272] Shelor, C. P.; Campbell, C. A.; Kroll, M.; Dasgupta, P. K.; Smith, T. L.; Abdalla, A.; Hamilton, M.; Muhammad, T. W. Fenton Digestion of Milk for Iodinalysis. *Anal. Chem.* **2011,** *83,* 8300-8307.

[273] Luong, H. V.; Lin, H. K. Controlling Fenton Reaction for Soil Remediation. *Anal. Lett.* **2000,** *33,* 3051–3065

[274] Coates, J. D.; Achenbach, L. A. Microbial perchlorate reduction: rocket-fuelled metabolism. *Nat. Rev Microbiol* **2004**, *2,* 569-580.

[275] Tan, K.; Anderson, T. A.; Jackson, W. A. Degradation kinetics of perchlorate in sediments and soils. *Wat. Air Soil Pollut.* **2004,** *151*, 245–259.

[276] Farhan, Y. H.; Hatzinger, P. B. Modeling the biodegradation kinetics of perchlorate in the presence of oxygen and nitrate as competing electron acceptors. *Bioremed. J.* **2009,** *13*, 65–78.

[277] Kengen, S. W. M.; Rikken, G. B., Hagen, W. R.; van Ginkel, C. G.; Stams, A. J. Purification and characterization of (per)chlorate reductase from the chlorate-respiring strain GR-1. *J. Bacteriol.* **1999,** *181,* 6706-6711.

[278] Moura, J. J.; Brondino, C. D.; Trincap, O. J.; Romao, M. J. Mo and W bis-MGD enzymes: nitrate reductases and formate dehydrogenases. *J. Biol. Inorg. Chem.* **2004,** *9,* 791-799.

[279] Eckburg, P. B.; Bik, E. M.; Bernstein, C. N.; Purdom, E.; Dethlefsen, L.; Sargent, M.; Gill, S. R.; Nelson, K. E.; Relman, D. A. Diversity of the human intestinal microbial flora. *Science* **2005,** *308,* 1635-1638.

[280] Iseki, K. Development of intestinal flora in neonates. *Hokkaido Igaku Zasshi* **1987**, *62,* 895-906.

[281] Kleesen, B.; Bunke, H.; Tovar, K.; Noack, J.; Sawatzki, J. Influence of two infant formulas and human milk on the development of faecal flora in newborn infants. *Acta Paediatr.* **1995,** *84*, 1347-1356.

[282] Harmsen, H.J.M.; Wildeboer-Veloo, A. C. M; Raangs, G. C.; Wagendorp, A. A.; Klijn, N.; Bindels, J. G.; Welling, G. W. Analysis of intestinal flora development in breast-fed and formula-fed infants by using molecular identification and detection methods. *J. Pediatr. Gastroenterol. Nutr.* **2000,** *30,* 61–67.

[283] Morelli, L. Postnatal development of intestinal microflora as influenced by infant nutrition. *J. Nutr.* **2008,** *138,* 1791S–1795S.

[284] Favier, C. F.; Vaughan, E. E.; De Vos, W. M.; Akkermans, A. D. L. Molecular monitoring of succession of bacterial communities in human neonates. *Appl Environ Microbiol.* **2002,** *68,* 219-226.

[285] Mullie,C., Romond, M. B.; Izard, D. Establishment and follow-up of bifidobacterial species in the gut of healthy bottle-fed infants of 1-4 months age. *Folia Microbiol*. **2006,** *51,* 473-477.

[286] Grönlund, M. M.; Gueimonde, M.; Laitinen, K.; Kociubinski, G.; Grönroos, T.; Salminen, S.; Isolauri, E. Maternal breast-milk and intestinal bifidobacteria guide the compositional development of the Bifidobacterium microbiota in infants at risk of allergic disease. *Clin Exp Allergy* **2007,** *37,* 1764-1772.

[287] Sjogren, Y. M.; Tomicic, S.; Lundberg, A.; Böttcher, M. F.; Björkstén, B.; Sverremark-Ekström, E.; Jenmalm, M. C. Influence of early gut microbiota on the maturation of childhood mucosal and systemic immune responses. *Clin Exp Allergy.* **2009,** *39,* 1842-1851.

[288] National Library of Medicine. Bifidobacteria. http://www.nlm.nih.gov/medlineplus/druginfo/natural/891.html Accessed November 25, 2011.

[289] Moro, G. E.; Arslanoglu, S. Reproducing the bifidogenic effect of human milk in formula-fed infants: why and how? *Acta Pædiatr.* **2005,** 94(Suppl 449), 14–17.

[290] Bomar, M. T. Bacteria and dietary fiber. *Z. Ernahrungswiss.* **1984,** *23,* 66-75.

[291] Sobko, T.; Reinders, C. I.; Jansson, E.; Norin, E.; Midtvedt, T.; Lundberg, J. O. Gastrointestinal bacteria generate nitric oxide from nitrate and nitrite. *Nitric Oxide* **2005**, *13*, 272-278.

[292] Caspi, R.; Altman, T.; Dreher, K.; Fulcher, C. A.; Subhraveti, P.; Keseler, I. M.; Kothari, A.; Krummenacker, M.; Latendresse, M.; Mueller, L. A. The MetaCyc database of metabolic pathways and enzymes and the BioCyc collection of

pathway/genome databases. *Nucleic Acid Res.* **2012,** *40,* D742-D753*.*

http://www.biocyc.org/META/NEW-IMAGE?type=ORGANISM&object=TAX-1681

[293] Nozawa-Inoue, M.; Scow, K. M.; Rolston, D. E., Reduction of perchlorate and nitrate by microbial communities in vadose soil. *Applied and Environmental Microbiology* **2005,** *71*, (7), 3928-3934.

[294] Goellner, M. H.; Ziegler, E. F.; Formon, S. J. Urination during the first three years of life. *Nephron*. **1981,** *28,* 174-178.

[295] US Environmental Protection Agency. Child-Specific Exposure Factors Handbook. 2008. Chapter 15. Human Milk Intake. http://cfpub.epa.gov/ncea/cfm/recordisplay.cfm?deid=199243 Accessed December 1, 2011.

[296] Delange, F.; Bourdoux, P.; Laurence, M.; Peneva, L.; Walfish, P.; Willgerodt, H. Neonatal thyroid function in iodine deficiency. In: Delange F, Dunn JT, Glinoer D, eds. Iodine Deficiency in Europe. A Continuing Concern. New York: Plenum Press, 1993. p199-210.

[297] Savin, S.; Cvejic, D.; Nedic, O.; Radosavljevic, R. Thyroid hormone synthesis and storage in the thyroid gland of human neonates. *J. Pediatr. Endocr. Met*. **2003,** *16,* 521-528.

[298] Zaichick, V.; Zaichick, S. Normal human intrathyroidal iodine. *Sci. Tot. Environ.* **1997,** *206,* 39-56.

[299] Zabala, J.; Carrión, N.; Murillo, M.; Quintana, M.; Chirinos, J.; Seijas, N.; Duarte, L.; Brätter, P. Determination of normal human intrathyroidal iodine in Caracas population. *J. Trace Elem. Med. Biol.* **2009,** *23,* 9-14.

[300] Milakovic, M.; Berg, G.; Eggertsen, R.; Nystrom, E.; Olsson, A.; Larsson, A.; Hansson, M. Determination of intrathyroidal iodine by X-ray fluorescence analysis in 60- to 65-year olds living in an iodine-sufficient area. *J. Intern. Med.* **2006,** *60,* 69-75.

[301] Food and Nutrition Board, Institute of Medicine. *Dietary reference intakes*; National Academy Press: Washington DC, 2001; p 258.

[302] Kratzsch, J.; Schubert, G.; Pulzer, F.; Pfaeffle, R.; Koerner, A.; Dietz, A.; Rauh, M.; Kiess, W. Thiery, J. Reference intervals for TSH and thyroid hormones are mainly affected by age, body mass index and number of blood leucocytes, but hardly by gender and thyroid autoantibodies during the first decades of life. *Clin. Biochem*. **2008,** *41*, 1091–1098.

[303] Sharma, A.; Ford, S. Calvert, J. Adaptation for life: a review of neonatal physiology. *Anaesthesia Intensive Care Med.* **2010,** *12(3),* 85-90.

[304] Laurberg, P.; Andersen, S.; Bjarnadóttir, R. I.; Carle´, T. A.; Hreidarsson, A. B.; Knudsen, N.; Ovesen, L.; Pedersen, I. B.; Rasmussen, L. B. Evaluating iodine deficiency in pregnant women and young infants – complex physiology with a risk of misinterpretation. *Public Hlth. Nutr.* **2008,** *10,* 1547-1552.

[305] Smyth, P. P.; Duntas, L. H. Iodine uptake and loss - can frequent strenuous exercise induce iodine deficiency? *Horm. Metabol. Res.* **2005**, *37*, 555-558.

[306] Vought, R.L., Londom, W.T., Lutwak, L., & Dublin, T.D. Reliability of estimates of serum inorganic iodine and daily faecal and urinary iodine excretion from single causal specimens. *J. Clin. Endocr. Metabol.* **1963,** *23,* 1218-1228.

[307] Wang, Y.; Ou, Y.-L.; Liu, Y.-Q. Xie, Q.; Liu, Q.-F.; Wu, Q.; Fan, T.-Q.; Yan, L.-L.; Wang, J.-Y. Correlations of Trace element levels in the diet, blood, urine, and

feces in the Chinese male. *Biol. Trace Elem. Res.* In press. doi: 10.1007/s12011-011-9177-8.

[308] Mao, I.-F.; Chen, M.-L., Ko, Y-C. Electrolyte loss in sweat and iodine deficiency in a hot environment. *Arch. Environ. Hlth.* **2001,** *56,* 271-277.

[309] Suzuki, M.; Tamura, T. Iodine intake of Japanese male university students: urinary iodine excretion of sedentary and physically active students and sweat iodine excretion during exercise. *J. Nutr. Sci. Vitaminol. (Tokyo)* **1985**, *31,* 409-415.

[310] Ariagno, R. L.; Glotzbach, S. F.; Baldwin, R. B.; Rector, D. M.; Bowley, S. M. Moffat, R. J. Dew-point hygrometry system for measurement of evaporative water loss in infants. *J. Appl. Physiol.* **1997,** *82,* 1008–1017.

[311] Clewell, R. A.; Merrill, E. A.; Gearhart, J. M.; Robinson, P.J.; Sterner, T. R.; Mattie, D. R.; Clewell, H. J. III. Perchlorate and Radioiodide Kinetics Across Life Stages in the Human: Using PBPK Models to Predict Dosimetry and Thyroid Inhibition and Sensitive Subpopulations Based on Developmental Stage. *Journal of Toxicology and Environmental Health,* Part A, **2007,** *70*, 408–428.

[312] R Development Core Team. R: A language and environment for statistical computing. **2011.** R Foundation for Statistical Computing, Vienna, Austria. http://www.R-project.org/ Accessed November 25, 2011.

[313] Valentin-Blasini, L.; Blount, B. C.; Otero-Santos, S.; Cao, Y.; Bernbaum, J. C.; Rogan, W. J., Perchlorate Exposure and Dose Estimates in Infants. *Environmental Science & Technology* **2011,** *45*, (9), 4127-4132.

[314] Ericksen, G. E. The Chilean nitrate deposits. *Am. Sci.* **1983,** *71,* 366-374.

[315] Beckurts, H. Uber den gehalt des salpeters an chlorsaurem salz. *Arch. Pharm.*
(Weinheim, Ger.) **1886**, *224*, 333-337.

[316] Bohlke, J. K.; Ericksen, G. E.; Revesz, K. Stable isotope evidence for an atmospheric
origin of desert nitrate deposits in northern Chile and southern California, USA.
Chem. Geol. **1997,** *136***,** 135-152.

[317] Rajagopalan, S.; Anderson, T. A.; Cox, S.; Harvey, G.; Cheng, Q. Q.; Jackson, W. A.
Perchlorate in wet deposition across North America. *Environ. Sci. Technol.* **2009,**
43, 616-622.

[318] Walser, M.; Rahill, J. W. Renal tubular reabsorption of iodide as compared with
chloride. *J. Clin. Invest.* **1965,** *44,* 1371-1381.

[319] Azroyan, A.; Morla, L.; Crambert, G.; Laghmani, K.; Ramakrishnan, S.; Edwards, A.;
Doucet, A. Regulation of pendrin by cAMP: possible involvement in β adrenergic-
dependent NaCl retention. *Am J Physiol Renal Physiol.* **2012**, Epub ahead of
print, PMID 22262479

[320] Alesutan, I.; Daryadel, A.; Mohebbi, N.; Pelzl, L.; Leibrock, C.; Voelkl, J.; Bourgeois,
S.; Dossena, S.; Nofziger, C.; Paulmichl. M.; Wagner, C. A.; Lang, F. Impact of
bicarbonate, ammonium chloride, and acetazolamide on hepatic and renal
SLC26A4 expression. *Cell Physiol Biochem.* **2011**, *28,* 553-558.

[321] Rozenfeld, J.; Tal, O.; Kladnitsky, O.; Adler, L.; Efrati, E.; Carrithers, S. L.; Alper, S. L.;
Zelikovic, I. The pendrin anion exchanger gene is transcriptionally regulated by
uroguanylin: a novel enterorenal link. *Am J Physiol Renal Physiol.* **2012**,
302,F614-624.

[322] The World Health Organiziation. I CD-10 Guide for Mental Retardation.
http://www.who.int/mental_health/media/en/69.pdf Accessed March 27, 2014

[323] M.B. Zimmerman, Endocr. Rev., 30(2009)376.

[324] F. Vermiglio, V.P. Lo Presti, M. Moleti, M. Sidoti, G. Tortorella, G. Scaffidi, M.G. Castagna, F. Mattina, M.A. Violi, A. Crisa, A. Artemisia, F. Trimarchi, J. Clin. Endocrinol. Meta., 89 (2004) 6054

[325] F. Delange, Postgraduate Medical Journal, 77 (2001)217

[326] P. Santiago-Fernande, R. Torres-Barahona, J.A. Muela-Martinez, G. Rojo-Martinez, E. Garcia-Fuentes, M.J. Garriga, A.G. Leon, F. Soriguer, J. Clin. Endocrinol. Metab. 89 (2004) 3851

[327] World Health Organization. Assessment of iodine deficiency disorders and monitoring their elimination. A guide for programme managers, 3rd ed. 2008.

[328] H. Backer, J. Hollowell, Environ. Health Perspect., 108 (2000) 679

[329] Food and Nutrition Board, Institue of Medicine. Dietary reference intakes; National Academy Press: Washington DC< 2001; p258

[330] J.G. Hollowell, N.W. Staehling, W.H. Hannon, D.W. Flanders, E.W. Gunter, G.F. Maberly, L.E. Braverman, S. Pino, D.T. Miller, P.L. Garbe, D.M. DeLozier, R.J. Jackson, J. Clin. Endocrinol. Metab., 83 (1998) 3401.

[331] Centers for Disease Control and Prevention (CDC). National Center for Health Statistics (NCHS). National Health and Nutrition Examination Survey Data

[332] K.B. Harris, K.A. Pass, Mol. Genet. Metab., 91 (2007) 268.

[333] E.B. Sandell, I.M. Kolthoff. Mikrochim. Acta 1937, 1, 9-25

[334] J.V. Dyke, P.K. Dasgupta. Anal. Chim. Acta. 2011, 702 16-36

[335] M. Haldimann, B. Zimmerli, C. Als, H. Gerber, Clin. Chem., 44 (1998) 817

[336] W. May, D. Wu, C. Eastman, P. Bourdoux, G. Maberly. Clin. Chem. 1990, 36, 865-869

[337] C.P. Shelor, P.K. Dasgupta. Anal. Chim. Acta. 1 (2011) 16-36

[338] K. A. Anderson and P. Markowski, *Journal of Aoac International*, 2000, 83, 225-230.

[339] S. P. Dolan, S. A. Sinex, S. G. Capar, A. Montaser and R. H. Clifford, *Analytical Chemistry*, 1991, 63, 2539-2542.

[340] Y.-q. Fei, G.-m. Luo, G.-d. Feng, H.-w. Chen, Q. Fei, Y.-f. Huan and Q.-h. Jin, *Chemical Research in Chinese Universities*, 2008, 24, 546-549.

[341] H. Matusiewicz and M. Slachcinski, *Analytical Methods*, 2010, 2, 1592-1598.

[342] E. A. Vtorushina, A. I. Saprykin and G. Knapp, *Journal of Analytical Chemistry*, 2008, 63, 643-648.

[343] E. A. Vtorushina, A. I. Saprykin and G. Knapp, *Journal of Analytical Chemistry*, 2009, 64, 129-135.

[344] M. C. Q. Ortega, J. C. Bautista, M. Saez, A. M. Garcia, J. E. S. Uria and A. S. Medel, *Spectrochimica Acta Part B-Atomic Spectroscopy*, 1992, 47, 79-87

[345] E. Niedobova, J. Machat, V. Otruba and V. Kanicky, *Journal of Analytical Atomic Spectrometry*, 2005, 20, 945-949.

[346] T. Nakahara and T. Mori, *Journal of Analytical Atomic Spectrometry*, 1994, 9, 159-165.

[347] F. Camuna, J. E. S. Uria and A. S. Medel, *Spectrochimica Acta Part B-Atomic Spectroscopy*, 1993, 48, 1115-1125.

[348] M. D. Calzada, M. C. Quintero, A. Gamero and M. Gallego, *Analytical Chemistry*, 1992, 64, 1374-1378.

[349] M. R. Cave and K. A. Green, *Journal of Analytical Atomic Spectrometry*, 1989, 4, 223-225.

[350] V. Karanassios. Spectrochimica Acta Part B-Atomic Spectroscopy 2004, 59 (7), 909-928

[351] M. Miclea, K. Kunze, J. Franzke, K. Niemax. Spectrochimica Acta Part B 57 (2002) 1585-1592

[352] U. Kogelschatz. Plasma Chemistry and Plasma Processing, 2003, 23 (1). 1-46

[353] Tendero, C.; Tixier, C.; Tristant, P.; Desmaison, J.; Leprince, P. *Spectrochimica Acta Part B-Atomic Spectroscopy* 2006, *61* (1), 2-30.

[354] Y.L. Yu, Z. Du, M.L. Chen, J.H. Wang, Angew. Chem. Int. Ed. 47 (2008) 7909

[355] Z.L. Zhu, G.C.Y. Chan, S.J. Ray, X.R. Zhang, G.M. Hieftje, Anal. Chem. 80 (2008) 8622–8627

[356] M. Puanngam, S-I Ohira, F. Unob, J-H Wang, P.K. Dasgupta. *Talanta*. 81 (2010) 110-9-1115

[357] Q. He, Z. Zhu, S. Hu, H. Zheng, L. Jin. *Analytical Chemistry*, 84 (2012) 4179-4184

[358] Y-L Yu, M-L Chen, J-H Wang, *Analytical Chimica Acta*. 809 (2014) 30-36

[359] Z. Zhu, H. He, D. He, H. Zheng, C. Zhang, S. Hu. *Talanta* 122 (2014) 234-239

[360] Z. Xing, B. Kuermati, J. Wang, G. Han, S. Zhang, X. Zhang, *Spectrochimica Acta Part B: Atomic Spectroscopy*, 65 (2010) 1056-1060

[361] H. Bingjun, X. Jian, X. Hou, C. Zheng. *Analytical Chemistry*, 86 (2014) 936-942

[362] W. Li, C. Zheng, G. Fan, L. Tang, K. Xu, Y. Lv, X. Hou. *Analytical Chemistry,* 83 (2011) 5050-5055

[363] Y-L Yu, S. Dou, M-L Chen, J-H Wang, *Analyst*, 138 (2013) 1719-1725

[364] Y-Q Fei, G-M Luo, G-D Feng, H-W Chen, Q. fei, Y-F Huan, Q-H Jin, Chemical Research in Chinese Universities, 24 (2008) 546-549

[365] S. P. Dolan, S. A. Sinex, S. G. Capar, A. Montaser and R. H. Clifford, Analytical Chemistry 63 (1991) 2539-254

[366] J-Y. Zhang, I.W. Boyd, Applied Physics B. 71 (2000) 177-179

[367] F.P. Scaringelli, A.E. O'Keeffe, E. Rosdenber, J.P. Bell. *Analytical Chemistry*, 8 (1970) 871-876

[368] C. Mathew, M.A. Majali, S.A. Balakrishnan. *Applied Radiation and Isotopes* 57 (2002), 359-367

[369] J. D. Way, P. Thoen, S. K. Gade. United States Patent US2009/0176012 A1, 2009

[370] T.T. Nham. Analysis of Urine and Seawater Samples by Ultrasonic Nebulization with a High Resolution ICP Spectrometer. Application Note, Agilent Technologies, ICPES-9

[371] L-F. Olsson, *Inorganic Chemistry* 24 (1985) 1398-1405

[372] D. L. Cason, H.M. Neumann, *Journal of the American Chemical Society* 83, 1822-1828

[373] P. Vanýsek, Electrochemical series, Handbook of Chemistry and Physics Online, http://www.hbcpnetbase.com/

[374] A. V. Hershey, W. C. Bray. *Journal of the American Chemical Society* 58 (1936) 1760-1772

[375] A. J. Fudge, K. W. Sykes. *Journal of the Chemical Society* (1952) 119-124

[376] J-L. Burgot. Ionic Equilibria in Analytical Chemistry. Springer, New York. 2012. Chapter 20.2 pg 391

[377] R. F. Beard, N. W. Taylor. *Journal of the American Chemical Society* 57 (1929) 1973-1985

[378] A.I Vogel. A tText-Book of Quantitative Inorganic Analysis, 3rd edition. Longmans, Green and Co LTD, London 1964

[379] M. Kimura, R. Ikawa, Y. Shiota, K. Tsukahara. *Bull. Chem. Soc. Jpn.* 71 (1998) 893-897

[380] L. M. Bharadwaj, D. N. Sharma, Y. K. Gupta. *Inorganic Chemistry* 17 (1978) 2469-2472

[381] M. Kimura, Y. Shiga, K. Tsukahara. *Bull. Chem. Soc. Jpn.* 71 (1998) 2345-2350

[382] M. Kimura, M. Takuda, K. Tsukahara. *Bull. Chem. Soc. Jpn.* 67 (1994) 2731-2735

[383] R. Sander . Compilation of Henry's Law Constants for Inorganic and Organic Species of Potential Importance in Envrionmental Chemistry. http://www.henrys-law.org/

[384] J. W. Dorman, S. M. Steinberg, *Environ. Monit. Assess* 161 (2010) 229-236

[385] P. Grinberg, Z. Mester, A. D'Ulivo, R. E. Sturgeon. *Spectrochimica Acta Part B* 64 (2009) 714-716

[386] M. B. Zimmermann, *Endocrine Reviews*, 2009, **30**, 376-408.

[387] F. Delange, *Postgraduate Medical Journal*, 2001, **77**, 217-220.

[388] P. Santiago-Fernandez, R. Torres-Barahona, J. A. Muela-Martinez, G. Rojo-Martinez, E. Garcia-Fuentes, M. J. Garriga, A. G. Leon and F. Soriguer, *Journal of Clinical Endocrinology & Metabolism*, 2004, **89**, 3851-3857.

[389] J. A. M. Martinez, A. G. Leon, R. T. Barahona, P. S. Fernandez and F. S. Escofet, *Psicothema*, 2008, **20**, 279-284.

[390] F. Vermiglio, V. P. Lo Presti, M. Moleti, M. Sidoti, G. Tortorella, G. Scaffidi, M. G. Castagna, F. Mattina, M. A. Violi, A. Crisa, A. Artemisia and F. Trimarchi, *Journal of Clinical Endocrinology & Metabolism*, 2004, **89**, 6054-6060.

[391] R. T. Zoeller and J. Rovet, *Journal of Neuroendocrinology*, 2004, **16**, 809-818.

[392] World Heath Organization, Assessment of Iodine Deficiency Disorders and Monitoring Their Elimination. A Guide for Programme Managers, 3rd ed., 2008. http://www.who.int/nutrition/publications/micronutrients/iodine_deficiency/9789241595827/en/ (accessed February 26, 2014)

[393] E. B. Sandell, I. M. Kolthoff, *Microchimica Acta*, 1937, **1**, 9-25

[394] M. Haldimann, B. Zimmerli, C. Als and H. Gerber, *Clinical Chemistry*, 1998, **44**, 817-824

[395] J. V. Dyke, P. K. Dasgupta and A. B. Kirk, *Talanta*, 2009, **79**, 235-242.

[396] W. May, D. Wu, C. Eastman, P. Bourdoux and G. Maberly, *Clinical Chemistry*, 1990, **36**, 865-869.

[397] C. P. Shelor and P. K. Dasgupta, *Analytica Chimica Acta*, 2011, **702**, 16-36.

[398] S. Grys, *Journal of Chromatography*, 1974, **100**, 43-48.

[399] M. Hu, H. Chen, Y. Jiang and H. Zhu, *Chemical Papers*, 2013, **67**, 1255-1261.

[400] T. Mitsuhashi and Y. Kaneda, *Journal of the Association of Official Analytical Chemists*, 1990, **73**, 790-791.

[401] H. S. Shin, Y. S. OhShin, J. H. Kim and J. K. Ryu, *Journal of Chromatography A*, 1996, **732**, 327-333.

[402] K. Reddy-Noone, A. Jain and K. K. Verma, *Journal of Chromatography A*, 2007, **1148**, 145-151.

[403] J. W. Dorman and S. M. Steinberg, *Environmental Monitoring and Assessment*, 2010, **161**, 229-236.

[404] P. Grinberg and R. E. Sturgeon, *Spectrochimica Acta Part B-Atomic Spectroscopy*, 2009, **64**, 235-241.

[405] P. Grinberg, Z. Mester, A. D'Ulivo and R. E. Sturgeon, *Spectrochimica Acta Part B-Atomic Spectroscopy*, 2009, **64**, 714-716.

[406] K. A. Anderson and P. Markowski, *Journal of Aoac International*, 2000, **83**, 225-230.

[407] S. P. Dolan, S. A. Sinex, S. G. Capar, A. Montaser and R. H. Clifford, *Analytical Chemistry*, 1991, **63**, 2539-2542.

[408] Y.-q. Fei, G.-m. Luo, G.-d. Feng, H.-w. Chen, Q. Fei, Y.-f. Huan and Q.-h. Jin, *Chemical Research in Chinese Universities*, 2008, **24**, 546-549.

[409] H. Matusiewicz and M. Slachcinski, *Analytical Methods*, 2010, **2**, 1592-1598.

[410] E. A. Vtorushina, A. I. Saprykin and G. Knapp, *Journal of Analytical Chemistry*, 2008, **63**, 643-648.

[411] E. A. Vtorushina, A. I. Saprykin and G. Knapp, *Journal of Analytical Chemistry*, 2009, **64**, 129-135.

[412] M. C. Q. Ortega, J. C. Bautista, M. Saez, A. M. Garcia, J. E. S. Uria and A. S. Medel, *Spectrochimica Acta Part B-Atomic Spectroscopy*, 1992, **47**, 79-87

[413] E. Niedobova, J. Machat, V. Otruba and V. Kanicky, *Journal of Analytical Atomic Spectrometry*, 2005, **20**, 945-949.

[414] T. Nakahara and T. Mori, *Journal of Analytical Atomic Spectrometry*, 1994, **9**, 159-165.

[415] F. Camuna, J. E. S. Uria and A. S. Medel, *Spectrochimica Acta Part B-Atomic Spectroscopy*, 1993, **48**, 1115-1125.

[416] M. D. Calzada, M. C. Quintero, A. Gamero and M. Gallego, *Analytical Chemistry*, 1992, **64**, 1374-1378.

[417] M. R. Cave and K. A. Green, *Journal of Analytical Atomic Spectrometry*, 1989, **4**, 223-225.

[418] N. Ratanawimarnwong, N. Amomthammarong, N. Choengchan, P. Chaisuwan, M. Amatatongchai, P. Wilairat, I. D. McKelvie and D. Nacapricha, *Talanta*, 2005, **65**, 756-761.

[419] D. Nacapricha, P. Sangkarn, C. Karuwan, T. Mantim, W. Waiyawat, P. Wilairat, I. Cardwell, I. D. McKelvie and N. Ratanawimarnwong, *Talanta*, 2007, **72**, 626-633.

[420] J. L. Burguera, M. R. Brunetto, Y. Contreras, M. Burguera, M. Gallignani and P. Carrero, *Talanta*, 1996, **43**, 839-850.

[421] F. Pena-Pereira, I. Lavilla and C. Bendicho, *Analytica Chimica Acta*, 2009, **631**, 223-228.

[422] F. Pena-Pereira, S. Senra-Ferreiro, I. Lavilla and C. Bendicho, *Talanta*, 2010, **81**, 625-629.

[423] J. Akhoundzadeh, M. Chamsaz, S. R. Yazdinezhad and M. H. Arbaz-zavvar, *Analytical Methods*, 2013, **5**, 778-783.

[424] V. S. Burakov, A. V. Isaevich, P. Y. Misakov, P. A. Naumenkov and S. N. Raikov, *Journal of Analytical Atomic Spectrometry*, 1994, **9**, 307-309.

[425] Y.-L. Yu, S. Dou, M.-L. Chen and J.-H. Wang, *Analyst*, 2013, **138**, 1719-1725.

[426] R. F. Taylor, *Chemical Engineering Science*, 1959, **10**, 68-79.

[427] W. C. Bray, H. A. Liebhafsky, *Journal of the American Chemical Society*, **1931**, 53 (1) 38-44

[428] W. C. Bray, A. L. Caulkins, *Journal of the American Chemical Society*, **1931**, 53 (1) 44-48

[429] H. A. Liebhafsky, *Journal of the American Chemical Society*, **1931**, 53 (3) 896-911

[430] H. A. Liebhafsky, *Journal of the American Chemical Society*, 1931, **53**, 2074-2090.

[431] H. A. Liebhafsky, *Journal of the American Chemical Society*, 1932, **54**, 3499-3503.

[432] H. A. Liebhafsky, W. C. McGavock, R. J. Reyes, G. M. Roe and L. S. Wu, *Journal of the American Chemical Society*, 1978, **100**, 87-91.

[433] H. A. Liebhafsky, R. Furuichi and G. M. Roe, *Journal of the American Chemical Society*, 1981, **103**, 51-56.

[434] E. Abel, *Z. Physik. Chim, 136:161 (1928)*

[435] E. C. Beahm, R. A. Lorenz, C. F. Weber, Oak Ridge National Laboratory, NUREG/CR-5950 ORNL/TM-1224

[436] M. Eigen, K. Kustin, *Journal of the American Chemical Society*, 1962, **84**, 1355-1361

[437] J. Paquette. B. Ford, *Canadian Journal of Chemistry,* 1985, **63**, 2444-2448

[438] D. A. Palmer, M. H. Lietzke, *Radiochimica Acta*, 1982, **31**, 37-44

[439] J. C. Wren and J. M. Ball, *Radiation Physics and Chemistry*, 2001, **60**, 577-596.

[440] C. B. Ashmore, J. R. Gwyther and H. E. Sims, *Nuclear Engineering and Design*, 1996, **166**, 347-355.

[441] R. Sander, Compilation of Henry's Law Constants for Inorganic and Organic Species of Potential Importance in Environmental Chemistry, Version 3, 1999. http://www.henrys-law.org/henry.pdf (Accessed March 3, 2014)

[442] J. Kleinberg and A. W. Davidson, *Chemical Reviews*, 1948, **42**, 601-609.

[443] Friedrich G. Helfferich. Ion Exchange. McGraw-Hill. New York, 1962

[444] N. Ahmad, *Australian Journal of Dairy Technology*, 1977, **32**, 103-106.

[445] Y. X. Duan, H. Q. Zhang, X. M. Jiang and Q. H. Jin, *Spectroscopy Letters*, 1996, **29**, 69-85.

[446] Z. Zhu, Q. He, Q. Shuai, H. Zheng and S. Hu, *Journal of Analytical Atomic Spectrometry*, 2010, **25**, 1390-1394.

[447] L. E. Strong, A. D. Pethybridge, *Journal of Solution Chemistry*, 1987, **16** 841-855

[448] G. Schmitz, *Physical Chemistry Chemical Physics,* 1999, **1**, 1909-1914

[449] Pino, S.; Fang, S. L.; Braverman, L. E. *Exp. Clin. Endocrinol. Diabetes,* **1998,** *106*, S22-S27.

[450] Ohashi, T.; Yamaki, M.; Chandrakand, S. P.; Madhu, G. K.; Minoru, I. *Clin.Chem.* **2000**, *46*, 529-536

[451] Carr MH. (1995) The Martian drainage system and the origin of valley networks and fretted channels. *Journal of Geophysical Research: Planets* 100: 7479-7507.

[452] Squyres SW, Grotzinger JP, Arvidson RE, et al. (2004) In Situ Evidence for an Ancient Aqueous Environment at Meridiani Planum, Mars. *Science* 306: 1709-1714.

[453] Bibring J-P, Langevin Y, Gendrin A, et al. (2005) Mars Surface Diversity as Revealed by the OMEGA/Mars Express Observations. *Science* 307: 1576-1581.

[454] Gendrin A, Mangold N, Bibring J-P, et al. (2005) Sulfates in Martian Layered Terrains: The OMEGA/Mars Express View. *Science* 307: 1587-1591.

[455] McLennan SM, Bell Iii JF, Calvin WM, et al. (2005) Provenance and diagenesis of the evaporite-bearing Burns formation, Meridiani Planum, Mars. *Earth and Planetary Science Letters* 240: 95-121.

[456] Ehlmann BL, Mustard JF, Fassett CI, et al. (2008) Clay minerals in delta deposits and organic preservation potential on Mars. *Nature Geosci* 1: 355-358.

[457] Wray JJ, Murchie SL, Squyres SW, et al. (2009) Diverse aqueous environments on ancient Mars revealed in the southern highlands. *Geology* 37: 10

[458] Grotzinger JP, Sumner DY, Kah LC, et al. (2014) A Habitable Fluvio-Lacustrine Environment at Yellowknife Bay, Gale Crater, Mars. *Science* 343.

[459] Harris RF. (1961) The effect of water potential on microbial growth and activity. In: Parr JF, Gardner WR and Elliot LF (eds) *Water Potential Relations in Soil Microbiology.* Madison, WI: Soil Scien Society of America, pp 23 - 95.

[460] Tapia MS, Stella MA and Chirife J. (2007) Effects of water activity (aw) on microbial stability as a hurdle in food preservation. In: Barbosa-Canovas GV, Fontana AJ, Schmidt SJ, et al. (eds) *Water Acitvity in Foods: Fundamental and Applications.* Ames, IA: Institute of Food Technologists and Blackwell Publishing, pp 239 - 271.

[461] Capone DG, Popa R, Flood B, et al. (2006) Follow the Nitrogen. *Science* 312: 708-709.

[462] Manning CV, McKay CP and Zahnle KJ. (2008) The nitrogen cycle on Mars: Impact decomposition of near-surface nitrates as a source for a nitrogen steady state. *Icarus* 197: 60-64.

[463] Pestova ON, Myund LA, Khripun MK, et al. (2005) Polythermal Study of the Systems M(ClO4)2-H2O (M2+ = Mg2+, Ca2+, Sr2+, Ba2+). *Russian Journal of Applied Chemistry* 78: 409-413.

[464] Stillman DE and Grimm RE. (2011) Dielectric signatures of adsorbed and salty liquid water at the Phoenix landing site, Mars. *Journal of Geophysical Research: Planets* 116: E09005.

[465] Chevrier VF, Hanley J and Altheide TS. (2009) Stability of perchlorate hydrates and their liquid solutions at the Phoenix landing site, Mars. *Geophysical Research Letters* 36: L10202.

[466] Renno NO, Bos BJ, Catling D, et al. (2009) Possible physical and thermodynamical evidence for liquid water at the Phoenix landing site. *Journal of Geophysical Research-Planets* 114.

[467] Davila AF, Duport LG, Melchiorri R, et al. (2010) Hygroscopic salts and the potential for life on Mars. *Astrobiology* 10: 617-628.

[468] Kounaves SP, Hecht MH, Kapit J, et al. (2010a) Wet Chemistry experiments on the 2007 Phoenix Mars Scout Lander mission: Data analysis and results. *Journal of Geophysical Research-Planets* 115

[469] Boynton WV, Ming DW, Kounaves SP, et al. (2009) Evidence for Calcium Carbonate at the Mars Phoenix Landing Site. *Science* 325: 61-64.

[470] Hecht MH, Kounaves SP, Quinn RC, et al. (2009) Detection of Perchlorate and the Soluble Chemistry of Martian Soil at the Phoenix Lander Site. *Science* 325: 64-67.

[471] Kounaves SP, Hecht MH, Kapit J, et al. (2010b) Soluble sulfate in the martian soil at the Phoenix landing site. *Geophysical Research Letters* 37.

[472] Stoker CR, Zent A, Catling DC, et al. (2010) Habitability of the Phoenix landing site. *Journal of Geophysical Research-Planets* 115.

[473] Navarro-Gonzalez R, Vargas E, de la Rosa J, et al. (2010) Reanalysis of the Viking results suggests perchlorate and organics at midlatitudes on Mars. *Journal of Geophysical Research-Planets* 115.

[474] Quinn RC, Martucci HFH, Miller SR, et al. (2013) Perchlorate Radiolysis on Mars and the Origin of Martian Soil Reactivity. *Astrobiology* 13: 515-520.

[475] Haddad PR, Nesterenko PN and Buchberger W. (2008) Recent developments and emerging directions in ion chromatography. *Journal of Chromatography A* 1184: 456-473.

[476] Paull B and King M. (2003) Quantitative capillary zone electrophoresis of inorganic anions. *Electrophoresis* 24: 1892-1934.

[477] Small H, Stevens TS, Bauman WC. (1975) Novel ion exchange chromatographic method using conductimetric detection. *Analytical Chemistry 47*: 1801-1809

[478] Christison T, Pang F, Madden J, et al. (2012) Dionex Technical note 112, Determination of trace anions in Ultrapure water uing capillary ion chromatography. Sunnyvale, CA: Thermo Fisher Scientific.

[479] Kirk AB, Martinelango PK, Tian K, et al. (2005) Perchlorate and iodide in dairy and breast milk. *Environmental Science & Technology 39*: 2011-2017.

[480] Kirk AB, Smith EE, Tian K, et al. (2003) Perchlorate in milk. *Environmental Science & Technology 37*: 4979-4981.

[481] Tian K, Dasgupta PK and Anderson TA. (2003) Determination of trace perchlorate in high-salinity water samples by ion chromatography with on-line preconcentration an preelution. *Analytical Chemistry 75*: 701-706.

[482] Dasgupta PK. (2009) Perchlorate: a cause for iodine deficiency? *Environmental Chemistry 6*: 7-9.

[483] Dasgupta PK, Kirk AB, Dyke JV, et al. (2008) Intake of Iodine and Perchlorate and Excretion in Human Milk. *Environmental Science & Technology 42*: 8115-8121.

[484] Shelor CP, Kirk AB, Dasgupta PK, et al. (2012) Breastfed Infants Metabolize Perchlorate. *Environmental Science & Technology 46*: 5151-5159.

[485] Kuban P and Dasgupta PK. (2004) Capillary ion chromatography. *Journal of Separation Science 27*: 1441-1457.

[486] Boring CB, Dasgupta PK and Sjogren A. (1998) Compact, field-portable capillary ion chromatograph. *Journal of Chromatography A 804*: 45-54.

[487] Kiplagat IK, Kuban P, Pelcova P, et al. (2010) Portable, lightweight, low power, ion chromatographic system with open tubular capillary columns. *Journal of Chromatography A* 1217: 5116-5123.

[488] Huang XJ, Foss FW and Dasgupta PK. (2011) Multilayer chitosan-based open tubular capillary anion exchange column with integrated monolithic capillary suppressor. *Analytica Chimica Acta* 707: 210-217.

[489] Kuban P, Dasgupta PK and Pohl CA. (2007) Open tubular anion exchange chromatography. Controlled layered architecture of stationary phase by successive condensation polymerization. *Analytical Chemistry* 79: 5462-5467.

[490] Jet Propulsion Laboratory CIoT. (2014) *Rover Speed*. Available at: http://mars.jpl.nasa.gov/msl/mission/rover/wheelslegs/.

[491] Kounaves SP, Hecht MH, West SJ, et al. (2009) The MECA Wet Chemistry Laboratory on the 2007 Phoenix Mars Scout Lander. *Journal of Geophysical Research-Planets* 114.

[492] Christian GD, Dasgupta PK and Schug K. (2013) *Analytical Chemistry, 7th ed.*: Wiley.

[493] Benner SA, Devine KG, Matveeva LN, et al. (2000) The missing organic molecules on Mars. *Proceedings of the National Academy of Sciences* 97: 2425-2430.

[494] Stalport F, Coll P, Szopa C, et al. (2009) Investigating the photostability of carboxylic acids exposed to Mars surface ultraviolet radiation conditions. *Astrobiology* 9: 543-549.

[495] Glavin DP, Freissinet C, Miller KE, et al. (2013) Evidence for perchlorates and the origin of chlorinated hydrocarbons detected by SAM at the Rocknest aeolian deposit in Gale Crater. *Journal of Geophysical Research-Planets* 118: 1955-1973.

[496] Dasgupta PK, Bligh RQ, Lee J, et al. (1985) ION PENETRATION THROUGH TUBULAR ION-EXCHANGE MEMBRANES. *Analytical Chemistry* 57: 253-257.

[497] Archer PD, Sutter B, Ming DW, McKay CP, Navarro-Gonzalez R, Franz HB, McAdam A, Mahaffy PR, MSL Science Team (2013) Possible detection of perchlorates by evolved gas analysis of racknest soils: global implications. *44th Lunar and Planetary Science Conference.* LPI Contribution No. 1719, p.2168

[498] Keller JM, Boynton WV, Karunatillake S, et al. (2006) Equatorial and midlatitude distribution of chlorine measured by Mars Odyssey GRS. *Journal of Geophysical Research: Planets* 111: E03S08.

[499] . Glavin DP, Freissinet C, Miller KE, et al. (2013) Evidence for perchlorates and the origin of chlorinated hydrocarbons detected by SAM at the Rocknest aeolian deposit in Gale Crater. *Journal of Geophysical Research-Planets* 118: 1955-1973.

[500] Kounaves SP, Chaniotakis NA, Chevrier VF, et al. (2014) Identification of the perchlorate parent salts at the Phoenix Mars landing site and possible implications. *Icarus* 232: 226-231.

[501] Leshin LA, Mahaffy PR, Webster CR, et al. (2013) Volatile, Isotope, and Organic Analysis of Martian Fines with the Mars Curiosity Rover. *Science* 341.

[502] Blake DF, Morris RV, Kocurek G, et al. (2013) Curiosity at Gale Crater, Mars: Characterization and Analysis of the Rocknest Sand Shadow. *Science* 341.

[503] Clark BC, Morris RV, McLennan SM, et al. (2005) Chemistry and mineralogy of outcrops at Meridiani Planum. *Earth and Planetary Science Letters* 240: 73-94.

[504] Gellert R, Rieder R, Bruckner J, et al. (2006) Alpha particle X-ray spectrometer (APXS): Results from Gusev crater and calibration report. *Journal of Geophysical Research-Planets* 111.

[505] Ericksen GE. (1983) THE CHILEAN NITRATE DEPOSITS. *American Scientist* 71: 366-374.

[506] Penrose RAF. (1910) The nitrate deposits of Chile. *Journal of Geology* 18: 1-32.

[507] Catling DC, Claire MW, Zahnle KJ, et al. (2010) Atmospheric origins of perchlorate on Mars and in the Atacama. *Journal of Geophysical Research-Planets* 115.

[508] Sutter B, Dalton JB, Ewing SA, et al. (2007) Terrestrial analogs for interpretation of infrared spectra from the Martian surface and subsurface: Sulfate, nitrate, carbonate, and phyllosilicate-bearing Atacama Desert soils. *Journal of Geophysical Research: Biogeosciences* 112: G04S10.

[509] Chyba C and Sagan C. (1992) Endogenous production, exogenous delivery and impact-shock synthesis of organic molecules: an inventory for the origins of life. *Nature* 355: 125-132.

[510] Martins Z. (2011) Organic Chemistry of Carbonaceous Meteorites. *Elements* 7: 35-40.

[511] Monroe AA and Pizzarello S. (2011) The soluble organic compounds of the Bells meteorite: Not a unique or unusual composition. *Geochimica Et Cosmochimica Acta* 75: 7585-7595.

[512] Kminek G and Bada JL. (2006) The effect of ionizing radiation on the preservation of amino acids on Mars. *Earth and Planetary Science Letters* 245: 1-5.

[513] Cartwright JA, Gilmour JD and Burgess R. (2013) Martian fluid and Martian weathering signatures identified in Nakhla, NWA 998 and MIL 03346 by halogen and noble gas analysis. *Geochimica Et Cosmochimica Acta* 105: 255-293.

[514] Kim YS, Wo KP, Maity S, et al. (2013) Radiation-Induced Formation of Chlorine Oxides and Their Potential Role in the Origin of Martian Perchlorates. *Journal of the American Chemical Society* 135: 4910-4913.

[515] Jakosky BM, J.P. A, W.M. B, et al. (2007) *An Astrobiology Strategy for the Exploration of Mars*: The National Academies Press.

[516] Ming DW, Archer PD, Glavin DP, et al. (2014) Volatile and Organic Compositions of Sedimentary Rocks in Yellowknife Bay, Gale Crater, Mars. *Science* 343.

[517] Davila AF, Willson D, Coates JD, et al. (2013) Perchlorate on Mars: a chemical hazard and a resource for humans. *International Journal of Astrobiology* FirstView: 1-5.

[518] Pappalardo RT, Vance S, Bagenal F, et al. (2013) Science Potential from a Europa Lander. *Astrobiology* 13: 740-773.

[519] International Technology Roadmap for Semiconductors. 2009 Edition. Yield Enhancement. pp. 11-12

[520] Semiconductor Equipment and Materials International. F63-0211. Guide for Ultrapure Water Used in Seminconductor Processing.

[521] The United States Pharmacopeia 35, The National Formulary 30. Volume 1. **2012**

[522] European Pharmacopoeia 5.0. 2.2.44 Total Organic Carbon in Water for Pharmaceutical Use. **2005**

[523] Bader, K.; Hyde, J.; Watler, P.; Lane, A. *Pharmaceutical Engineering* **2009**.

[524] Baffi, R.; Dolch, G.; Garnick, R.; Huang, Y. F.; Mar, B.; Matsuhiro, D.; Niepelt, B.; Parra, C.; Stephan, M. *Journal of Parenteral Science and Technology* **1991**, *45*. 13-19.

[525] Clifford, R. H. *American laboratory* **2010**, *42*.

[526] Jenkins, K. M.; Vanderwielen, A. J.; Armstrong, J. A.; Leonard, L. M.; Murphy, G. P.; Piros, N. A. *PDA journal of pharmaceutical science and technology / PDA* **1996**, *50*. 6-15.

[527] Strege, M. A.; Stinger, T.; Farrell, B.; Lagu, A. L. *BIOPHARM-EUGENE-* **1996**, *9*. 42-45.

[528] Wallace, B.; Stevens, R.; Purcell, M. *Pharmaceutical Technology* **2004**, *28*. 40-43.

[529] United States Food and Drug Administration, Validation of Cleaning Processes, July 1993. http://www.fda.gov/ICECI/Inspections/InspectionGuides/ucm074922.htm Accessed July 16, 2013

[530] Bevilacqua, A.; Dowd, N. *The Pharmaceutical Solutions Update* **2008,** March. 36-38

[531] Van Hall, C. E.; Stenger, V. A. *Analytical Chemistry* **1967**, *39*. 503-507.

[532] Huber, S. A.; Frimmel, F. H. *Analytical Chemistry* **1991**, *63*. 2122-2130.

[533] Huber, S.; Frimmel, F. *International journal of environmental analytical chemistry* **1992**, *49*. 49-57.

[534] Steele, J. W.; Birbara, P. J.; Nalette, T. A.; United States Patent 5,106,754, 1992.

[535] Inoue, K.; Morita, Y.; United States Patent 5,425,919, 1995.

[536] Bernard, B. B.; United States Patent 4,619,902, 1986.

[537] Godec, R.; O'neill, K.; Hutte, R.; United States Patent 5,902,751, 1999.

[538] Godec, R. D.; Kosenka, P. K.; Hutte, R.; United States Patent 5,132,094, 1992.

[539] Davenport, R. J.; Godec, R. D.; Unites States Patent 6,723,565, 2004.

[540] Thomas, R. C.; Cravens, E. D.; Carter, M. T.; United States Patent 6,444,474, 2002

[541] Blades, F. K.; Godec, R. D.; United States Patent 5,047,212, 1991.

[542] Bender, D.; Bevilacqua, A. C. *Ultrapure Water* **1999**, *16*. 58-68.

[543] DeGenova, J.; Donovan, R.P.; Morrison, D. *Ultrapure Water Journal.* **1998**, Nov.

[544] Matthews, R.W.; Abdullah, M.; Low, G.K.-C. *Analytica Chimica Acta.* **1989.** 233, 171-179

[545] Izumi, I.; Dunn, W. W.; Wilbourn, K. O.; Fan, F. R. F.; Bard, A. J. *Journal of Physical Chemistry* **1980**, *84.* 3207-3210.

[546] Emery, R. M.; Welch, E. B.; Christman, R. F. *Journal (Water Pollution Control Federation)* **1971**. 1834-1844.

[547] Godec, R. In *Semiconductor Pure Water and Chemicals Conference*, 2000, pp 61-112.

[548] Peyton, G. R. *Marine Chemistry* **1993**, *41*. 91-103.

[549] Rydzewski, J.; Godec, R. *Proceedings of the Semiconductor Pure Water and Chemicals Conference*, 2002.

[550] Godec, R. In *ULTRAPURE WATER Europe,* **2002.**

[551] Bevilacqua, *16th Annual Seminconductor Pure Water and Chemical Conference*. **1997**, pp 131-160

[552] Cutler, F. *Ultrapure Water*. **1988**, Sep. 40-48

[553] Emery, A.P.; Girard, J.E.; Jandik, P. *Ultrapure Water.* **1988,** Oct. 49-54

[554] Emery, R. M.; Welch, E. B.; Christman, R. F. *Journal (Water Pollution Control Federation)* **1971**. 1834-1844.

[555] Dobbs, R. A.; Wise, R. H.; Dean, R. B. *Water Research* **1972**, *6*. 1173-1180.

[556] MacCraith, B.; Grattan, K.; Connolly, D.; Briggs, R.; Boyle, W.; Avis, M. *Sensors and Actuators B: Chemical* **1994**, *22*. 149-153.

[557] Naffrechoux, E.; Fachinger, C.; Suptil, J. *Analytica chimica acta* **1992**, *270*. 187-193.

[558] Edwards, A.; Cresser, M. *Water Research* **1987**, *21*. 49-56.

[559] Power, J. F.; Langford, C. H. *Analytical Chemistry* **1988**, *60*. 842-846.

[560] Pages, J.; Gadel, F. *Science of the total environment* **1990**, *99*. 173-204.

[561] Sheppard, C. *Water Research* **1977**, *11*. 979-982.

[562] Ferrari, G. M. *Marine Chemistry* **2000**, *70*. 339-357.

[563] Ferrari, G. M.; Dowell, M. D.; Grossi, S.; Targa, C. *Marine Chemistry* **1996**, *55*. 299-316.

[564] Blades, F. K.; United States Patent 4,304,996, 1981.

[565] Klinkhammer, G.P.; McClelland, P.H.; Jackson, D.; Russo, C.J. United States Patent 2012/0205547 A1, **2012**

[566] Weishaar, J. L.; Aiken, G. R.; Bergamaschi, B. A.; Fram, M. S.; Fujii, R.; Mopper, K. *Environmental Science & Technology* **2003**, *37*. 4702-4708.

[567] Zaps Technologies LiquID Total Organic Carbon monitoring data sheet. http://www.zapstechnologies.com/wp-content/uploads/2012/05/ZAPS_How-It-Works_TOC2.pdf. Accessed July 16, 2013

[568] White, J. U. *J. Opt. Soc. Am* **1942**, *32*. 285-288.

[569] Herriott, D. R.; Schulte, H. J. *Applied Optics* **1965**, *4*. 883-889.

[570] Dasgupta, P. K. *Analytical Chemistry* **1984**, *56*. 1401-1403.

[571] Dasgupta, P. K.; Rhee, J. S. *Analytical Chemistry* **1987**, *59*. 783-786.

[572] Okeefe, A.; Deacon, D. A. G. *Review of Scientific Instruments* **1988**, *59*. 2544-2551.

[573] O'Keefe, A. *Chemical Physics Letters* **1998**, *293*. 331-336.

[574] O'Keefe, A.; Scherer, J. J.; Paul, J. B. *Chemical Physics Letters* **1999**, *307*. 343-349.

[575] Kiwanuka, S.-S.; Laurila, T.; Kaminski, C. F. *Analytical chemistry* **2010**, *82*. 7498-7501.

[576] Seetohul, L. N.; Ali, Z.; Islam, M. *Analyst* **2009**, *134*. 1887-1895.

[577] Simon, R. *Lab on a Chip* **2011**, *11*. 3953-3955.

[578] van der Sneppen, L.; Hancock, G.; Kaminski, C.; Laurila, T.; Mackenzie, S. R.; Neil, S. R.; Peverall, R.; Ritchie, G. A.; Schnippering, M.; Unwin, P. R. *Analyst* **2010**, *135*. 133-139.

[579] Weidner, V. R.; Hsia, J. J. *JOSA* **1981**, *71*. 856-861.

[580] Hannon, G.E.; McGregor, G.L.; Minor, R.B. United States Patent 5,781,342

[581] Minor, R. B.; McGregor, G. L.; Wu, H. S.; Lash, D. J.; United States Patent 6,015,610, 2000.

[582] Tsai, B. K.; Allen, D. W.; Hanssen, L. M.; Wilthan, B.; Zeng, J. In *Optical Engineering+ Applications*; International Society for Optics and Photonics, 2008, pp 70650Y-70650Y-9.

[583] Silva, C.; Pinto da Cunha, J.; Pereira, A.; Chepel, V.; Lopes, M.; Solovov, V.; Neves, F. *Journal of Applied Physics* **2010**, *107*. 064902-064902-8.

[584] Janecek, M. *Nuclear Science, IEEE Transactions on* **2012**, *59*. 490-497.

[585] Nutter, S.; Bower, C.; Gebhard, M.; Heinz, R.; Spiczak, G. *Nuclear Instruments and Methods in Physics Research Section A: Accelerators, Spectrometers, Detectors and Associated Equipment* **1991**, *310*. 665-670.

[586] Platt, U.; Perner, D.; Pätz, H. *Journal of Geophysical Research: Oceans (1978–2012)* **1979**, *84*. 6329-6335.

[587] Wei, L.; Fujiwara, K.; Fuwa, K. *Analytical Chemistry* **1983**, *55*. 951-955.

[588] Fuwa, K.; Lei, W.; Fujiwara, K. *Analytical Chemistry* **1984**, *56*. 1640-1644.

[589] Fujiwara, K.; Fuwa, K. *Analytical Chemistry* **1985**, *57*. 1012-1016.

[590] Peters, D.G.; Hayes, J.M.' Hieftje, G.M. A brief introduction to modern chemical analysis, Saunders, 1976.

[591] P. K. Dasgupta, R. P. Bhawal, Y.-H. Li, *Analytical Chemistry*. DOI: 10.1021/ac404251wl

[592] Esource optics VUV-UV flat mirrors. http://www.esourceoptics.com/vuvmirrors.html. Accessed July 7, 2013

[593] Torchio, P.; Gatto, A.; Alvisi, M.; Albrand, G.; Kaiser, N.; Amra, C. *Applied optics* **2002**, *41*. 3256-3261.

[594] Fry, E. S.; Kattawar, G. W.; Pope, R. M. *Applied Optics* **1992**, *31*. 2055-2065.

[595] Schauss, A. G. Açaí, an Extraordinary Antioxidant Rich Palm Fruit. 2nd ed. Biosocial Publications, Tacoma, WA, 2006.

[596] Seeram, N. P.; Aviram, M.; Zhang, Y.; Henning, S. M.; Feng, L.; Dreher, M.; Heber, D. Comparison of Antioxidant Potency of Commonly Consumed Polyphenol-Rich Beverages in the United States. *J. Agric. Food Chem.* **2008,** *56*, 1415-1422.

[597] Rodrigues, R. B.; Lichtenthäler, R.; Zimmermann, B. F.; Papagiannopoulos, M.; Fabricius, H.; Marx, F.; Maia, J. G.; Almeida, O. Total Oxidant Scavenging Capacity of Euterpe oleracea Mart. (Açaí) Seeds and Identification of Their Polyphenolic Compounds. *J. Agric. Food Chem.* **2006,** *54*, 4162-4167.

[598] Hassimotto, N. M.; Genovese, M. I.; Lajolo, F. Antioxidant Activity of Dietary Fruits, Vegetables, and Commercial Frozen Fruit Pulps. *J. Agric. Food Chem.* **2005,** *53*, 2928-35.

[599] Matheus, M. E.; de Oliveira Fernandes, S. B.; Silveira, C. S.; Rodrigues, V. P.; de Sousa Menezes, F.; Fernandes, P. D. Inhibitory effects of *Euterpe oleracea* Mart. on nitric oxide production and iNOS expression *J. Ethnopharmacol.* **2006,** 107, 291-296.

[600] Schauss, A. G., Wu, X., Prior, R. L., Ou, B., Patel, D., Huang, D.; Kababick, J. P. Antioxidant capacity and other bioactivities of the freeze-dried Amazonian palm berry, *Euterpe oleraceae* Mart. (Açaí). *J. Agric. Food Chem.* **2006,** *54*, 8604-10.

[601] Noratto, G. D.; Angel-Morales, G.; Talcott, S.T.; Mertens-Talcott, S.U. Polyphenolics from açaí (*Euterpe oleracea* Mart.) and red Muscadine grape (*Vitis rotundifolia*) protect human umbilical vascular endothelial cells (HUVEC) from glucose- and lipopolysaccharide (LPS)-induced inflammation and target microRNA-126. *J. Agric. Food Chem.* **2011,** *59*, 7999-8012.

[602] Del Pozo-Insfran, D.; Percival, S. S.; Talcott, S. T. Açaí (*Euterpe oleracea* Mart.) polyphenolics in their glycoside and aglycone forms induce apoptosis of HL-60 leukemia cells *J. Agric. Food Chem.* **2006,** *54*, 1222-1229.

[603] Smith, R. E.; Eaker, J.; Tran, K.; Goerger, M.; Wycoff, W.; Sabaa-Srur, A. U. O.; Menezes, E. M. S.; Insoluble solids in Brazilian and Floridian açaí. *Nat. Prod. J.* **2012**, *2*, 95-98.

[604] Zhang, Y.; Krueger,D.; Durst, R.; Lee, R.; Wang, D.; Seeram, N.; Heber, D. International Multidimensional Authenticity Specification (IMAS) Algorithm for Detection of Commercial Pomegranate Juice Adulteration. *J. Agric. Food Chem.* **2009,** 57, 2550-2557.

[605] Smith, J. Your Açaí Didn't Work? http://www.aprovenproduct.com/acailand.php Accessed May 6, 2012

[606] Hamilton Media LLC. The Açaí Berry Scam. A Briefing for Attorneys, Regulators and Victims. http://www.scribd.com/doc/51511856/The-Acai-Berry-Scam. Accessed December 25, 2012.

[607] Madden, J. E.; Shaw, M. J.; Dicinoski, G. W.; Avdalovic, N.; Haddad, P. R. Simulation and optimization of retention in ion chromatography using virtual column 2 software. *Anal. Chem.* **2002,** *74,* 6023–6030.

[608] Mato, I.; Suarez-Luque, S.; Huidobro, J. F. A review of the analytical methods to determine organic acids in grape juices and wines. *Food Res. Int.* **2005,** *38*, 1175-1188.

[609] Widodo, S. E.; Shiraishi, M.; Shiraishi, S. Organic acids in the juice of acid lemon and Japanese acid citrus by gas chromatography. *J. Fac. Agric. Kyushu Univ.* **1995,** *40*, 39-44.

[610] Shiraishi, S. C.; Kawakami, K.; Widodo, S. E.; Shiraishi, M.; Kitazaki, M. Organic acid profiles in the juice of fig fruits. *J. Fac. Agric. Kyushu Univ.* **1996,** *41*, 29-33.

[611] Barden, T. J.; Croft, M. Y.; Murby, E. J.; Wells, R. J. Gas chromatographic determination of organic acids from fruit juices by combined resin mediated methylation and extraction in supercritical carbon dioxide. *J. Chromatogr. A* **1997,** 785, 251-261.

[612] Jurado-Sanchez, B.; Ballesteros, E.; Gallego, M. Gas chromatographic determination of 29 organic acids in foodstuffs after continuous solid-phase extraction. *Talanta* **2011,** *84*, 924-930.

[613] Irudayaraj, J.; Tewari, J. Simultaneous monitoring of organic acids and sugars in fresh and processed apple juice by Fourier transform infrared–attenuated total reflection spectroscopy. *Appl. Spectrosc.* **2003,** *57,* 1599-1604

[614] Bureau, S.; Ruiz, D.; Reich, M.; Gouble, B.; Bertrand, D.; Audergon, J. M.; Renard, C. M. G. C. Application of ATR-FTIR for a rapid and simultaneous determination of sugars and organic acids in apricot fruit. *Food Chem.* **2009,** *115*, 1133-1140.

[615] Loredana, L.; Diehl, H.; Socaciu, C. HPLC fingerprint of organic acids in fruit juices. *Bull. Univ. Agric. Sci. Vet. Med.* **2006,** *62,* 288-292.

[616] Santalad, A.; Teerapornchaisit, P.; Burakham, R.; Srijaranai, S. Capillary zone electrophoresis of organic acids in beverages. *LWT-Food Sci. Technol*. **2007,** *40* 1741-1746.

[617] Nutku, M. S.; Erim, F. B. Polyethyleneimine-coated capillary electrophoresis capillaries for the analysis of organic acids with an application to beverages. *J. Microcol. Sep.* **1999,** *11*, 541-543

[618] Tezcan, F.; Gultekin-Ozguven, M.; Diken, T.; Ozcelik, B.; Erim, F. B. Antioxidant activity and total phenolic, organic acid and sugar content in commercial pomegranate juices. *Food Chem.* **2009,** *115*, 873-877.

[619] Cámara, M. M.; Diez, C.; Torija, M. E.; Cano, M. P. HPLC determination of organic acids in pineapple juices and nectars. *Z. Lebensm. Unters. Forsch.* **1994,** *198,* 52-56.

[620] Grosheny, B.; Isengard, H. D.; Philipp, O. Determination of twelve organics acids and 5-Hydroxymethylfurfural in fruit juices by HPLC. *Deut. Lebensm. Rundsch.* **1995,** *91,* 137-140.

[621] Huopalahti, R.; Järvenpää, E.; Katina, K. A novel solid-phase extraction-HPLC method for the analysis of anthocyanin and organic acid composition of Finnish cranberry *J. Liq. Chromatogr. Related Technol.* **2000**, *23*, 2695-2701.

[622] Koyuncu, F. Organic acid composition of native black mulberry fruit. *Chem. Nat. Compd.* **2004,** *40,* 367-369.

[623] Raffo, A.; Paoletti, F.; Antonelli, M. Changes in sugar, organic acid, flavonol and carotenoid composition during ripening of berries of three seabuckthorn

(*Hippophae rhamnoides* L.) cultivars. *Eur. Food Res. Technol.* **2004,** *219*, 360-368.

[624] Gao, H. Y.; Liao, X. J.; Wang, S. G.; Hu, X. S. Simultaneous determination of eleven organic acids in fruit juice by reversed phase high performance liquid chromatography. *Chin. J. Anal. Chem.* **2004,** *32*, 1645-1648.

[625] Marconi, O.; Floridi, S.; Montanari, L. Organic acids profile in tomato juice by HPLC with UV detection. *J. Food Qual.* **2007,** *30*, 253-266.

[626] Cunha, S. C.; Fernandes, J. O.; Ferreira, I. M. HPLC/ UV determination of organic acids in fruit juices and nectars. *Eur. Food Res. Technol.* **2002,** *214*, 67-71.

[627] Nour, V.; Trandafir, I.; Ionica, M. E. Ascorbic acid, anthocyanins, organic acids and mineral content of some black and red currant cultivars. *Fruits* **2011,** *66*, 353-362.

[628] Chinnici, F.; Spinabelli, U.; Riponi, C.; Amati, A. Optimization of the determination of organic acids and sugars in fruit juices by ion-exclusion liquid chromatography. *J. Food Comp. Anal.* **2005,** *18,* 121-130

[629] Ergoenuel, P. G.; Nergiz, C. Determination of organic acids in olive fruit. *Czech J. Food Sci.* **2010,** *28*, 202-205.

[630] Lin, J. T.; Liu, S. C.; Shen, Y. C.; Yang, D. J. Comparison of various preparation methods for determination of organic acids in fruit vinegars with a simple ion-exclusion liquid chromatography. *Food Anal. Met.* **2011,** *4*, 531-539.

[631] Eyeghe-Bickong, H. A.; Alexandersson, E. O.; Gouws, L. M.; Young, P. R.; Vivier, M. A. Optimisation of an HPLC method for the simultaneous quantification of the major sugars and organic acids in grapevine berries. *J. Chromatogr. B.* **2012,** *885,* 43-49.

[632] Muñoz-Robredo, P.; Robledo, P.; Manríquez, D.; Molina, R.; Defilippi, B. G. Characterization of sugars and organic acids in commercial varieties of table grapes. *Chil. J. Agric. Res.* **2011,** *71,* 452-458.

[633] Shui, G. H.; Leong, L. P. Separation and determination of organic acids and phenolic compounds in fruit juices and drinks by high-performance liquid chromatography. *J. Chromatogr. A* **2002,** *977*, 89-96.

[634] Veberic, R.; Jakopic, J.; Stampar, F.; Schmitzer, V. European elderberry (Sambucus nigra L.) rich in sugars, organic acids, anthocyanins and selected polyphenols. *Food Chem.* **2009,** *114,* 511-515.

[635] Hernández, Y.; Lobo, M. G.; Gonzalez, M. Factors affecting sample extraction in the liquid chromatographic determination of organic acids in papaya and pineapple. *Food Chem.* **2009,** *114,* 734-741.

[636] Silva, B. M.; Andrade, P. B.; Ferreres, F.; Domingues, A. L.; Seabra, R. M.; Ferreira, M. A. Phenolic profile of quince fruit (*Cydonia oblonga* Miller) (pulp and peel). *J. Agric. Food Chem.* **2002,** *50,* 4615-4618.

[637] Suarez, M. H.; Rodriguez, E. R.; Romero, C. D. Analysis of organic acid content in cultivars of tomato harvested in Tenerife. *Eur. Food Res. Technol.* **2008**, *226*, 423-435.

[638] Arslan, D.; Ozcan, M. M. Influence of growing area and harvest date on the organic acid composition of olive fruits from Gemlik variety. *Sci. Hort.* **2011,** *130,* 633-641.

[639] Zhang, A.; Fang, Y. L.; Meng, J. F.; Wang, H.; Chen, S. X.; Zhang, Z. W. Analysis of low molecular weight organic acids in several complex liquid biological systems

via HPLC with switching detection wavelength. *J. Food Comp. Anal.* **2011,** *24*, 449-455.

[640] Oatway, L.; Vasanthan, T.; Helm, J. H. Phytic acid. *Food Rev. Int.* **2001**, *17*, 419-431.

[641] Schlemmer, U.; Frolich, W.; Prieto R. M.; Grases, F. Phytate in foods and significance for humans: Food sources, intake, processing, bioavailability, protective role and analysis. *Mol. Nutr. Food Res*. **2009**, *53*, S330-S375.

[642] Kell, D. B. Towards a unifying, systems biology understanding of large-scale cellular death and destruction caused by poorly liganded iron: Parkinson's, Huntington's, Alzheimer's, prions, bactericides, chemical toxicology and others as examples. *Arch. Toxicol*. **2010**, *84*, 825-889.

[643] Horwitz, W. Association of Official Analytical Chemists. AOAC method 986.11, Phytate in foods, anion exchange method, in: Methods of Analysis, Association of Official Analytical Chemists, Arlington, VA, 2000, pp. 57-58.

[644] Smith, R. E.; Macquarrie, R. A. Determination of inositol phosphates and other biological anions by ion chromatography. *Anal. Biochem*. **1988**, *170*, 308-315.

[645] Skoglund, E.; Carlsson, N.-G.; Sandberg, A.-S. Analysis of inositol mono- and diphosphate isomers using high-performance ion chromatography and pulsed amperometric detection. *J. Agric. Food Chem.* **1997,** *45,* 4668-4673.

[646] Carlsson, N.-G.; Bergman, E.-L.; Skoglund, E.; Hasselblad, K.; Sandberg, A.-S. Rapid analysis of inositol phosphates. *J. Agric. Food Chem.* **2001,** *49,* 1695-1701.

[647] Chen, Q. C.; Li, B. W. Separation of phytic acid and other related inositol phosphates by high-performance ion chromatography and its applications. *J. Chromatogr. A*. **2003**, 1018, 41-52.

[648] Blaabjerg, K.; Hansen-Moller, J.; Poulsen, H. D. High-performance ion chromatography method for separation and quantification of inositol phosphates in diets and digesta. *J. Chromatogr. B.* **2010**, *878*, 347-354.

[649] Saccani, G.; Gherardi, S.; Trifirò, A.; Soresi Bordini, C.: Calza, M.; Freddi, C. Use of ion chromatography for the measurement of organic acids in fruit juices. *J. Chromatogr. A*. **1995**, *706*, 395-403.

[650] Kupina, S. A.; Pohl, C. A.; Gannotti, J. L. Determination of tartaric, malic, and citric acids in grape juice and wine using gradient ion chromatography. *Am. J. Enol. Viticult* **1991,** *42,* 1-5.

[651] Masson, P. Influence of organic solvents in the mobile phase on the determination of carboxylic acids and inorganic anions in grape juice by ion chromatography. *J. Chromatogr. A*. **2000**, *881*, 387-394.

Charles (Phillip) Shelor received his B.S. in Chemistry from the University of Texas at Arlington in 2007. Phillip went on to work for the Cott Beverage corporation from 2007 to 2009 as a quality control technician. Phillip left Cott to pursue his PhD at the University of Texas at Arlington working for Purnendu Dasgupta. While in Professor Dasgupta's lab Phillip worked on a large number of projects, largely related to measuring iodine and perchlorate in biological fluids. During his time at UTA, Phillip earned the Chemistry Department Graduate Research Award, Graduate Teaching Award, and Charles K. Baker Character Fellowship. He additionally earned the 2012 Environmental Chemistry Graduate Student Award and earned an American Chemical Society department of Analytical Chemistry 2013 summer fellowship.